The University Of Sheffield.

ESCAPE FROM BREAST CANCER THERAPY, ARE NEUROPILINS THE KEY?

SAPNA LUNJ

Thesis submitted for the degree of
Doctor of Philosophy.

University of Sheffield
Department of Oncology

August 2013
(corrections resubmitted in October 2014)

"Make yourself familiar with the angels, and behold them frequently in spirit; for without being seen, they are present with you."

- Francis de Sales

I would like to dedicate my PhD Thesis to my granddad, Ved Pall Lunj and my uncle, Vijay Rajput. I always get the feeling, that you are looking down on me from heaven, protecting and guiding me. If you were both here today, I hope you would be proud of, what I have become.

CONTENTS

TITLE **PAGE**

I ACKNOWLEDGEMENTS

I would like to thank my supervisors, Prof. Nicola Brown, Dr Carolyn Staton, Dr Ingunn Holen and Prof. Malcolm Reed for one giving me the opportunity to work on this project but also for their constant support and guidance throughout my research. I could not have asked for nicer or more inspiring supervisors.

I wish to thank the Breast Cancer Campaign, for funding research project. I would also like to acknowledge Prof. Kurt Ballmer-Hofer for supplying us with the Np1 binding peptides used in the *in vitro* experiments. Additionally I would like to acknowledge Dr Kim Reeves for conducting the intra-cardiac injections on my behalf and Dr Hannah Brown for providing technical advice. I would like to acknowledge Alyson Evans, Matt Fisher, Claire Greaves, Jenny Globe, Sue Higham and Carmel Nichols for providing me with technical support and advice throughout my PhD. In addition I would like to thank everyone else in the department for making me feel welcome and part of the family. I would like to thank my friends and colleagues Rachel Daniel, Gemma Foulds, Aliya Hasan, Katerina Nanou, Rohini Raman, Kim Reeves, Lucy Shaw, Manoj Valluru, Abi Welford, Jessie Wu and Robin Young for their constant friendship, help and advice, you have all in one way or another kept me sane during this testing period of me life.

I would like to thank my granddad, grandma and uncle for their constant support and encouragement. The faith that you all have in me, keeps me going always. I would also like to thank my sister, brother and sister-in-law for being there for me; you have always been understanding and supportive of me and provided me with so much love and encouragement. A special acknowledgement goes out to my little nephew, Neel who at the moment is too young to realise just what a little ray of sunshine he is. Your cheeky little face keeps me happy and optimistic in life.

Last but not least I would like to thank my parents without whom none of this would have been possible. You have always been so supportive of all my decisions and have encouraged me in every aspect of my life. Your constant love and encouragement has always made me believe that hard work and dedication will keep you on the right track and will lead you to your goals. I can not express just how grateful I am to you both for everything that you have done for me.

II ABSTRACT

Background

Angiogenesis is the formation of new blood vessels from the pre-existing vasculature and is crucial for the development and progression of solid tumours. Vascular Endothelial Growth Factor (VEGF) is the most potent angiogenic factor identified to date and mediates its mitogenic and angiogenic activity on endothelial cells via tyrosine kinase receptors VEGF-R1 and VEGF-R2. Bevacizumab (Bz) is a humanised antibody to VEGF and prevents VEGF binding to VEGF-R1 and VEGF-R2 thereby inhibiting angiogenesis, and has been shown to increase progression free survival in breast cancer. However, tumours treated with Bz eventually acquire resistance and subsequently escape treatment control.

Aim

The aim of the study was to assess if combining Bz with a neuropilin 1 targeted peptide would enhance the inhibitory effects observed with Bz on breast cancer growth.

Methods

Three cell types were utilised the *in vitro* studies; human dermal microvascular endothelial cells (HuDMECs) and two breast cancer cell (MDA-MB-231 and MDA-MB-436). A number of *in vitro* functional assays were carried out to assess if any of the neuropilin1 peptides demonstrated biological activity. Based on the *in vitro* data a primary sub-cutaneous tumour model was set up to assess the effects of Bz in combination with the neuropilin1 peptides in a more relevant and dynamic setting.

Results

Overall the Np1 peptides failed to demonstrate additive effects on inhibiting breast cancer growth and activity. The 'true' inhibitory effects of Bz were observed in the bone metastasis *ex vivo* analysis, whereby the health of the bone in a animal with bone metastases was significantly healthier in the Bz treated animals compared with the control vehicle.

Conclusion

To conclude the effects of the neuropilin 1 peptides in enhancing inhibitory effects on breast cancer growth when combined with Bz remains inconclusive due to a number of reasons discussed in this thesis. In addition, the thesis highlighted that going forward differentiating the actions of Bz from those observed with the vehicle control is crucial and needs to be bought to light. Finally, expanding on the bone metastasis model is key, as preliminary data with Bz looks promising.

III ABBREVIATIONS

ABC	Avidin/ Biotinylated enzyme Complex
ALDH	Aldehye Dehydrogenase
Ang-2	Angiopoeitin 2
ATCC	American Type Culture Collection
BCA	Bicinchonic Acid Protein Assay
BrDU	Bromodeoxyuridine
BSA	Bovine Serum Albumin
Bz	Bevacizumab
Cu^{+}	Calcium ion
CV	Control Vehicle for Bz
DAB	3'3' Diaminobenzidine
DCIS	Ductal Carcinoma *in situ*
dH_20	Distilled Water
DMEM	Dulbecco's Modified Eagle Medium
DMSO	Dimethyl Sulfoxide
DNA	Deoxyribonucleic Acid
DPX	Distyrene Plasticiser Xylene
E-selectin	Endothelial leukocyte Adhesion Molecule
EBM2	Endothelial Cell Basal Growth Media 2
EC	Endothelial Cells
ECM	Extra Cellular Matrix
EDTA	Ethylenediaminetetraacetic Acid
ELISA	Enzyme Linked
EOP	End of Procedure
ER	Estrogen Receptor
EtOH	Ethanol
FCS	Fetal Calf Serum
FDA	Federal Drugs Agency
FGF	Fibroblast Growth Factor
FLK	Fetal Liver Kinase
FLT	Fms-related Tyrosine Kinase
GFP	Green Fluorescent Protein
h	Hour
HBSS	Hank's Balanced Salt Solution

HCL	Hydrochloric Acid
H&E	Haematoxylin and Eosin
HER	Human Epidermal Receptor
HIF-1α	Hypoxia Inducible Factor 1 alpha
HIF-1β	Hypoxia Inducible Factor 1 beta
HR	Hazard Ratio
HRE	Hypoxia Responsive Element
HRP	Horse Radish Peroxidise
HSP	Heparin Sulphate Proteins
HuDMEC	Human Dermal Microvascular Endothelial Cells
HuVECs	Human Umbilical Vein Endothelial Cells
i.c	Intra-cardiac
IgG	Immunoglobulin
IHC	Immunohisochemistry
i.p	Intra-peritoneal
i.v	Intra-venous
IVIS	Interactive Video Information System
kDa	Kilo Dalton
MAPK	Mitogen-Activated Protein Kinase
mBC	Metastatic Breast Cancer
MITC	Mitomycin C
MMPs	Matrix Metalloproteinase's
MMP1	Matrix Metalloproteinase 1
MMP2	Matrix Metalloproteinase 2
mRNA	Messenger RNA
Micro-CT	Microscopic Computed Tomography
MTS	DiMethylthiazlotetrazolium Salt
NADH	Nicotinamide Adenine Dinucleotide
NAOH	Sodium Hydroxide
Np1	Neuropilin 1
Np2	Neuropilin 2
ORR	Overall Response Rate
OS	Overall Survival
P1	Peptide 1
P2	Peptide 2
P7b	Peptide 7b
P10	Peptide 10

PBS	Phosphate Buffered Saline
PBST	Phosphate Buffered Saline Tween
PCR	Polymerase Chain Reaction
PDGF	Platelet Derived Growth Factor
PFS	Progression Free Survival
PI3-kinase	Phosphoinositide 3-kinase
Pimo	Pimonidazole
PLCγ	Phospholipase C
PLGF	Placenta Growth Factor
PR	Progesterone Receptor
P/S	Penicillin/Streptomycin
PVDF	Polyvinylidene difluoride
rh	Recombinant
RNA	Ribonucleic Acid
RPMI	Rosewell Park Memorial Institute 1640 Medium
rtp	Room Temperature
SDS-PAGE	Sodium Deoxy Sulphate Polyacrylamide Gel Electrophoresis
SEMA	Semaphorin
s.c	Subcutaneous
SNP	Single Nucleotide Polymorphism
SPR	Surface Plasmon Resonance
TBST	Tris Buffered Saline Tween
TGF-β	Transforming Growth Factor Beta
TK	Tyrosine Kinase
TKRs	Tyrosine Kinase Receptors
TRAP	Tartrate-Resistant Acid Phosphatase
VE	Vascular Endothelial
VEGF	Vascular Endothelial Growth Factor
VEGF-R1	Vascular Endothelial Growth Factor Receptor 1
sVEGF-R1	Soluble Vascular Endothelial Growth Factor Receptor 1
VEGF-R2	Vascular Endothelial Growth Factor Receptor 2
VHL	Von-Hippal Lindau
VPF	Vascular Permeability Factor
w.r.t	with respect to

IV LIST OF TABLES

V LIST OF FIGURES

Chapter 1- Introduction

Chapter 2- Materials & Methods

Chapter One

Introduction

1. Introduction

Breast cancer is a life threatening disease that has an incidence rate of 47,693 cases per annum in the UK alone and is the most commonly diagnosed cancer type in the UK (Cancer Research UK, 2008). Surgery is the first line of treatment for primary breast cancer and current treatment for metastatic breast cancer (mBC) includes chemotherapy or radiotherapy used in an adjuvant setting sometimes in combination with anti-angiogenic drugs including Bevacizumab (Avastin®). However, since the approval of Bevacizumab (Bz) for mBC treatment in 2008, it has become clear that resistance to anti-angiogenic therapy is rapid and that the initial promise of such therapy is proving less efficacious than initially hoped. Despite disappointing outcomes in the clinic, the anti-angiogenic approach to mBC treatment may still hold some promise and greater knowledge of the mechanisms of action and a more selective use of the therapy may prove beneficial. This introduction discusses the clinical significance of anti-angiogenic therapy in breast cancer treatment with the main focus being the vascular endothelial growth factor pathway. The challenges that anti-angiogenic therapy has encountered in the clinic and the Food and Drug Administration (FDA) withdrawal of approval will also be discussed, in particular the potential mechanisms that lead to Bz resistance in breast cancer therapy.

1.1 Breast Cancer

1.1.1 Morphology of Breast Cancer

Breast carcinomas mostly present as discrete lumps, usually within the upper quadrant of the breast and histological examination is required to ensure correct diagnosis (***Underwood, 1996***). A high majority of breast carcinomas are adenocarcinomas that arise from either glandular or ductal epithelium. The clinical manifestations of invasive breast cancer occur in a progressive manner. A normal duct may progress through several different proliferative conditions that will not necessarily result in a malignant disease; these conditions include fibrocystic changes, adenosis, epithelial hyperplasia and cysts. Breast carcinomas do not develop rapidly from the normal breast; there is a morphological change in the cells in the ducts or lobules, which eventually leads to a malignant disease. The following lists the morphological states in order of lesion severity; (1) Hyperplasia, (2) Atypical hyperplasia, (3) Ductal Carcinoma *in situ* (DCIS) and (4) Invasive Carcinoma (***Underwood, 1996***). However it is important to note that breast cancer progression does not necessarily follow each step in this order of severity, unlike the adenoma-carcinoma sequence in colorectal cancer (CRC) (***Frank, 2007***).

1.1.2 Breast Cancer (Sub-Types)

Breast cancer is not defined as one disease as there are many sub-classifications. This makes the treatment of the disease difficult, as sub-types can present with different risk factors, clinical

symptoms, pathological features and response to therapy (***Weigeit et al*, *2010***). Recent microarray technology has allowed sub-classification of invasive breast cancer based on the molecular profile of the disease. Invasive breast cancer can now be categorised as either (1) Luminal A (2) Luminal B (3) Oestrogen and progesterone negative and human epidermal receptor positive (ER-/PR-/HER+) (4) Basal like and (5) Normal Breast-like.

Luminal tumours are the most commonly observed sub-type of invasive breast cancer and are further divided into two separate groups; luminal A and Luminal B. Both are ER/PR hormone receptor positive however, luminal A breast tumours usually have a lower Ki67 count (proliferative index), have a better prognosis as they are usually classified as low/moderate grade tumours compared to luminal B tumours. Luminal B tumours are usually of a higher grade and are lymph node positive (***Eroles et al, 2011***). The third sub-type of invasive breast cancer account for 10-15% of invasive breast cancer cases and are classified as HER2 tumours that are ER/PR hormone receptor negative but HER2 positive, and are usually lymph node positive and have a poorer prognosis compared to luminal breast cancer, with patients more prone to recurrence and metastasis (***Eroles et al, 2007***).Basal like breast tumours also referred to as triple negative breast cancer (TNBC) lack expression of ER, PR and HER2 but are classified as basal like because they express genes that are commonly expressed by basal epithelial cells, such as cytokeratin 5/6 (***Ishihara et al, 2009***). Basal like breast tumours account for 15-20% of invasive cases and characteristically present with an aggressive phenotype and are commonly observed in younger patients. TNBC is one of the most difficult disease states to treat (***Eroles et al, 2011***). The best treatment strategy for basal like carcinomas is targeted systemic chemotherapy (***Ishihara et al, 2009***). The fifth sub-group is the Normal Breast-like tumours; these are the least common type of invasive breast cancer observed, accounting for approximately 6-10% of cases and are small in size and have a good prognosis. The above sub-classification can also be applied to human breast cancer cell lines that are frequently used for research purposes (***Holliday and Speirs, 2011***). The grouping of different breast cancer cell-lines based on the molecular profile is potentially an excellent tool in research to allow identification of therapy for specific breast cancer sub-types that could potentially translate to the clinic.

However the onset of abnormal cell and cancer development is the initial step of the process. It is well understood that once a tumour has established within its primary location, the tumour cells must be able to create a microenvironment in which growth and progress is possible. In order to survive and metastasise, tumours promote the formation of a blood supply (***Amini et al, 2012***). Initially tumours obtain oxygen and nutrients via simple diffusion from neighbouring cells; however, for tumours to grow beyond $2mm^3$ there is a requirement to stimulate the

formation of a new micro-vascular network by a process known as angiogenesis (***Folkman, 1971***).

1.2 Developing the Primary Vasculature

The vascular system is one of the first processes to develop in the embryo, due to its importance in supporting and maintaining all aspects of organ development (***Carmeliet, 2005***). Establishing the primary vasculature in the early embryo occurs through a process known as vasculogenesis, which effectively forms the vasculature network through differentiation of endothelial progenitor cells, haemangioblasts (***Patan, 2004***) Expansion of this primary network is required and occurs through the process of angiogenesis, which is explained in detail in the following section.

1.3 Angiogenesis

Angiogenesis is the formation of new blood vessels from pre-existing vasculature and plays an important role in physiological processes such as wound healing, menstruation and inflammation (***Papetti and Herman 2002***). It is thought that in general living cells are located within 100-200µm of a blood supply (***Carmeliet and Jain 2000***) emphasising the need to maintain a well regulated blood system that will efficiently deliver oxygen and nutrients at the same time as removing waste products from all tissues. Hence as a tissue attempts to grow, the metabolic demands exerted on the system are increased and therefore the vascular network must grow in a concurrent manner to maintain healthy growth of the tissue. This is particularly evident when considering the key role angiogenesis plays in many pathological diseases which are characterised by an increase in cell proliferation such as psoriasis and cancer. Oxygen and nutrients diffuse adequately over a distance of 100-200µm, subsequently for tumours to grow beyond $2mm^3$ in volume they must elicit a vasculature to meet nutritional requirements (***Carmeliet and Jain 2000***).

1. 3.1 Physiological Angiogenesis

Physiological angiogenesis occurs initially during early embryonic development to form a functional vasculature. It is a multistep process that is tightly regulated to maintain physiological integrity of the blood network. There are a number of different stimuli that are capable of inducing angiogenesis, including hypoxia and angiogenic growth factors, one of the most potent being vascular endothelial growth factor (VEGF) (***Ferrara 2004***) (**section 1.3.3**). The initial stage is once an angiogenic stimulus has been received, the de-attachment of pericytes from endothelial cells (ECs) to induce vascular destabilisation of the host vasculature which is thought to be mediated by the actions of angiopoeitin 2 (Ang-2) (***von Tell et al. 2006***).

Then proteases such as matrix metalloproteinases (MMPs) are secreted, which loosen the cell-cell and cell-basement membrane interactions by degrading the adhesion molecules and surrounding matrix (***Papetti and Herman 2002***). The breakdown of the basement membrane and the extracellular matrix (ECM) not only allows EC migration but also causes the release of many pro angiogenic factors that are sequestered within the ECM, thereby increasing the number of circulating pro angiogenic factors such as VEGF ***(Plank and Sleeman 2003*)**. Adhesion molecules including the integrins also play an important role in angiogenesis as they allow ECs to interact with ECM components aiding formation of the sprouting capillary. Integrins also have the ability to transmit signals from the extracellular environment, thus mediating many pro-angiogenic events including promotion of calcium signalling which in turn mediates cell motility ***(Brooks et al. 1994*)** and cell adhesion.

ECs migrate along a concentration gradient towards the chemo-attractant e.g. VEGF and then proliferate, differentiate to form tubes and finally secrete a basement membrane and recruit pericytes to induce vascular stability (***Papetti and Herman 2002***). The process of physiological angiogenesis is subject to tight control whereby the balance between pro and anti-angiogenic factors shifts slightly towards the positive regulators of angiogenesis. Under normal physiological conditions this shift is only transient and it is this crucial difference that distinguishes physiological angiogenesis from tumour induced (or pathological) angiogenesis.

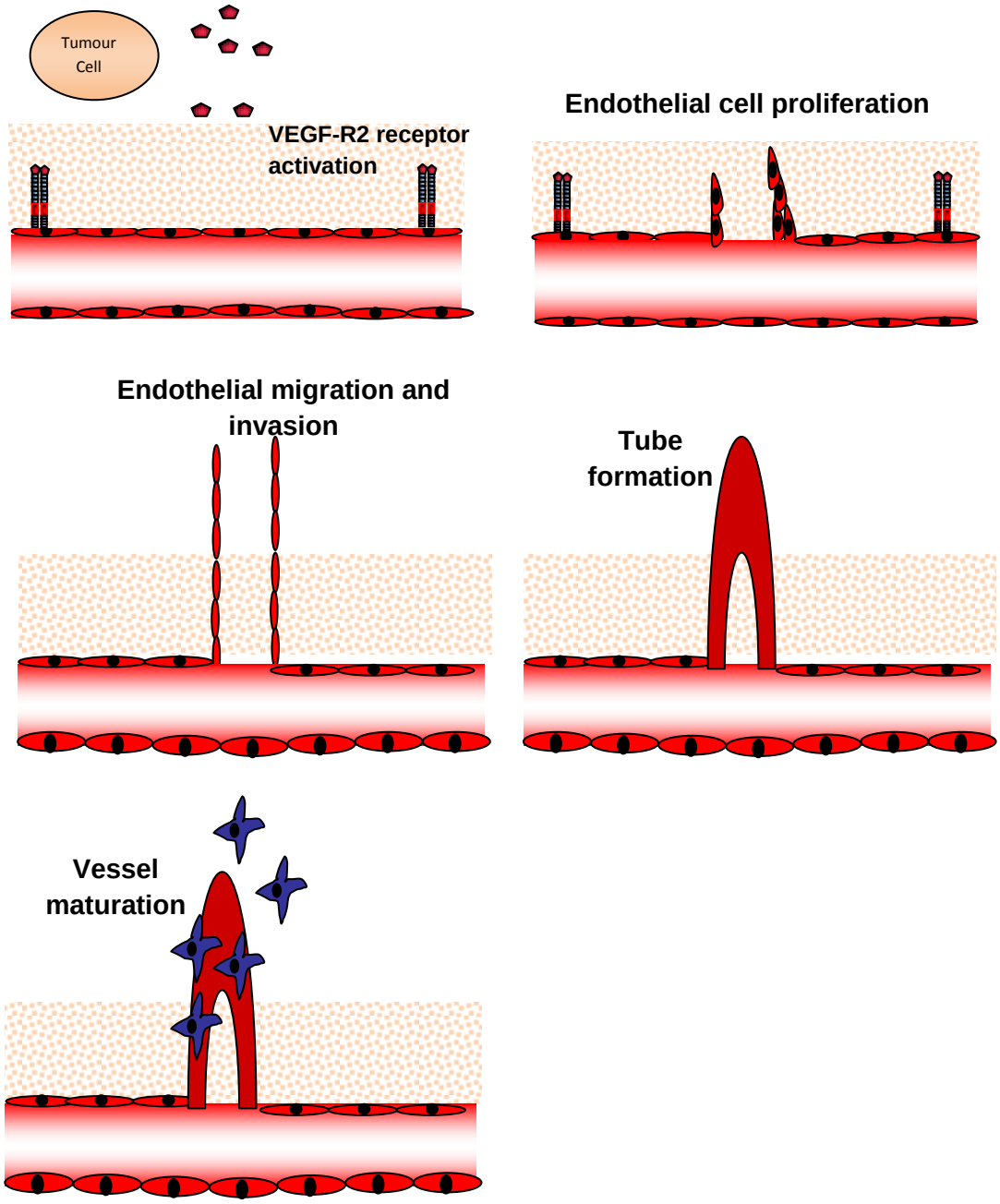

Figure 1.1 The Process of Tumour Angiogenesis:
Tumour angiogenesis is a complex and multi-step process that involves a number of different factors. Tumour cell production and secretion of pro-angiogenic factors such as VEGF can be initiated by a number of factors such as hypoxia. Receptor binding of VEGF leads to the **activation of ECs** and degradation of the vessel wall by proteinases such as MMP1 &2. The degradation of the wall facilitates **EC proliferation**, **directional migration** and **invasion** towards the angiogenic stimulus. ECM remodelling and reorganisation of ECs aid the **formation of tubular vessel structures**. The final stage of the process is **vascular maturation/stabilisation** which is facilitated by the recruitment of pericytes (via the release of PDGF).

Adapted from; Angiogenesis foundation. The angiogenesis process: how do new blood vessels grow? 2009.

1. 3.2 Tumour Angiogenesis

While the process of tumour angiogenesis (**Figure 1.1**) demonstrates some similarities to physiological angiogenesis, there are a number of key differences. The main difference is that during tumour angiogenesis regulatory controls are lost; the shift towards positive regulators is no longer transient and pro-angiogenic signals appear permanently switched on and anti-angiogenic signals are often lost, a process known as the 'angiogenic switch'. Moreover, the tumour vasculature is chaotic and tumour associated capillaries have been shown to have three times greater diameter than normal capillaries ***(Weinberg 2007***). The process of tumour angiogenesis also gives rise to relatively unstable vessels with chaotic and sparse dispersion of pericytes, as well as being approximately 10 times more permeable than normal capillaries (***Morikawa et al. 2002; Weinberg 2007***). This extensive permeability seen within tumour vessels is thought to be due to the up regulation of VEGF which was initially defined as vascular permeability factor (VPF) (***Senger et al, 1983***). Accumulation of fluid that results from extensive leaking can result in high fluid pressure within the tumour mass which makes administration of anti-cancer therapeutic drugs difficult (***Jain 2001***).

The basement membrane of tumour vessels also differs in protein composition, assembly and structure ***(Cao, 2004***) Furthermore there is no hierarchy present within the tumour vasculature as there is no clear distinction between the microvascular components; arterioles, capillaries and venules (***Shojaei and Ferrara 2008***) (**Figure 1.2**). Regardless of the chaotic and unstable nature of the tumour vasculature it does have the ability to provide tumours with the required oxygen and nutrients needed to progress. Interestingly these differences observed between the normal and tumour vasculature could prove beneficial in terms of tumour targeting therapeutics, especially since tumour ECs divide up to 50 times more frequently and express higher levels of specific cell surface molecules such as αVβ3, E-selectin, endoglin, DLL4, Robo4 and VEGF receptor 1 and 2 (***Gasparini et al, 2005***). During tumour angiogenesis the balance of pro-angiogenic versus anti-angiogenic factors shifts to aid tumour progression (**Figure 1.3**) and although there are a plethora of pro-angiogenic factors identified, Vascular Endothelial Growth Factor A (VEGF-A) is the most potent stimulator of tumour angiogenesis identified to date (***Amini et al, 2012; Prager et al, 2012***).

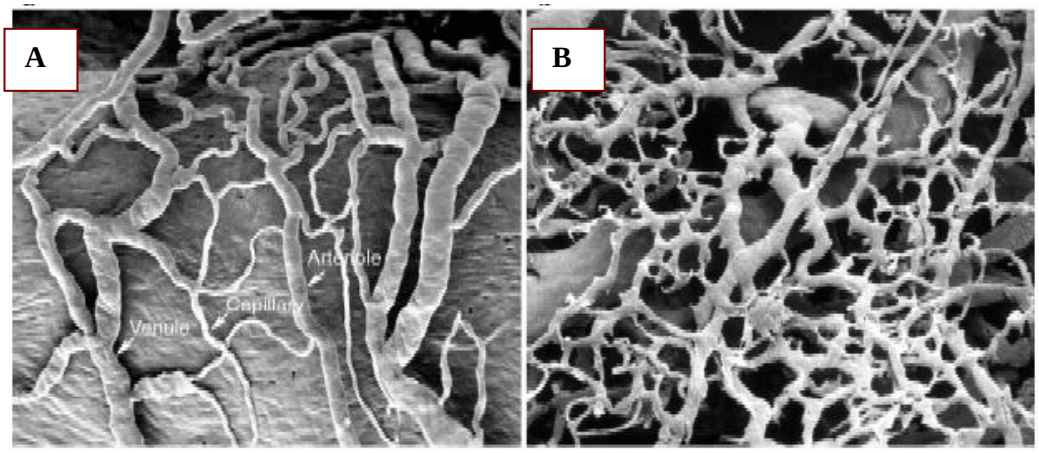

Figure 1.2 ***Differences between Physiological and Pathological Vasculature*:**

(A) Shows the normal physiological blood network, with the different components of the vasculature being distinct and ordered. In contrast (**B**) shows the tumour-associated vasculature, the network has lost order, and distinction between the capillaries, venules and arterioles is difficult. The tumour associated vasculature shows evidence of increased and chaotic sprouting.

Photograph reproduced by kind permission of Professor Donald McDonald. Taken from Imaging of angiogenesis: from microscope to clinic. Nature Medicine 9(6); 713-725 (2003).

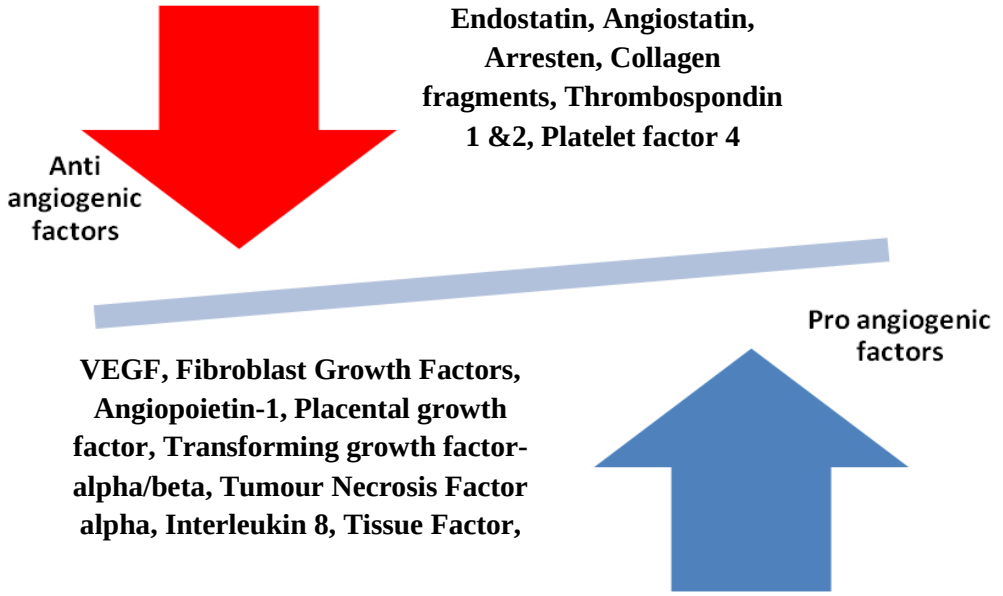

Figure 1.3 ***Factors Involved in Angiogenesis:***
During physiological angiogenesis pro- and anti-angiogenic factors are tightly regulated. However, during tumour angiogenesis, a shift towards the pro-angiogenic factors occurs. This imbalance caused by excessive up-regulation of pro-angiogenic factors causes the 'angiogenic switch' to occur; which in turn allows tumours to assume a vascular phenotype, favouring progression and metastasis.

1.3.3 Vascular Endothelial Growth Factor

Vascular Endothelial Growth Factor (VEGF-A/VEGF) belongs to a family of six structurally related glycoproteins; VEGF-A, VEGF-B, VEGF-C, VEGF-D, viral VEGF-E and placenta growth factor (PLGF). VEGF is a multifunctional cytokine which was initially identified as a vascular permeability factor (VPF) (***Senger, et al. 1983***) and, to date is the most extensively studied pro-angiogenic factor and thought to be the most potent factor involved in physiological and pathological angiogenesis (***Holmes and Zachary 2005***).

VEGF gene and protein structure

The human VEGF gene consists of eight exons that are separated by seven introns and is subject to alternative gene splicing, giving rise to a number of isoforms that differ in amino acid length; $VEGF_{121}$, $VEGF_{145}$, $VEGF_{148}$, $VEGF_{162}$, $VEGF_{165}$, $VEGF_{183}$, $VEGF_{189}$ and $VEGF_{206}$ (***Robinson and Stringer 2001***). The VEGF isoforms differ in their ability to bind heparin sulphates (HSP) on both the cell surface and the ECM and it is this difference in affinity to HSP that determines whether the various isoforms are freely soluble or membrane bound (***Park et al. 1993; Stimpfl et al, 2002***) (**Figure 1.4 and Table 1.1**).

Until recently it was assumed that the different isoforms had similar biological activities, however, it is now becoming apparent that the VEGF isoforms may play distinct roles in tumour angiogenesis (**Table 1.1**) (***Tozer et al, 2008***; ***Akerman et al, 2013***). The ability of the VEGF isoforms to bind ECM is important in the bioavailability of VEGF, to allow creation of a VEGF gradient. Studies have revealed $VEGF_{121}$, $VEGF_{165}$ and $VEGF_{189}$ as the most abundant tumour isoforms of VEGF, with $VEGF_{165}$ being the most characterised in relation to tumour angiogenesis (***Park et al. 1993***). The role of the other VEGF isoforms in cancer progression is however currently under investigation (***Tozer et al, 2008***; ***Akerman et al, 2013***).

The discovery of additional VEGF-A isoforms ($VEGF_{xxxb}$) have also been reported, with some studies suggesting that these so called 'b' isoforms are anti-angiogenic (***Rennel et al. 2008***) however, the role of these isoforms needs to be fully elucidated. $VEGF_{165b}$, *in vitro* binds VEGF-R2 with the same affinity as $VEGF_{165}$, but does not transmit a signal (***Woolard et al. 2004***). The ratio of $VEGF_{xxx}/VEGF_{xxxb}$ present within the tumour micro-environment, could have implications for treatment efficacy as the $VEGF_{xxxb}$ isoforms also bind Bz in addition to $VEGF_{xxx}$ isoforms thus may potentially reduce the efficacy of Bz, if these $VEGF_{xxxb}$ isoforms are truly endogenous anti-angiogenic agents (***Varey et al, 2008***).

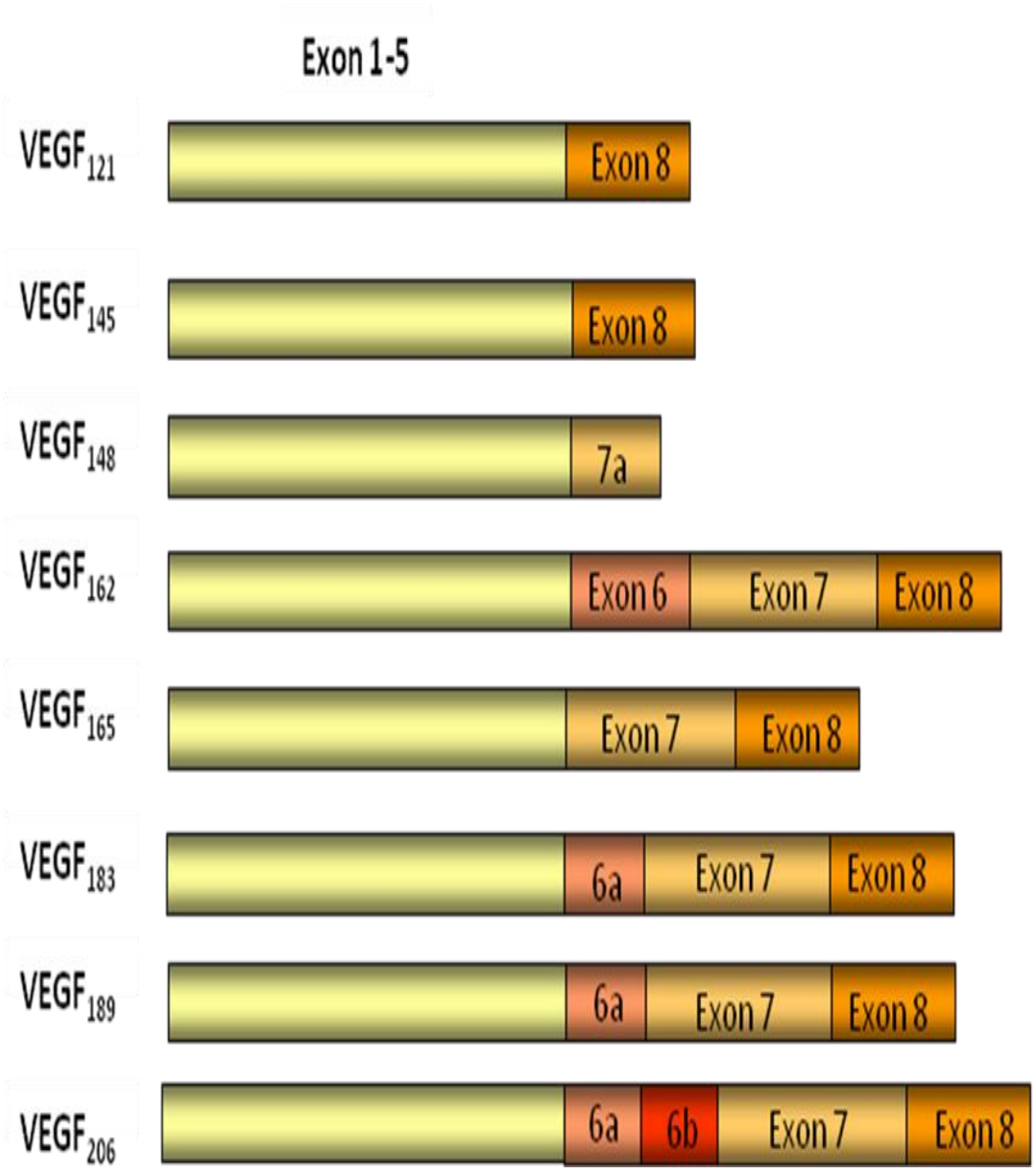

Figure 1.4 Gene Structure of VEGF isoforms:

The figure illustrates the gene arrangement of the eight VEGF isoforms. All eight variants contain exons 1-5. Exons 6-8 determine the binding to HSP and other receptors such as the neuropilins receptors.

Adapted from Shibuya M. (2001) Structure & Function of VEGF/VEGF Receptor System Involved in Angiogenesis. Cell Structure and Function 26: 25-35 & Nowak et al. (2008) Expression of pro-and anti-angiogenic isoforms of VEGF is differentially regulated by splicing and growth factors. J Cell Sci October 15; 121 (Pt 20): 3487-3495

VEGF ISOFORM	HEPARIN BINDING	PROPERTIES
121	No- freely diffusible	▪ Stimulates angiogenesis ▪ Induces breast cancer proliferation (T47Ds) (***Liang et al, 2006***).
145	-	unknown
148	-	unknown
162	-	unknown
165	Yes- intermediate binding affinity thus exists as ECM bound and diffusible form	▪ Potent pro-angiogenic factor ▪ Induces breast cancer proliferation (MDA-MB-231, MCF-7, T47Ds) (***Liang et al, 2006***).
183	-	unknown
189	Yes- strong binding affinity thus is ECM bound	unknown

Table 1.1 Properties of VEGF isoforms:
There is increased interest in the VEGF isoforms and the distinct role played by each one. Research into these isoforms is important in terms of establishing response to anti-VEGF agents such as Bz.

Regulation of VEGF Expression

During early organ development VEGF expression can be regulated by the onset of cellular differentiation, cytokine regulation, hypoxia and tissue remodelling (during the formation of the corpus luteum, wound healing and menstruation) (***Claffey 1996***), with hypoxia being thought of as the major inducer of VEGF expression especially in tumours (***Amini et al, 2012***). Hypoxia or low oxygen tension is a common hallmark of solid tumours and it has been observed that mice deficient in hypoxia inducible factor 1 alpha (HIF-1α) show lower levels of angiogenic activity (***Boudreau and Myers 2003; Hanahan and Weinberg, 2011***). Under normoxic conditions, the HIF-1α subunit undergoes ubiquitination and protesomal degradation via the Von-Hippal Lindau (VHL) protein. However low oxygen tension allows HIF-1α to accumulate to threshold levels and translocate to the nucleus where it binds HIF-1β at the hypoxia responsive element (HRE) in the promoter region of the VEGF gene which leads to subsequent up-regulation of VEGF gene transcription and enhances VEGF mRNA stability (***Jones et al, 2001***) (**Figure 1.5**). Even though hypoxia is major regulator of VEGF expression, it is important to note that a number of tumour cells constitutively express VEGF under normoxic conditions (***Heinzman et al, 2008***) including breast cancer cells (***Marxsen et al, 2001***).

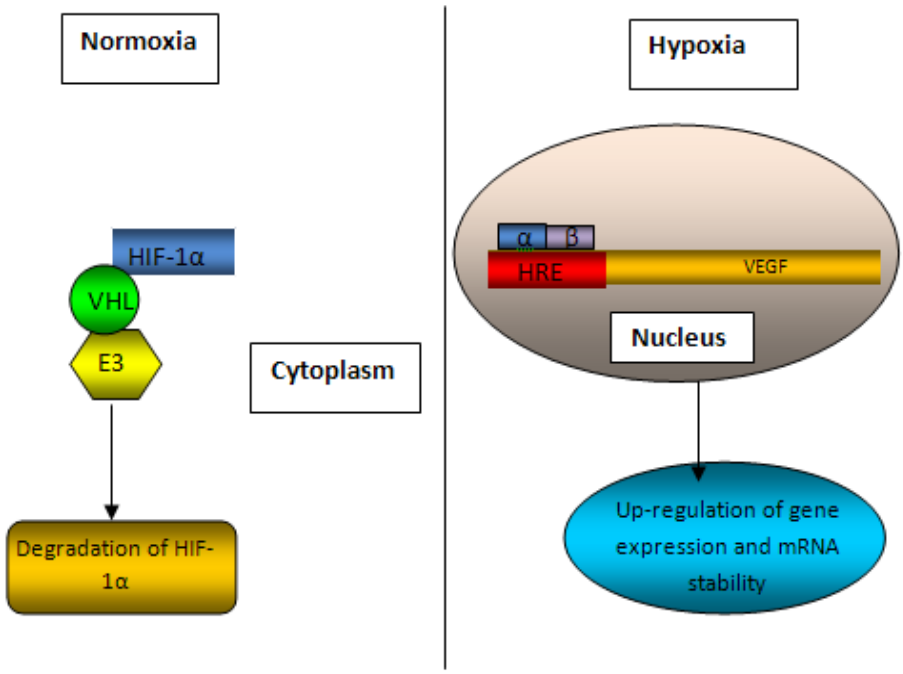

Figure 1.5 ***HIF-1α Regulation of VEGF Gene Expression*****:**
Low oxygen tension is one of the major inducers of VEGF expression. Under normoxic conditions HIF-1α is modified by oxygen dependent prolyl-hydroxylases which allows for binding of the VHL protein to HIF-1α, which in turn results in recognition of the molecule by the E3 ubiquitination-protein ligase resulting in rapid degradation of HIF-1α. Whereas under hypoxic conditions HIF-1α is stable, reaches threshold levels and translocates to the nucleus where it binds to the HRE of VEGF in concordance with the β subunit and enhances VEGF expression.

Adapted from Huang & Bao. (2004). Roles of main pro- and anti-angiogenic factors in tumour angiogenesis. World J Gastroenterol; 15:10463-70

Endothelial Cells and VEGF

VEGF plays a key role in vascular development as knockout a single allele of the VEGF gene results in embryonic lethality at day 11/12 due to vascular impairment ***(Ferrara et al. 1996***). VEGF acts as a permeability factor by inducing an up-regulation of matrix metalloproteases (MMPs) including MMP2, MMP9 and MTI-MMP that allows breakdown of the ECM (***Funahashi et al, 2011***), extravasation of angiogenic factors and induces proliferation and tubule formation of ECs. Experimental data shows that not only does VEGF induce a two-fold increase in human dermal microvascular endothelial cell (HuDMECs) proliferation, but it also protects the ECs from apoptosis *in vitro* (***Nor et al. 1999***) . The latter observation confirms the notion that VEGF also acts as an EC survival factor, up-regulating a number of anti-apoptotic factors such as Bcl2 and A1 (5.2 & 2.7 fold increase respectively) and is important for EC maintenance (***Gerber et al. 1998***). VEGF also acts as a chemotactic factor, inducing migration and stimulating differentiation of ECs which is required for tubular morphogenesis.

1.3.4 VEGF Receptors

VEGF activity is mediated via three transmembrane tyrosine kinase receptors, VEGF receptor 1 (VEGF-R1), VEGF receptor 2 (VEGF-R2) (**Figure 1.6**) and VEGF receptor 3 (VEGF-R3). VEGF-R3 is widely expressed in the early embryonic vasculature but becomes restricted to the lymphatic endothelium in post natal life (***Robinson and Stringer 2001***). Other than EC expression, the profile of both receptors is quite distinct, with VEGF-R1 being found on inflammatory cells such as monocytes and macrophages, osteoclasts, pericytes and trophoblasts in the placenta (***Shibuya & Claesson-Walsh et al, 2006***). Whereas VEGF-R2 is commonly found in osteoblasts, haematopoietic stem cells and megakaryocytes. More recently the neuropilins have been identified as co receptors for VEGF, augmenting signalling through VEGF-R1 and VEGF-R2 and can also act as direct receptors, signalling through intracellular neuropilin interacting protein (NIP) (***Staton et al,2007***).

VEGFR1 (flt-1) is 180kDa in size and binds all forms of VEGF-A, VEGF-B and PIGF (***Robinson and Stringer 2001***). Its role in early development is important as VEGF-R1 null mice die at embryonic day 8.5 due to disorganised vasculature (***Fong et al. 1995***). VEGF-R1 is also present in a soluble form (sVEGFR1), and the presence of sVEGFR1 results in significant reduction in tumour growth *in vivo* (***Goldman et al. 1998***). VEGF-R2 (KDR) is 200-230kDa and binds all VEGF-A isoforms, VEGF-C, VEGF-D and VEGF-E. It is crucial for normal development of the embryonic vasculature as VEGF-R2 knock-out mice are embryonic lethal and display minimal or no vasculature (***Shalaby et al. 1995; Staton 2007***).

Both VEGF-R1 and VEGF-R2 are predominantly expressed on ECs and are similar in structure. The two receptors contain 7 IgG-like extracellular domains, a transmembrane domain, a tyrosine kinase domain (that has a 70 amino acid kinase insert) followed by the C-terminus (***Shibuya & Claesson-Walsh et al, 2006***). The IgG-like domains of VEGF-R1 and VEGF-R2 are responsible for different elements of VEGF receptor binding and signalling. Domain 2 and 3 are responsible for ligand binding, domain 2 and 4 are required for ligand association and domain 5 and 6 are required for retention of bound ligand (**Figure 1.6**). The tyrosine kinase domains of both receptors share approximately 80% homology. Interestingly, the VEGF receptors are thought to differ from the majority of tyrosine kinase receptors (TKRs) as they lack a characteristic YxxM motif within the kinase insert domain, suggesting that the intracellular signalling associated with the VEGF receptors is distinct from other TKRs (***Shibuya, 2010***).

VEGF-R3 (flt-4) is a 195kDa tyrosine kinase receptor for VEGF-C and VEGF-D and in humans exists as two splice variants (***Cross et al, 2003***) (**Figure 1.7).** During embryonic development, VEGF-R3 is expressed on both vascular and lymphatic ECs. Mice lacking VEGF-R3 die at E9.5

due to deficient vessel remodelling, with large vessels exhibiting a disorganised pattern which leads to accumulation of fluid cardio-vascular failure (***Cross et al, 2003***). In adults, VEGF-R3expression is largely restricted to lymphatic endothelial cells and blocking the receptor with soluble VEGF-R3 causes regression of lymphatic vessels and features of lymphoedma but no apparent effects on the blood vasculature (***Cross et al, 2003***) suggesting a potential role for VEGF-R3 in tumour metastasis . Activation of VEGF-R3 by VEGF-C or VEGF-D induces proliferation, migration and survival of lymphatic ECs (***Cross et al, 2003***). Inhibiting VEGF-R3 *in vivo*, demonstrates inhibitory effects on breast cancer induced metastasis to the lymph nodes and the lungs (***Matsui et al, 2008 and Kodera et al, 2011***). As the data concerning VEGF-R3 suggests a role mainly in lymphangiogenesis, the role of this receptor will not be discussed further.

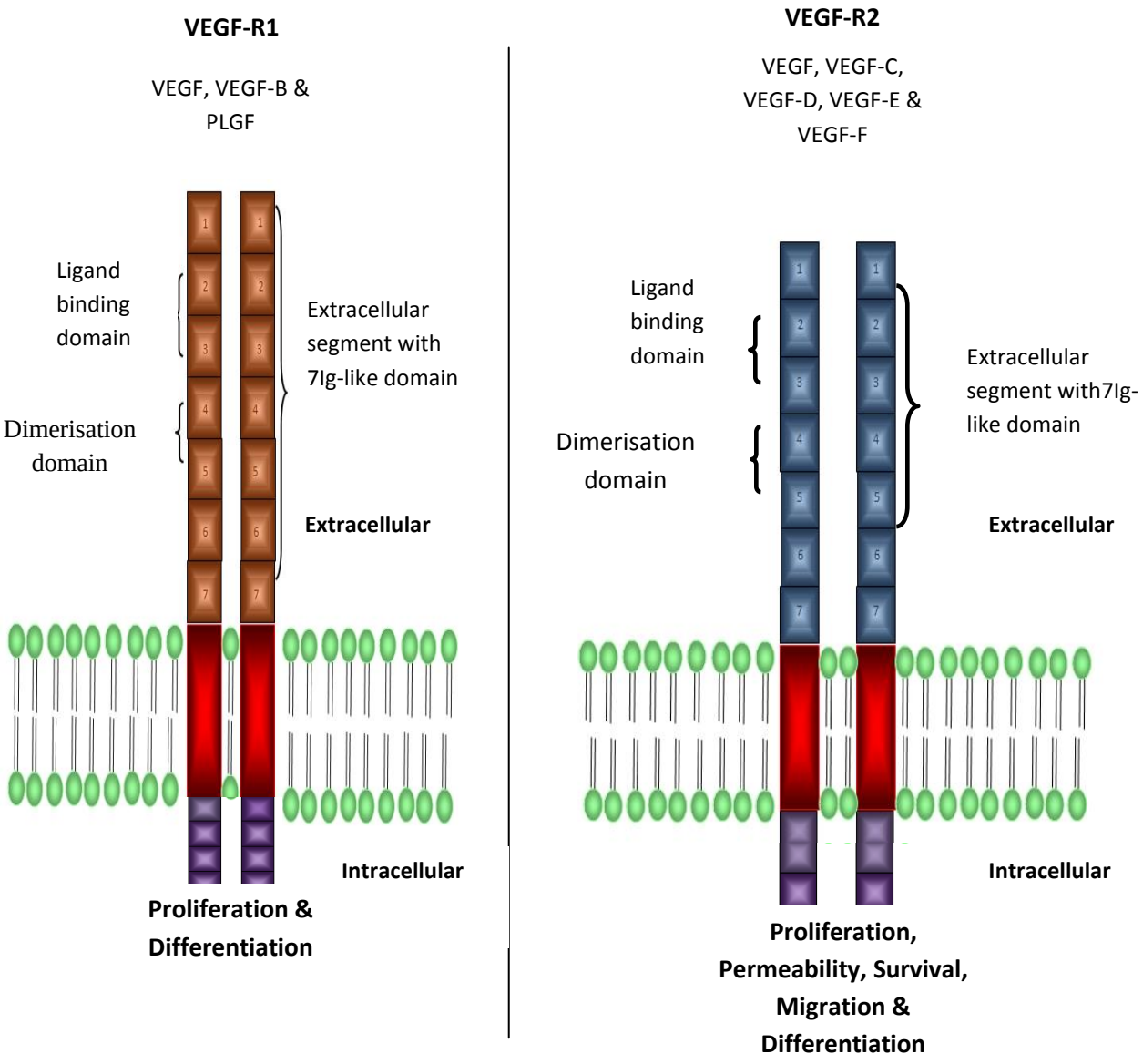

Figure 1.6 ***The Structure of VEGF Receptors 1 and 2:***
VEGF angiogenic activity is primarily mediated via two tyrosine kinase receptors; VEGF-R1 & R2. The structure of the two receptors is similar but the associated signalling differs; VEGF-R2 is considered the predominant receptor for mediating angiogenic signals. Upon ligand binding the receptors dimerise, are autophosphorylated and activate a number of downstream signals leading to the activation of a number of angiogenic processes such as EC permeability, survival and proliferation.

Adapted from; Staton et al (2007). Neuropilins in Physiological and Pathological Angiogenesis. Journal of Pathology; 212:237-248

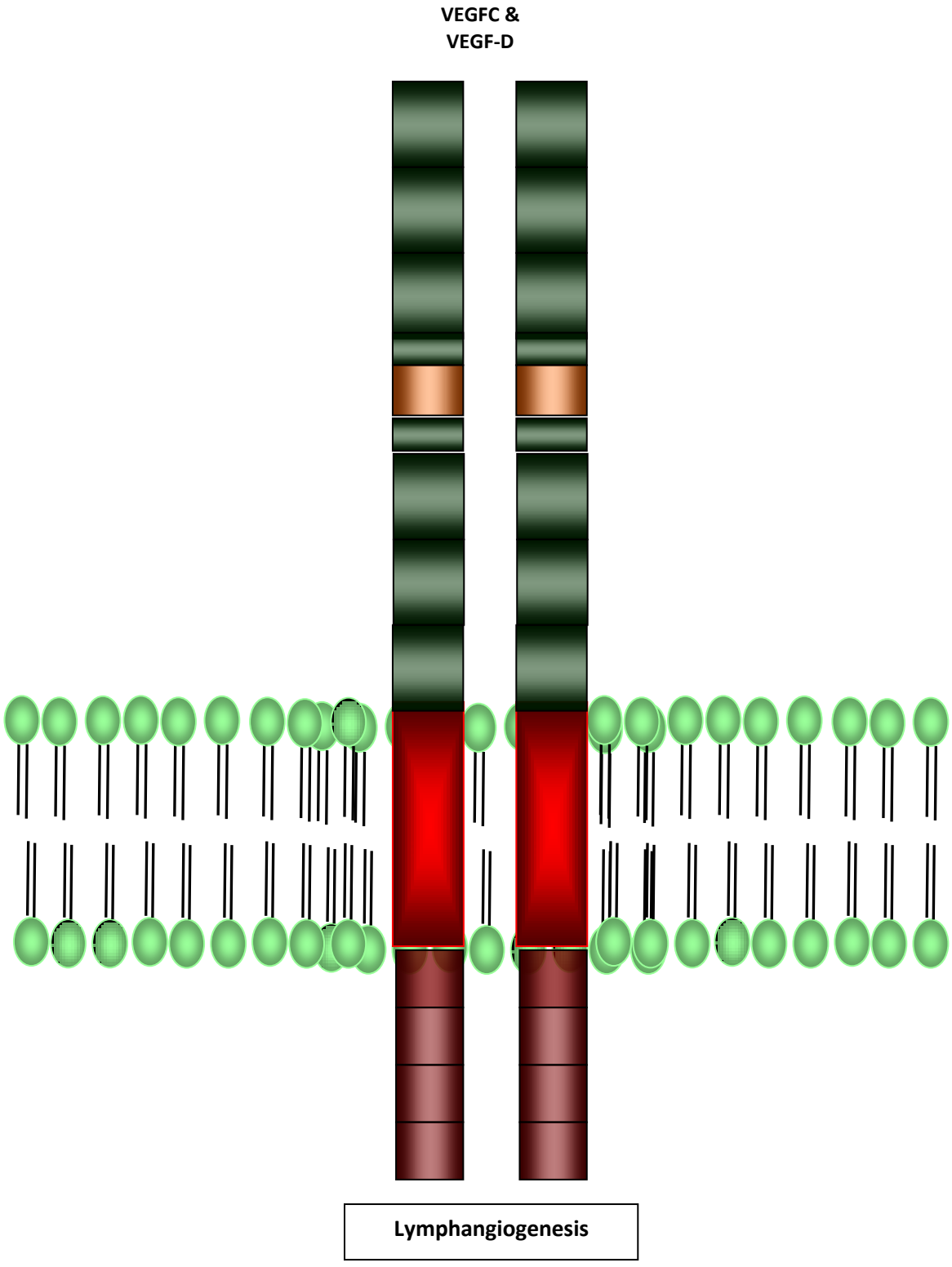

Figure 1.7 ***Structure of Vascular Endothelial Growth Factor Receptors 3.***
VEGF-R3 is thought to play an important role in lymphangiogenesis. It binds to other VEGF family members; VEFG-C and VEGF-D and potentially has an important role in tumour metastasis.

Adapted from Shibuya M. (2001) Structure and Function of VEGF/VEGF Receptor System Involved in Angiogenesis.

1.3.5 Effects of VEGF Receptors on EC function

Upon VEGF binding, VEGF-R1 and VEGF-R2 dimerise and are autophosphorylated which leads to activation of downstream signalling pathways (**Figure 1.6**). VEGF-R1 and VEGF-R2 can form either hetero- or homo dimers with one another (***Guo et al, 2010***).

VEGF-R1

VEGF-R1 is thought to act predominantly as a negative regulator of VEGF activity, with an increased affinity for VEGF ($Kd=1\text{-}10x10^{-12}M$). However, the associated tyrosine kinase activity is thought to be considerably weaker, being approximately, one order of magnitude less than that associated with VEGF-R2 (***Miguel JV 2008*** & ***Shibuya, 2010***).

VEGF-R1 null mice are embryonic lethal and are characterised by the presence of excessive haemangioblasts (***Shibuya, 2010***). The same study assessed the effects of deleting the tyrosine kinase (TK) domain of VEGF-R1 on development and interestingly VEGF-R1 tyrosine kinase null embryos developed normally with no detectable defects. This suggests that the presence of VEGF-R1 is required solely to regulate the availability of VEGF for ECs. However, interestingly, the migration of macrophages towards VEGF is hindered in VEGF-R1 TK null mice (***Fong et al, 1995***) suggesting a potential role for VEGF-R1 in regulating this cell type in the tumour microenvironment, which is potentially important in cancer metastasis and priming the pre-metastatic niche (***Kaplan et al, 2005***; ***Shibuya 2006;***).

Experimental studies identifying the main sites for autophosphorylation on VEGF-R1 are Y1169, Y1213, Y1242, Y1327 & Y1333, with the Y1169 postulated as being responsible for regulating EC proliferation via the downstream activation of phospholipase Cγ (PLCγ) (***Olsson et al, 2006***). However a number of other studies have shown that the interaction of VEGF with VEGF-R1 fails to stimulate EC proliferation (***Waltenberger, 1994; Price et al. 2001***) which may have been due to the models used. These studies, suggest that VEGF-R1 exhibits little or no pro-angiogenic activity which further confirms the negative feedback role that VEGF-R1 has on regulating VEGF activity on ECs.

A number of studies have demonstrated that VEGF-R1 fails to induce porcine aortic endothelial cell (PAE) migration in response to VEGF stimulation *in vitro* (***Waltenberger et al, 1994; Gille et al, 2000***). Interestingly, when chimera VEGF receptors were constructed so that VEGF-R1 contained the intracellular juxtamembrane region of VEGF-R2 and vice versa, the ability of VEGF-R1 chimera to transduce VEGF mediated PAE migration was dramatically enhanced. A VEGF-R2 chimera that contained the intracellular domain of VEGF-R1 failed to induce the typically observed VEGF-mediated PAE cell migration *in vitro,* suggesting that a sequence within the intracellular domain of VEGF-R2 is vital for EC migration (***Gille et al, 2000***). The

juxtamembrane region appears to be highly conserved between the two receptors; however a sequence of three serine residues in the juxtamembrane region of VEGF-R1 that is not present in VEGF-R2 appears to be responsible for the lack of PAE migration observed in the presence of VEGF/VEGF-R1 interactions. Replacing the three serine residues with the corresponding sequence in VEGF-R2 (ANGG) or removing the serine sequence completely, results in VEGF-R1 mediated PAE migration *in vitro*, comparable to migration observed in wild type VEGF-R2. (***Gille et al, 2000***).

From the studies utilising the different VEGF receptor chimeras and mutants it appears that PLCγ activation is not required for PAE cell migration *in vitro* since the VEGF-R1 mutants with mutated intracellular sequences stimulate PAE cell migration but do not activate PLCγ (***Gille et al, 2000***). The role of VEGF-R1 as a regulator of VEGF signalling in endothelial cells is further confirmed in studies whereby VEGF-R1 inhibits both PAE and HuVEC cell proliferation induced by VEGF-R2 (***Zeng et al, 2001***). This inhibition is not due to VEGF-R1 sequestering VEGF or due to the formation of VEGF-R1/2 hetero-dimers but is a result of PI-3K signalling.

In contrast however, other studies have suggested a role for VEGF-R1 in promoting tumour angiogenesis. VEGF-R1 appears important in VEGF-mediated tissue factor (TF) production in PAE cells expressing VEGF-R1 (***Zeng et al, 2001***). Quantification of the response to an anti-VEGF-R1 antibody on HuVEC tube formation in a co-culture assay, demonstrated that inhibiting $VEGF_{165}$/VEGF-R1 reduced *in vitro* tube formation, using several different parameters including total tube length and capillary connections, however, VEGF-R1 inhibition induced tube thickness (***Bussolati et al, 2001***). These studies provide evidence that VEGF-R1 has a wider portfolio of responses than simply regulating VEGF-mediated EC activity. The role that VEGF-R1 plays in vascular biology needs further investigation, as therapies targeting the VEGF-R1 pathway, must consider the dual role of this receptor and thus design VEGF-R1 inhibitors accordingly.

VEGF-R2

The role of VEGF-R2 signalling in tumour angiogenesis is well recognised with a large body of evidence suggesting that VEGF-R2 is involved in a diverse range of EC functions, including EC migration, survival, differentiation, proliferation and vascular permeability (***Olsson et al, 2006***). Over the years a number of key tyrosine residues have been identified as important in mediating VEGF/VEGF-R2 signals, these include Y951, Y1054, Y1059, Y1175 and Y1214 (***Shibuya 2006***). Phosphorylation at the 1175 tyrosine residue appears vital for VEGF-R2 function, as a mutant mouse model lacking the Y1175 residue was found to be embryonic lethal (E.9) due to a lack of angiogenesis, displaying a phenotype similar to that observed in the VEGF-R2 null mouse (***Sakurai et al, 2005***). In addition, downstream activation of PLCγ-1 subsequent to

Y1175 phosphorylation induces EC mitogenesis (***Cebe-Suarez et al, 2006***). Vascular permeability was the first function of VEGF to be identified and is partly regulated by VEGF-R2 (***Olsson et al, 2006***).

VEGF-R2 signalling is important in the differentiation of vascular endothelial cells, as demonstrated by assessing the ability of HuVEC to undergo tubular morphogenesis (*in vitro*). VEGF mutants with varying capacity to bind either VEGF-R1 or R2 were constructed and their ability to induce the tubular structure formation in a 3D collagen gel HuVEC assay was assessed (***Yang et al, 2001***). Wild type VEGF in addition to the mutant VEGF is selective for VEGF-R2 induced HuVEC cell differentiation *in vitro* with no comparable observations in the presence of the VEGF-R1 selective VEGF mutant suggesting that VEGF-R2 and not VEGF-R1 is required for VEGF induced HuVEC differentiation (***Yang et al, 2001***). This was confirmed in a follow up experiment whereby wild type VEGF was pre-incubated with a VEGF-R1 or R2 antibody prior to adding to the 3D assay. Inhibiting VEGF/VEGF-R2 interactions resulted in a dramatic decrease in the average tube length (microns) compared to the control and the anti-VEGF-R1 treated cells, which was thought to be via alterations of MAPK and p38 signalling (***Yang et al, 2001***).

VEGF-R2 is also important in $VEGF_{165}$ (VEGF-A isoform) induced endothelial cell proliferation as suggested by a number of different studies (***Bernatehez et al, 1999***; ***Cai et al, 2006***; ***Olsson et al, 2006***). PAE cells were incubated with $VEGF_{165}$ (0-100ng/ml) for 24 hours after which [^{3}H] thymidine incorporation was measured. PAE cells transfected with VEGF-R2 showed increased cell proliferation in the presence of $VEGF_{165}$, with no stimulatory effects using the control PAE or the VEGF-R1 transfected cells (***Waltenberger et al, 1994***).

The *in vitro* regulation of VEGF mediated EC proliferation by VEGF-R2 is thought to be enhanced in the presence of cell adhesion molecules. Adherent HuVECs have increased VEGF-R2 phosphorylation after $VEGF_{165}$ stimulation (10 min at 10ng/ml) compared to HuVECs in suspension (***Soldi et al, 1999***). HuVECs plated on vitronectin, a ligand for $\alpha_v\beta_3$ showed the greatest level of VEGF-R2 phosphorylation *in vitro* and which resulted in enhanced functional activity; HuVECs plated on vitronectin and fibrinogen (ligands for $\alpha_v\beta_3$) resulted in enhanced cell proliferation compared to cells plated on other ECM molecules such as fibronectin and collagen (***Soldi et al, 1999***).

VEGF-R2 has also been implicated in mediating VEGF stimulated cytoskeletal reorganisation and migration. PAE cells transfected with VEGF-R2 and HuVECs induced changes in cell shape in the presence of $VEGF_{165}$ (exposure to 100ng/ml for 2-20mins) as measured by the level of cytoplasmic protrusions and membrane ruffling with no morphological changes observed in control PAE or PAE/VEGF-R1 transfected cells exposed to $VEGF_{165}$, suggesting that $VEGF_{165}$

induced endothelial cell migration is mediated via VEGF-R2 (***Waltenberger et al, 1994***). When these cells were utilised in a modified Boyden chamber assay, the VEGF-R2 transfected PAE cells demonstrated increased migration towards $VEGF_{165}$ compared to the full media control (***Waltenberger et al, 1994***).

There are a number of different mechanisms by which VEGF-R2 is thought to mediate VEGF induced EC migration. VEGF/VEGF-R2 interactions result in the activation of Rho small GTPases (***Lamalice et al, 2007***). VEGF-R2 activation leads to the activation of Cdc42, which is involved in the formation of filopodia. Phosphorylation of Y951 and nitric oxide are also thought to be important regulators of VEGF-R2 mediated EC migration (***Lamalice et al, 2007***).

VEGF-R2 migration of HuVEC cells may also be dependent on the urokinase receptor (uPAR) (***Prager et al, 2004***). The number of focal adhesions after $VEGF_{165}$ (50ng/ml for 2h) stimulation increased by ~ 2.5 fold, with the number of uPAR positive focal adhesions also increasing. This re-distribution of uPAR at focal adhesions was mediated via VEGF-R2 since the VEGF-R1 specific ligand, PIGF did not increase uPAR positive focal adhesions whereas VEGF-E, a specific ligand for VEGF-R2 did. Interestingly, the number of focal adhesions formed after PIGF treatment was similar to that observed with both $VEGF_{165}$ and VEGF-E treated cells suggesting that the induction of uPAR is not required for the formation of focal adhesions in VEGF-R1 mediated migration (***Prager et al, 2004***). When uPAR expression was inhibited, the migration of HuVECs towards VEGF-E was blocked suggesting that VEGF-R2 mediated HuVEC migration is dependent on the presence of uPAR within focal adhesion formed at the leading edge of these cells.

VEGF-R2 is likely to be an important mediator of EC survival via activation of the PI3K and Akt pathways. HuVEC cells serum starved for 4 days in the presence or absence of wildtype $VEGF_{165}$ or $VEGF_{165}$ mutants selective for binding to either VEGF-R1 or VEGF-R2, demonstrated that VEGF-R2 selective mutants induced a survival effect on HuVEC cells *in vitro* that was similar to the wildtype VEGF control, with no discernable survival activity observed in the presence of the VEGF-R1 mutants (***Herber et al, 1998***). HuVECs were then incubated with a PI3K specific inhibitor (wortmannin, 2h prior to serum starvation) in the absence of $VEGF_{165}$ for 24-36h, after which FACS analysis was performed. The presence of wortmannin resulted in a loss of cell survival activity, suggesting that the initial anti-apoptotic effects observed on HuVEC cells by $VEGF_{165}$ was a result of downstream PI3K activation. The addition of $VEGF_{165}$ to the HuVEC cells incubated with wortmannin resulted in a slight 'rescue' effect, suggesting the importance of VEGF in this VEGF/VEGF-R2/PI3K signalling loop (***Herber et al, 1998***). VEGF-R2 mediated EC survival is also thought to be enhanced in the presence of certain intergrins, as when $\alpha_v\beta_3$ interacts with VEGF-R2, downstream Akt activity is

increased (***Soldi et al, 1999***). Activation of the PI 3-kinase/Akt by VEGF-R2 is also important for EC survival. A study found that VE-cadherin was integral in mediating VEGF-R2 survival signals when in a complex with VEGR-R2, PI 3-kinase and β-catenin, since loss of VE-cadherin resulted in EC apoptosis (***Cebe-Suarez et al, 2006***).

Upon ligand binding, VEGF-R1 and VEGF-R2 can form both homo and heterodimers, with the resulting downstream signalling properties in ECs varying (***Huang et al, 2001***). Interestingly, VEGF induced migration of PAE cells (after 4h in the Boyden chamber) was significantly ($p<0.05$) more efficient when VEGF-R1 and VEGF-R2 heterodimers were formed compared to VEGF-R2 homodimers (***Huang et al, 2001***). With increasing evidence a role for VEGF-R1, studies utilising VEGF-R1 and R2 heterodimers, may provide more information about which VEGF induced signalling pathways/functions in EC overlap between the two receptors and which are more specific. One such study, using a ligand that binds only the heterodimer form of the VEGF receptors was constructed and demonstrated that EC migration, tube formation and NO mediated vasorelaxation was induced by the ligand to levels comparable with those observed with VEGF and VEGF-E alone (***Cudmore et al, 2012***).

Overall, the VEGF/VEGF receptor signalling pathway is complex and induces the activation of various downstream signalling pathways which are summarised in **Figure 1.8.** This complex network of downstream signalling needs to be taken into account when designing inhibitors that target the angiogenesis pathway.

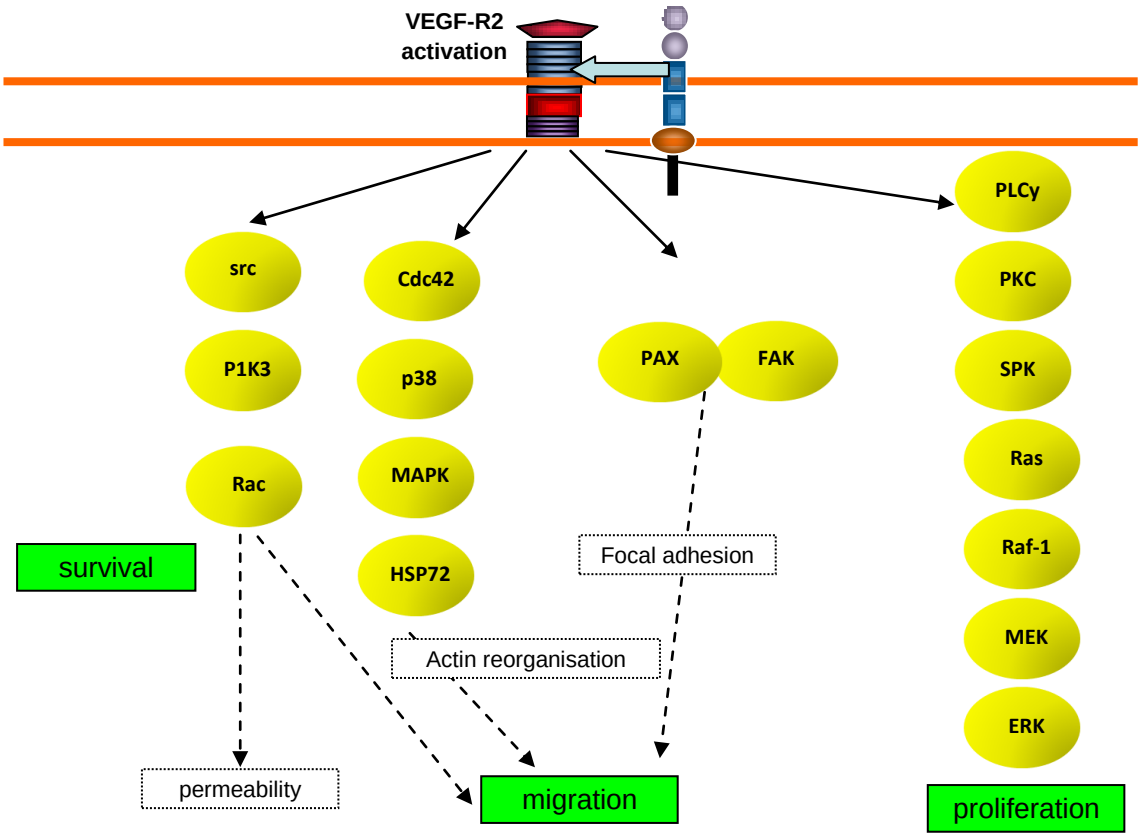

Figure 1.8 VEGF Signalling Pathway:
The VEGF signalling pathway way involves the interplay of a number of downstream effectors. Upon VEGF binding, VEGF-R2 is activated. This in turn phosphorylates major effectors such as PLCy, FAK, p38 and Akt, which results in EC apoptosis, migration and proliferation.

Adapted from SABiosciences. VEGF signalling pathway. (www.SABiocsciences.com)

1.3.6 VEGF- Expression and Role in Breast Cancer

VEGF has a large array of effects on EC function which were initially thought to be EC-specific. However more recently, it had been demonstrated that VEGF has effects on and is produced by breast cancer cells. These observations have been investigated in both an *in vivo* setting and *in vitro* and are explored in the following sections.

Breast Tumour Samples

VEGF tissue expression under physiological conditions is relatively low in comparison with tumour tissue; tumour tissue is thought to express approximately 7-fold higher than the surrounding normal tissue (***Price et al, 2001***). Moreover, necrotic tumours express high levels of VEGF mRNA in hypoxic regions that are adjacent to the necrotic to stimulate angiogenesis in these areas (***Prudence, 1998***). Increased expression of VEGF has been demonstrated in many human tumours, including breast (***Anan 1996; Gasparini et al. 1997***). The association of VEGF

expression with clinically relevant factors (diagnostic and prognostic features) is important and has been investigated (***Fuckar et al, 2006***). VEGF expression is often linked to an increase in micro-vessel density (MVD- a surrogate measure of angiogenesis), tumour size and advanced disease stage along with shorter survival ***(Guetz, et al. 2006***), suggesting that VEGF expression is associated with a more aggressive tumour phenotype. Correlation between VEGF expression in 233 breast cancer tissue samples with a number of key prognostic factors of breast cancer have been evaluated (***Fuckar et al, 2006***). Of the 233 patient samples tested, 222 were positive for cytoplasmic VEGF staining; however, intensity of staining was variable, potentially reflecting the heterogeneous nature of breast cancer, suggesting that not all cells within the same tumour are responsive or as susceptible to anti-VEGF therapy, making treatment difficult. In this cohort of patient samples, no correlation was observed between VEGF expression and (a) tumour size, (b) histological grade, (c) vascular invasion, (d) lymph node status, (e) Ki67 expression, (f) PR status and (g) HER-2 expression. However, a significant inverse correlation between VEGF expression and ER status was observed, with ER negative samples showing greater VEGF expression (***Fuckar et al, 2006***).

Another study demonstrated the use of VEGF as a predicative marker for relapse-free survival and overall survival in patients with invasive breast cancer (***Linderholm et al, 2000***). VEGF expression has also been demonstrated to positively correlate with HER2/neu expression in both node negative and node positive breast tumour samples (***Konecny et al, 2004***). A more recent study evaluating the prognostic and predicative value of VEGF mRNA in 308 patients with high-risk operable breast cancer, demonstrated a significant association of high VEGF expression with negative ER/PR status, a positive HER2 status, high histological grade (III-IV), no adjuvant hormonal therapy, higher age and post-menopausal status (***Linardou et al, 2012***), this contrasts to previously reported IHC data (***Fuckar et al, 2006***) which demonstrated no correlation with the majority of parameters described in the ***Linardou et al, 2012*** paper. The technique used to assess the prognostic role of VEGF in breast cancer patients differ between groups, as ELISA, RT-PCR and IHC analysis have been carried out. Currently, the majority of studies assessing the value of VEGF as a predictive marker in breast cancer report conflicting data. Thus, to date the use of VEGF as a routine prognostic marker in breast cancer remains to be fully determined as to date there is no consistent data that correlates VEGF expression with routinely used clinical markers.

Breast Cancer Cell Lines

VEGF expression is evident in a number of breast cancer cell lines tested. *In vitro* studies have shown that VEGF is a potent survival factor for metastatic breast cancer cells (MDA-MB-231), such that when VEGF is depleted from the cells and the medium, the presence of other factors in the serum is not sufficient to fully rescue the apoptotic effects observed in the absence of VEGF (***Bachelder et al, 2001***). The advantage of using an *in vitro* system is that this allows the direct functional effects of VEGF on the breast cancer cells to be investigated, without other external influences.

VEGF has also been shown to stimulate proliferation of a range of breast cancer cells *in vitro* (including MCF-7 and MDA-MB-231*)* (***Liang et al, 2006***). A range of VEGF concentrations (0-200ng/ml) were evaluated and demonstrated that the rate of proliferation of a high and low metastatic breast cancer cell line (MDA-MB-231 and MCF-7 respectively) both increased in response to VEGF but reached a saturation point (100ng/ml & 50ng/ml respectively) after which proliferation decreased (***Liang et al, 2006***). The T47Ds which are a non-metastatic breast cancer cell line in contrast, continue to grow in an exponential manner in response to all VEGF doses. This is not surprising as it is thought that once a tumour has established itself, it potentially becomes less dependent on the actions of VEGF for progression and other cytokines may begin to play a greater role and this may be reflective in the more aggressive breast cancer cell types. Another explanation is that MDA-MB-231 and MCF-7 cells have higher levels of endogenous VEGF than the T47Ds, resulting in saturation levels of VEGF to be reached more rapidly, compared with those breast cancer cell lines that have low constitutive expression levels of basal VEGF.

1.3.7 VEGF Receptor- Expression and Role in Breast Cancer

Breast Cancer Patient Samples

Up-regulation of the VEGFR2 has been demonstrated in some tumour tissue samples. The expression pattern of VEGF/VEGFR2 was analysed using IHC in tumour tissue from 102 breast cancer patients (***Rydén et al. 2003***). VEGF/VEGFR2 staining correlated significantly (p=0.005) and was co-expressed in the tumours. Interestingly VEGFR2 expression was only associated with histological grade (p=0.002) whereas VEGF expression was associated with both histological grade (p=0.003) and tumour size (p=0.022). It is also worth noting that neither VEGF nor VEGFR2 expression was associated with hormone receptor status, node status or tumour stage (***Rydén et al. 2003)*** suggesting that expression of VEGF and its receptor may not be reliable prognostic markers of disease progression.

A study comprising of 642 primary breast cancer samples aimed to investigate the expression profile of VEGF and its receptors VEGF-R1/2 and to determine if there was any correlation between the expression patterns and patient outcome (***Ghosh et al, 2008).*** VEGF and its receptors were mostly expressed within the membrane/cytoplasmic regions of the tumour. The patient data revealed a significant (p=<0.001) association of high VEGF and VEGF-R1/2 expression with poor survival rates (***Ghosh et al, 2008)***. However, there was insufficient data regarding treatment of all the patients, thus treatment-specific effects on VEGF and receptor expression and patient outcome could not be evaluated. Despite high levels of VEGF being associated with poor survival, the use of VEGF as a marker in response to anti-vascular therapy such as Bz, has yet to be established (***Ghost et al, 2008***).

Breast Cancer Cell Lines

VEGF receptor expression in human breast cancer cell lines is somewhat controversial with data showing the presence of either one or both VEGF receptors whilst other studies have failed to determine any expression at all. One group demonstrated that the metastatic MDA-MB-231 breast cancer cells expressed VEGF-R2 but not VEGF-R1 mRNA whereas the low metastatic MCF-7 and the non-metastatic T47D breast cancer cell lines expressed both VEGF-R1/2 mRNA. A critical question that arises from VEGF-R1 and VEGF-R2 expression profiling in breast cancer cells, is that when (and if) the receptors are present, do they play a functional role in breast cancer cell activity and behaviour.

VEGF-R1

VEGF-R1 in breast cancer cells appears to be predominantly expressed internally, localised within the nuclear envelope of MDA-MB-231 and MCF-7 breast cancer cells (***Lee et al, 2007***). VEGF-R1 has been shown to play a role in autocrine survival of MDA-MB-231 and MCF-7 breast cancer cells *in vitro* potentially through activation of the Akt pathway (***Lee et al, 2007***). VEGF-R1 also appears important in MDA-MB-231 tumour growth *in vivo* (***Lee et al, 2007***). Interestingly, only siRNA knock down of VEGF-R1 inhibited breast cancer cell proliferation and survival, whereas VEGF antibodies or addition of soluble VEGF-R1 had no inhibitory effects. This suggests that the role that VEGF/VEGF-R1 play in breast cancer survival appears to be internally regulated (***Lee et al, 2007***) and inhibitors that target cell surface VEGF-R1 may not be therapeutically effective.

Interestingly, a study published a year prior to the one detailed above investigated the effects of a human VEGF–R1 neutralising monoclonal (mAb 6.12) on a range of breast cancer cell lines and demonstrated inhibition of the activation of Akt in BT-474 breast cancer cells when stimulated with either VEGF or PIGF (***Wu et al, 2006***) whereas no activation of Akt via the

VEGF-R1 pathway was observed in MCF-7, DU4475 and MDA-MB-231 breast cancer cells. This suggests significant heterogeneity amongst breast cancer cell lines, with differential activation of VEGF receptor pathways. Targeting VEGF-R1 in breast cancer appears to be an effective target as the VEGF-R1 specific mAb 6.12 significantly inhibited xenograft tumour growth of a number of breast cancer cell lines (DU4475, BT-474, MCF-7 and MDA-MB-231) *in vivo*. This further suggests that the role of VEGF-R1 in tumour biology has greater significance than initially thought (***Wu et al, 2006***).

More recently a family of intracellular VEGF-R1 receptors have been identified. The intracellular VEGF-R1 receptors appear to have a role in MDA-MB-231 breast cancer cell invasion *in vitro* possibly through activation of the Src pathway (***Mezquita et al, 2010***). In addition, there is also evidence suggesting that VEGF-R1 signalling associated with PIGF ligand stimulation is important in the autocrine effects of VEGF-R1 on breast cancer cells, such as *in vitro* proliferation (***Wu et al, 2006***).

VEGF-R2

VEGF-R2 signalling is important in breast cancer cell activity, especially since VEGF-R2 appears constitutively active, even in the absence of exogenous VEGF (***Lee et al, 2007***). Treatment of T47D and BT-474 breast cancer cells with a VEGF-R2 specific antibody (2C3) and a tyrosine kinase inhibitor (SU1498) for 72h resulted in decreased cell proliferation of both breast cancer cell lines *in vitro* compared with the VEGF alone treated cells (***Liang et al, 2006***). VEGF-R2 signalling is important for tumour survival of both ER positive MCF7 and ER negative MDA-MB-468 breast cancer cells lines (***Aesoy et al, 2008; Svensson et al, 2005***). In addition, VEFG-R2 signalling plays a role in tamoxifen resistance (***Aesoy et al, 2008)*** which is thought to occur by increased breast cancer cell proliferation (***Qu et al, 2008***), which is induced by the interplay between VEGF and VEGF-R2, which subsequently activates the p38 signalling pathway (***Aesoy et al, 2008***).

Overall VEGF-R2 is a critical receptor in VEGF-mediated EC activity, but less is known about any role in breast cancer cell activity. There is a larger body of evidence for a direct role of VEGF-R1 in breast cancer cell activity *in vitro* suggesting that the role of both classical VEGF receptors need to be considered when targeting different aspects of the VEGF pathway in breast cancer therapy (i.e. epithelial vs. endothelial cells).

The classical VEGF receptors demonstrate a functional role on breast cancer cell activity. However, there is minimal literature available regarding the autocrine role of these receptors on breast cancer cells compared with vascular endothelial cells biology. This is not surprising as initially, the role of VEGF-R1 and VEGF-R2 was almost exclusively thought to be on

endothelial cells. In addition to this, the identification of the neuropilins, a second family of VEGF receptors, suggests that these alternative receptors may play a more direct role in VEGF-mediated breast cancer activity.

VEGF-R2 inhibition effectively reduces breast cancer growth in an MDA-MB-231 orthotopic model, with significant ($p<0.05$) inhibition by 2C3 (100μg three times weekly) after 20 days of treatment compared to control IgG treated animals (***Zhang et al, 2002***). 2C3 is a monoclonal mouse anti-human antibody that prevents VEGF interacting with VEGF-R2 but not VEGF-R1. The group suggested that the inhibition in MDA-MB-231 breast cancer growth was a result of direct vascular effects of 2C3, since a ~70% decrease in tumour microvessel density (MVD) was observed with 2C3 treated tumours and when the MVD data was plotted against the percentage tumour growth inhibition in individual mice a linear correlation was observed ($R=0.82$) (***Zhang et al, 2002***). Targeting VEGF-R2 with 2C3 caused a reduction in the tumour microvessel number with larger diameter vessels, but very few capillaries found in deeper tumour regions (***Zhang et al, 2002***) and only a few vessels in central regions of the tumours, with the tumour edges demonstrating the most expansive areas of vascularisation. Inhibition of VEGF-R2 also reduced the number of metastatic colonies formed in the lung (77 vs. 157 colonies) and lung weight (0.18g vs. 0.24g), six weeks after intra-venous injection of MDA-MB-231 breast cancer cells compared to the IgG control respectively. These studies suggest that VEGF-R2 is important in some aspects of the metastatic process in breast cancer.

Another study investigated the DC101 murine VEGF-R2 antibody (***Franco et al, 2006***). MDA-MB-231 breast cancer cells were implanted into the mammary fat pad of CB-17 severe combined immunodeficiency (SCID) and then treated with DC101 (800μg/mouse) twice weekly or a PBS control for 3 weeks (***Franco et al, 2006***). Treatment with DC101 resulted in a significant ($p<0.001$) decrease in MDA-MB-231 growth (65%) compared to the PBS treated group (***Franco et al, 2006***). The group reported (although data was not shown) that DC101 had no inhibitory effects on MDA-MB-231 breast cancer cell proliferation or survival *in vitro*. This result is not surprising as DC101 is an antibody that only recognises murine VEGF-R2 and since MDA-MB-231 breast cancer cells are of human origin, no direct effects on these cells is expected. However, this is an important study suggesting that inhibition of VEGF-R2 alone, can exert significant inhibitory effects on breast cancer growth, via an anti-angiogenic mechanism. This was confirmed when microvessel density (MVD) analysis demonstrated a decrease in CD31 positive vessels in the DC101 treated tumours compared to controls. Treatment with DC101 also resulted in more extensive hypoxia in treated tumours (***Franco et al, 2006***). This is an interesting finding, and might partially explain why resistance to anti-angiogenic therapy occurs, since hypoxic regions tend to harbour cells with a more aggressive and resilient phenotype.

DC101 appears to exhibit effects that are widespread and not confined to the tumour microenvironment as suggested by a study investigating the effects of anti-VEGF treatment on VEGF induced cancer associated systemic syndrome (CASS) (***Xue et al, 2008***). Over-expression of VEGF by tumours can lead to defective vasculature in 'healthy' organs and result in CASS, which is characterised by a number of different clinical features including, defective haematopoiesis, endocrine system, ascites, gastrointestinal track disorders and impaired liver, spleen and kidney function (***Xue et al, 2008***). A spontaneous breast cancer murine model, MMTV*neu* was utilised in this study along with xenografts of other cancer types. Treatment with DC101 (800µg/mouse i.p.) commenced when MMTVneu tumours reached approximately $1cm^3$ in size, and was administered twice weekly for a total of two weeks, which resulted in normalisation of the histology and vascular networks in the liver, spleen and adrenal glands as well as the reversal of the severe anaemia and enlargement of the spleen and liver observed in the PBS treated MMTV*neu* tumour bearing animals (***Xue et al, 2008***). In this study the effects of DC101 on tumour growth in the spontaneous model was a secondary objective, and the group observed that although there was a trend towards MMTV*neu* tumour growth inhibition, the nature of the model made quantifying this inhibition difficult (***Xue et al, 2008***). This study suggests an additional mechanism by which anti-VEGF agents such as DC101 may prove beneficial for breast cancer patients, by blocking VEGF/VEGF-R2 interactions this aids in normalising function of other organs that may be affected by systemic increases in tumour VEGF and thus may reduce the number of complications and associated mortality that arise in cancer patients. Thus, VEGF-R1/2 may play a potential role in autocrine signalling on breast cancer cells; however, it is worth noting that the presence of other receptors on or in association with the breast cancer cells, such as the neuropilin receptors, may exert a greater role on the function of breast cancer cells.

1.4 Neuropilins and Their Role in Breast Cancer

1.4.1 Neuropilin Receptors

Neuropilin 1 and 2 (Np1 and Np2) are transmembrane receptors that have an observed molecular weight of 130 and 135kDa respectively (***Barr et al, 2005***) and were originally identified as receptors for Class 3 Semaphorins (SEMA) with a role in axonal guidance (***Staton, 2007***). Both Np1 and Np2 share approximately 45% amino acid (a.a) sequence homology and are structurally very similar. The neuropilin receptors consist of a large extracellular domain, a membrane spanning domain and a short cytoplasmic domain (40 a.a) that lack tyrosine kinase activity (***Staton et al, 2007***). The extracellular domain of Np1/2 is separated into three distinct domains, the a1/a2 domain, b1/b2 domain and the CUB domain (***Staton et al, 2007***) (**Figure 1.9**). The binding region for the SEMA proteins lies within the a1/a2 domain; the b1/b2 domain is responsible mainly for VEGF binding. There is however a slight overlap within the b1

domain where both SEMA and VEGF bind Np1/2 and the CUB domain is responsible for receptor dimerisation.

Due to the fact that Np1 and Np2 lack tyrosine kinase activity, it was initially assumed that Np1 and Np2 could only mediate VEGF associated intracellular signals when complexed with other cell receptors and were therefore thought to act as co-receptors for the classical VEGF receptors (***Staton et al, 2007***). However, over the past few years, the ability of Np1 to transduce signals independently of the classical VEGF receptors has been recognised with the identification of the neuropilin interacting protein (NIP) which binds a highly conserved C terminal region of Np1 (the last 3 amino acids- SEA-COOH). Interestingly the cardiovascular defects associated with NIP knockdown are more severe than those associated with Np1 null mice and are specific to arterial development and adult arteriogenesis, with reduced arterial density and branching in the retina, heart and kidney (***Miguel, 2008***). The importance of NIP in Np1signaling makes this a potential therapeutic target and strengthens the theory that Np1 is important in VEGF-mediated angiogenesis, activating signals in a VEGF-R1/2 independent manner.

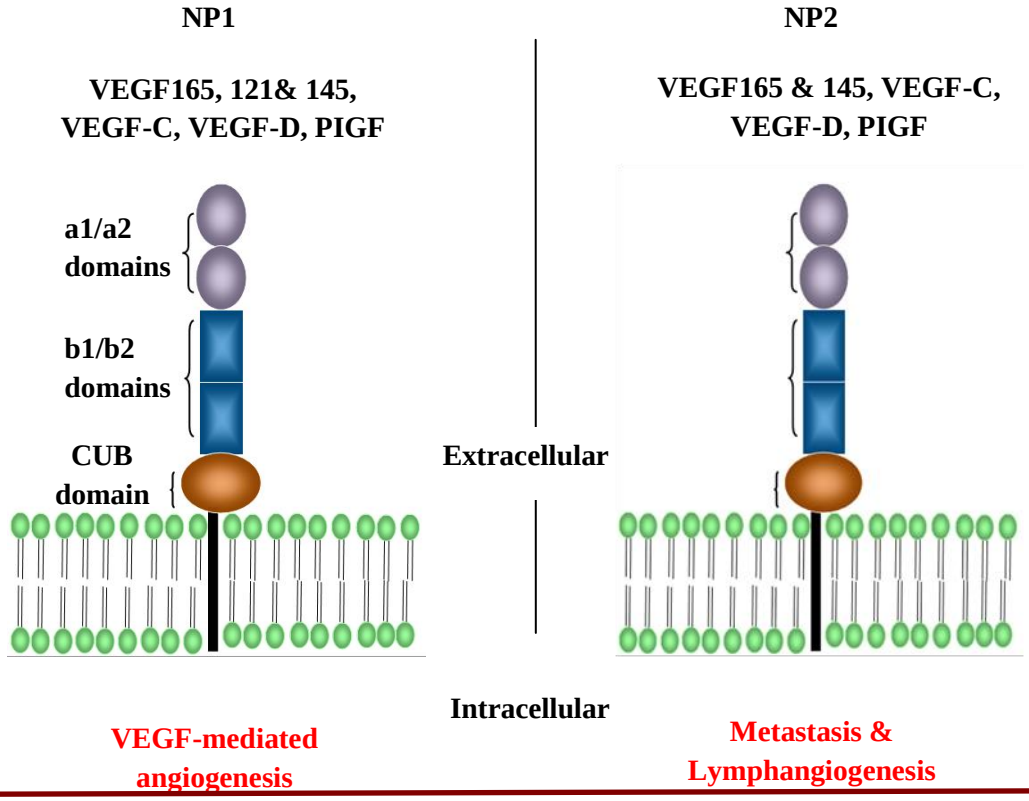

Figure 1.9 *Structures of the Neuropilin Receptors:*
The neuropilin receptors have a large extracellular domain, consisting of 860 amino acids, a short transmembrane domain containing 23 amino acids and an intracellular domain consists of 40 amino acids. The extracellular domain consists of 5 subunits; a1/a2, which are responsible for VEGF binding and b1/b2 which are responsible for SEMA binding but can also enhance VEGF binding to the neuropilins and the c domain which is involved in Np1 dimersation.

Adapted from Staton et al (2007). Neuropilins in physiological and pathological angiogenesis. J.Pathol. 212;3: 237-248.

1.4.2 Expression and Signalling

Neuropilin receptor expression on vascular endothelial cells is observed during the developing vasculature, which appears critical since Np1 null mice are embryonic lethal (E12.5-13.5) and exhibit cardiovascular defects (***Kawasaki et al, 1999***). Over-expression of Np1 results in excessive vessel formation and haemorrhaging, a phenotype typical of VEGF-R2 over-expression or VEGF-R1 deletion (***Kawasaki et al, 1999***). Np2 null mice are viable but display lymphatic defects. A Np1/Np2 double knockout results in embryonic lethality earlier (E8.5) than a Np1 knockout (E12.5-13.5) and is characterised by impaired capillary formation, defective blood vessel branching and avascular embryos (***Takashima et al, 2002***).

The expression profile of the two receptors differs during development, with Np1 being mostly expressed by arterial ECs and Np2 being expressed by venous and lymphatic ECs. Later expression differs with Np1 being predominantly expressed on vascular endothelial cells and Np2 being expressed on lymphatic endothelial cells (***Favier et al, 2006***). The expression of Np1 is regulated by a number of different factors including hypoxia and an array of growth factors, including tumour necrosis alpha and FGF (***Staton et al, 2007***).

1.4.3 Neuropilin 1 and VEGF Interactions

Although originally identified as SEMA binding, the neuropilin receptors also act as VEGF isoform specific receptors (***Barr et al, 2005***). Np1 binds $VEGF_{165}$ and $VEGF_{189}$ whereas $VEGF_{121}$ does not bind to Np1 on porcine aortic endothelial cells (PAE) (***Soker et al, 1998***) or HuVECs (***Soker at al, 1996***). However there is some controversy surrounding the ability of $VEGF_{121}$ to bind Np1 on ECs with a more recent study observing binding of $VEGF_{121}$ to Np1 on HuVECs (***Pan et al, 2007***).

Endothelial Cells

The binding sites for VEGF-R1/2 (a.a. 8-109 across exon 3 and 4) and the neuropilin receptors on VEGF are distinct (a.a. 141-165 across exon 7) (***Soker et al 1997; Muller et al, 1998***) thus VEGF can simultaneously bind both receptors. The presence of Np1 on the same cell or a neighbouring cell forms a receptor-ligand bridge that increases the binding of VEGF to VEGF-R2 PAE by 4 fold and enhances VEGF/VEGF-R2 signalling (***Starzec et al. 2007***; ***Soker et al, 1998***). The ***Soker et al*** study observed a 2.5 fold increase in the migration (when stimulated with 10ng/ml $VEGF_{165}$) of VEGF-R2/Np1-expressing PAE compared to cells expressing VEGF-R2 only, suggesting that the interaction of Np1 with $VEGF_{165}$ on EC results in functional activity. Interestingly, PAE cells that only expressed Np1 did not migrate towards $VEGF_{165}$, suggesting that signalling via Np1 alone is not sufficient to induce migration of PAE. This supports the role of Np1 as a co-receptor for the classical VEGF receptors at least for PAE migration. In this study no enhanced migration was observed when the cells were stimulated

with $VEGF_{121}$. However, $VEGF_{121}$ and Np1 activity is yet to be fully determined, as in contrast to the above study, a different group found that $VEGF_{121}$ induces EC migration via Np1 signalling (***Pan et al, 2007***).

Endothelial cell over-expression of a mutant form of Np1 (Y297A) that lacked any binding ability to VEGF had reduced migration towards a VEGF gradient. The Y297A mutant receptor also disrupted the formation of the Np1/VEGF-R2 complex, resulting in reduced phosphorylation of focal adhesion kinases at the tyrosine kinase 407 residue (***Herzog et al, 2011***) thus suggesting a role for Np1 in actin arrangement and cell motility.

Np1 appears to have role in HuVEC proliferation (measured by H-Thymidine uptake and pERK activity), as siRNA targeted knock down of Np1 in HuVECs resulted in a modest decrease in cell proliferation compared to the control siRNA treated cells (***Murga et al, 2005***). However, this decrease in cell proliferation was significantly less than when VEGF-R2 was depleted in these cells, suggesting that Np1 alone does not regulate HuVEC cell proliferation (***Murga et al, 2005; Pan et al, 2007; Herzog et al, 2011)***.

It is clear that Np1 is important in enhancing a number of VEGF-R2 associated signalling pathways in ECs (***Starzec et al, 2007***), however there is also ample evidence suggesting, that Np1 has more actions than simply a co-receptor for VEGF-R1/2 in ECs. One such study observed the importance of Np1 in a number of activities required for HuVEC functionality (***Murga et al, 2005***). Both VEGF-R2 and Np1 were equally important for HuVECs to form tube-like structures on Matrigel, with the decreased number of tube-like structures formed in the presence of the VEGF-R2 and Np1 siRNA compared with the control being comparable. This suggests that Np1 alone is important in tubular morphogenesis of ECs. In addition, Np1 alone is central for HuVEC cell migration in response to VEGF, with decreased migration of cells in Np1 siRNA and VEGF-R2 siRNA treated cells being comparable. Interestingly, this observation contrasts with previous studies in PAE, where Np1 expressing PAE failed to migrate when stimulated with $VEGF_{165}$ (***Soker et al, 1998***). The observation that Np1 knock down had such dramatic inhibitory effects on HuVEC migration was unexpected. Further investigation revealed the mechanism by which Np1 alone was regulating HuVEC migration in response to VEGF (***Murga et al, 2005***), with the down regulation of Np1 reducing the ability of HuVECs to adhere to ECM molecules (laminin, fibronectin and gelatin. This suggests that VEGF-R2 and Np1 regulate VEGF-stimulated HuVEC migration via two distinct mechanisms since siRNA knock down of VEGF-R2 had no significant inhibitory effects on cell adhesion (***Murga et al, 2005***). In addition to observing impaired attachment to ECM components, Np1 siRNA treated cells failed to form the stress fibers (F-actin) required for cytoskeleton re-arrangement within the same time frame (24h after plating on gelatin). However, the Np1

defective HuVECs did form stress fibers after 48h gelatin incubation, similar in intensity compared to the control/VEGF-R2 defective cells. There is now growing evidence supporting these observations that Np1 plays an important role in EC actin arrangement, cell motility and tube formation (***Wang et al, 2003; Herzog et al, 2011***). Np1 mediated HuVEC migration has also been shown to be mediated via activation of the p130cas pathway (***Wang et al. 2003)***

Over recent years a potential role for Np1 in tumour angiogenesis has become apparent, however the mechanism by which this angiogenic stimulation occurs is not fully understood. In an attempt to investigate the mechanism by which Np1 activates ECs during angiogenesis, the effects of dimeric rat Np1 versus that of soluble Np1 (truncated form that lacks the c domain of the receptor) were evaluated (***Uniewicz et al, 2011***). A tube formation revealed that both forms of the Np1 receptor were capable of inducing HuDMEC or HuVEC tube formation *in vitro*. However, the dimeric form of the receptor had a more potent effect on EC tube formation *in vitro* suggesting that either the dimerisation process of Np1 and /or the c domain of the receptor are important in the extent of tubular morphogenesis (***Uniewicz et al, 2011***). The level of tube formation observed with the dimeric Np1 protein alone was increased compared with $VEGF_{165}$ and the dimeric form activated phosphorylation of VEGF-R2 even in the absence of recombinant $VEGF_{165}$. These findings suggested that Np1 has the ability to drive EC angiogenesis in a VEGF-R2 dependent but $VEGF_{165}$ independent manner (***Uniewicz et al, 2011*).**

Breast Cancer

Studies to further support the hypothesis that Np1 is important in tumour progression have shown that Np1 may act as the primary VEGF receptor on tumour cells in different cancer types including breast cancer (***Soker et al, 1998; Starzec et al, 2006***) and expression is also thought to correlate with tumour invasion and aggression (***Starzec et al, 2006***). $VEGF_{165}$ (***Soker et al, 1998***) and $VEGF_{189}$ (***Herve et al, 2008***) bind Np1 directly on breast cancer cells (MDA-MB-231) but not $VEGF_{121}$ (***Soker et al, 1998***).

VEGF is important in the autocrine survival of breast cancer cells (***Bachelder et al, 2001***). When VEGF mRNA was knocked down in MDA-MB-231 and MDA-MB-435 cells using anti-sense oligonucleotide treatment (15h or 40h treatment respectively), the levels of apoptosis (Annexin V) increased by 33% and 18% respectively compared to the control sense treated cells (***Bachelder et al, 2001***). Thus, Np1 appeared to play an important role in VEGF mediated breast cancer survival *in vitro*. The group investigated this hypothesis in two ways; (1) the survival of MDA-MB-231 breast cancer cells in the presence of VEGF anti-sense oligonucleotides was determined followed by treatment with exogenous $VEGF_{165}$ or $VEGF_{121}$ and found that the MDA-MB-231 cells treated with $VEGF_{165}$ demonstrated an increased survival compared to

those treated with $VEGF_{121}$ (since $VEGF_{121}$ is thought to not bind Np1 it was suggested that the survival potential was due to interactions of $VEGF_{165}$ with Np1). (II) Secondly MDA-MB-453 which do not express Np1 were transfected with a plasmid encoding Np1, and the level of apoptosis present in the transfected cells was lower compared to the control cells (26% apoptosis vs. 58% apoptosis respectively). A later study confirmed this initial observation whereby treatment with a 24-mer peptide derived from exon 7 of $VEGF_{165}$ (the binding region for $VEGF_{165}$ to Np1) for 24h significantly increased the level of apoptosis of human MDA-MB-231 breast cancer cells and murine 4T1 breast cancer cells *in vitro* compared to cells that were either untreated or treated with a control peptide (***Barr et al, 2005***). Both MDA-MB-231 and 4T1 breast cancer cells were also treated with an anti VEGF-R2 peptide but there was no decreased cell survival in any of these cell lines. Interestingly $VEGF_{189}$ that also binds to Np1 has been shown to induce opposing effects to $VEGF_{165}$ on breast cancer cell survival *in vitro* (***Vintonenko et al, 2011***). The ability of MDA-MB-231 cells cloned to over-express either $VEGF_{165}$ or $VEGF_{189}$ to survive under stress conditions (0.5% serum treatment) was tested over a 24-96h time period and surprisingly at the 72h time point the MDA-MB-231 breast cancer cells that over-expressed $VEGF_{189}$ had a higher level of late stage apoptotic cells compared to cells over-expressing $VEGF_{165}$ and control transfected cells that were wild type VEGF expression (***Vintonenko et al, 2011***). This suggests that not all VEGF isoforms aid breast cancer progression and that the level of each splice variant present may have therapeutic implications.

It has been suggested that Np1 is important in breast cancer migration. However, MDA-MB-231 breast cancer cell migration in the presence of an anti-Np1 antibody was significantly increased (2 fold increase) compared with control cells (***Bachelder et al, 2003***). This study suggests that Np1 is potentially required for MDA-MB-231 breast cancer migration however the ratio of SEMA3A compared with VEGF in the breast cancer cells is important in determining the rate of migration observed and subsequently whether an anti-Np1 treatment proves effective in inhibiting breast cancer migration (***Bachelder et al, 2003***). The formation of lamellipodia on migrating cells is the first step in this process, however, when these lamellipodia form, weak adhesions tend to result in membrane ruffles that are visible at the edge of the cell (*Borm et al, 2005*). VEGF promotes the *in vitro* formation of membrane ruffles on breast cancer cells (***Nasarre et al, 2003***), which is most likely due to an inhibitory effect on focal adhesion molecules. The formation of weaker adhesions on the surface of breast cancer cells is advantageous as it increases the ability of the tumour cells to migrate and metastases and it is thought that Np1 may play a role in this VEGF mediated effect (***Nasarre et al, 2003***). In this study two distinct breast cancer cell lines were utilised, MCF7 cells which exhibit low metastatic potential and C100 (which is a derivative of MDA-MB-435 breast cancer cells) that are highly motile and exhibit high metastatic potential (***Nasarre et al, 2003***). The MCF7 cells

were treated with medium that contained SEMA 3F (1h) and an inhibition in MCF7 cell spreading and membrane ruffling was observed suggesting that the presence of SEMA 3F competes with VEGF for binding to the neuropilin receptors. This study supported data from the ***Bachelder*** group which suggested that the SEMA/VEGF ratio present in breast cancer cells an important determinant in the effective migration of breast cancer cells.

Np1/VEGF interactions and breast cancer metastatic potential are regulated via SNAIL (***Wanami et al, 2008***). SNAIL is a transcriptional repressor for E-cadherin which is a transmembrane glycoprotein involved in epithelial cell-cell adhesion (***Wanami et al, 2008***) and it is thought to also act as a tumour suppressor (***Kowalski et al, 2003***). This study observed a reduction in cell-cell adhesion in MCF7 and T47D breast cancer cells 24h post VEGF transfection, with the mRNA/protein extracted from these cells showing increased SNAIL expression and reduced levels of E-cadherin. The addition of an anti-Np1 antibody reversed these effects, suggesting that Np1 mediated breast cancer cell adhesion is via regulation of SNAIL expression. Interestingly, Bz had similar effect on SNAIL expression, suggesting that SNAIL regulation can possibly be via distinct pathways, supporting the notion that dual therapy (Bz/anti-Np1) may enhance efficacy of current breast cancer treatment.

Autocrine VEGF has been shown to be important for breast cancer invasion *in vitro* (***Bachelder et al, 2002***). Treatment of MDA-MB-231 breast cancer cells with VEGF anti-sense oligonucleotides resulted in a significant decrease (64%) in the ability of these cells to invade a Matrigel layer (4h), with inhibition reversed by the addition of exogenous VEGF (***Bachelder et al, 2002***). This VEGF mediated breast cancer invasion is thought to be regulated by Np1 *in vitro* since the addition of a Np1 antibody significantly inhibited MDA-MB-231 breast cancer invasion compared to an IgG control whereas no inhibitory effects on MDA-MB-231 invasion *in vitro* were observed with the addition of a VEGF-R2 antibody (***Bachelder et al, 2002***).

Np1- ***In vivo***

The existing literature supports a role for Np1 in regulating key activities in both EC and breast cancer cells *in vitro*. However it is important that these effects are also verified *in vivo* in order to establish Np1 as an effective and clinically relevant target for breast cancer treatment.

ATWLPPR (A7R) is a heptapeptide that binds Np1 and subsequently blocks $VEGF_{165}$ from binding (***Starzec et al, 2006***). An orthotopic breast cancer murine model using MDA-MB-231 breast cancer cells found that A7R significantly reduced breast cancer growth by 45% compared with control tumours (mean volume: 1.82cm^3 control vs. 1.00cm^3 A7R treated) (***Starzec et al, 2006***). The mechanism by which this occurred are not clear, however the inhibition of tumour growth is likely to be a result of inhibitory actions on ECs rather than on the MDA-MB-231 breast cancer cells directly since no difference was observed in the proliferation of the MDA-

MB-231 breast cancer cells between the two groups (Ki67 staining). A modest yet significant decrease in tumour endothelial cell area (stained ECs measured in pixels) and intratumour vessel density (Chalkley grid method) was observed in the A7R treated tumours (22% reduction in area and 25% reduction in vessel density compared to control tumours) (***Starzec et al, 2006***).

Neuropilin 1- Effects on other cancer types

The focus of this project is on the role of Np1 in breast cancer; however the effects of Np1 on other cancer types may also aid our understanding of how the neuropilin receptors modulate tumour progression, allowing for different avenues of research in breast cancer therapy to be investigated. In pancreatic cancer Np1 appear to play a role in promoting chemoresistance (***Wey et al, 2005***) and in skin tumours the deletion of the Np1 gene impaired the ability of VEGF to promote cancer 'stemness' in cancer stem cells (***Beck et al, 2011***). The presence of cancer like stem cells in tumours is thought to aid the aggressive nature of tumours and cause cells to become chemoresistant (***Abdullah and Chow, 2013***). It has now thought that breast cancer cells with a CD44+/CD24-/ALDH^{high} phenotype are representative of a stem cell like population and if these cells express neuropilin receptors, this would be an important area to investigate especially since both chemotherapy and anti-angiogenic treatment eventually leads to resistance (***Glinka et al, 2012***).

1.4.4 Neuropilin 2

The majority of research into the role of the neuropilins in tumour progression has been carried out on Np1 however the role of Np2 is becoming more apparent. Np2 expression in breast cancer patient tumour samples has been correlated with a poor prognosis (***Yasuoka et al, 2009***). However there is minimal literature available on the molecular mechanisms by which Np2 augments tumour progression.

Endothelial Cells

Np2 binds to both $VEGF_{165}$ and $VEGF_{145}$ with $VEGF_{165}$ displaying a greater affinity for Np2 (5 fold greater then that of $VEGF_{145}$ ($VEGF_{165}$ $-1.3x10^{-10}{}_{M}$ vs. $VEGF_{145}$ $7x10^{-10}{}_{M}$)) (***Gluzman-Poltorak et al, 2000***). Despite the fact that Np2 binds to $VEGF_{145}$ and $VEGF_{165}$, the majority of literature available on the role of Np2 in cancer in mostly related to the interaction of Np2/VEGF-C. Np2 binding to VEGF-C is thought to lead to lymphangiogenesis. The presence of VEGF-C is required to promote a VEGF-R2/Np2 complex (***Favier et al, 2006***).

Np2 is important in VEGF and VEGF-C EC survival *in vitro* (***Favier et al, 2006***). HuDMECs that over-expressed Np2 were incubated with VEGF (10ng/ml) or VEGF-C (100 and 300ng/ml) for five days, after which cell viability was quantified. VEGF and VEGF-C in the presence of an empty vector increased HuDMEC cell survival compared to un-stimulated cells, with both

ligands stimulating survival to a relatively similar extent (***Favier et al, 2006***). Interestingly, over-expression of Np2, further enhanced cell survival of HuDMECs in the presence of both VEGF and VEGF-C, suggesting that Np2 does play an important role in EC survival of both vascular and lymphatic endothelial cells *in vitro*. Interestingly, the addition of SEMA3F inhibited the survival activity induced by VEGF and VEGF-C on HuDMECs. This observation is important as it suggests that SEMA-3F and VEGF/VEGF-C compete for Np2 binding on HuDMECs, and may have important implications in Np2 targeted therapy. Np2 has also been implicated in HuDMEC migration *in vitro*. HuDMECs displayed increased cell migration towards both VEGF (50ng/ml) and VEGF-C (100ng/ml) after 24h, which was inhibited in the presence of Np2 siRNA knock down treatment (36h) (***Favier et al, 2006***). Similar to the cell survival assay described above, the presence of SEMA3F inhibited VEGF and VEGF-C induced HuDMEC migration, further confirming that the SEMA proteins may compete with the VEGF proteins for Np2 binding on ECs. It was suggested that the role of Np2 in EC activity is a result of co-receptor actions since VEGF-R2 and Np2 formed complexes, however this does not rule out Np2 as an independent receptor for VEGF or VEGF-C mediated EC activity. The majority of data concerning the role of Np2 on EC biology appears to be related to lymphangiogenesis; however, there are suggestions that Np2 may also play an important role in tumour angiogenesis.

Breast Cancer Cells

Again data us scarce concerning the role of Np2 on breast cancer cells. However the limited data suggests that Np2 potentially plays a role in breast cancer cell motility (***Yasuoka et al, 2009***). When $Np2^{high}$ and $Np2^{low}$ expressing breast cancer cells are isolated from an invasive breast tumour the ability of these two sub-populations demonstrate differential adhesion to ECM molecules (***Goel et al, 2012***). The $Np2^{high}$ expressing breast cancer cells readily adhered to laminin which appeared due to interactions of Np2 with α6β1 integrin (***Goel et al, 2012***). MDA-MB-435 breast cancer cells were utilised in subsequent experiments as these cells express both Np2 and α6β1 integrin. Interestingly it was observed that depletion of Np2 expression via short hairpin RNA resulted in a significant reduction in cell attachment and cell morphology when coated on a laminin surface but not collagen, suggesting the Np2 plays a role in α6β1 integrin regulation on breast cancer cells and thus potentially cell migration. (***Goel et al, 2012***). More recently, it has been suggested that Np2 may also play an important role in tumour initiation of triple negative breast cancer, as oncogenic transformation of normal mammary epithelial cells appears to be associated with increased Np2 expression whereas no increase in Np1 expression was observed. This suggests that Np2 may play a role in regulating the tumour initiating cell population in triple negative breast cancer (***Goel et al, 2013***). At present there is no *in vivo* data concerning a specific role for Np2 specifically on breast cancer progression.

The literature surrounding the neuropilin receptors supports the idea that these receptors play an important role in VEGF signalling on both ECs (vascular and lymphatic) and breast cancer cells. The nature of the neuropilins as both co-receptors and independent receptors suggests that a number of functional effects on different factors involved in breast cancer progression. There is sufficient compelling experimental evidence both *in vitro* and *in vivo* to suggest that Np1 is a key player in breast cancer progression and thus a valid target for breast cancer therapy.

1.5 Clinical Significance for Anti-Angiogenic Therapy

The clinical importance of angiogenesis in tumour growth was initially described in the early 1970s, when Judah Folkman suggested that targeting the tumour vasculature would prove to be an effective method to prevent tumour progression (Folkman 1971). The leaky tumour vasculature allows tumour cells to escape from the primary tumour and circulate through the bloodstream to an alternative site (often liver, lungs and bone) where they seed and form metastases. Clinically there is a definitive correlation between angiogenesis and metastasis which supports the theory that a highly vascularised tumour will rapidly grow and progress (***Guidi et al, 2000; Schneider and Miller, 2005***).

Current anti-tumour strategies include chemotherapy which targets the rapidly proliferating tumour cells. However these are genetically unstable and likely to acquire resistance to therapy after continued use. Moreover drugs must pass through endothelial barriers before reaching the target tumour and high interstitial pressure within tumours makes delivery of cytotoxic drugs difficult (***Eichhorn, 2007***). In contrast anti-angiogenic agents target the relatively stable ECs which are less likely to acquire resistance to therapy. Moreover anti-angiogenic therapies are not restricted to a certain histological tumour type as all solid tumours ultimately depend on angiogenesis, making the application of anti-angiogenic therapies across many oncology indications.

Preclinical and clinical success has been observed with a number of anti-angiogenic agents, with the preclinical data showing elimination of tumour blood vessels and tumour burden in a number of murine solid tumours including breast cancer ***(Lin and Sessa 2004; Xue et al, 2008***) and clinical results observing a reduction in both vascular density and tumour burden (***Kerbel and Folkman 2002)***. It is thought that the anti-angiogenic agents act by causing collapse of immature vessels, prevent further vessel initiation, reducing vascular permeability and increasing pericyte coverage on vessels stimulating vascular maturity (***Lin and Sessa 2004***). It has also been suggested that anti-angiogenic agents may produce a window of opportunity for more effective delivery of cytotoxic agents by 'normalising' the vasculature and reducing intratumoural pressure (***Jain, 2001; Goel et al, 2011; Goel et al, 2012; Huang et al, 2012***).

It is important that anti-angiogenic therapy may not completely remove a tumour, but by causing it to regress, may allow for more complete surgical removal of the tumour. The actions of anti-angiogenic therapy are also more specific than those associated with chemotherapy, thus the associated toxicities tend to be less severe, moreover they will simultaneously target any existing metastases (***Eichhorn, 200***7). Due to the pivotal role played by VEGF in tumours there are now a large number of inhibitors being developed to inhibit VEGF mediated activity, for example Bevacizumab (**section 1.6**).

Pre-clinical data (***Xue et al, 2008***) and clinical data (***Miller et al, 2007; Goel et al, 2011; Goel et al, 2012***) emphasises the clinical relevance of anti-angiogenic therapy in breast cancer, however the complexity of the disease challenges the success of anti-angiogenic in breast cancer treatment, as suggested by recent 'gap' analysis reviews (***Thompson et al, 2012***).

1.5.1 Therapeutic Strategies for Inhibiting the VEGF Pathway

As VEGF is the most potent pro-angiogenic stimulus identified to date and its clinical significance appear pivotal to tumour angiogenesis, this makes it a major target for the development of anti-angiogenic therapy. Currently, there are a number of therapeutic measures targeting the VEGF pathway (**Figure 1.10** and **Table 1.2**) including synthesis of antisense oligonucleotides to inhibit secretion of endogenous tumour VEGF, and neutralising VEGF in the microcirculation using soluble receptors such as VEGF-Trap (***McMahon, 2000***). An alternative method of preventing VEGF binding to its receptor and subsequent signalling is the use of blocking antibodies to either VEGF the ligand or to VEGF-R2. Furthermore small molecule drugs which target the tyrosine kinase receptors (VEGF-R1 and VEGF-R2) thereby preventing downstream signalling have now been developed e.g. Sunitinib. Targeting the mTOR (rapamycin) pathway provides an alternative method for targeting VEGF, as inhibitors of mTOR such as Temsirolimus inhibit the expression of VEGF in EC (***Del Bufalo et al, 2006***).

There are a number of VEGF targeted agents that are currently undergoing clinical trials in a number of different tumour types. Targeted therapy offers the benefit in that, in theory it should reduce the toxicities associated with more systemic treatments such as chemotherapy. Despite minimal success with Bz, the approach to breast cancer treatment and other such tumours ins promising. However, more bench to bedside research needs to be performed to establish the mechanism of these different targeting agents (**Table 1.2**).

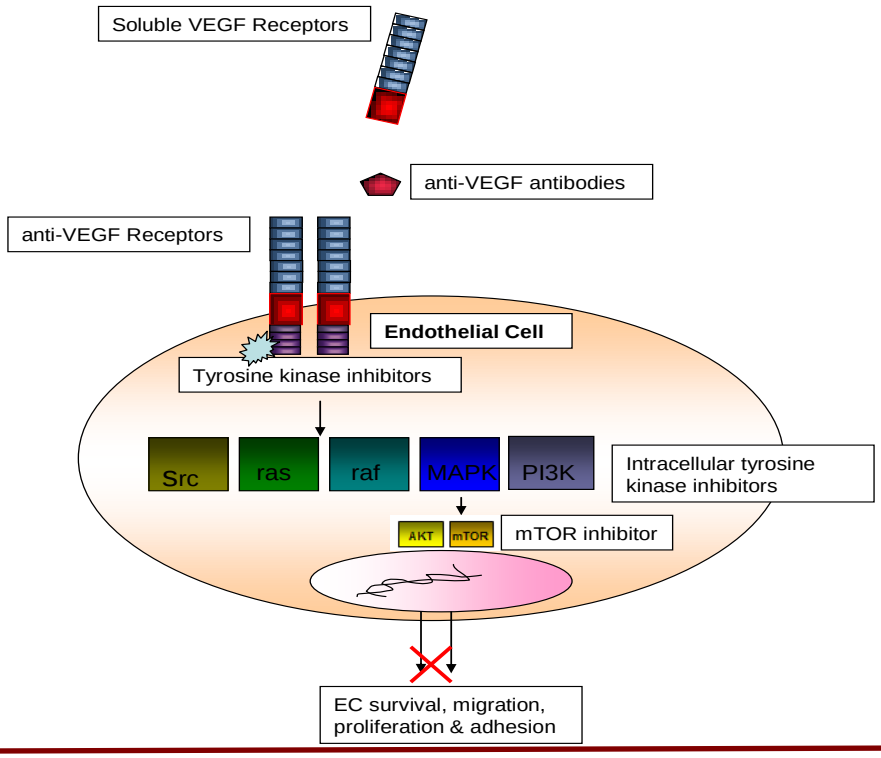

Figure 1.10 ***VEGF Targeting Agents*** **:**
There are a number of different strategies currently being investigated for inhibiting the VEGF pathway and thus inhibiting angiogenesis. The main focus for my project is Bz, which is a mAb that inhibits VEGF from binding to its receptors; VEGF-R1/R2 and thus subsequent signalling. The targets for therapy are vast and, developed for a number of different stages in the VEGF pathway from inhibiting EC survival signals (Rapamycin) through to intracellular tyrosine kinase inhibitors that targets downstream signalling molecules such as ras & raf.

Adapted from Eichhorn et al, 2007.Angiogenesis in cancer: molecular mechanisms, clinical impact. Langenbecks Arch Surg 392; 3:371-9

AGENT	TARGET	STATUS
Aflibercept	Binds VEGF isoforms and PIGF and inhibits interaction with VEGF-R1 and VEGF-R2	Clinical Trials- for use for mCRC patients in combination with chemotherapy – clinically successful, demonstrated extension of PFS and OS. Potential second line treated for non-responders to Bz
Vandetanib	Oral inhibitor, blocks VEGF receptor signalling via downstream kinase blockade	Clinical Trials- for use in advanced breast cancer patients in combination with docetaxel
Cilengitide	Avβ3/5 integrin inhibitor	Clinical Trials- for use in glioblastoma and other cancer types including breast cancer
Pazopanib	Tyrosine kinase inhibitor that targets VEGF-R1, VEGF-R2, VEGF-R3, PDGFR and c-kit	Approved for use in renal cell carcinoma
Angiostatin/ Endostatin	Inhibits the expression of VEGF-A, VEGF-C and VEGF-D	Pre-clinical studies for colon cancer

Table 1.2 ***VEGF Targeting Agents:***
Outlines some of the targeted therapies that are currently undergoing clinical trials or have been approved for use in a number of cancer patients, including breast cancer.

Adapted from Angiogenesis in cancer: anti-VEGF escape mechanisms. Prager et al, 2012. Translational lung cancer research; 1(1): 14-25

1.6 Bevacizumab in the Treatment of Breast Cancer

When this current project commenced (2008), Bevacizumab (Bz) had recently been approved for the mBC indication and was at the fore-front of anti-angiogenic therapy. However, over the past four years the clinical studies data have failed to reach clinically meaningful study outcomes. The lack of significant benefit to patients and a rise in safety concerns led to the withdrawal of Bz in mBC by the FDA (Nov 2011). This section discusses the early clinical data, the challenges faced in the clinic and the new knowledge that can be exploited to overcome these challenges. It is important to state that the clinical use of Bz in combination with chemotherapy in other solid tumours such as metastatic colorectal cancer (FDA) has proved successful. Thus, the question remains is to why Bz, an anti-angiogenic agent which in theory has the same mechanism of action across all solid tumours is not translating to successful application in mBC.

Bevacizumab is the first angiogenic inhibitor to be approved for use in the clinic by the FDA. Metastatic colorectal cancer was the first indication for which Bz was approved followed by breast cancer in February 2008; where it was granted accelerated approval for use in advanced (HER2/neu negative) breast cancer treatment (FDA) (section 1.6.5 for clinical studies in breast cancer). It is a humanised monoclonal antibody that binds all known human VEGF isoforms,

preventing interactions with VEGF-R1 and VEGF-R2 and subsequent signalling (***Shih and Lindley 2006***). The human region (93%) constitutes the framework of the antibody and the murine region (7%) constitutes the complementary determining regions that bind VEGF (***Shih and Lindley 2006***). The biochemical and pharmacological properties of Bz are the same as its parent antibody A4.6.1. (murine antihuman antibody), however has the advantage of inducing a reduced immune response and exhibiting a longer biological half-life of 17-21 days in humans (***Gerber and Ferrara 2005***).

1.6.1 *In vitro* effects of Bz on Endothelial Cells

A dose dependent inhibition on $VEGF_{165}$ mediated HuVECs cell proliferation *in vitro* was observed with the addition of Bz (96h experimental time point) at a range of doses with maximum inhibition of HuVECs cell proliferation observed with Bz at 500ng/ml (***Wang et al, 2004***). $VEGF_{165}$ (50ng/ml) and Bz were pre-incubated for 2h prior to addition to the cells. An IgG1 control was also used to assess any non-specific effects observed with the addition of a monoclonal antibody; however the data from these control experiments were not shown (***Wang et al, 2004***). Similarly, $VEGF_{165}$ mediated HuVECs cell survival was also inhibited in a dose dependent (100, 200 and 500ng/ml) manner by Bz (***Wang et al, 2004***). No inhibitory effects were observed on HuVECs cell survival in the presence of a control IgG (500ng/ml). Bz also inhibited the *in vitro* vascular permeability effects of $VEGF_{165}$ on HuVECs. Minimal inhibitory effects were also observed with the control IgG but the level of permeability observed with $VEGF_{165}$ alone and $VEGF_{165}$ plus the control IgG was not significant (it is important to note that statistical analysis was not presented) (***Wang et al, 2004***). Nitric oxide (NO) production is important in a number of EC associated process such as permeability and migration (***Wang et al, 2004***) and likely to be regulated by VEGF , thus the effects of Bz on NO production by HuVECs were also evaluated. Again, Bz exerted an inhibitory effect on NO production compared to cells treated with $VEGF_{165}$ alone, with no effect with the control IgG (***Wang et al, 2004***).

VEGF-induced tissue factor expression in HuVECs was also inhibited by Bz (62.5ng/ml-1000ng/ml). Interestingly, when Bz (500ng/ml) was pre-incubated with a range of $VEGF_{165}$ doses (2.5-50ng/ml) an inhibitory effect with Bz on HuVECs migration was observed in the presence of three $VEGF_{165}$ doses (2.5, 5 and 10ng/ml) however this inhibitory effect was negated in the presence of Bz and 50ng/ml $VEGF_{165}$, suggesting that a much higher $Bz/VEGF_{165}$ ratio is required to maintain inhibitory effects on HuVECs migration *in vitro* (***Wang et al, 2004***). It is interesting that inhibition of $VEGF_{165}$ mediated tissue factor production and HuVECs cell migration required much higher doses of Bz compared to the doses used in the other functional

assays in these experiments, suggesting differences in the extent to which downstream HuVEC pathways are activated by $VEGF_{165}$ in the different cellular processes *in vitro*.

Another study investigated the effects of Bz on functional HuVEC activity *in vitro* (***Carneiro et al, 2008***). Exogenous VEGF was not added but assays were carried out in the presence 2% serum containing media, thus creating a different micro-environmental setting from the studies above (***Wang et al, 2004***), where $VEGF_{165}$ was pre-incubated with Bz 2h prior to adding to the HuVECs. In this more recent study the appropriate vehicle control was used rather than an IgG control since Bz is purchased as a re-suspended liquid, with the vehicle control containing (51mM sodium phosphate ph 6.2, 60mg/ml Trehalose.$2H_2O$, 0.04% polysorbate 20) European Medicines Agency 2005. No *in vitro* cytotoxic effect on HuVECs was observed 24h after treatment with Bz (0.25-2.5mg/ml) (***Carneiro et al, 2008***). Bz significantly ($p<0.01$) inhibited HuVECs cell proliferation at all doses tested (0.25-2.5mg/ml) compared to vehicle control treated cells (***Carneiro et al, 2008***), at a much earlier time point (24h) then previously reported (96h) (***Wang et al, 2004***). Bz significantly ($p<0.01$) inhibited HuVECs cell survival in a dose dependent manner, compared to the vehicle control treated cells (***Carneiro et al, 2008***). The effects of Bz on HuVECs cell migration was tested using the 0.25mg/ml and 2.5mg/ml dose only, with the higher dose of Bz (2.5mg/ml) significantly ($p<0.05$) inhibiting HuVECs cell migration *in vitro* compared to the vehicle control. Low and high Bz doses (0.25 and 2.5mg/ml respectively) significantly ($p<0.05$) inhibited HuVECs cord formation compared to the vehicle control (***Carneiro et al, 2008***). These two studies described, are important even using different experimental conditions both confirm that ability of Bz to effectively inhibit cellular functions associated with HuVECs *in vitro*. However, it is important to note that the majority of *in vitro* studies thus far have assessed the effects of Bz on HuVECs rather than HuDMECs. HuDMECs are microvascular ECs and thus a more relevant cell type when studying angiogenesis *in vivo*. However, they are technically more demanding than HuVECs to culture. However, recently, during the review of this current project the effects of Bz on the microvascular ECs have been investigated.

Bz used at two different doses (0.125 and 0.25mg/ml) demonstrated similar inhibitory effects on HuDMECs function *in vitro* when compared to HuVECs despite the use of lower concentrations of Bz (***Costa et al, 2009***). Bz (0.25mg/ml) significantly inhibited *in vitro* HuDMEC cell proliferation and survival after 24h treatment compared to the vehicle control (***Costa et al, 2009***). Interestingly, both doses of Bz (0.125 and 0.25mg/ml) significantly ($p<0.05$) inhibited HuDMEC cell migration and cord formation after 24h compared to the vehicle control. The presence of Bz reduced the level of VEGF released by the HuDMEC cells with a significant ($p<0.001$) reduction in response to higher dose (0.25mg/ml) compared with the vehicle control (***Costa et al, 2009***).

Breast Cancer Cells

With the controversy surrounding the expression of VEGF-R1 and VEGF-R2 on breast cancer cells and the mechanism of anti-angiogenic agents are thought to predominantly target ECS. Consequently, there is limited literature available on any direct effects of Bz on breast cancer cells *in vitro*. However a few studies have been performed *in vitro*.

Treatment of Luciferase labelled MDA-MB-231 (Luc-MDA-MB-231) breast cancer cells with Bz alone with a dose much lower then used for ECs (10μg/ml)) for 14 days resulted a decrease (23%) in the number of colonies formed compared to the control (***Volk et al, 2008***). Combining Bz with nab- paclitaxel (a albumin bound form of paclitaxel), dramatically enhanced the inhibition on Luc-MDA-MB-231 colony-formation compared to nab-paclitaxel alone (43% vs. 76%) (***Volk et al, 2008***). It is possible that increasing the molecular weight of paclitaxel by the addition of albumin leads to greater retention of the drug, thus more effective delivery into the tumour, resulting in enhanced inhibitory effects. However, a separate study demonstrated conflicting results with no inhibition of breast cancer cell proliferation in the presence of Bz (***Gerber & Ferrara, 2005***). Breast cancer cells that express HER2 at high levels may respond to Bz treatment to a greater extent, demonstrated by using the HER2 positive SKBR3 cell line, which demonstrated enhanced inhibition of cell proliferation when compared to the low HER2 expressing breast cancer cell lines, MCF7 and MDA-MB-231 (***Emlet et al, 2007***).

1.6.2 Pre-clinical Studies

A4.6.1 and Bz

Over the years since the approval of Bz for clinical use in breast cancer patients, a number of pre-clinical *in vivo* studies have been performed assessing the effects of A4.6.1 or Bz in combination with a number of different agents.

Preclinical studies using the murine parent antibody, A4.6.1 against a breast carcinoma cell line (MDA-MB-435) revealed a significant decrease ($p<0.05$) in tumour permeability but no change in tumour fractional blood volume 24 hours after a single dose of A4.6.1 (1mg dose) (***Brasch, 1997***). A further study demonstrated a reduction in tumour growth rates and microvascular permeability after three 1mg doses of A4.6.1 at 3 day intervals (***Pham et al. 1998***). The efficacy of A4.6.1 in combination with doxorubicin was also investigated in three different human breast cancer cell lines implanted as xenografts in nude mice. The combination of A4.6.1 with doxorubicin significantly reduced tumour mass ($P<0.001$) in all three cell lines tested (***Gerber and Ferrara 2005***).

Pre-clinical studies investigating A4.6.1 efficacy demonstrated incomplete tumour inhibition

as A4.6.1 only inhibits human VEGF isoforms, and therefore endogenous murine forms of VEGF are freely available to bind and activate VEGF receptors (***Ryan et al. 1999***). Indeed, studies have shown that the degree of inhibition of Bz is inversely related to the content of stromal-derived mouse VEGF that is present within the tumour xenografts (***Ferrara et al. 2005***). A recent pre-clinical study assessed the effects of Bz on HCC1806, a cancer cell line thought to represent a clinically relevant model for triple negative breast cancer (***Volk-Draper et al, 2012***). HCC1806 breast cancer cells were injected orthotopically, tumours were allowed to grow to 150mm^3 after which treatment with either saline control or nab-paclitaxel alone (10mg/kg i.v.) for five consecutive days, Bz alone (4mg/kg i.p.) twice weekly or a combination of nab-paclitaxel and Bz commenced (***Volk-Draper et al, 2012***). Interestingly, Bz had no significantly inhibitory effect on HCC1806 breast cancer growth *in vivo* compared with the saline control (mean±SEM tumour volume, mm^3; Bz vs. control; 2126 vs. 1799mm^3). In contrast, Nab-paclitaxel alone significantly ($p<0.01$) inhibited HCC1806 breast cancer growth (180mm^3) compared with the saline control. However, when nab-paclitaxel treatment was discontinued approximately 15 days later, the nab-paclitaxel alone treated tumours all started to re-grow, which was not evident when Bz was combined with nab-paclitaxel using a similar regime (***Volk-Draper et al, 2012***). The data from this HCC1806 study is important for future pre-clinical studies investigating the more aggressive sub-type of breast cancer that frequently present in clinical setting.

The majority of breast cancer pre-clinical studies begin treatment once palpable tumours of approximately100-200mm^3 are reached. However in the clinic, breast cancer patients are routinely diagnosed when they present with metastatic breast cancer. Thus the following group designed a pre-clinical study that commenced treatment when tumours were larger in volume (450-600mm^3) and distant metastases were present. Luc-MDA-MB-231 and Luc-MDA-MB-435 breast cancer cells were injected into the mammary fat pad of SCID mice, tumours were allowed to grow and then treated with a saline control, nab-paclitaxel alone (10 or 30mg/kg i.v.) for five consecutive days, Bz alone (4mg/kg i.p.) twice weekly or a combination of nab-paclitaxel and Bz began (***Volk et al, 2011***). Interestingly, in the Bz (4mg/kg) treated group, a varied response in the Luc-MDA-MB-231 tumours was observed in the two different cohorts, with the first cohort demonstrating a significant (p=0.006) inhibitory effect on advanced Luc-MDA-MB-231 breast cancer growth compared to the control group (1332 vs. 2095mm^3 respectively). In the second cohort Bz at the same dose demonstrated no inhibitory effects on Luc-MDA-MB-241 tumour growth compared to the control (1933 vs. 1973mm^3 respectively). This suggests that tumour responses to Bz are diverse and that personalised treatment is required to identify patients that are likely to respond to anti-angiogenic treatment.

Bz significantly (p<0.001) inhibited advanced Luc-MDA-MB-435growth compared to the control group (1030 2157 and 2151mm^3 respectively) (***Volk et al, 2011***). Nab paclitaxel (10 and 30mg/kg) significantly (p<0.001) inhibited both breast cancer cell lines at the advanced stage compared to the control with a further inhibition in tumour growth being observed when Bz was combined with nab paclitaxel (Luc-MDA-MB-231-10mg/kg nab-paclitaxel dose; 469 vs. 26mm^3 respectively: Luc-MDA-MB-435-10mg/kg nab-paclitaxel dose; 642 vs. 174mm^3 respectively) (***Volk et al, 2011***). The effects of Bz on distant metastasis in the lungs and lymph nodes was also assessed in this study. Bz alone had no effect on the incidence of metastasis in the lymph node (LN) however, Bz alone significantly (p=0.005) reduced the Luc-MDA-MB-231 metastatic tumour burden in the LN present in the advanced diseased state compared to the control group (***Volk et al, 2011***). Nab paclitaxel alone (10 and 30mg/kg) also significantly (p=0.003 and p=0.001 respectively) reduced Luc-MDA-MB-231 tumour burden in the LN and combining Bz with nab paclitaxel further reduced the metastatic burden present in the LN. Interestingly, advanced tumour growth of the primary tumour formed by the Luc-MDA-MB-435 cells responded to both Bz alone and nab paclitaxel but no such response was observed in the metastatic setting (***Volk et al, 2011***). Nab-paclitaxel alone increased incidence of distant metastasis in the LN compared to the control group, this was significant (p=0.041).

Preclinical efficacy of A4.6.1/Bz has also been shown in a variety of solid tumours other than breast carcinoma. Preclinical studies showed 90-95% growth reduction in rhabdomyosarcoma xenografts when the drug was administered at the same time or shortly after injection of the tumour cell lines into nude mice. Administration of Bz or A4.6.1 in a colorectal cancer xenograft showed 90% inhibition of primary tumour and a 10-18 fold reduction in the number of liver metastases present (***Melnyk et al. 1999; Gerber and Ferrara 2005***). Tumour inhibition occurred in a dose dependent manner irrespective of the route of administration or tumour location (***Gerber et al. 2000***) suggesting that bioavailability or barrier problems are not encountered and suggested that Bz offered an advantage over cytotoxic drugs. Interestingly if tumour growth was significant prior to the addition of Bz, the tumour was able to escape treatment and continue to progress (***Gerber et al. 2000***), providing possible evidence that tumours may eventually become VEGF independent. Therefore, the screening for VEGF levels prior to VEGF based therapy may assist in stratification of patients who may respond to VEGF therapy.

1.6.3 Mechanism of action of Bz

It is thought that Bz reduces tumour growth by causing regression of existing vessels and eventually inhibiting new blood vessel formation which supports tumour growth (***Gerber and Ferrara 2005***) (**Figure 1.11**). Since Bz targets tumour-associated vasculature, it is accepted that Bz suppresses tumour growth via indirect effects on tumour cells. Bz treatment appears to

increase pericyte coverage on tumour associated vessels thus leading to restoration of a mature vascular lining. It has been speculated that the 'normalisation' of the tumour associated vasculature leads to restoration of blood flow and interstitial pressure, thereby creating a window of opportunity which allows for more efficient delivery of chemotherapeutic drugs and radiotherapy (***Goel et al, 2011; Goel et al, 2012; Jain et al, 2013***). Thus vascular normalisation may explain why the clinical effects of Bz are increased when Bz is combined with chemotherapy. There is also a suggestion that Bz reduces the level of bone marrow derived cells infiltrating into the tumour, which may reduce the chance of the vascular 'rebound' (***Roland et al, 2009***).

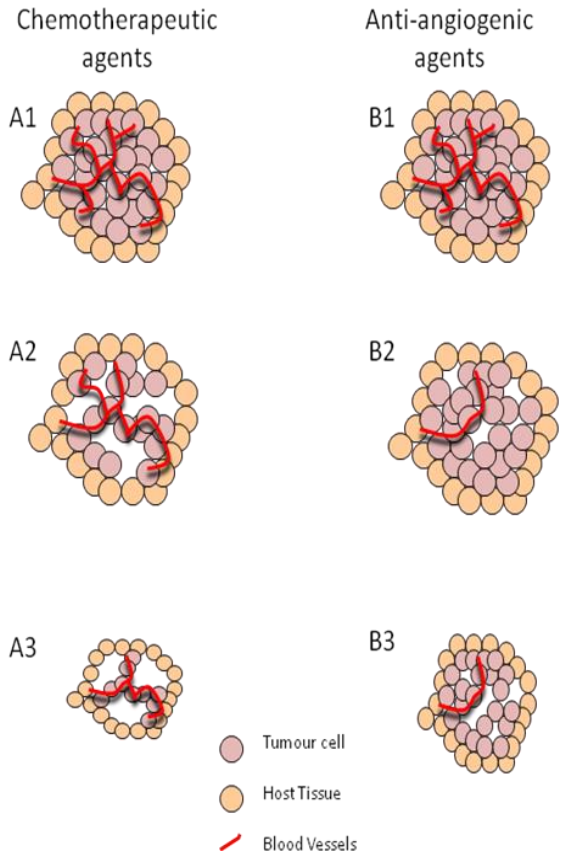

Figure 1.11 ***Chemotherapy versus Angiogenesis Inhibitors.***

This diagrammatic representation shows the different mechanisms of action observed with chemotherapy and anti-angiogenic inhibitors. Anti-angiogenic inhibitors will primarily target tumour cells indirectly by acting on the blood vessels that have established within the tumour, whereas standard chemotherapy directly targets and kills the tumour cells. Although some chemotherapeutic agents, such as Paclitaxel have been shown possess anti-angiogenic activity. The different targets for the two therapies results in different outcomes. Treatment with chemotherapy, results in shrinkage of the tumour and if successful, elimination of the primary tumour (cytotoxic effects). Anti-angiogenic agents cause regression of the tumour but more notably stabilisation of the disease (cytostatic) due to reduced oxygen and nutrients required for growth.

Adapted from Loges et al, 2009. Silencing or Fuelling Metastasis with VEGF inhibitors: Anti-angiogenesis Revisited.

1.6.4 Toxicity Profile

Pre-clinical safety of Bz in monkeys (share 99% homology to human VEGF) showed no real toxicities, pathological changes or unexpected adverse effects after Bz treatment even after prolonged treatment with high doses of Bz (up to 50mg/kg/dose for 13 weeks). Pre-clinical trials confirmed that anti-VEGF therapy with Bz/A4.6.1 exhibited significant anti-tumour activity in a range of primary and metastatic tumours including breast, with relatively mild associated side effects, which resulted in the progression of Bz to clinical trials to assess safety and efficacy in humans (***Ryan et al. 1999***).

1.6.5 Clinical Trials

Monotherapy

The first Phase I trial measuring the safety and pharmacokinetic profile of Bz recruited 25 patients with solid tumours; sarcoma (n=8), renal cell carcinoma (n=7), breast cancer (n=5), lung cancer (n=2) and other (n=3) (***Gordon et al, 2001***). The patients were treated with a range of Bz doses (0.1-10mg/kg) with 90 minute i.v infusions at day 0, 28, 35 & 42, with a linear pharmacokinetic profile being observed between 0.3-10mg/kg, and inhibition of serum free VEGF being observed within this range (***Gordon et al, 2001***). Bz was reasonably tolerated; the majority of patients presented with manageable grade 1-2 side effects (asthenia, nausea, low-grade fever and head-ache), with grade 3-4 adverse events (anaemia, dyspnea and serious bleeding) occurring in four patients only, over the entire course of the study (6 weeks). These adverse events were thought not to be a result of Bz dose-dependent treatment but due to disease progression (***Gordon et al, 2001***).

Bz as a single agent in the treatment of previously treated (chemotherapy) metastatic breast cancer (mBC) patients was evaluated in a Phase I/II trial. This trial that assessed the safety and efficacy of Bz administered at increasing doses of 3, 10 & 20mg/kg twice weekly as i.v. infusion until disease progression or to a maximum of 13 doses, with tumour response being assessed on days 70 & 154 after start of the initial treatment (***Cobleigh et al, 2003***). The aim of the study was to establish an optimal dosage to be used in subsequent trials and the primary end point of the study was objective response rate (ORR). The trial observed an ORR of 9.3% with median duration of response observed at 5.5%; ~17% had stable disease or showed ongoing objective response (***Eskens and Sleijfer, 2008***). Adverse effects at higher doses of Bz (20mg/kg) were detected, such as severe headaches, nausea and vomiting in 4/16 patients treated at this dose. From this study, the optimal dose was administration of Bz at 10mg/kg (i.v. infusion) every other week. These Phase I/II trials using Bz alone showed Bz to generally be well tolerated but overall Bz monotherapy had proven to have only modest anti-tumour effects (***Eskens and Sleijfer ,2008; Gerber and Ferrara, 2005***).

Combination Therapy

Preclinical experiments suggested that the anti-tumour activity of Bz was enhanced by combining with cytotoxic chemotherapy, radiation and other angiogenic inhibitors (***Gerber and Ferrara 2005***). The first successful clinical trial that led to the approval of Bz in combination with standard chemotherapy was in 2004 for the treatment of untreated metastatic colorectal cancer (mCRC) (***Hurwitz et al, 2004***). In this study, patients received Iriontecan, Fluorouracil and Leucovorin (IFL) in combination with Bz (5mg/kg every two weeks) or IFL with a placebo. The primary endpoint of overall survival (OS) and the secondary end point progression free

survival (PFS), response rate (RR), duration of response (DR), safety and quality of life were all successfully met. The patients in the Bz group demonstrated a significant ($p<0.001$) increase in OS compared to the placebo group (20.3 vs. 15.6 months respectively). Progression free survival, RR and DR (10.6months, 44.8% and 10.4months respectively) were also significantly improved in the patients receiving Bz and chemotherapy compared to the chemotherapy alone group (6.2months, 34.8% and 7.1months respectively). Grade 3 hypertension was considerably increased in the Bz treated patients compared to placebo (11% vs. 2.3% respectively) however this was stated to be managed with the use of standard anti-hypertensive agents (***Hurwitz et al, 2004***). With the successful trial in mCRC and the pre-clinical data suggesting that combining Bz with standard chemotherapy regimens did not result in enhanced chemotherapy-associated toxicities (***Margolin et al. 2001***) the majority of clinical studies in breast cancer focused on the role of Bz in adjuvant therapy for the first line treatment of MBC.

Phase II Trial

XCALIBr, a Phase II clinical trial investigating capecitabine alone (1000mg/m^2) vs capecitabine/Bz (15mg/kg every 3weeks) in 106 mBC patients observed an increase in time to progression in the combination arm (4mths vs 5.7 mths) in addition to therapeutic response rate. Interestingly, the study also observed combination therapy to be more efficacious in mBC patients with HER positive status; this however is undergoing further investigation in further trials (*Roche*).

Phase III Trial

Unfortunately the first published Phase III trial proved unsuccessful. The study evaluated second line treatment of mBC patients using Bz in combination with capecitabine (2500mg/m2/d, twice daily for 14 days followed by a 7 day rest period then Bz 15mg/kg on day one of each 3 week cycle) compared with capecitabine monotherapy (2500mg/m2/d, twice daily for 14 days followed by a 7 day rest period) in 462 patients who had undergone previous anthracyclines and taxanes treatment (***Miller et al. 2005***). There was increased overall response rate (9.1 vs. 19.8%) in patients treated with the combination therapy; however median progression free survival (PFS; 4.9 vs. 4.2 months) and overall survival (OS; 15.1 vs. 14.5 months) remained relatively unchanged between the two groups (***Miller et al. 2005***).

However, a second Phase III (E2100) trial followed, where previously untreated mBC patients were administered with either paclitaxel alone (90mg/m^2 weekly for 3 of 4 weeks) or in combination with Bz (10mg/kg every 2 weeks). There were significant increases in PFS in the combination group (11.8 vs. 5.9 months), increased ORR (36.9%vs. 21.2%) but the OS however remained unchanged (***Miller et al. 2007***). Interestingly a follow up investigated any role of

polymorphisms in the VEGF or VEGF-R2 gene on the efficacy and safety profile of Bz combination treatment and any value as biomarkers, found that certain SNPs increased the OS observed in response to Bz combination therapy (***Schneider et al. 2008***). The E2100 study resulted in Bz being granted FDA accelerated approval on the basis that further investigations would follow, thus the AVADO and RiBBON studies were instigated.

AVADO

The AVADO study was a randomised, double-blind trial that investigated the effects of Bz (7.5mg/kg and 15mg/kg every 3 weeks) in combination with 3-weekly docetaxel (100mg/m2) as first line treatment for HER2 negative mBC (***Miles et al, 2010***). The primary endpoint for this study was PFS and a large number of other parameters such as OS, DR, safety, premature withdrawal due to adverse effects and best overall response observed at secondary endpoints. The primary endpoint of this study was met, with PFS being statistically (p=0.006) increased in the Bz (15mg/kg) combination treated patients compared to the placebo group (10.1 vs. 8.2 months respectively). The lower dose of Bz (7.5mg/kg) also resulted in increased PFS compared to the placebo (9.0 vs. 8.2 months respectively) however this increase was not statistically significant (***Miles et al, 2010***). Of the secondary endpoints only the overall response rate was statistically improved in Bz treated groups, with no significant differences being observed in OS, a similar finding to the E2100 trial. Grade 3-4 adverse events of particular interest (e.g. hypertension, neutropenia and febrile neutropenia) were more commonly observed in both the Bz groups compared to the placebo group (78% and 75% vs. 67% respectively). In addition, other grade 3-4 events (such as peripheral odema) were higher in the placebo group compared to the Bz treated groups (2.6% vs. 1.2% and 0.4% respectively). However this is largely expected as, Bz potentially acts by 'normalising' the vasculature, thus making it less leaky, hence decreasing the incidence of odema present. However, the overall safety profile of Bz was reported in the AVADO trial was that of reasonable tolerance.

The first clinical investigation combining Bz with standard chemotherapy in breast cancer observed that previously treated patients exhibited a 2.2% increase in congestive heart failure (3.1% vs. 0.9%) (***Miller et al. 2005***). The safety profile of Bz is still under investigation and the RiBBON1/2 studies have been designed to determine whether previous treatment increases the incidence and severity of adverse effects of Bz combination therapy (***O'Shaughnessy and Brufsky 2008***).

RiBBON-1 and RiBBON-2

Despite the accelerated approval of Bz following the E2100 trial, there were still a number of key questions that needed further addressing with regards to Bz treatment in mBC, in particular the safety profile of Bz. The RiBBON trials have been designed to determine whether previous

treatment increases the incidence and severity of the adverse effects of Bz combination therapy, since previous studies looked at Bz in the first line therapy setting (***O'Shaughnessy and Brufsky, 2008***). The Phase III RiBBON-1 and RiBBON-2 studies assessed the safety and efficacy of Bz in combination with a broad spectrum of chemotherapeutic agents (taxane based therapy, anthracycline based regimens or capecitabine) in two groups of HER2 negative patients, (1) patients with untreated mBC (RiBBON-1) and (2) patients with previously treated mBC (RiBBON-2).

The RiBBON-1 trial demonstrated a similar profile of response to the AVADO study, whereby the more severe adverse events were higher in the Bz combination (***Robert et al, 2011***). Due to the high incidence of adverse events that were grade 3 or above associated with the addition of Bz to the chemotherapeutic drugs, the addition of further treatment agents are limited.

In the RiBBON-2 trial the addition of Bz to taxane, gemcitabine or capecitabine improved PFS marginally (~2.1 month improvement) whereas adding Bz to vinorelbine resulted in no further efficacy. In the RiBBON-2 study the number of severe events was much higher in the Bz treated group, and the number of patients that discontinued treatment due to severe adverse events was twice that in the Bz treated group compared to the control group (13.3% vs. 7.2% respectively) (***Brufsky et al, 2011***).

Recent/On-going Trials with Bevacizumab

In 2011, Bz was withdrawn by the FDA for use in mBC, following much deliberation. Withdrawal of Bz in the indication of mBC treatment was due to the lack of clinical benefit in patients and severe toxicity. However despite the withdrawal of Bz from breast cancer treatment by the FDA, clinical trials assessing Bz in combination with a number of different agents under different clinical settings are currently still underway. These studies are important to determine the reasons that Bz failed to reach the initial expectations for use in breast cancer, and may allow more optimal regimes of the drug to be instigated.

A recent study consisting of 1206 patients with primary operable HER2 negative breast cancer, evaluated the effects of Bz in combination with capecitabine or gemcitabine plus docetaxel followed by doxorubicin and cyclophosphamide (***Bear et al, 2012***). Patients were randomised into one of three chemotherapy groups and received either (1) four cycles of docetaxel (100mg per square metre, i.v. on day one of each cycle) every three weeks followed by four cycles of doxorubicin-cyclophosphamide (60mg and 600mg per square metre respectively, i.v.) every three weeks, (2) capecitabine (825mg per square metre, orally) twice a day for the first 14 days followed by docetaxel (75mg per square metre, i.v. on day one) followed by doxorubicin-cyclophosphamide (as above) or (3) gemcitabine (1000mg per square metre, i.v.) on day 1 and 8 followed by docetaxel (75mg per square metre, i.v. on day one) followed by doxorubicin-

cyclophosphamide (as above). From the three chemotherapy groups, half of the patients in each group was randomised to receive Bz (15mg/kg i.v.) every three weeks (***Bear et al, 2012***).

Pathological complete response (pCR) was the primary endpoint for the trial. This trial suggests that in this particular cohort of patients, the addition of capecitabine or gemcitabine to the docetaxel/doxorubicin/cyclophosphamide (DDC) regimen has no additive effect on the pCR rate compared to DDC alone (29.7%, 31.8% and 32.7% respectively) (***Bear et al, 2012)***. Interestingly the addition of Bz improved the rate of pCR, with hormone receptor positive tumours demonstrating an increased response to Bz treatment compared to hormone receptor negative (***Bear et al, 2012***), suggesting that Bz may be more effective in the less aggressive hormone positive phenotype.

Bz was initially approved as first line therapy for patients with HER2 negative metastatic breast cancer however after the withdrawal of Bz in the over-arching classification of patients, the use of Bz in other breast cancer settings is being investigated. A single-arm Phase II clinical trial (EGF103890) assessed the efficacy and safety of combining Bz with lapatinib (dual tyrosine kinase inhibitor of both HER2 and epidermal growth factor receptor) on 52 patients with HER2 positive metastatic breast cancer (***Rugo et al, 2012***). It has previously been shown that HER2 over-expressing tumours also have increased expression of VEGF (***Rugo et al, 2012***) thus combining a HER2 targeting antibody with Bz is a valid approach in overcoming the resistance observed in breast cancer patients treated with HER2 targeting agents alone. Most patients in this study had previously been treated with chemotherapy and/or Herceptin prior to participation. The patients were considered as heavily pre-treated, as most had previously received a median of 3 chemotherapy regimes and Herceptin (median exposure 84.1 weeks) treatment for the metastatic disease (***Rugo et al, 2012***). Patients received lapatinib (1500mg, orally) daily with Bz (10mg/kg i.v.) every two weeks until disease progression, the presence of severe toxicities or withdrawal of consent from the patient with the primary endpoint being PFS at the end of week 12 of the trial (clinical data not yet published) (***Rugo et al, 2012***)

In addition to the trials described, there are still a large number of clinical trials underway, evaluating the most appropriate regime for using Bz in the treatment of breast cancer, these include; BEATRICE (triple negative patients, treated with Bz after surgery), BETH (HER2 positive patients after tumour has been resected), MO19391 (safety trial of Bz in combination with taxane based chemotherapy) and the E5103 (non-metastatic BC) trials.

1.6.6 Clinical side effects of Bz

Since Bz targets VEGF signalling but does not differentiate between the tumour vasculature and the normal vasculature, it is possible that side effects such as impaired wound healing may be present with Bz treatment. The clinical side effects of Bz as stated by the FDA are divided into (**1**) serious side effects associated with Bz and (**2**) milder, more commonly observed side effects due to drug interaction. The serious side effects caused by Bz administration include gastrointestinal perforation, impaired wound healing, serious bleeding that potentially leading to stroke or death, heart failure and kidney damage. The more commonly seen adverse effects include high blood pressure, proteinuria, weakness, thrombophlebitis, diarrhoea, reduced white cell count, headaches, loss of appetite and mouth sores.

All of the studies following on from the E2100 trial, although have shown an increase PFS and ORR with Bz added to a number of different standard chemotherapeutic agents currently used for the treatment of mBC, no study has reproduced the results originally observed in the E2100, where a doubling of the PFS was observed in the Bz arm. Thus, with the results from the AVADO and RiBBON trials, actual clinical benefit of Bz when compared to the increased severe adverse events must be considered. The use of Bz in mCRC has proven successful in the clinic which further questions the benefit of using Bz for the treatment of mBC, especially with Bz being an extremely costly drug. Consequently Bz was withdrawn by the FDA in 20122 for use in mBC, however there are still a number of ongoing studies evaluating the use of Bz in different breast cancer sub-types and biomarker based studies suggest that the clinical benefit of Bz may be masked by treatment of a mixed population of breast cancer patients. The identification of breast cancer sub-populations from these biomarker studies may indicate which patients are most likely to benefit from Bz treatment (***Schneider et al, 2008; Miles et al, 2013***). These biomarker studies may also allow potential identification of resistance pathways to Bz treatment.

1.7 Modes of Anti-Angiogenic Resistance

Despite some clinical success being observed with Bz in the treatment of mBC, OS remains relatively unchanged and eventually patients relapse. There are several possibilities as to why initial response to Bz treatment is not maintained and tumours escape this therapy. One reason for eventual resistance to Bz therapy is that tumours become less dependent on VEGF. VEGF is crucial in stimulating the process of blood vessel development but maintenance of the vasculature may not be dependent on the continual presence of VEGF. Inhibition of VEGF signalling may initiate production of other pro-angiogenic factors (FGF-2, PDGF, Delta/Jagged family and Angiopoietins) by the tumour or surrounding stroma (***Prager et al, 2012***) thereby allowing progression of the tumour in the presence of Bz. This re-iterates that VEGF targeted

treatment such as Bz would prove to be more efficient if administered as first line therapy. Secondly, other components of the tumour vasculature, such as pericytes, fibroblasts, macrophages and mesenchymal stem cells are not targeted by Bz and have not been considered in terms of the role that they may play in the efficacy of drug treatment (***Shojaei and Ferrara 2008; Roland et al, 2009; Prager et al, 2012)***. Thirdly, anti-angiogenic agents such as Bz, although thought to normalise the vasculature, if successful, eventually cause the collapse of existing tumour associated vessels. Following this, intra-tumoural hypoxia levels are thought to increase. Hypoxia induced post treatment, can induce a number of mechanisms which lead to resistance, potentially resulting in selection of more aggressive tumour cells leading to increased metastasis (***Grepin and Pages, 2010; Loges et al, 2010; Shojaei, 2012***). Fourthly, sprouting angiogenesis is not the only process by which a functional vasculature is formed, other processes include vasculogenesis, vessel 'cooption' and vascular mimicry, which are not necessarily dependent on VEGF (***Azam et al, 2010*** ; ***Loges et al, 2010***).

The existence of biomarkers and polymorphic genetic analysis indicate that certain mutations in the VEGF or VEGF receptor gene may render the patients more or less likely to respond to Bz treatment. This is turn suggests that only certain individuals will benefit from Bz treatment and thus identifying these niche patients may be the key to improving the efficacy of Bz treatment in mBC (***Schneider et al, 2008; Shojaei, 2012***). Lastly, the other possible reason for resistance to Bz treatment is the existence of alternative VEGF signalling pathways (***Shojaei, 2012***). It is possible that continual inhibition of VEGF receptor signalling prompts VEGF to find alternative receptor pathways such as the recently identified neuropilin receptors. This possibility forms the basis of the hypothesis for my PhD project and is discussed in further detail in (**section 1. 4**).

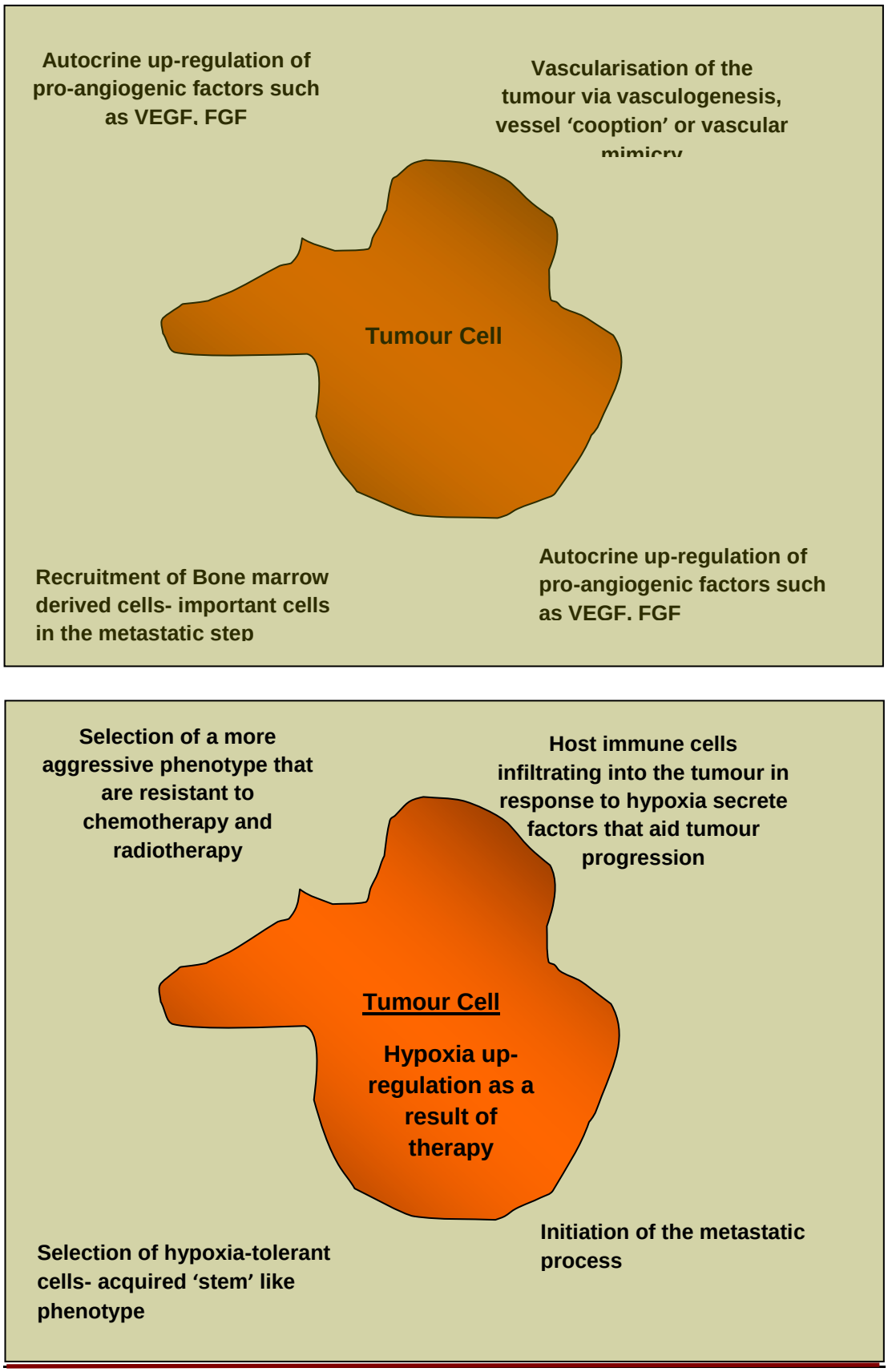

Figure 1.12 Modes of Resistance. There are a number of mechanism of escape for tumours, especially after treatment (bottom panel), a more aggressive phenotype evoked by the harsh micro-environment induced by either targeted vasculature therapy or chemotherapy. ***Adapted from Loges et al, 2010, Mechanism of Resistance to anti-angiogenic therapy and development of third generation anti-angiogenic drug candidates.***

1.7.1 Targeting Neuropilin Receptors

The rationale for targeting the neuropilin receptors is twofold, (I); there is a wealth of *in vitro* and *in vivo* data suggesting that the neuropilin receptors are important during the angiogenic process and may also directly influence breast cancer activity and (II); in the presence of Bz, the neuropilin receptor binding site on VEGF is not inhibited (**Figure 1.13**). Therefore, it is possible that the neuropilin receptors provide an alternative signalling pathway for $VEGF_{165}$ (***Loges et al, 2010***). Additionally treatment with Bz results in increased Np1 expression in patients with rectal cancer (***Xu et al, 2009***) thus may be demonstrated in breast cancer patients. More recently, a retrospective biomarker analysis of a proportion of tumour samples (n=462) from AVF2119g study (***Miller et al, 2005***) identified that patients with lower EC Np1 expression tended to respond better to combined capecitabine/Bz treatment when considering PFS, however this trend did not reach significance (***Jubb et al, 2011***). Despite this observation not proving significant, it provides evidence that Np1 may be a route via which there is escape from VEGF from anti-angiogenic therapy. Identifying relevant sub-groups of breast cancer patients is crucial in isolating those more likely to respond to Bz treatment. Possible mechanisms for inhibiting $VEGF_{165}$ and Np1 interactions for therapeutic targeting can be categorised as (**I**) inhibiting Np1 protein expression, (**II**) administration of a peptide that competes with $VEGF_{165}$ for the Np1 binding site and (**III**) inhibition of the interactions between the neuropilins and the VEGF receptors (***Gabhann and Popel 2006***).

1.8 Conclusion & Hypothesis

It is evident that tumour angiogenesis is not only a critical but also a complex process in tumour progression. The fact that tumour angiogenesis is a multi-step pathway offers many targeting options and a number of 'windows of opportunities'. However, the complexity and mechanism of the components regulating the process must be fully understood if successful long term therapy is to be achieved. VEGF is a key player in both initiating and maintaining tumour angiogenesis and thus is an ideal candidate for anti-tumour targeting. Anti-VEGF therapies have shown some clinical success, such as Bz, but unfortunately the efficacy of the treatment is short-lived since OS of mBC patients remains relatively unchanged in the presence of Bz in combination with chemotherapy. The introduction to this project discusses the possible mechanisms of tumour escape from Bz treatment, with a particular focus on neuropilins. The neuropilins evidently play a role in both enhancing VEGF signalling via VEGF-R1/R2 and by independent signalling via NIP, with experimental data revealing the reduction of tumour growth via EC regulation in the presence of anti-neuropilin treatment. Based on the information available in the literature, the following hypothesis has been proposed (**Figure 1.13**) and will be evaluated in this thesis.

Hypothesis:

"The addition of a neuropilin peptide will increase efficacy of Bz therapy in breast cancer."

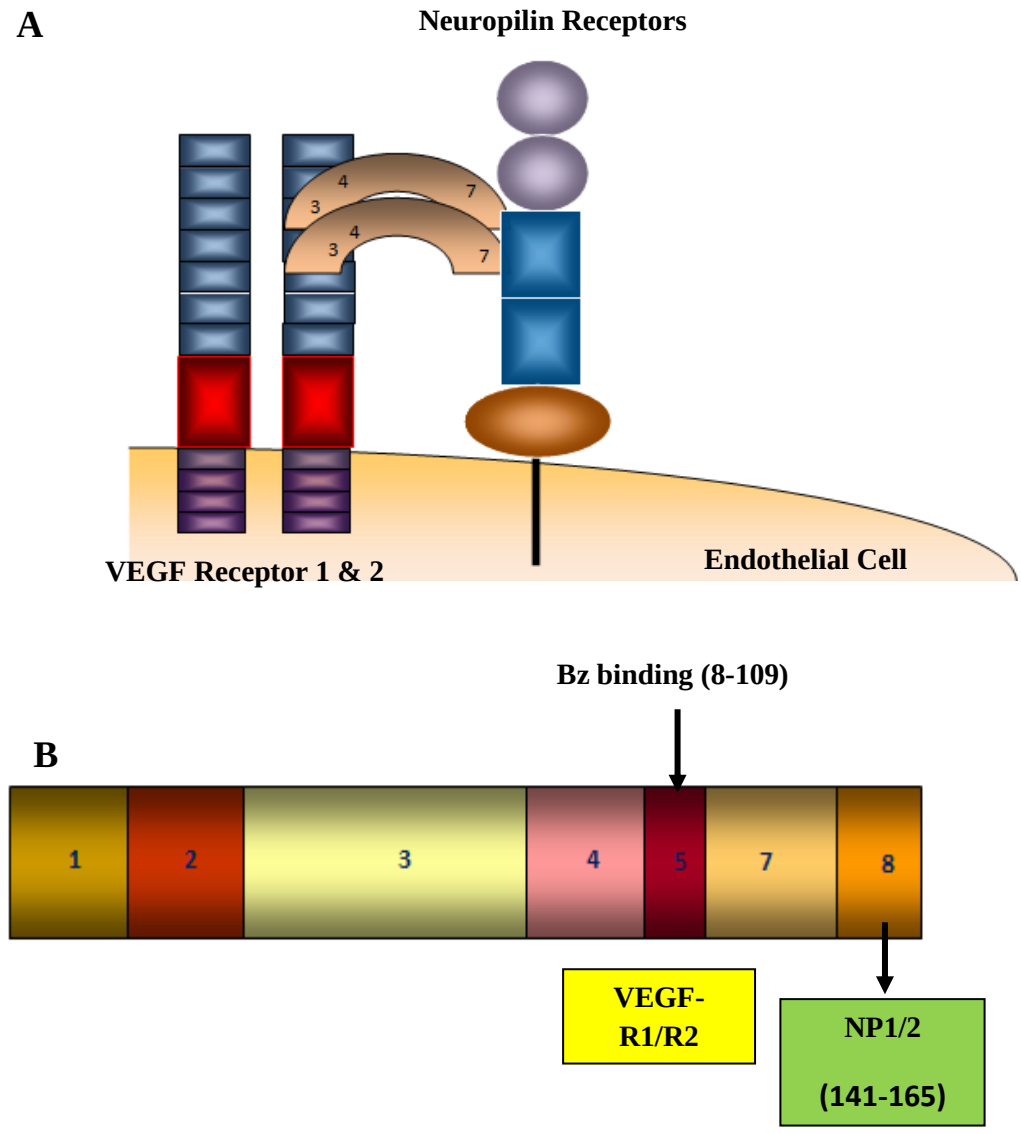

Figure 1.13*Possible Mechanism of Escape:*

A diagram to illustrate the proposed mechanism by which may escape Bz treatment control. (**A**) VEGF can to bind either VEGFR1 or VEGFR2 and neuropilin receptors simultaneously as the binding sites on the VEGF gene differ, with VEGFR1 & R2 binding at VEGF exon 3 and 4 respectively and neuropilin binding occurring at exon 7 of the VEGF gene. (**B**) In the presence of Bz, the VEGF binding site for the neuropilin receptors remains uninhibited potentially providing VEGF with an alternative pathway for action.

1.8. 1 Project Aims

The hypothesis will be tested by the following aims:

1. Investigate protein expression of $VEGF_{165}$ and it's four receptors, VEGFR1, VEGFR2, Np1 & Np2 in the following cell lines: (1) Human Dermal Micro-Vascular Endothelial cells (HuDMECs) and (2) two breast cancer cell lines (two highly metastatic; MDA-MB-231 and MDA-MB-436).
2. Investigate the *in vitro* effects of Bz and four Np1 binding peptides either alone or in combination on the functional activity of both endothelial and breast cancer cells.

Evaluate the most active Np1 peptides identified *in vitro*, in both the primary and metastatic disease *in vivo* model.

EQUIPMENT AND PLASTICS

ITEM	SUPPLIER
Anaesthetic Machine	Biological Services
7ml Bijou Tubes	Corning
Centrifuge	Sanyo Harrier 18/80
Coverslips	Fischer Scientific
0.5ml and 1.5ml Eppendorf	Sarstedt
Filter Pads	Biorad
Glass Slides	Fischer
1ml Insulin Syringes	Biological Services
Inverted Phase Contrast Microscope	Leica
IVIS Lumina II	Caliper
Micro-CT Machine	SkyScanner
Pasteur Pipettes	Costar
8µM Pore Membrane (Polycarbonate)	Neuro Probe
Pipette Bouy	Starlabs
P2, P10, P20, P200 and P1000 Pipettes	Gilson
P2, P10, P20, P200 and P1000 Pipette Tips	StarLabs
Plate Reader	Fluorstar
Rocking Platform	Sanyo
SDS PAGE Tank	Biorad
Semi-Dry Western Blot Transfer	Biorad
5ml, 10ml and 25ml Stripettes	Corning
96-well Tissue Culture Flat Bottomed Plate	Costar
T25cm^3, T75cm$_3$ and T`175cm^3 Tissue Culture Vented Flasks	Corning
Tissue Culture Cabinet Hoods (Cell Line & Primary Cells).	Heraeus
Vortex	Whirlmixer
ViCell Counter	Beckman Coulter
Western Blot Film	GE Healthscience

REAGENTS

REAGENT	SUPPLIER
ABC Standard Peroxidase Kit	Vector
Acetic acid (Analar)	VWR
30% Acrlaymide	Geneflow
APS (10%) 50mg stored at r.tp (500µl dH_2O added prior to use).	Sigma
BCA Solution	Sigma
Bz	Roche
Blocking Milk 5g dried milk powder in 100ml PBST/TBST	Marvel
BSA	Sigma
BSA Standards 2mg/ml stock diluted to various concentrations (0-1mg/ml) using dH_2O. Store at 4^0C.	Sigma
saturated Butan-2-ol	Sigma
Caesin	Vector
anti-Caspase 3 antibody ()	Abcam
anti-CD34 antibody (ab8158)	Abcam
Copper II Sulphate Solution	Sigma
DAB In 2.5ml add 1 drop of buffer, 2 drops DAB solution and 1 drop	Vector
Developing Solution Add 105ml developing solution to 473ml dH_2O.	Kodak
Dimethylformamide	Fischer
DMEM Media (with ultraglutamine) Cell culture medium used for culturing human MDA-MB231 breast cancer cells. Supplemented with 5%v/v P/S, 5% Fungizome and 10% v/v FCS. Media was stored at 4^oC and was brought to r.t.p prior to use.	Lonza

EBM2 Media	Lonza
Eosin	Sigma
Ethanol (100%)	Sigma
FCS	Lonza
Fibronectin	Sigma
Fixing Solution Add 105ml fixing solution to 473ml dH_2O.	Kodak
Fungizone	Lonza
Gill's Haematoxylin	Sigma
Anti-goat biotinylated secondary antibody	Vector
Goat Serum	Vector
Growth Factor Reduced Matrigel Aliquot and stored at -20^{O}c. Defrosted on ice prior to use.	BD Biosciences (VWR Supplier)
L-Glutamine	Lonza
Hamatoxylin Solution	Sigma
HBSS	Promo Cell
HCL	Sigma
Horse Serum	Vector
Hydrogen Peroxidase	Sigma
HuDMECs	Promo Cell
Isoflurane	Biological Services
anti-Ki67	DAKO
Lectin	Vector
D-Luciferin, Potassium Salt (#122796)	Caliper Life Science
Mammalian Cell Lysis Kit Stored at 4^{0}c, bring to r.t.p prior to use. Add 200µl of each component to adherent cells in culture prior to use	Sigma
MDA-MB-231 Human Breast Cancer Cells	ATTC- kindly gifted by Dr. Ingunn Holen
MDA-MB-231 Luciferase Labelled Human Breast Cancer Cells	Caliper Life Sciences, UK
MDA-MB-436 Human Breast Cancer Cells	ATTC
Methanol	Sigma
MITC	Sigma

Anti-mouse biotinylated secondary antibody	Vector
Mouse Serum	Vector
MTS Reagent	Promega
NaOH	Sigma
Naphthol AS-BI phosphate (sodium salt)	Sigma
Anti-Neuropilin 1 (Western Blot Analysis)	Abcam
Anti-Neuropilin 1 (IHC Analysis)	Santa Cruz Biotechnology
Neuropilin 1 Binding Peptides	Prof. Kurt Ballmer-Hofer (*in vitro* use) Severn (*in vivo* use)
Anti-Neuropilin 2 (Western Blot Analysis)	Abcam
Anti-Neuropilin 2 (IHC Analysis)	Santa Cruz Biotechnology
Paraformaldehye	Sigma
Pararosaniline	Sigma
Penicillin/Streptomycin Store at -20^{o}C in 5ml aliquots.	Invitrogen
PBS for tissue culture	Lonza
PBS Tablets	Lonza
PBST	Sigma
Pimo	Hydroprobe
Pimo antibody ()	Hydroprobe
Protease Inhibitor Tablets	Roche
Protein plus Precision Standards	Biorad
PVDF Membrane	Millipore
Rabbit Serum	Vector
Anti-rat Biotinylated	Vector
Resolving Gel 1.5M Tris HCL pH 8.8	Geneflow
RPMI Media Used for culturing human MDA-MB-436 breast cancer cells. Supplemented with 5%v/v P/S, 5% Fungizome, 1% L-Glutamine and 10% v/v FCS. Once supplemented, media was stored at 4^{o}C and was brought to r.t.p prior to use.	Lonza

Saline	Field Labs
SDS (10%) 10g in 100ml dH_2O. Stored at r.t.p	Biorad
Sodium acetate trihydrate	Sigma
Sodium Citrate	Sigma
Sodium nitrite	Sigma
Sodium tartrate (dihydrate)	Sigma
Stacking Gel 0.5M Tris HCL pH 6/8	Geneflow
Stripping Buffer	Pierce
Super Signal West Dura Mix 1ml Reagent A and B	Pierce
TEMED	Sigma
Transfer Buffer (10x) For 1x buffer, add 100ml methonal to 100mls 10x buffer and make up to 1L with dH_2O. Stored at r.t.p	Geneflow
Tris Base	Sigma
Trypsin/EDTA Store at -20^{o}C in 50ml aliquots.	Sigma
Tween20	Sigma
anti-VEGF antibody (IHC)	Santa Cruz Biotechnology
anti-VEGF antibody (Western Blotting)	Abcam
anti-$VEGF_{165b}$	R&D systems
Recombinant VEGF165 Stock concentration at 2μg/ml stored at -20^{0}C.	R&D systems
Recombinant VEGF165b Stock concentration at 2μg/ml stored at -20^{0}C.	R&D systems
anti-VEGF-R1 antibody (IHC)	abcam
anti-VEGF-R1 antibody (Western Blotting)	Santa-Cruz Biotechnology
anti-VEGF-R2 antibody (IHC)	abcam
anti-VEGF-R2 antibody (Western Blotting)	Santa-Cruz Biotechnology
Wax pen (IHC)	Vector
Xylene	VWR

Chapter Two

Materials & Methods

2.1 Cell Culture

All cell culture work was carried out in a Class II safety cabinet under sterile conditions. The cabinets were switched on 15 minutes prior to use and were thoroughly cleaned with 70% ethanol before and after use and between different cells lines. A lab coat and gloves were worn at all times and all equipment and bottles were cleaned with 70% ethanol prior to placing in the cabinet. All reagents used during cell work were opened in the cabinet to sustain sterile conditions. A change over time of 10-15 minutes was allowed between different cell lines to minimise potential cross contamination.

2.1.1.Cell Line Characteristics

The human dermal microvascular endothelial cells (HuDMECs) used for experiments are primary endothelial cells derived from the dermis, purchased as proliferating cells from Promo Cell, UK: (it is also important to note that the HuDMECs reach senescence at higher passages and can also differentiate over time; therefore were always used at passage 6 or less). The MDA-MB-436 breast cancer cell lines were obtained from the American Type Tissue Culture Collection (ATCC), USA: and the MDA-MB-231 cells (from the ATCC) were kindly donated by Dr Ingunn Holen. Both breast cancer cells were isolated by pleural effusion from patients with primary adenocarcinomas in the mammary gland. Both the MDA-MB-231 and MDA-MB-436 breast cancer cells lines are oestrogen (ER) and progesterone (PR) receptor negative and are tumourgenic *in vivo* (**Table 2.1**). Two metastatic breast cancer cells were used as the main focus was targeting breast cancer cells with a metastatic potential. In addition, with the increased interest in personalised medicine (***Cho et al, 2012***) and the further sub-classification of breast cancer (***Kao et al, 200; Holliday and Speirs, 2011***), the use of two metastatic breast cancer cell lines, that are seemingly similar were used to allow identification of downstream effectors that may be responsible for any differential responses to therapy.

	ER receptor status	PR receptor status	HER status	p53 status	Tumourgenicity	Breast Classification
MDA-MB-231	Negative	Negative	Negative	Mutant	Highly Metastatic	Basal-like
MDA-MB-436	Negative	Negative	Negative	Mutant	Metastatic	Basal-like

Table 2.1 ***Breast Cancer Cell Line Characteristics:***
Summarises the properties of the two human breast cancer cell lines used. Although the breast cancer cell lines are similar in many aspects, there are mutational differences that could result in differential response to treatment. The use of two metastatic breast cancer cell lines may provide means of identifying markers or downstream activators involved in resistance to therapy in advanced breast cancer.

2.1.2 Cell Sub-Culture

The HuDMECs were maintained in Microvascular Endothelial Media (EBM-2) supplemented with 0.4% ECGS/H, 5% FCS, 10ng/ml epidermal growth factor and 1µg/ml hydrocortisone. The breast cancer cell lines were maintained in either DMEM Ultraglutamine (MDA-MB-231) or RPMI 1640 media supplemented with 1% L-Glutamine (MDA-MB-436) with 10% FCS, 1% P/S & 1% fungizone. Cells were monitored daily using an inverted phase light microscope and alternate days cells were washed with PBS/HBSS and media replaced to keep the cells nourished. Cells were allowed to proliferate to x~80% confluency after which they were harvested. Prior to harvesting, the cell media, trypsin-EDTA, trypsin inhibitor and PBS/HBSS were brought to room temperature to avoid any cell damage.

When harvesting the HuDMECs, old media was aspirated and discarded, and cells were then washed twice with 5ml HBSS to remove any excess FCS in the media, that may have inhibited the detachment of the cells from the flask. The adherent HuDMECs were detached from the flask by adding 3ml trypsin solution; the detachment of the cells was monitored under the microscope until ~90% of the cells were observed to be rounded up. At this point the flask was gently tapped to lift the cells from the surface and 3ml of trypsin neutralising solution was added. Cells were then centrifuged at room temperature for 5 minutes at 1000rpm, the supernatant discarded and the cells re-suspended in 3-4ml of cell culture media, and the relevant volume of cells was added to a new, sterile T75 flask containing 10ml media and then placed in the primary cell incubator (37^0C, 5% CO_2).

When harvesting the breast cancer cell lines, the same procedure was followed as described above except that detachment of the cells was carried out by adding 3ml trypsin solution followed by incubation of the cells for no longer than 5 minutes in the 37^{o}C cell line incubator. The trypsin reaction was inhibited by adding, 7ml of the relevant cell culture media; cells were then pelleted at 1000rpm for 5 minutes and re-suspended as previously described for the HuDMECs.

2.1.3 Freezing Cells

HuDMECs

Upon receiving a fresh batch of HuDMEC cells, the cells were placed in the 37^{o}C incubator for a minimum of 2 hours to allow the cells to acclimatise, after which the cells were trypsinised and pelleted (section 2.1.2). The cells were re-suspended in Cryo-SFM (serum free media) and counted before diluting to a minimum of 1x10^{6} cells/ml. The cryogenic vials containing 1ml cells were placed in a Mr Frosty, containing isopropanol solution and stored at -20^{o}C for an hour and than -80^{0}C overnight, to freeze the cells gently, after which the cells were placed in liquid nitrogen.

Breast Cancer Cells

The breast cancer cells were frozen down when they were ~ 70% confluent and were still in exponential growth phase to ensure that cells would be healthy when thawed for use. Breast cancer cells were trypsinised as described above (2.2.1) and centrifuged at 1000rpm for 5 minutes, the supernatant was discarded and the cells were re-suspended in normal culture media containing 10% DMSO. 1ml of the cell solution at a minimum cell density of 5x10^{5} cells/ml was then aliquoted into cryovials and stored at -20^{o}C for an hour and than -80^{0}C overnight, before moving into liquid nitrogen storage.

2.1.4 Thawing Cells

Prior to removing the cells from liquid nitrogen the relevant culture media was pre-warmed and 9ml was added to a sterile T75cm^{3} flask. The vial of cells was placed in the 37^{o}C water-bath until ~ 90% of the cell solution had thawed. The vial was thoroughly wiped with 70% ethanol, after which the cells were added to the sterile flask and placed in the incubator. After 24 hours the media containing DMSO was replaced with fresh media and the cells cultured as described previously.

2.1.5 Mycoplasma Testing

Routine mycoplasma testing was carried out by PCR on cell culture on initial arrival and every six months thereafter. The cell cultures were also tested after revival from frozen stocks.

2.2 Protein Expression-Western Blotting

Protein expression was determined using SDS-PAGE/Western Blot analysis, which is a highly selective technique that is used for detecting proteins in a given sample. The proteins are resolved by SDS-PAGE and are then detected using specific antibodies raised against the protein of interest.

2.2.1 Protein Extraction

Cells were grown to 70-80% confluency, then serum starved overnight prior to protein extraction. 70-80% confluency is considered optimum for protein extraction as over confluent cells generally show reduced levels of protein production. Prior to carrying out the cell lysis procedure, the cell lysis buffers were allowed to reach room temperature. Following this, conditioned media from the cells was aspirated and collected in a 15ml falcon tube for analysis of proteins released by the cells. The media was centrifuged at 1000rpm for 4-5minutes to remove any debris and 5ml of this conditioned media was retained and stored at -20^{o}C until use. Protein extraction was carried out using a mammalian cell lysis kit (Sigma) which contained 200µl of each of five different denaturing detergents (section 2.1) that cause the cell membrane to rupture, allowing cellular proteins to be suspended in the solution for subsequent isolation. The cells were washed twice with 5ml PBS to remove any residual FCS followed by the addition of 1ml of the mammalian cell lysis buffer containing 20µl of protease inhibitor. The cells were then placed on a mechanical rocker for 20 minutes at room temperature, then scraped off the surface of the flask and added to a 15ml falcon tube. The cell suspension was then syringed using a 25mm gauge needle to further disrupt the cell membrane before centrifugation at 1000rpm for 4-5 minute. The supernatant containing the proteins of interest was then pipetted into a sterile 1.5ml eppendorf tube and stored at -20^{o}C till required or -80^{o}C for long term storage.

2.2.2 Protein Estimation: Bicinchonic Acid Protein Assay

Protein quantification is a vital step when investigating protein expression, especially when comparing expression levels of a particular protein in a number of different cell types as it allows the protein concentration to be normalised between different samples so that the differences observed in protein expression can be confidently assumed as a difference in the microenvironment in different cell types or treatment groups rather than any inconsistency

in protein levels loaded onto the SDS-PAGE gel. Ideally a minimum of 20µg/sample should be loaded on the gel to ensure detection.

The Bicinchonic Acid Protein Assay (BCA) quantifies protein concentration on the ability of proteins to reduce Cu^{2+} to Cu^{1+}. BCA is able to then form a complex with the $Cu1^{+}$ ion, which in turn causes a colorimetric reaction (from light green to purple) and the intensity of the purple colour is directly proportional to the levels of protein in the solution. The assay works by generating a standard curve of known protein concentrations (Bovine serum albumin, BSA) and then extrapolating the concentrations of the unknown samples from the graph plotted (**Figure 2.1**). The BCA assay was performed in triplicate for individual samples each time protein extracts were isolated.

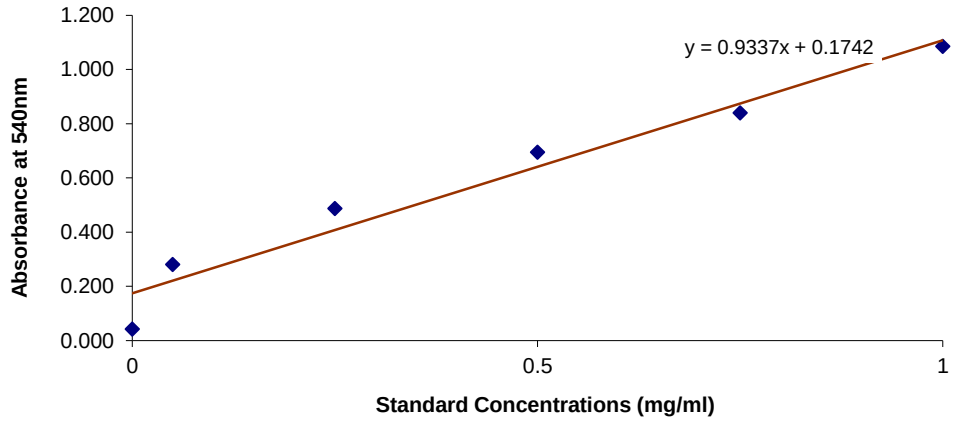

Figure 2.1 ***Protein Estimation-BCA Assay***:
Absorbance values of the standards were plotted onto a graph and then the protein concentration of the cell lines were extrapolated from the line of best fit from the standard curve. The BCA assay was repeated each time protein lysates were extracted.

2.2.3 SDS-PAGE

In order to separate the different proteins contained within the each sample, the protein samples were resolved on a Sodium Dodecyl Sulfate Polyacrylamide gel Electrophoresis (SDS-PAGE) gel. The SDS-gel technique allows separation of proteins on the basis of size in the presence of an electrical field.

Prior to casting the SDS gel, 1.5mm Biorad glass plates were cleaned using 70% ethanol to remove any residual particles that may interfere with the even running of the gel. The resolving gel was then pipetted between the two glass plates using a 5ml pipette, leaving a gap of approximately 1-1.5cm from the top of the plates. A thin layer of water saturated

butan-2-ol was added to the resolving gel (**see appendix**) to ensure that an even surface was produced thus allowing uniform separation of the individual bands in the sample to occur. The gel was left to set for ~45 minutes, using the excess resolving gel as a guide and once the gel had set, the butan-2-ol was thoroughly washed off using distilled water. The stacking gel (**see appendix**) was then added on top of the resolving gel and a 9 well (1.5mm) comb was placed between the two glass plates. The gel was then left to set for 20-30 minutes, again using the excess gel as a guide. Once the stacking gel had set, the well combs were carefully removed to avoid tearing of the wells. The plates were then placed in the Biorad gel running apparatus, the tank was filled and the wells rinsed out with 1x Running Buffer (**see appendix**) to remove any unattached acrylamide.

Samples were diluted to the same concentration (~20µg/well) and 4x loading dye or 10x reducing agent (**see appendix**) was added to each sample. The samples were then mixed by briefly vortexing and centrifuging, prior to further denaturation by heating to 95^{o}C for 5 minutes, with the lids of the tubes open. Using the fine western pipette tips, 10µl of the Precision Plus Kaleidoscope protein marker was loaded into the first well and 60µl of each sample in the subsequent wells. The SDS tank lid was connected to the Biorad power pack and the gel was then left to run at 100V until the markers had appropriately separated. Once the gel had finished running, the plates were removed from the apparatus and were carefully opened. The stacking gel was removed using the Biorad plate separator and discarded and the resolving gel was then placed in 1x transfer buffer (**see appendix**).

2.2.4 Western Blotting

Once the proteins had been separated on the SDS gel, they were transferred onto a PVDF membrane using the Semi-Dry western blotter. Prior to loading on the semi-dry blotter, the filter pads and the SDS gel were equilibrated in 1x transfer buffer for approximately 20 minutes. The PVDF membrane was activated prior to use by incubation for 5 minutes in methanol and then transferred to the 1x transfer buffer for ~ 10 minutes. Forceps were always used to handle the PVDF membrane to minimise any background interference that may arise from non-specific proteins.

Once all the separate components of the western were fully equilibrated, they were loaded onto the Semi-Dry transfer blot apparatus. Firstly one of the pre-soaked filter pads was placed on the anode side of the apparatus and rolled out using a sterile pipette to ensure removal of air bubbles that may interfere with the transfer process. The PVDF membrane was then placed on top of the filter pad using tweezers and again rolled out to remove any air bubbles. An incision was made at the bottom right hand corner of the membrane for orientation in later stages. The SDS gel was then carefully placed on top of the membrane,

taking care not to tear the gel and lastly the second filter pad was placed on top if the gel and rolled out (**Figure 2.2**). The power pack was then set at 15V and the blot was left to transfer, with the transfer time being dependent on the size of the protein of interest. It is important to optimise transfer time, as too little transfer time meant that the proteins did not fully transfer onto the membrane and if the transfer time was too long then there was a risk that the proteins may transfer through the membrane onto the filter pad.

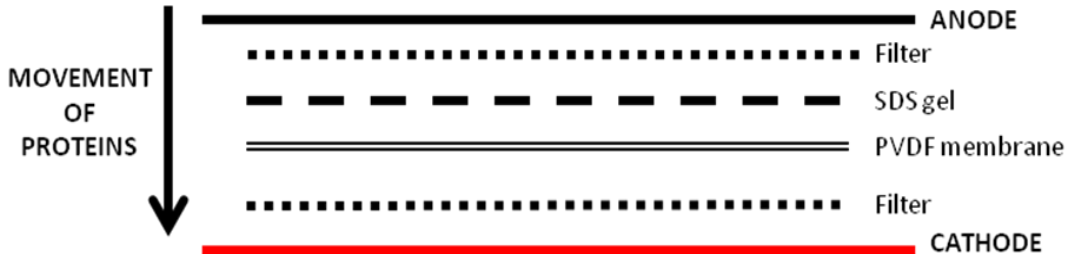

Figure 2.2: Semi-dry protein transfer set up:
Proteins move from the negatively charged anode to the positive cathode and are transferred onto the PVDF membrane during this movement. The rate of transfer is determined by the size of the protein of interest and the voltage set.

Once the transfer was complete the gel was placed in Commassie Blue Dye to check the efficiency of the transfer process. The membrane was transferred to a clear box and blocked with either 5% milk or a combination of 3% BSA/5% milk solution for 1 hour to minimise non-specific interactions occurring with the antibodies. The blocking solution was then removed and the primary antibody, which is raised to recognise a specific epitope within the protein of interest was added to the membrane and left to incubate overnight at 4^0C in milk.

After the overnight incubation, the membrane was incubated in the primary antibody for a further 2 hours at room temperature on the shaker to maximise binding. The membrane was then washed with PBST/TBST (**see appendix**) 3 x10 minutes after which the secondary antibody was added to the membrane and left on the shaker for 1.5 hours at room temperature. The secondary antibody was specific to the species in which the primary antibody was raised and was conjugated with Horse Radish Peroxidise (HRP). The membrane was then washed with PBST/TBST 4x 10 minutes following which 500µl of chemilluminescence super signal mix (1ml of reagent A & 1ml of reagent B) was added to each membrane and incubated for 5 minutes. Excess substrate was removed by blotting tissue paper and the membrane was placed between the plastic sheets of an x-ray cassette.

In the dark room under a red light, an x-ray film was placed above the plastic sheets and the lid of the cassette was then closed and the film was exposed for different time intervals. After exposure the film was placed in developing solution and gently swirled until bands appeared, at which point it was placed into a tray of water to remove any excess developing solution prior to placing in fixing solution until the film turned clear. Finally the film was rinsed in water and allowed to dry. A number of pilot studies were performed to optimise the conditions for each protein and these are detailed in **Table 2.2**.

Protein ⟶	**$VEGF_{165}$**	**$VEGF_{165b}$**	**VEGF-R1**	**VEGF-R2**	**NP1**	**NP2**
Blocking Reagent	5% milk in 1XPBST	-	5% milk in 1XPBST	5% milk in 1XPBST	5% milk in 1XTBST	5% milk in 1XTBST
Company	Abcam	RnD Systems	RnD Systems	Cell Signalling	RnD Systems	RnD Systems
Concentration	1:500	-	1:500	1:1000	1:1000	1:500
Incubation Time	overnight	-	overnight	overnight	overnight	overnight
Temperature	4°C	-	4°C	4°C	4°C	4°C
Secondary antibody	Anti-rabbit	-	Anti-rabbit	Anti-rabbit	Anti-sheep	Anti-rabbit
Concentration	1:5000	-	1:5000	1:5000	1:5000	1:5000
Incubation Time	2 hours	-	2 hours	2 hours	2 hours	2 hours
Temperature	rtp	-	rtp	Rtp	rtp	rtp
Exposure Time	1 minute	-	10 minutes	1 hour	5 minutes	10 minutes

Table 2.2 ***Optimised Protein Detection***:
The above table summarises the conditions used for the detection of protein expression of $VEGF_{165}$ & $VEGF_{65b}$ and the four receptors. $VEGF_{165b}$ was not detected in any of the cell lines; therefore appropriate conditions were not determined.

2.2.5 Beta actin Control

Beta actin (β-actin) is a house keeping gene that is present in all human cells, thus probing for it enables protein levels to be measured in each sample and hence acts as a loading control. Therefore after exposure and development, the membrane was stripped and re-probed for β-actin as follows. Firstly the membrane was incubated with 5ml stripping buffer

on a shaker for 10 minutes. The membrane was then washed thoroughly with PBST to ensure that any trace of the stripping buffer was removed, to avoid the protein of interest being removed from the membrane. The membrane was then incubated with a β actin primary antibody (1:15,000) for 20 minutes on a shaker at room temperature and then washed with PBST on three occasions for 15 minutes. This was followed by 30 minute incubation with the secondary antibody (1:30,000) and three further, 15 minute washes, after which the membrane was developed (**section 2.2.4**). Western blotting analysis was performed a minimum of three times for each protein of interest in each cell type.

2.3 Neuropilin 1 Peptides

Targeting the neuropilin receptors is a feasible option for anti-tumour therapy as not only is the receptor expressed on cancer cells but also has shown to influence cancer cell activity. ECs also express the neuropilin receptors therefore offering a potential for dual targeting. Np1 or Np2 may provide VEGF with an alternative pathway when the classical receptors are blocked, thus providing an escape mechanism for the tumours.

The four neuropilin peptides used in my *in vitro* experiments were created and kindly supplied by Prof. Ballmer-Hofer (***Paul Scherrer Institute***). The ability of these four peptides to bind Np1 has previously been measured using surface plasmon resonance (SPR) analysis (***Cebe-Suarez et al, 2008***). Peptide 1(p1) was derived from the viral member of the VEGF-E super-family, and peptide 2 (p2) was essentially designed as a control peptide as it does not bind Np1. Peptide 7b (p7b) binds Np1 and is a human $VEGF_{165}$ variant, whilst peptide 10 (p10) is a VEGF-E derived peptide that bind Np1 and has the potential to bind Np2 also, but this was not confirmed (**Table 2.3**). Peptides were supplied as lyophilised powder. Upon arrival in the laboratory, peptides were dissolved in PBS at a concentration of 1mg/ml and then aliquoted and stored in the -80^0C freezer until use in the phenotypic assays. Due to the quantities required for the *in vivo* studies, additional peptides were ordered from a commercial source (Severn Biotech) and treated the same way.

PEPTIDE	ORIGIN	SEQUENCE	NP1 BINDING
1	Viral VEGF-E protein	GSGST**RPPR**	Yes
2	Human VEGF-A protein (control)	GSGST**EPPR**	No
7b	Human VEGF-A protein	GSGST**DKPRR**	Yes
10	Viral VEGF-E protein	GSGST**RPPR**RRR	Yes

Table 2.3 ***Np1 Binding Peptides***:
Summaries the key properties of the four Np1 peptides that were used in the *in vitro* and *in vivo* experiments. The peptides were derived from the VEGF-A and VEGF-E (based on the Np1 binding sequence of each respective variant).

2.4 Cell Differentiation-Matrigel Assay

Microvascular endothelial cells are the primary cells involved in angiogenesis and *in vitro* the human dermal micro-vascular endothelial cells (HuDMECs) have the ability to mimic the *in vivo* process of capillary formation when plated on Matrigel. Matrigel is a basement membrane preparation isolated from the Engelbreth-Holm-Swarm (EHS) mouse sarcoma, which is rich in proteins found in the extracellular matrix (BD Biosciences). The major component of Matrigel is laminin but it also contains other essential proteins that stimulate endothelial cell differentiation (**Table 2.4**). The Matrigel used in this thesis was growth factor-reduced to ensure that sufficient stimulation was observed with the addition of exogenous VEGF; if cells have ample growth factors present prior to the assay then the cells will be unresponsive to additional growth factors due to saturation.

Matrigel Component	Properties	Reference
60% Laminin	Stimulates cell adhesion, growth, differentiation & migration	Kubota et al,1988
30% Collagen IV	Promotes adhesion	Kubota et al,1988
Heparan sulphate proteoglycans (perlecan)	-	-
8% Entactin	Briding molecule, involved in structutal organisation of ECM molecules	BD Biosciences

Table 2.4 ***Components of Growth-Factor Reduced Matrigel:***
The different components that are present in the Matrigel are summarised above. Each component displays varying properties that allow for the formation of cord-like structures.
(Table adapted from BD Biosciences datasheet).

A confluent flask of HuDMECs (70-80% confluency) was serum starved (using EBM2 media with 1% FCS) for 6 hours prior to starting the Matrigel assay. The required volume of Matrigel was removed from the -20^{o}C freezer and allowed to thaw on ice in a fridge (Matrigel will set even at slightly elevated temperatures in a fridge-**see section 2.4.1** for optimisation of the Matrigel assay and **Table 2.5** for finalised conditions). All tips and the 96 well plate(s) used during the assay were pre-chilled at -20^{o}C.

Thirty minutes prior to the end of the 6 hour time point, 40µl of Matrigel was added to each test well of the 96 well plate and then placed into a 37^{o}C incubator for 30 minutes to allow the Matrigel to set. During this time, the HuDMECs were trypinised and re-suspended in 1.5mls of 1% EBM2 media; 0.5mls of the cell solution was counted using the Vi-Cell counter, which gave a total cell count of cells/ml. The relevant volume of cells was then added to sterile 1.5ml eppendorfs containing the relevant treatments and mixed by gently pipetting. 100µl of the cell/treatment solution was then added to the corresponding wells in the 96-well plate, which was allowed to sit without movement to allow the cells to adhere for 20 minutes prior to incubation at 37^{o}C incubator. Each test condition was repeated four times per experiment and each experiment was repeated a minimum of three times to allow for reproducibility and statistical analysis to be performed (student's T test or Mann Whitney U test, Sigmaplot 11 software). The cells were incubated for 16 hours, after which photographs of the whole well were taken. Two parameters for the Matrigel assay were measured; the average number of cords per field of view and the average number of branch points (**Figure 2.3**).

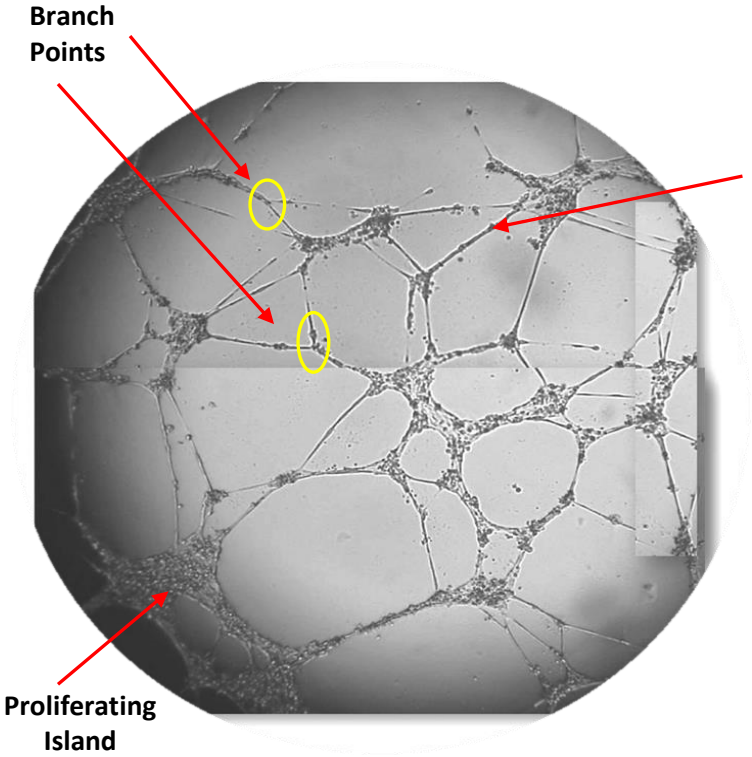

Figure 2.3 *Matrigel*
Representative image of a well (96 well plate) in the Matrigel assay observed using a phase contrast light microscope. The parameters measured for the assay were average number of cords and branch points.

2.4.1 Optimisation of the Matrigel Assay

Seeding Density

Optimisation of the number of cells seeded per well in a 96 well plate was carried out prior to beginning the test experiments. The seeding densities tested were as follows; $7x10^3$, $10x10^3$, $12x10^3$ and $15x10^3$ cells per well (**Figure 2.4**). It was decided that $7x10^3$ and $10x10^3$ cells per well were too few cells and resulted in minimal cord formation, whereas $15x10^3$ cells/well resulted in optimal cord formation and thus would be used for subsequent experiments.

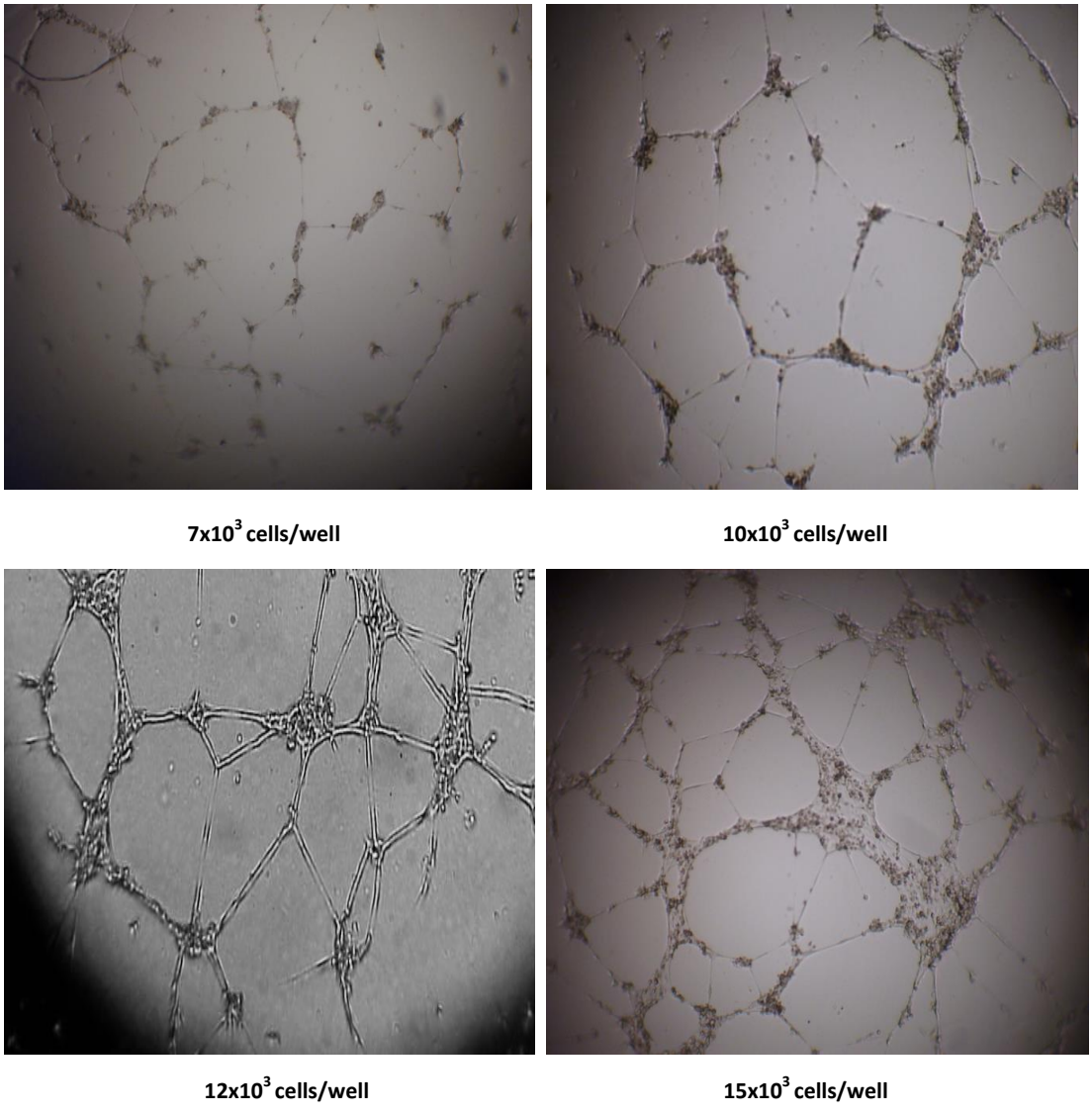

Figure 2.4 ***Matrigel Seeding Density:***
Cells were plated at varying densities in the presence of 20ng/ml recombinant $VEGF_{165}$. Optimisation of the Matrigel assay determined that sufficient cord-like structures were formed using $12x10^3$ cells/well after a 16 hour incubation period.

Determination of VEGF Concentration for the Differentiation Assay

VEGF is a potent stimulator and required for EC differentiation *in vivo* and *in vitro* and thus optimising the concentration of VEGF was necessary. A range of $VEGF_{165}$ concentrations (0-50ng/ml) were assessed (**Figure 2.5**). From the data obtained it was decided that 20ng/ml $VEGF_{165}$ would be used for subsequent experiments as this yielded a good network of cords, demonstrating defined cord formation , minimal proliferating islands and a reasonable number of cords which could be modified by treatment. This concentration also correlated with the concentration of VEGF used in the literature, where 20ng/ml of $VEGF_{165}$ is used in standard *in vitro* assays using HuDMECs (***Cross et al, 2005***; ***Hsu et al, 2012***).

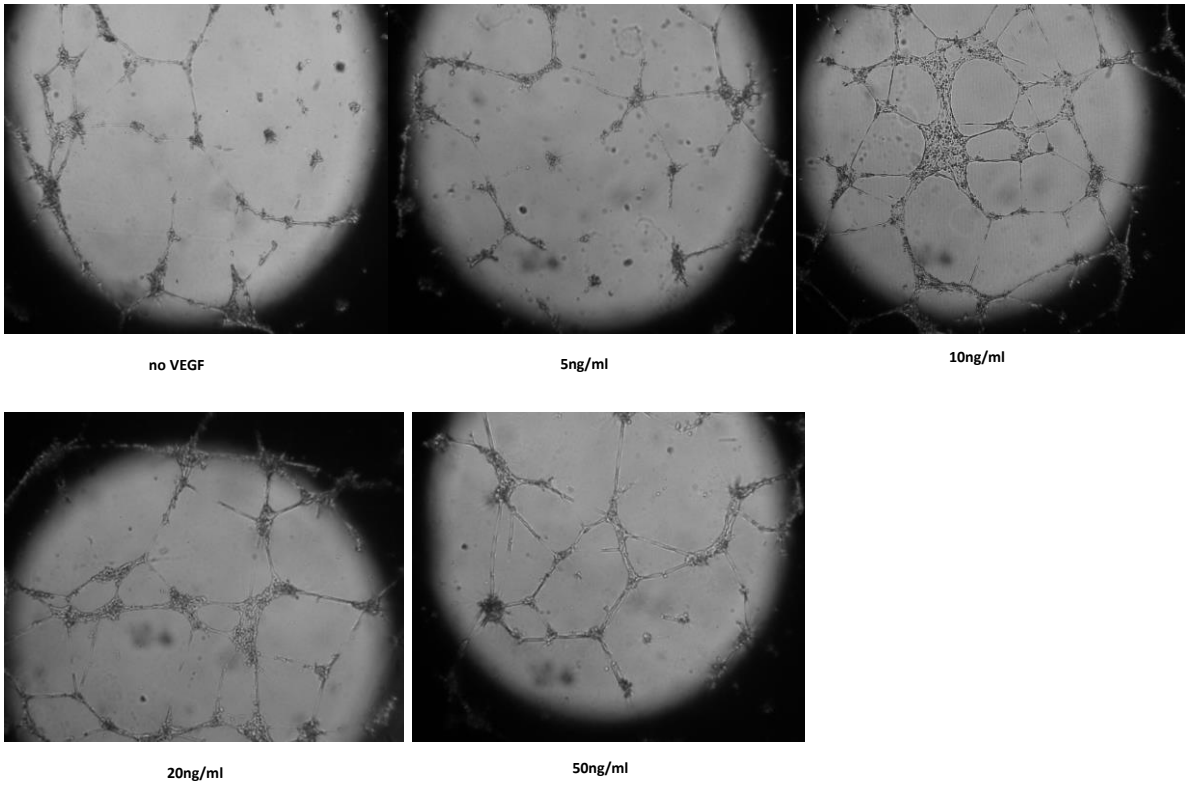

Figure 2.5 ***VEGF Concentration Curve.***:
Representative images of the stimulatory effects seen with a range of exogenous $VEGF_{165}$ concentrations. From the images it can be observed that HuDMEC tube formation *in vitro* is $VEGF_{165}$ dose dependent, with stimulatory effects plateuing at 20ng/ml. 20ng/ml was decided upon as the optimal dose of $VEGF_{165}$, with saturation being observed at 50ng/ml VEGF.

Conditions to Optimise	Comments	Finalised conditions
Matrigel volume	Too little causes meniscus effect	40µl
Seeding density	Too few = no tubule formation Too many = large clumps	15,000 cells/well
Serum starvation time	Too short = no response to VEGF Too long = cell death	6 hours
VEGF concentration	There is a bell shaped curve of response	20ng/ml
Experiment incubation time	Too short = little/no tubule formation Too long = cell death	16 hours

Table 2.5 ***Optimised Matrigel Conditions*****:**
Summaries the optimised conditions to be used in all subsequent Matrigel assays. All aspects of the assay are important in ensuring the assay is working effectively to allow for standardised conditions when adding different drug treatments.

2.5 Cell Proliferation

Cell proliferation is an important step in tumour angiogenesis and tumour development. During capillary formation proliferation of endothelial cells behind the leading migrating tip cell is important in forming the newly sprouted tubes that give rise to the new tumour microvasculature (***Gerhardt et al, 2003***).

2.5.1 MTS Assay

The MTS (3-4,5-dimethylthiazol-2-yl)-5-(3-carboxymethoxyphenyl)-2-(4-sulfophenyl)-2H-tetrazolium), assay differs from some of the more classical techniques used for measuring cell proliferation e.g. BrDU, as rather than measuring DNA incorporation, the assay quantifies mitochondrial metabolic activity and thus is thought to be a more accurate measure of cell viability rather than cell proliferation *per se*. (***Mo et al, 2013; Prabhakaran et al, 2013***) However, cell metabolic activity it is accepted as an alternative measure for cell proliferation. The MTS assay involves a reduction reaction, whereby the MTS compound is reduced into formazan (a yellow coloured product) by NO reductase, a mitochondrial enzyme, which is produced by metabolically active cells. The quantity of formazan produced

(measured as absorbance at 490nm) is directionally proportional to the number of actively metabolic and therefore viable cells present (***Promega Datasheet***).

A confluent flask of cells (70-80% confluency) was serum starved (1% FCS medium) for 6 hours prior to starting the MTS assay. After this time the cells were trypinised and re-suspended in 1.5ml of 1% FCS media, 0.5ml of which was counted using the Vi Cell counter, which gave a total cell count of cells/ml. The relevant volume of cells was then added to sterile 1.5ml eppendorfs containing the treatments and mixed by gently pipetting (see **section 2.5.2** for MTS optimisation). 100µl of the treatment solution (treatments made up in 1% serum media) was then added to the corresponding wells in the 96-well plate and incubate at 37^{o}C for 24 and 48 hours.

The experimental incubation times for the assay were optimised at 24 and 48 hours (see section), and 3 hours prior to the end of each time point, 20µl of MTS solution was added to each well, including the background control wells, the plate was then wrapped tightly with tin foil and then returned to the 37^{o}C incubator. Note, the MTS solution is light sensitive, thus all experiments were performed in the dark, with all MTS solutions wrapped and stored in tin foil to minimise the exposure to natural light. At the end of each experimental time point, the absorbance of the samples was measured at 490nm.

Each test condition was repeated 6 times per experiment and each experiment was carried out a minimum of 3 times to allow for reproducibility and subsequent statistical analysis (student's t test or Mann Whitney U test, Sigmaplot 11 software). Analysis of the raw data was carried out by subtracting the background control values from each of the test wells, and then the data was presented as percentage proliferation compared with the 24 hour cells alone control.

2.5.2 Optimisation of the MTS Assay

When measuring the effects of drugs on cell proliferation it is essential to establish a time point in which the cells are in the exponential stage of growth, thus optimisation of the cell density and time were carried out. Also, VEGF has been shown to stimulate endothelial cell proliferation therefore optimisation was carried out in the presence and absence of exogenous $VEGF_{165}$. The optimisation of the MTS assay outlined in (**Figure 2.6)**, led to the following conditions; 5000cells/well for all four cell types tested and an experimental time point of 24 and 48 hours (after 48 hours the rate of proliferation decreased). Only HuDMEC proliferation was increased in the presence of exogenous VEGF (20ng/ml) therefore it was decided that the MTS for the HuDMECs would be carried out in the presence of recombinant $VEGF_{165}$ (**Figure 2.6**). The addition of exogenous $VEGF_{165}$ did not further enhance the rate of proliferation of the two breast cancer cell lines; this was expected, as the breast cancer

cells already express relatively high levels of endogenous VEGF and the $VEGF_{165}$ response may already be saturated.

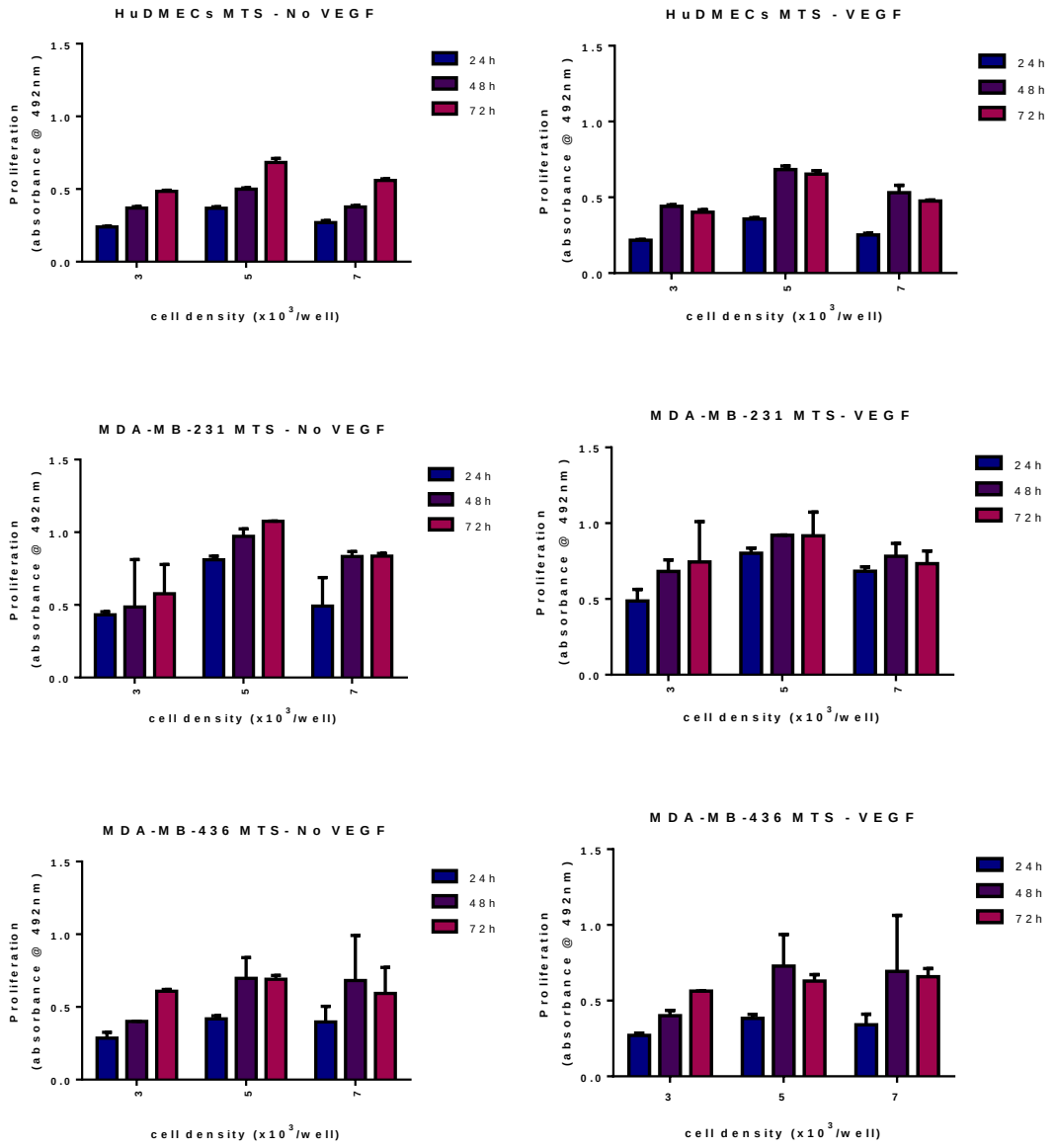

Figure 2.6 ***Optimisation of the MTS Assay***:
Experimental variables being measured were cell density, experimental time point and the effects of exogenous VEGF on cell proliferation. The HuDMEC cell proliferation was increased in the presence of exogenous VEGF165, whereas no change in the rate of MDA-MB-231 or MDA-MB-436 breast cancer proliferation was observed when VEGF165 was added to the cells. The 24 and 48 hour time-points were chosen as optimal experimental times to assess cell proliferation *in vitro.*

Data presented as mean ±SEM of the raw absorbance data minus the background controls. n=2

2.6 Cell Migration

Cell migration is an extremely important step in tumour angiogenesis and metastasis. The ECs must be able to move towards a chemotactic factor effectively, to establish local new vessels in the developing tumours and the breast cancer cells must be able to effectively move through the tumour micro-environment and vascular system to disseminate to distant organs to form metastasis.

2.6.1 Scratch/Wound Healing Assay

The scratch assay or 'wound healing' assay unlike the Boyden Chamber or Transwell method does not work on the principle that cells must migrate from an upper chamber to a lower chamber towards a chemo-attractant nor does it create a chemo-attractant gradient for cells to migrate towards (**Figure 2.7**). Since cells in the scratch assay are not moving towards a growth factor in a unidirectional manner, through a membrane, an anti-proliferative agent is usually used to ensure that any observations made in this assay are largely due to effects on cell migration and not cell proliferation.

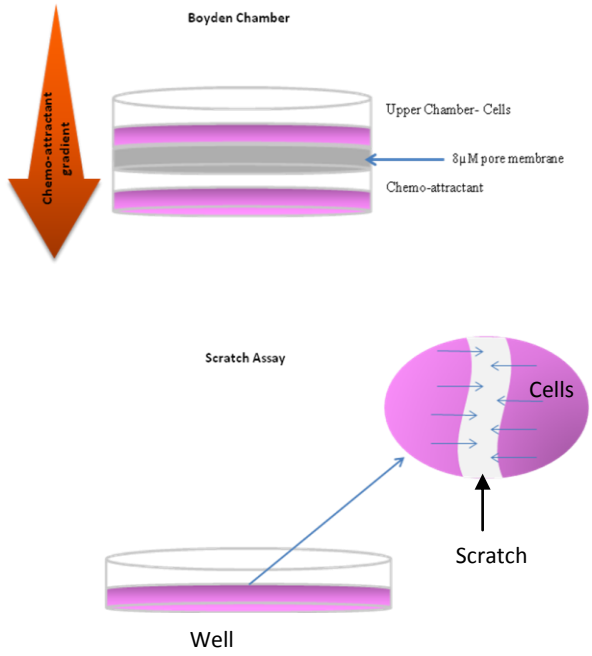

Figure 2.7 Principles of the Scratch Assay versus the Boyden Chamber for measuring cell migration:

The Boyden Chamber allows for directional migration to be assessed as the use of a top and bottom chamber allows for a chemotactic (e.g.VEGF) gradient

For this assay, cells were plated ($1.5x10^4$ and $2x10^4$, HuDMECs and breast cancer cells respectively) into a 96 well plate and left overnight in the 37°C incubator to allow the cells in each well to form a confluent monolayer. Once a confluent monolayer was achieved, 3µg/ml and 30 µg/ml Mitomycin C (MITC) (breast cancer cells and HuDMECs respectively) added to each test well and left to incubate for an hour at 37°C (see section for scratch optimisation). MITC is an anti-proliferative agent and was used to prevent cell proliferation. Since it is a

toxic agent, all media, tips, plates and eppendorff tubes that were in contact with MITC were soaked in 4% sodium hydroxide solution for a minimum of 12 hours to neutralise the toxic activity of MITC after which they were washed with running tap water and disposed of as usual.

After incubating the cells with MITC for an hour, the media was removed and 100µl fresh media was added to the cells and replaced in the incubator for 30 minutes, during which time the relevant treatment solutions were prepared. After 30 minutes, a scratch was made in the middle of each well using a 100µl Gilson pipette tip. The media was then aspirated off and the cells were gently washed once with 100µl PBS to remove any cells and debris from each well. 100µl of the treatment solution (treatments made up in 1% serum media) was then added to each relevant well, after which the cells were imaged at 0 hours time point and then left to incubate until the next time point (32 hours and 24/48 hours, HuDMECs and breast cancer cells respectively).

Each test condition was repeated 4 times per experiment and each experiment was carried out a minimum of 3 times to allow for reproducibility and statistical analysis (student's t test or Mann Whitney U test, Sigmaplot 11 software). Analysis of the raw data was carried out as follows, the percentage closure of the gap was calculated using Image J software (distance of gap in pixels) and then presented as percentage gap closure compared with the relevant control (VEGF alone control for the HuDMECs and the cells alone control for the breast cancer cells).

Optimisation of the Scratch Assay

The stimulatory effects of exogenous $VEGF_{165}$ on breast cancer cell migration in a 96 well format were assessed. However, addition of $VEGF_{165}$ did not enhance breast cancer cell migration, so this was not included in the assay (**Figure 2.8**). Optimisation of the HuDMECs in this assay had recently been carried out within the lab and therefore was not repeated.

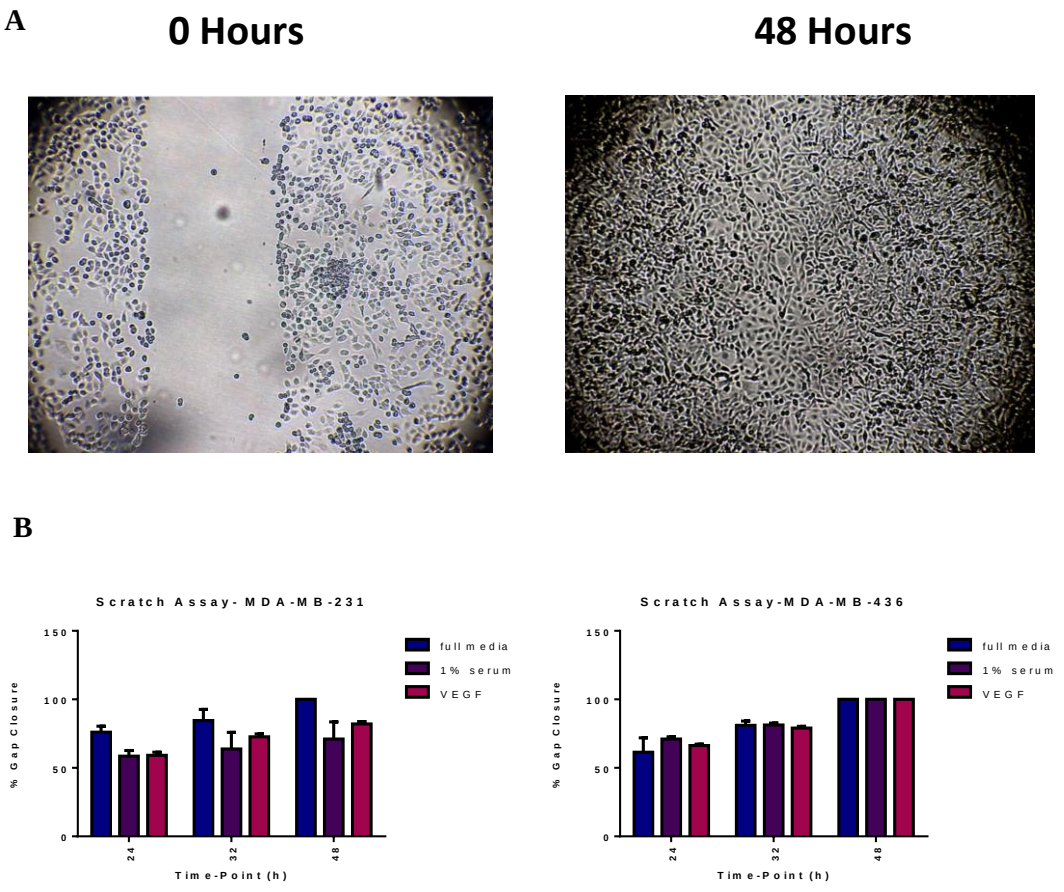

Figure 2.8 Optimisation of the Scratch Assay
(**A**)Representative image of MDA-MB-231 migration in scratch assay (in the absence of MITC). A scratch was made in a confluent monolayer of cells, after which treatments were added. Cell migration was measured by the ability of both the HuDMECs and the breast cancer cells to 'close' the gap created by the initial scratch (**B**) Assessing the effects of exogenous $VEGF_{165}$ on breast cancer migration.

MITC Optimisation

MITC was used in the scratch assay to minimise cell proliferation to ensure that the gap closure measured was due to cell migration. The concentration of MITC when working with the HuDMECs had been previously optimised at 30µg/ml and therefore was not repeated. The breast cancer cells appeared more sensitive to MITC treatment in comparison to the HuDMECs and therefore a lower concentration was used (1-5µg/ml) (**Figure 2.9**). A final concentration of 3µg/ml MITC was determined as optimal with a balance between the anti-proliferative effects of MITC without being cytotoxic to the cells or causing complete detachment from the surface of the wells.

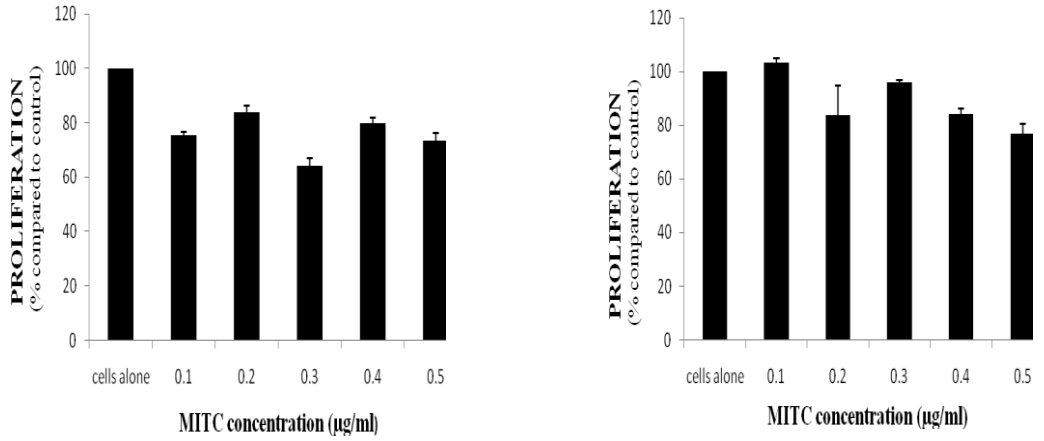

Figure 2.9 *MITC Concentration Curve*:
The above graphs show the effects of MITC treatment on (A) MDA-MB-436 and (B) MDA-MB-231 breast cancer cell proliferation after 48 hours incubation with MITC. The concentration curve was carried out to allow the optimal concentration of MITC to be used in the scratch assay.

2.6.2 Boyden Chamber

The Boyden chamber was used to confirm the data observed with the scratch assay. HuDMECs and the breast cancer cells were serum starved for 24 and 6 hours respectively prior to setting up the assay.

The 8µM pore membrane was coated in 50ng/ml fibronectin on both sides for 10 minutes each and then air dried for a further 10 minutes. The membrane was than equilibrated in growth medium for 10 minutes on both sides and then air-dried again for 10 minutes. Whilst the membrane was being coated the cells were trypinised, pelleted and counted. Approximately 27.5µl-28µl of treatment media was pipetted into the bottom chamber, the fibronectin membrane was then laid on top followed by the gasket and the top chamber which was bolted into place. $1.5x10^3$ and $2.0x10^3$ cells/well (HuDMECs and breast cancer cells respectively) were pipetted into the top chamber and the chamber was then incubated at 37^oC for 4 or 24 hours (HuDMECs and breast cancer cells respectively). After the incubation period, the chamber was removed from the incubator and disassembled, the membrane was removed using tweezers and the top side of the membrane was scraped gently to remove any cells that had not migrated during the 4 or 24 hour experimental time. The membrane was then washed with PBS for 5 minutes and the cells were fixed by washing the membrane with 100% methanol for 5 minutes. Gills hemotoxylin (4%) was then used to stain the cells (for 5 minutes) after which any excess stain was removed by washing the membrane with distilled water for 5 minutes. The membrane was then mounted using DPX on a slide, and was imaged for analysis (**Figure 2.10**). One central image was taken of each well and the number

of cells that had migrated per field of view were counted and presented as a % of the VEGF control cell migration. The Boyden chamber was carried out in triplicate to allow for reproducibility and statistical analysis to be performed (student's t test or Mann Whitney u test, Sigmaplot 11 software).

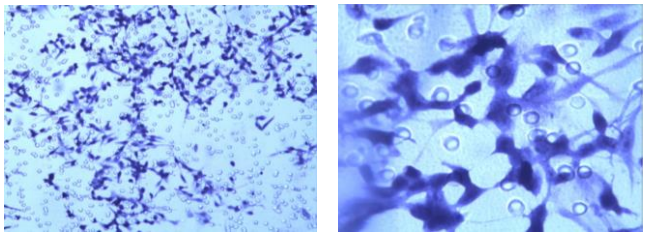

Figure 2.10 ***Boyden Chamber:***
Representative image of MDA-MB-231 breast cancer cell migration after 48 hours (x20 and x 40 magnification)

2.7 Statistical Analysis

For all the *in vitro* assays, all experiments were carried out in triplicate (minimum). Following assessment of normality, statistical analysis was performed using either the student's t test or the Mann Whitney U test (Sigmaplot 11 software). Statistical significance was considered at $p=0.05$.

2.8 *In Vivo* Studies

In vivo experiments for cancer research play an important part in understanding the mechanism by which different anti-cancer treatments exert inhibitory effects. *In vitro* work is important when focusing on a particular pathway or receptor/ligand interactions whereas *in vivo* work allows for a more dynamic assessment, with all components of the tumour micro-environment potentially influencing response.

2.8.1 Primary Breast Cancer Growth: Sub-Cutaneous Model

Animal Husbandry

CD1 nude female mice were delivered at 4-5weeks of age from Charles River, the animals were allowed to acclimatise to the housing facility (*University of Sheffield, Field Labs*) for a one week period following which experimental procedures were performed. Animals were exposed to a 12:12 hour light-dark cycle in humidity and temperature controlled environment and allowed access to water and food *ad libitum*. CD1 nude mice are immuno-compromised used in xenograft models, which allow for the growth of human tumour cells, and are therefore housed in a 'sterile' environment, where all food and bedding is appropriately autoclaved. For recovery procedures such as tumour implantation, sterile techniques were essential and were carried out where possible. All surfaces and equipment to be in direct contact with the animals were sprayed and cleaned with 70% ethanol. All procedures were performed in accordance with UK Home Office Animal Procedures Act (1986) under project license number 40/3531 (NJB).

Growth Kinetics

MDA-MB-436 green fluorescent protein (GFP) labelled breast cancer cells were used for the *in vivo* experiments as a result of the *in vitro* characterisation stage (**Chapter 4**). A pilot study was initially performed to determine the appropriate cell densities to determine growth kinetics and to establish a minimum treatment window. MDA-MB-436 breast cancer cells were implanted (1 x 105, $1x10^6$ and $5x10^6$; in a total volume of 100µl) via a sub-cutaneous (s.c.) injection into the left flank of CD1 nude females (n=3/4 per group) under gas anaesthesia (isoflurane).

The animals were then monitored for signs of tumour development three times a week. Once a palpable tumour developed, tumour volume was measured three times a week using callipers until the end of procedure (EOP). Tumour volume was calculated using the following calculation: $(a^2 \times b)/2$, where a, is the smaller tumour diameter and b is the larger diameter. The EOP was determined when either (**1)** Home Office maximum tumour diameter permissible was reached (15mm, NCRI guidelines, ***Workman et al. 2010***), (**2**) the tumour

ulcerated or (**3**) animals lost greater than 10% body weight due to tumour development. Following cull, tumours were excised, divided into two and either formalin (10%) or zinc fixed prior to wax embedding. Tumour sections were cut (5µM from the blocks) and used for optimisation of the immunohistochemistry (IHC) staining protocols (**Section 2.8.2**). The growth kinetics study determined that the optimal cell density for MDA-MB-436 tumour implantation into the flank (s.c) as $1x10^6$/100µl as this cell density demonstrated 100% tumour take and a minimum treatment period of approximately four weeks thus was used in all subsequent sub-cutaneous studies.

Combination Studies

CD1 nude females were anaesthetised using isoflurane and each mouse was subsequently injected subcutaneously (s.c.) with $1x10^6$ (in a total volume of 100µl) MDA-MB-436 breast cancer cells into the left flank region. The animals were placed in a 37^{o}C incubator to allow recovery from the anaesthesia and then returned to the cages. The animals were monitored three times a week for signs of tumour development and body weight was measured throughout the entire experiments. Once a palpable tumour was detected (on average 2 weeks post implantation of MDA-MB-436 GFP breast cancer cells), calliper measurements were taken three times a week, when tumour volume reached $100mm^3$ treatment began (approximately four weeks post implantation of MDA-MB-436 GFP cells). A treatment regime was established on the basis of previous literature available on pre-clinical work carried out using Bz (***Higgins et al, 2007; Xue et al, 2008; Borgan et al, 2012***). Bz and the control vehicle for Bz (CV) were administered via intra-peritoneal (i.p.) injection, twice weekly as was administration of p7b and p10. In the Bz and peptide combination groups, Bz was administered 1 hour prior to peptide injection.

During the treatment period tumour growth was quantified three times a week and EOP was determined as described in the growth kinetics section. Fluorescently labelled pectin (inject a 1/4 dilution in 200µl from 1mg/ml stock/ 20g mouse) and pimonidazole (pimo; 60mg/kg) were injected intravenously (i.v.) five minutes and two hours prior to culling respectively to allow for post *in vivo* staining. Lectin identifies functional vessels (***Hunter et al, 2006***) and pimo is a standard marker used to identify areas of hypoxia (***Przybyla et al, 2012; Sun et al, 2012***). After culling tumours were removed, divided in two, formalin fixed prior to wax embedding for IHC analysis or snap frozen (in OCT buffer) using liquid nitrogen for protein, RNA, lectin or pimo analysis. In addition, lungs, liver, kidney and spleen were also removed, divided in two and formalin fixed or frozen.

2.8.2 *Ex Vivo* Analysis of Tumour Sections and Normal Tissue

Post *in vivo* analysis of the tumour is important as it allows for differences in morphology, receptor/ligand expression and the vasculature in the control and treated tumour sections to be determined. This is allows for assessment of how a drug exerts its effects which is especially important in cancer research especially when determining how tumours initiate a resistance response to therapy. Analysis of normal tissue is also important to determine any off-target effects of drug treatment.

Haematoxylin and Eosin (H&E) Staining

Morphology of the tumour and the organs is assessed using H&E staining. Tumour necrosis can also be quantified using a H&E stain. The sections were de-waxed in xylene twice for 5 minutes each to remove the paraffin from the tissue sections. After which the sections were dehydrated in a series of alcohol incubations for 3 minutes each (100% EtOH, 100% EtOH, 95% EtOH and 70% EtOH). The sections were then washed with dH_20 twice for 3 minutes each and then stained in Gill's Haematoxylin (for nuclei staining) for 5 minutes and then 'blued' under running water until the excess stain was removed. The sections were then counterstained with Eosin (cytoplasmic staining) for 1 minute and then re-hydrated through the alcohols, incubated in xylene twice for 15 minutes each and then mounted with coverslips with DPX and left to dry for a minimum of 48 hours.

Immunohistochemistry

Post analysis of the tumour sections was carried out using Immunohistochemistry (IHC). IHC staining is a useful tool for assessing differences in the molecular phenotype of the tumour under different treatment conditions. It is important to be able to measure these differences as it provides useful information with regards to the potential mechanism of a drug or specific treatment group.

Paraffin embedded tumour sections were de-waxed in xylene twice for 5 minutes each to remove the paraffin from the tissue sections. After which the sections were hydrated in a series of alcohol incubations for 3 minutes each (100% EtOH, 100% EtOH, 95% EtOH and 70% EtOH). The sections were then washed with dH_20 twice for 3 minutes each. Horseradish Peroxidise (HRP) was used as the antigen detecting method in this project, thus, endogenous peroxidises activity must be blocked to minimise non-specific staining. In order to minimise endogenous peroxidise activity, the tumour sections were quenched with 3%methnaol/hydrogen peroxidise for 30 minutes at room temperature. The sections were then washed once in PBS for 5 minutes and then antigen retrieval was carried out in sodium citrate buffer (**appendix**). Antigen retrieval is required when working with formalin fixed

sections, as the formalin can form cross links in the sample, and potentially mask the antigen epitopes, which require unmasking to allow the antibody access to the desired antigen epitope in the tissue section.

After antigen retrieval, the sections were washed in PBS once for 5 minutes and then blocked in blocking serum for an hour at room temperature to minimise non-specific binding of the antibody to other non-relevant epitopes. The blocking serum was made up of 10% from the species in which the secondary antibody was raised. After the blocking step, the primary antibody was added to the tissue and incubated for either an hour at room temperature or overnight at 4^{o}C, depending on the stain (**Table 2.6**). The sections were then washed three times for 5 minutes each in PBST after which the biotinylated secondary antibody was added to the sections and incubated at room temperature for an hour. During this secondary antibody incubation the ABC (Avidin Biotin Complex) solution required for recognising the biotiylated secondary antibody was prepared and allowed to set for a minimum of 30 minutes. After the secondary antibody step, the tissue was washed 3 times for 5 minutes each in PBST and then the ABC solution was added and allowed to incubate for 30 minutes at room temperature. The sections were then washed twice for 5 minutes each in PBST and incubated with DAB solution for 2-10 minutes or until brown the DAB stain was visible. The sections were then washed in dH_2O for 5 minutes, and then 'blued' for 30 seconds in Gill's Haematoxylin. After which the sections were washed in running water for 3 minutes (or until all the excess haematoxylin was removed) and then de-hydrated through a series of EtOH washes for 3 minutes each (70%, 95%, 100% and 100%). The sections were then left in xylene mount twice for 10 minutes each and then mounted with a glass coverslip using DPX. The slides were allowed to dry for 48 hours before imaging or analysis could be carried out. The conditions used for each protein/receptor is detailed in **Table 2.6.**

Factor	Company	Antigen Retrieval Method	Antigen Retrieval Buffer	Blocking	1^0an Conc.	2^0 Ab Conc.
VEGF	Santa-Cruz	Microwave	Sodium citrate	serum	1:100 overnight at 4^0C	1:250 for 1 hour
VEGF-R1	Santa-Cruz	Heat Pressure	Sodium citrate	serum	1:100 overnight at 4^0C	1:250 for 1 hour
VEGF-R2	Santa-Cruz	Heat Pressure	Sodium citrate	serum	1:100 overnight at 4^0C	1:250 for 1 hour
Np1	Santa-Cruz	Heat Pressure	Sodium citrate	serum	1:100 overnight at 4^0C	1:250 gor 1 hour
Np2		Heat Pressure	Sodium citrate	serum	1:100 overnight at 4^0C	1:250 for 1 hour
CD34	Abcam	Heat Pressure	Sodium citrate	serum	1:50 overnight at 4^0C	1:250 for 1 hour
Ki67	DAKO	Heat Pressure	Sodium citrate	serum	1:100 for an hour at room temperature	1:250 for 1 hour
Caspase 3	Abcam	Heat Pressure	Sodium citrate	serum	1:50 for an hour at room temperature	1:250 for 1 hour

Table 2.6 ***IHC Conditions:***
The table summaries the optimised conditions used in the IHC staining protocol for each of the different proteins of interest that was required for post-*in vivo* tumour analysis.

IHC Analysis

CD34 staining was analysed using the chalkley grid method with 5 regions of the tumour section being analysed. Ki67 and Caspase 3 staining was analysed by imaging 5 regions of each tumour section and the number of positively stained cells were counted and the average of the 5 regions was calculated.

Chalkley Grid

H&E stains were performed prior to necrosis being established. The chalkley grid was used to measure tumour necrosis in the tumours. The 25-point grid was placed in the lens of the Leica upright microscope and the number of corresponding points that were in contact with both a necrotic area and a viable area to allow percentage necrosis to be calculated. Necrosis scoring was performed on the entire tumour tissue to accurately measure the level of necrosis.

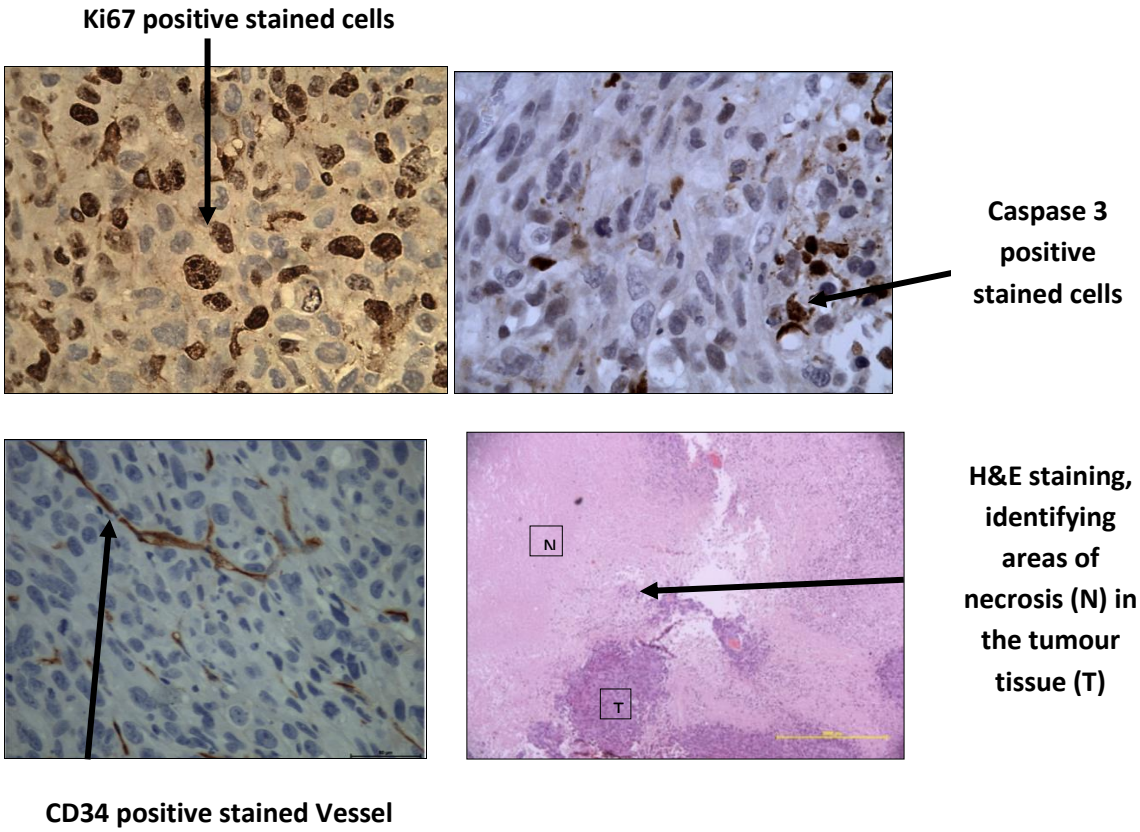

Figure 2.11 Markers of Tumour Activity:
Representative images of the different parameters measured to assess the effects of drug treatment on the tumour. H&E staining allows analysis and quantification of tumour morphology and necrosis. Ki67 measures tumour cell proliferation. Caspase 3 measures apoptotic activity and CD34 quantifies newly formed vessels

2.8.3 Bone Metastasis Model

Bone metastasis is a frequent occurrence in breast cancer, and is more commonly the cause of morbidity and mortality then the primary disease itself (***Lu et al, 2009***) and therefore is an important process to investigate.

Models of Bone Metastasis

There are three commonly used models for assessing bone metastasis using injection of tumour cells, (1) intra-cardiac, (2) intra-tibial and (3) mammary fat pad (***Campbell et al, 2012***). All three offer advantages as models of bone metastasis depending on the primary aim of investigation. The intra-cardiac model allows assessment of the tumour cells to migrate and survive in the bone environment (and other metastatic sites) and form established tumours. Whereas the intra-tibial model looks more closely at the interaction of the tumour and surrounding bone cells once the tumour cells have successfully established themselves in the bone environment (***Campbell et al, 2012***). The mammary fat pad (MFP) model does not consistently result in metastasis to the bone from the primary site and very few cell lines have success in this model, with the most commonly used cell line being the 4T1 cells (***Campbell et al, 2012***). Since we were interested in the effects of Bz on reducing the metastatic tumour burden, the intra-cardiac model of bone metastasis was most appropriate, and we had already determined that the MDA-MB-231 cell line pre-dominantly metastasises to the bone when administered via this route (***Yoneda et al, 1994; Yoneda, 1997; Jenkins et al, 2005***).

IVIS Lumina II Imaging

The IVIS Lumina II imaging system allows for live non-invasive imaging of pre-clinical tumour models over time, which allowed monitoring and quantification of tumour metastasis/burden in the intra-cardiac model. In the bioluminescent system, tumour cells tagged with luciferase are injected into the animals. D-Luciferin (firefly potassium salt) is a freely diffusible organic compound that is oxidised by luciferase (tagged to the tumour cells) to oxyluciferin in the presence of oxygen and co-factors, ATP and Mg^{2+}. This oxidation reaction at 37^0C is visualised at ~ 560nm (***Caliper Life Sciences, UK***).

Animal Husbandry

Athymic BALB/C nude female mice were delivered at 4-5 weeks of age from Harlan, the animals were allowed to acclimatise to the housing facility (University of Sheffield, Field Labs) for a one week period following which experimental procedures were performed. Animals were exposed to a 12:12 hour light-dark cycle in humidity and temperature controlled environment and allowed access to water and food *ad libitum*. BALB/C nude

mice are immuno-compromised and are therefore housed in a 'sterile' environment, where all food and bedding is appropriately autoclaved. For recovery procedures such as tumour implantation, sterile techniques were essential and were carried out where possible. All surfaces and equipment to be in direct contact with the animals were sprayed and cleaned with 70% ethanol. All procedures were performed in accordance with UK Home Office Animal Procedures Act (1986) under project license number 40/3531 (NJB).

2.8.4 Intra-cardiac Bone Metastasis Model

Six week old BALB/C nude females were anaesthetised using isoflurane (2.5%) and each mouse was subsequently injected via an intra-cardiac injection into the left ventricle with luciferase2 tomato labelled MDA-MB-231 breast cancer cells ($1x10^5$/100µl). MDA-MB-231 cells were used in this model because they have previously been shown to metastasise to the bones following intra-cardiac injection (***Brown et al, 2012***) whereas 'homing' of MDA-MB-436 breast cancer cells via intra-cardiac injection to the bone *in vivo* has not been published (**PubMed**). The animals were placed in a 37ºC incubator to allow recovery from the anaesthesia and returned to the cages. Two days after the initial injection of MDA-MB-231 cells the animals were anaesthetised and imaged using the IVIS Lumina II (**described above**).

After injection of cells into the left ventricle, generally the tumours cells initially migrate to the skull of the animal, after which the cells then slowly begin to migrate through the body and eventually form distant metastasis in the bones. Animals were imaged twice a week, once a signal was detected in any of the hind legs, treatment with either Bz (0.1mg/kg and 0.5mg/kg) or the control vehicle for Bz (CV) was commenced (twice weekly i.p injection, n=10/group). IVIS imaging was carried out to monitor tumour growth in the bone twice a week on the same day as the i.p injections. Once treatment began the experiment lasted for a maximum experimental time of six weeks. During this time the animals were monitored 3 times a week, body weight was measured throughout the entire experiment, if a loss of more than 10% body weight was observed, the animal was culled. Neurological side effects, such as the ability to walk properly were also monitored throughout the entire experiment to ensure that brain metastasis had not occurred. At the end of the experiment the hind legs of the animals that had a tumour signal were removed. The skin and muscle was removed from the bone and then the harvested tibia was fixed in ice-cold 4% paraformaldehyde (PFA) solution (**appendix**) that was freshly prepared at 4ºC for a maximum of 72 hours. Once fixed, the bones were scanned using the X-ray computated micro-tomograph (Micro-CT-Skyscan), after which the bone tissue was decalcified at 4ºC using an EDTA decalcifying buffer (**appendix**). Decalcification removes the mineral from the bone to preserve the integrity of bone elements. The decalcification process takes 14-18 days, during which time,

fresh decalcification buffer was added every 2 days to ensure complete removal of calcium salts. Once the bones were decalcified, they were washed in 1xPBS three times for an hour each, at room temperature, after which the bones were wax embedded.

2.8.5 *Ex Vivo* Analysis of Bone Sections

IVIS Analysis

Tumour burden analysis was performed (from ventral images) with use of the Living Image acquisition and analysis software (***Caliper Life Sciences, UK***). Signal intensity was quantified as the total photon count, manually selected within individual regions of interest (ROI) present in each animal (**Figure 2.12** and **Figure 2.13**).

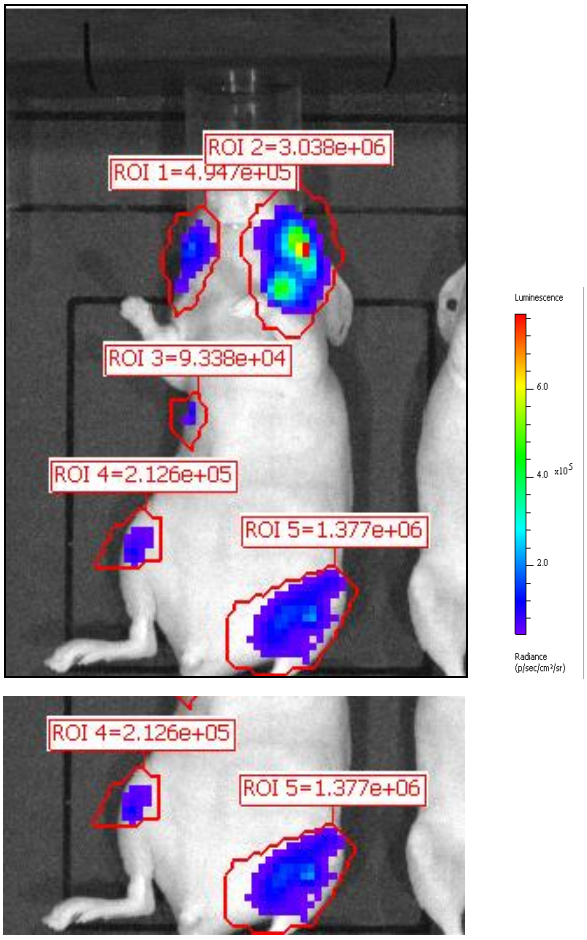

Figure 2.12

Total Tumour Burden

The total radiance corresponding to tumour burden in each individual animal is the sum of the radiance in each of the ROIs.

Figure 2.13

Hind Limb Tumour Burden

The total radiance corresponding to tumour burden in each individual animal for the hind limbs only is the sum of the radiance in each of the ROIs drawn around tumours in the hind limbs only.

Micro-CT

Prior to decalcification, micro-CT analysis was performed using the Skyscan 1172 X-ray micro-CT (Skycan) on representative animals (n=3/group). Imaging was carried out at a voltage of 49kV and a current of 200μA, an aluminium filter of 0.5mm and a pixel size set to a dimension of 4.3μm, with scanning initiated from the growth plate of the tibia. Cross-sectional images were reconstructed using NRecon software (version 1.4.3 Skyscan). Following re-construction trabecular volume, trabecular number and thickness amongst other parameters were also defined using a manual drawing tool on the 2D acquisition images. 3D modelling and analysis to measure bone mineral density were performed using CTAn software (version 1.5.02). Below is a representative image (**Figure 2.14**) of the reconstructions of the micro-CT scanned bones. These images were used to manually draw around the trabecular bone region, from which the bone histophometry parameters were calculated.

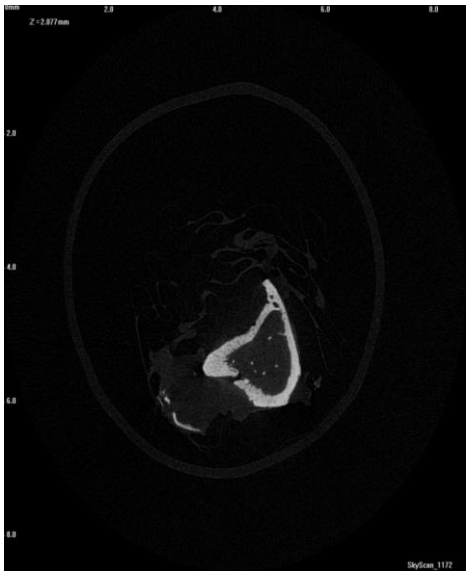

Figure 2.14

Micro-CT reconstruction

Representative images of the micro-CT scan that were used to measure bone density parameters.

H&E Staining

Bone sections (3μM) were incubated in xylene twice for five minutes each, and hydrated through a series of alcohol (IMS) washes (99% x2, 95% x1 and 70% x1) for five minutes each. Following de-hydration, the bone sections were washed with tap water for a minutes, incubated in Gill's II haematoxylin for 90 seconds and 'blued' in running tap water for five minutes. The sections were then incubated in 1% aqueous eosin (with 1% calcium carbonate) for five minutes, washed in tap water for 30 seconds and then hydrated through a series of alcohols for ten seconds each (70%, 95%, 99% x2). The sections were then incubated in xylene for three minutes and the mounted with DPX and left to dry prior to analysis or imaging.

TRAP Staining

Tartrate-resistant-acid-phosphatase (TRAP) staining is a marker for osteoclasts. Bone sections (3μM) were de-waxed and hydrated (as in the H&E protocol) and then incubated in pre-warmed (2-4 hours) acetate buffer (**appendix**) in a pre-warmed coplin jar at 37°C for five minutes. The bone sections were then incubated in Napthol/dimethylformamide buffer (**appendix**) for thirty minutes at 37°C. The sections were then transferred and incubated in sodium nitrite solution (**appendix**) for fifteen minutes, after which the sections were rinsed gently in running tap water and counter-stained for twenty minutes with Gill's haematoxylin and 'blued'. The bone sections were then de-hydrated quickly through ethanol and mounted in DPX as in the H&E staining protocol. TRAP stained osteoclast were quantified (per mm trabecular bone surface not in contact with the tumour) using a Leica RMRB upright microscope with a 10x objective and Osteomeasure software (**Osteometrics 31**). Osteoblast quantification was performed on the same sections that were TRAP stained. Osteoblast were identified and quantified based on morphology.

2.8.6 Statistical Analysis

Following assessment of normality, statistical analysis was performed using either the One Way ANOVA followed by the Holm-Sidak post-hoc test or the Kruskal-Wallis (Sigmaplot 11 software).

Chapter Three

In Vitro Results
Targeting the Angiogenic Pathway

3. Introduction

Microvascular endothelial cells are the key components of angiogenesis, and when activated undergo a number of key steps that leads to the formation of new vessels from the pre-existing vasculature. VEGF was initially identified as a vascular permeability factor, acting primarily on endothelial cells (***Senger et al. 1983***) and over the years it has become apparent that VEGF is important in exerting stimulatory effects on survival, migration, proliferation and differentiation of endothelial cells.

The expression of VEGF-R1 and VEGF-R2 on endothelial cells has been well defined as has the functional role of VEGF-R2 on these cells. The role of VEGF-R1 has for a long time been thought to be solely as a negative regulator of VEGF function. However, it has become apparent that VEGF-R1 also plays an important role in promoting tumour angiogenesis (***Zeng et al, 2001***). The dual role that VEGF-R1 plays in tumour angiogenesis may be important to assess, if the role of VEGF-R1 in endothelial cell function is unclear, the implications of blocking this receptor alongside VEGF-R2, may not be clearly understood which could result in ineffective use of receptor targeting agents such as Bz.

The neuropilin receptors have been identified as alternative VEGF receptors and the role played by Np1 in endothelial activity *in vitro* appears to be increasingly evident. There is evidence to suggest that Np1 plays an important role in EC migration and differentiation thus the following experiments aimed to assess whether 4 Np1 peptides exerted any biological activity in inhibiting HuDMEC function in a number of *in vitro* functional assays. If any inhibitory effects with the Np1 peptides were observed, combination experiments with Bz were carried out.

3.1 Materials & Methods

Initially, Western blot analysis was carried out to establish VEGF and VEGF receptor expression (**section 2.2.4**) on HuDMECs. Cells were serum starved overnight in 1% serum media after which protein was extracted and quantified using the BCA method. The samples were stored at -80ºC in aliquots until required. Once receptor expression was established functional angiogenesis related assays were performed.

The Matrigel assay (**section 2.4**) was used to measure the effects of Bz, the four Np1 peptides and a commercially available Np1 and Np2 blocking antibody on HuDMEC differentiation *in vitro*. The Matrigel assay mimics the process of tubular morphogenesis and capillary formation resulting in the formation of cord like structures *in vitro*. HuDMECs were serum starved for 6 hours in 1% serum media to deplete the cells of endogenous growth factors, so that the effects of exogenous $VEGF_{165}$ at a known concentration (20ng/ml) could be analysed. HuDMECs were then plated on growth factor reduced Matrigel in the presence or absence of 20ng/ml $VEGF_{165}$ either alone or in combination with the above treatments and then incubated at 37ºC for 16 hours, after which images were taken and then analysed. Data from the Matrigel assay is presented either as percentage cord or branch point formation compared with the $VEGF_{165}$ alone control (as all drug treatments were carried out in the presence of exogenous $VEGF_{165}$).

The MTS assay (**section 2.5.1**) was used to measure the effects of Bz and the four Np1 peptides on HuDMEC proliferation *in vitro*. HuDMECs were serum starved for 6 hours in 1% serum media to deplete the cells of endogenous growth factors. HuDMECs were plated in the presence or absence of 20ng/ml $VEGF_{165}$ either alone or in combination with the treatments and incubated at 37ºC for 24 and 48 hours. The MTS solution was added to the cells 3 hours prior to the end of each experimental time point, after which absorbance readings were taken. Data from the MTS assay is presented as percentage absorbance compared with the $VEGF_{165}$ alone control at 24h (as all the drug treatments were carried out in the presence of exogenous $VEGF_{165}$).

The scratch assay (**section 2.6.1**) was used to measure the effects of Bz and the four Np1 peptides on HuDMEC cell migration *in vitro*. A central scratch was made on a confluent monolayer of HuDMECs and then incubated with 1% media alone or media containing 20ng/ml $VEGF_{165}$ in the presence or absence of the treatments at 37ºC for 32 hours. Images of the gap were taken at 0 and 32 hours after which the gap closure was calculated using ImageJ software (**version 1.42q**). Data from the scratch assay is presented as percentage gap closure

compared with the $VEGF_{165}$ alone control at 0 hours (as all the drug treatments were carried out in the presence of exogenous $VEGF_{165}$).

All assays that investigated the effects of Bz *in vitro,* also included a control vehicle (CV). In breast cancer patients, Bz is reconstituted in this control vehicle and then administered via i.v. infusion (***Avastin® SPC, 2010***). Thus, it was vital to include this control, in order to confidently attribute any biological effect observed with Bz, to the targeted therapy itself and not due to non-specific actions of the vehicle components.

Statistical Analysis

After assessment of normality statistical analysis was performed using a student's t test or Mann-Whitney U Test (**Sigmaplot 11 software**).

3.2 Results

3.2.1 Protein Expression

VEGF protein expression was detected in the cell lysate of cultured HuDMECs, with a range of bands being observed between 42-50kDa (**Figure 3.1a**) which was expected as the antibody used in the western blot experiments is known to detect the different pro-angiogenic VEGF isoforms. Only the dimeric form of VEGF was detected in the HuDMECs as no smaller bands (21-25kDa) that would correspond to the monomeric forms of VEGF were detected. No protein expression was detected in the conditioned media from the HuDMECs. $VEGF_{165b}$ protein expression was undetected in both the cell lysate and media of cultured HuDMECs (**Figure 3.1b**).

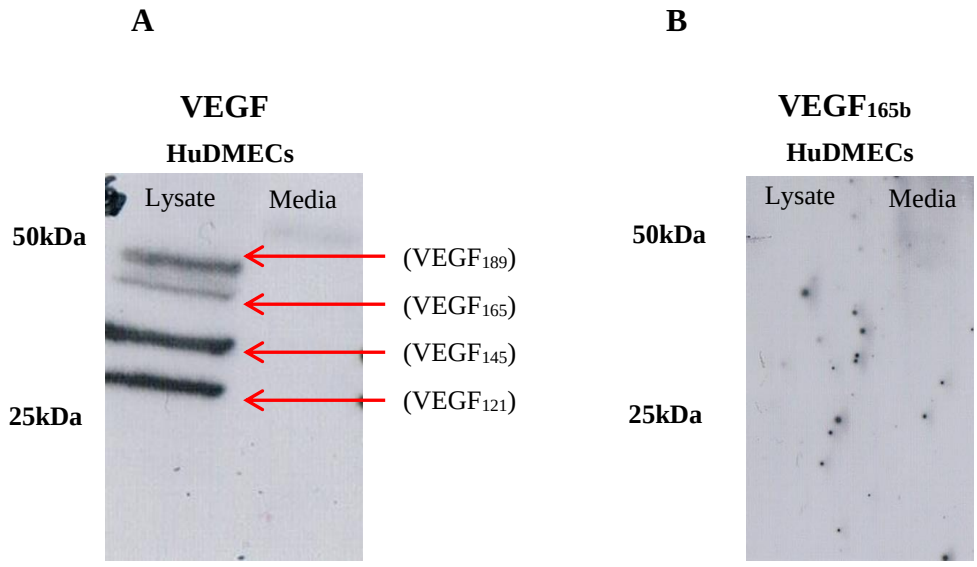

Figure 3.1 ***VEGF$_{165}$ and VEGF$_{165b}$ Protein Expression:***
(**A**) VEGF$_{165}$ protein expression was detected in the cell lysate fraction of cultured HuDMECs. Additional bands in the blot represent the different VEGF isoforms. Secreted VEGF was not detected in the conditioned media. **(B**) VEGF$_{165b}$ remained undetected in both cell lysate and conditioned media

VEGF-R1 protein expression was detected in the cell lysates of cultured HuDMEC cells, with two bands being observed, one at approximately 180kDa and the other at ~200kDa. VEGF-R1 protein expression was not detected in the conditioned media of the HuDMEC cells (**Figure 3.2a**). VEGF-R2 protein expression was also detected in the cell lysates of cultured HuDMEC cells, with two bands spanning approximately 200-230kDa being observed (**Figure 3.2b**). These two bands are thought to correspond to the glycosylated form of VEGF-R2 (***Takahashi & Shibuya. 1996***). Similar to VEGF-R1, VEGF-R2 protein expression was not detected in the conditioned media of cultured HuDMEC cells.

Np1 protein expression was also detected in the cell lysates of cultured HuDMEC cells with a large singular band observed at approximately 130kDa (**Figure 3.2c**). Np1 protein expression was not observed in the conditioned media from cultured HuDMEC cells. Np2 protein expression was observed in the cell lysates and conditioned media of cultured HuDMEC cells, with several bands observed in the cell lysate fraction and a single secreted band in the media (**Figure 3.2d**). In the cell lysate fraction of the cultured HuDMEC cells 3 distinct bands were observed at ~135kDa, ~90kDa and ~75kDa. The ~135kDa band corresponds to the known size of full length Np2 (***Barr et al, 2005***) and it is possible that the lower two bands correspond to soluble forms of the Np2 receptor (***Lu et al. 2009***). A soluble form of the

Np2 receptor also appears to be present in the conditioned media of the cultured HuDMECs at ~75kDa.

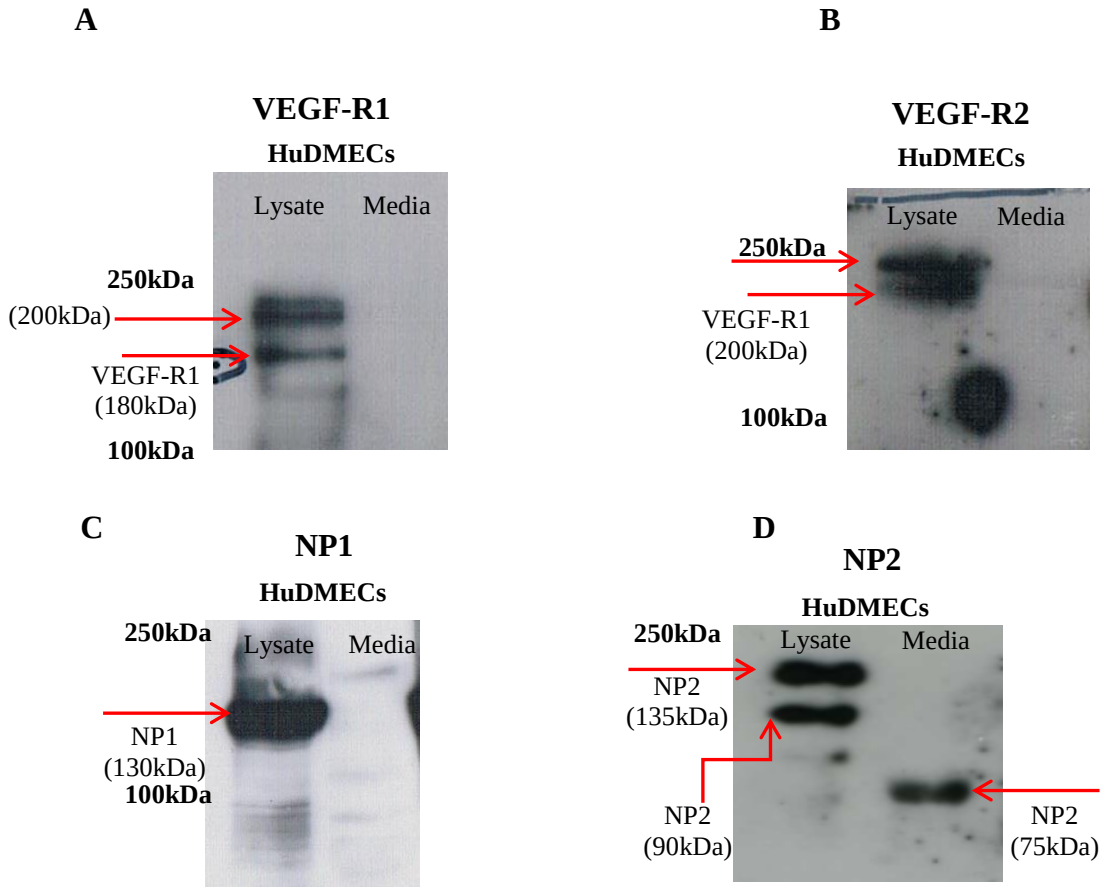

Figure 3.3 ***Protein Expression; VEGF Receptors:***
Expression of all the VEGF receptors were observed in the cell lysates of cultured HuDMECs ***(A)*** VEGF-R1 (**B**) VEGF-R2 (**C**) Np1 (**D**) Np2 with soluble Np2 also being observed in the conditioned media. Several forms of VEGF-R1, VEGF-R2 and Np2 were observed, whereas only a single band corresponding to the full length Np1 receptor was observed.

Images are representative of protein expression detected in triplicate experiments

3.2.2 Effects of Bz on HuDMEC Function

Differentiation

The majority of *in vitro* data that is published in the literature assess the effects of Bz using macrovascular endothelial cells; human umbilical vein endothelial cells (HuVECs). However, the main cells to undergo angiogenesis *in vivo* are microvascular endothelial cells; therefore HuDMECs were the chosen as the relevant cell type, in all the following experiments. Previous experiments measuring the effects of Bz on endothelial cells used a range of

concentrations and since the current experiments were assessing the effects of Bz on microvascular endothelial cells, it was decided that the effects of both high and low concentrations of Bz would be tested. *In vitro*, endothelial cell differentiation is represented by the formation of cord-like structures on a thin layer of growth factor reduced Matrigel. Representative images of these cord-like structures after 16h are shown in **Figure 3.3**.

Bz significantly (P = 0.008) inhibited HuDMEC cord formation *in vitro* at both the 2.5mg/ml and 5mg/ml dose compared with the $VEGF_{165}$ alone control (85.9% SEM± and 79.1% SEM± versus 100% respectively) (**Figure 3.4a**). In addition, Bz (1mg/ml and 5mg/ml) significantly (P = 0.008) inhibited, the complexity of the network when measured as percentage branch point formation at the compared with the $VEGF_{165}$ alone control (79.5% SEM± and 75.1% SEM± versus 100% respectively) (**Figure 3.4b**). Interestingly, the control vehicle (CV) also exhibited similar significant (P = 0.008) inhibitory effects on HuDMEC cord formation at the 2.5mg/ml and 5mg/ml equivalent dose compared with the $VEGF_{165}$ alone control (85.9% SEM± and 80.5% SEM± versus 100% respectively) (**Figure 3.5a**). However, unlike Bz, CV, had no inhibitory effect on the complexity of the network (**Figure 3.5b**).

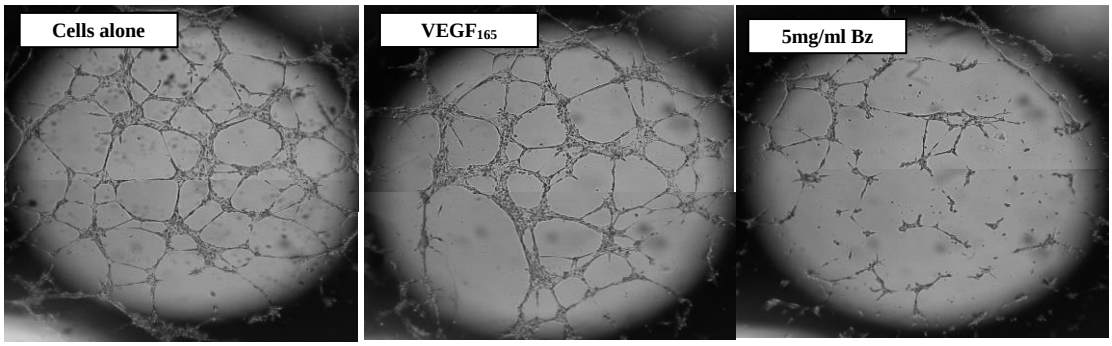

Figure 3.3 ***Matrigel Assay:*** Representative images of cord-like structures formed when HuDMECs are plated alone, in the presence of $VEGF_{165}$ alone (20ng/ml) and Bz (5mg/ml). The number of cord like structures was manually counted to determine the level of *in vitro* endothelial cell differentiation.

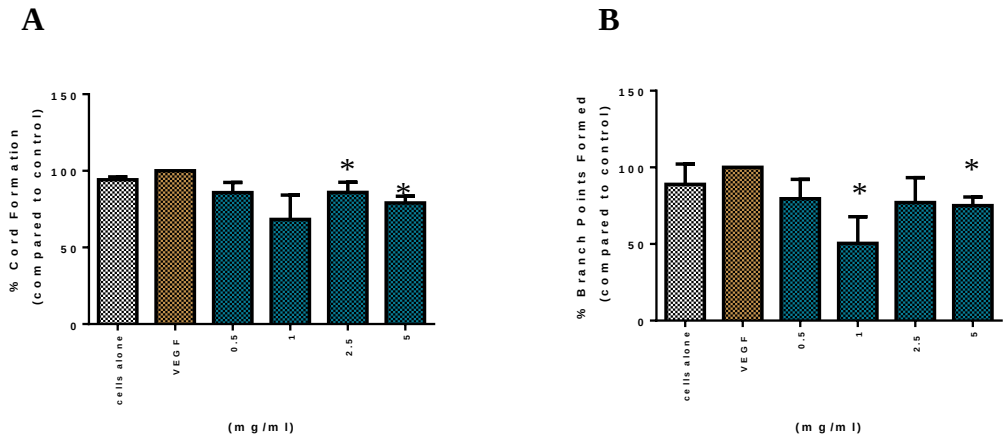

Figure 3.4 ***Effects of High Doses of Bz on HuDMEC Differentiation*****.**
In the presence of recombinant $VEGF_{165}$, plus varying doses of Bz, HuDMEC differentiation was inhibited. (**A**) Bz at 2.5 and 5mg/ml exerted a significant (*P = 0.008*) inhibitory effect on HuDMEC cord formation when expressed as a percentage of the $VEGF_{165}$ alone control. (**B**) Bz at 1 and 5mg/ml significantly (*P =0.008*) inhibited HuDMEC branch point formation when expressed as a % of the $VEGF_{165}$ alone control.

Data is presented as mean±SEM (% cord or branch point formation compared with $VEGF_{165}$ alone; n=5, p=0.008. Statistical analysis was carried out using the Mann-Whitney U Test (Sigmaplot 11 software).

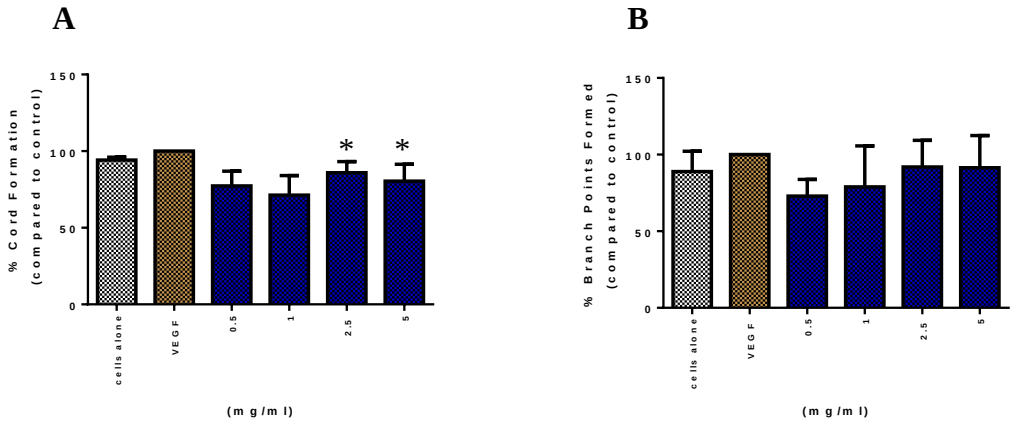

Figure 3.5 ***Effects of High Doses of CV on HuDMEC Differentiation*****:**
In the presence of recombinant $VEGF_{165}$, plus varying doses of CV, HuDMEC differentiation was inhibited. (**A**) CV at 2.5 and 5mg/ml exerted a significant (*P = 0.008*) inhibitory effect on HuDMEC cord formation when expressed as a % of the $VEGF_{165}$ alone control (**B**) No effects on HuDMEC branch point formation were observed in the presence of CV when expressed as a % of the $VEGF_{165}$ alone control.

Data is presented as mean±SEM (% cord or branch point formation compared with $VEGF_{165}$; n=5, p=0.008. Statistical analysis was carried out using the Mann-Whitney U Test (Sigmaplot 11 software).

Since CV, exerted similar inhibitory effects as those observed with Bz on HuDMEC cord formation *in vitro*, it was important to further investigate this effect. CV is made up of sodium salts and tween20 (***Avastin® SPC***), and since tween20 is used as a detergent in many denaturing solutions, it was decided that the effects of tween20 in CV, should be tested. All the different components of CV exerted an inhibitory effect on HuDMEC differentiation *in vitro,* and the data is summarised below in **Table 3.1**. This assay aimed to determine which particular component of CV was responsible for the inhibitory effects observed in the Matrigel assay. However, unfortunately, differentiation was not achieved, due to varying effects on endothelial cell differentiation in the presence of all the components of CV.

Experimental condition	**Cord formation (% compared with the $VEGF_{165}$ alone control; 100%)**	***P* value**	**Branch point formation (% compared with the $VEGF_{165}$ alone control; 100%)**	***P* value**
Bz (5 mg/ml)	38±12	<0.001	29±15	0.001
CV	71±12	0.044	82±20	NS
Tween20 alone	76±8	0.015	63±18	NS
CV minus tween20	43±11	<0.001	62±17	0.008

Table 3.1 ***Inhibitory Effects of the Different Components of CV on HuDMEC Differentiation:***
The Matrigel assay determined that the different components of the control vehicle for Bz display biological activity. Differentiation of the different component of CV was not achieved, due to various inhibitory effects observed with all the different components.

The data in the table is presented as mean±SEM (% cord or branch point formation compared with the $VEGF_{165}$ control; n=5). Statistical analysis (t-test) was performed using Sigmaplot 11 software.

Lower doses of Bz (0.5mg/ml) exerted significant yet minimal inhibitory effects on $VEGF_{165}$ mediated HuDMEC differentiation (mean±SEM; Bz 0.5mg/ml versus $VEGF_{165}$; 89±3.6% versus 100±0%; n=3, *P* = 0.034) when measured as cord formation (**Figure 3.6a**), however no inhibitory effects on branch point formation was observed. A stimulatory trend on network complexity was observed with Bz, compared with the $VEGF_{165}$ alone control (mean±SEM; Bz 0.125, 0.25 and 0.5 mg/ml versus $VEGF_{165}$; 213±87%, 195±81% & 190±88% respectively versus 100±0%; n=3, NS) (**Figure 3.6b**). However, this was not significant (*P* = 0.263, 0.303 & 0.363 respectively). No inhibitory effects were observed on HuDMEC differentiation in the presence of the control vehicle when measured as cord formation (**Figure 3.7a**). Similar to Bz, branch point formation was stimulated (153, 218 & 203%) compared with the $VEGF_{165}$ control (**Figure 3.7b**), this was not significant (*P* = 0.167, 0.302 & 0.382 respectively).

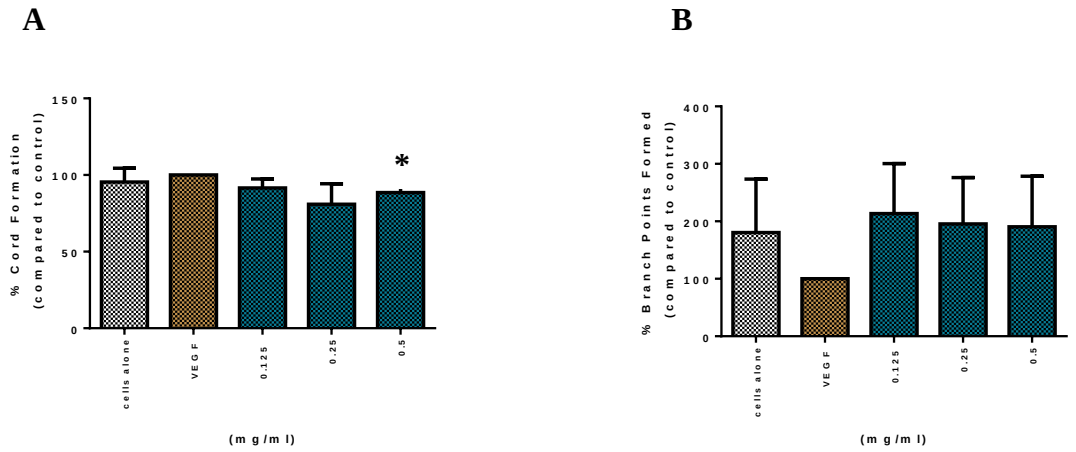

Figure 3.6 ***Effects of Low Doses of Bz on HuDMEC Differentiation:***
(**A**) In the presence of recombinant $VEGF_{165}$, Bz at 0.5mg/ml exerted significantly (*P=0.034*) inhibited HuDMEC cord formation when expressed as a % of the $VEGF_{165}$ alone control. (**B**) No significant effects were observed on branch point formation when expressed as a percentage of the $VEGF_{165}$ alone control.

Data is presented as mean±SEM (% cord or branch point formation compared with the $VEGF_{165}$ control; n=3, P = 0.034). Statistical analysis (t test) was performed using Sigmaplot 11 software.

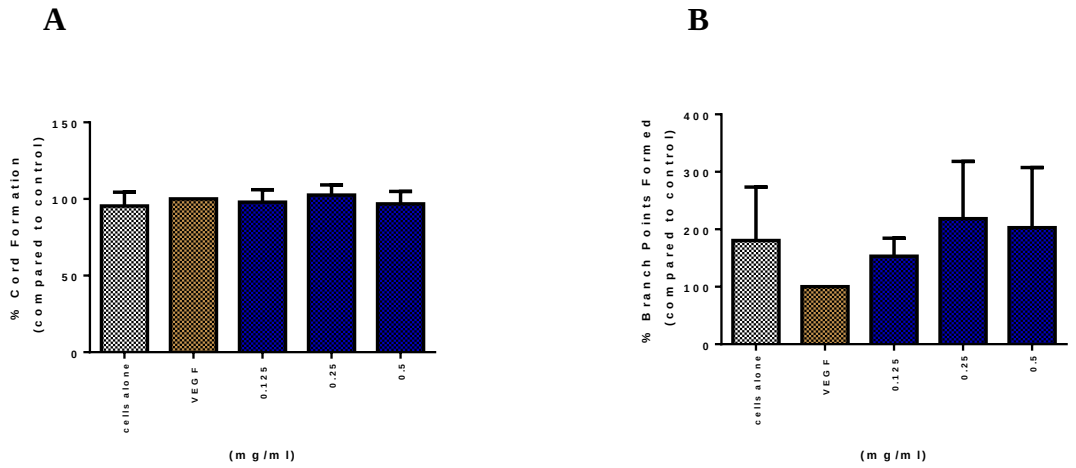

Figure 3.7 ***Effects of Low Doses of Control Vehicle on HuDMEC Differentiation:***
In the presence of recombinant $VEGF_{165}$ plus varying doses of CV, no inhibitory effects were observed on (**A**) cord formation or (**B**) branch point formation when expressed as a % of the $VEGF_{165}$ alone control.

Data is presented as mean±SEM (% cord or branch point formation compared with the $VEGF_{165}$ control; n=3, NS). Statistical analysis (t test) was performed using Sigmaplot 11 software.

Proliferation

Under normal physiological conditions EC turnover is slow, with proliferation occurring very rarely. However, during tumour angiogenesis the rate of EC proliferation is increased to allow for the rapid expansion of the microvasculature that supports the growth of solid tumours.

The addition of exogenous $VEGF_{165}$ exerted a minimal yet significant increase in HuDMEC cell proliferation at 24h compared with cells alone (mean±SEM; $VEGF_{165}$ vs. cells alone; 100±0% vs. 96±%; n=4, *P = 0.008*). Although an increase in HuDMEC cell proliferation was maintained in the presence of exogenous $VEGF_{165}$ at 48h (mean±SEM; $VEGF_{165}$ vs. cells alone; 136±20% vs. 125±12%; n=4, NS) this was not significant (*P = 0.841*) (**Figure 3.8**). In the presence of $VEGF_{165}$, the addition of high doses of Bz had no effect on HuDMEC cell proliferation at 24 or 48h (**Figure 3.8a**). A lack of inhibitory effects was also observed with equivalent volumes of CV (**Figure 3.8b**).

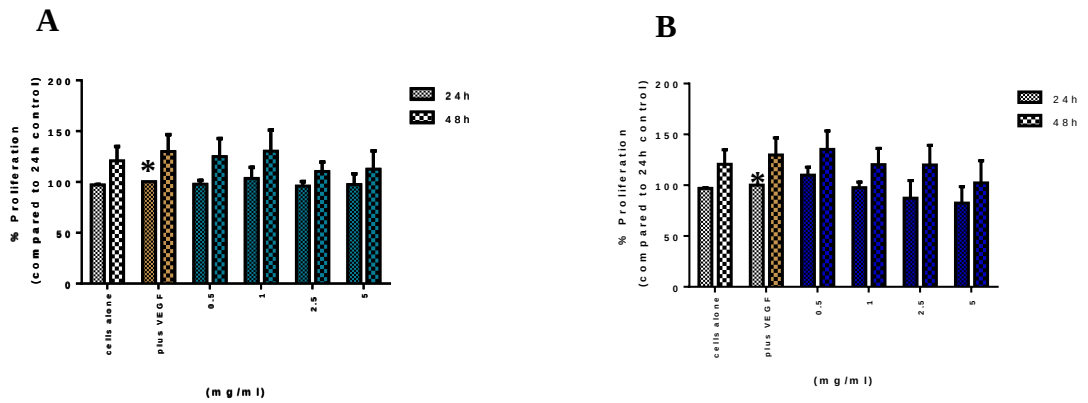

Figure 3.8 ***Effects of High Doses of Bz and CV on HuDMEC Proliferation:*** (**A**) In the presence of recombinant $VEGF_{165}$ with varying doses of (A) Bz, no significant inhibitory effects were observed on HuDMEC cell proliferation. (**B**) Similarly, no inhibitory effects were observed in the presence of equivalent volumes of CV at 24 or 48h.

Data is presented as mean±SEM (% proliferation compared with the 24h $VEGF_{165}$ control; n=4, p=0.008). Statistical analysis was performed using a Mann-Whitney U test (Sigmaplot 11 software).

Low doses (0.125, 0.25 and 0.5mg/ml) of Bz exerted a significant (*P= 0.029*), yet minimal inhibitory effect on HuDMEC cell proliferation at 24h (**Figure 3.9a**) (mean±SEM; Bz 0.125 and 0.25 and 0.5 vs. $VEGF_{165}$ alone control; 95±2% and 95±1% and 92±2% vs. 100±0%; n=4, *P* = 0.029). However, this initial inhibition was not maintained at 48h (**Figure 3.9a**). HuDMEC cell proliferation remained uninhibited in the presence of CV (**Figure 3.9b**).

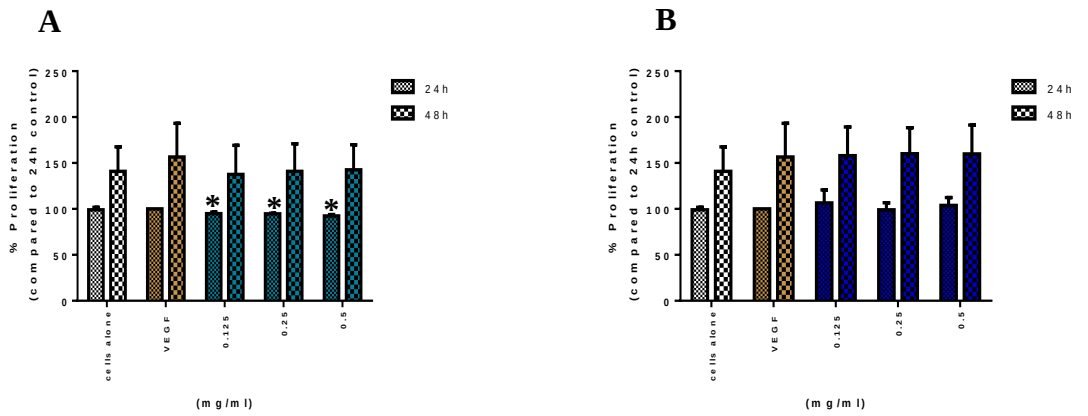

Figure 3.9 ***Effects of Low Doses of Bz and the CV on HuDMEC Proliferation:***
In the presence of recombinant $VEGF_{165}$, with varying low doses of (**A**) Bz, a significant (*P=0.029*) inhibitory effect was observed on HuDMEC cell proliferation, compared with the $VEGF_{165}$ alone control at 24h. However, this was not maintained at the 48h time-point. (**B**) No inhibitory effects were observed in the presence of equivalent volumes of CV at 24 or 48h.

Data is presented as mean±SEM (% proliferation compared with the 24h $VEGF_{165}$ control; n=4, p=0.029). Statistical analysis was performed using the Mann-Whitney U test (Sigmaplot 11 software).

Migration

Migration of endothelial cells *in vitro* can be measured by measuring the percentage gap closure formed on a monolayer of endothelial cells; this is represented in **Figure 3.10**.

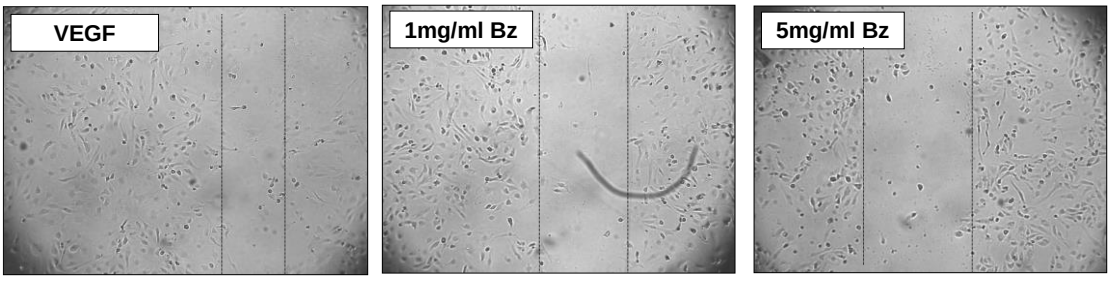

Figure 3.10 ***HuDMEC Migration*** (**A**) Representative images of HuDMEC gap closure at 32h after creating a scratch in the presence $VEGF_{165}$ alone (20ng/ml) or Bz at varying doses (1mg/ml and 5mg/ml).

High doses of Bz in the presence of recombinant $VEGF_{165}$ (1 and 5mg/ml) significantly (*P* = 0.010 and <0.001 respectively) inhibited VEGF-mediated HuDMEC migration, compared with the $VEGF_{165}$ alone control at 32h (mean±SEM; Bz 1 and 5mg/ml versus $VEGF_{165}$; 65±8% and 50±6% versus 100±0%; n=3) (**Figure 3.11a**). Unfortunately, a similar significant

inhibition was observed with the equivalent volume of CV (5mg/ml) (mean±SEM; CV versus $VEGF_{165}$; 31±15 versus 100±0%; n=3, *P* = 0.009) (**Figure 3.11b**). The CV at the equivalent volume (0.5 and 1mg/ml) exerted a stimulatory effect on HuDMEC migration (mean±SEM; CV 0.5 and 1 versus $VEGF_{165}$; 113±51% and 195±66% versus 100±0%; n=3, ns) however, this did not reach significance (*P* = 0.814 and 0.221 respectively).

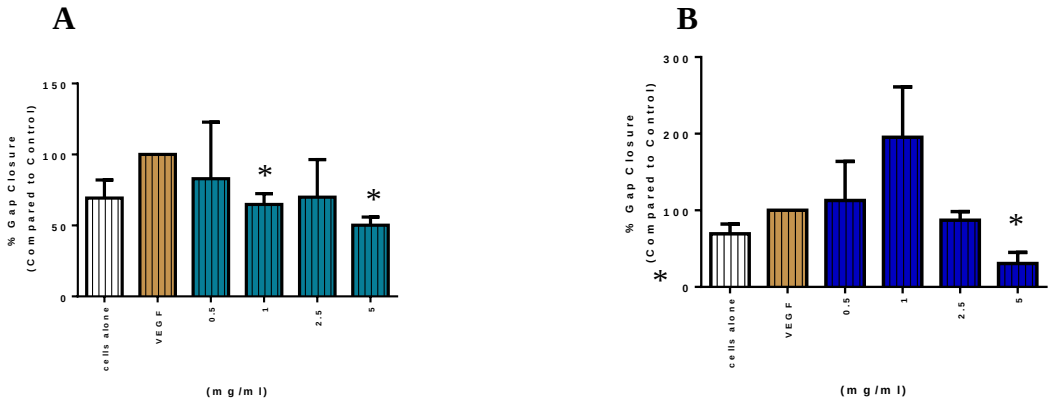

Figure 3.11 ***Effects of High Doses of Bz and the Control Vehicle on HuDMEC Migration***:
In the presence of recombinant $VEGF_{165}$, plus varying doses of (**A**) Bz (1mg/ml and 5mg/ml), resulted in significant (*P= 0.010 and P= < 0.001* respectively) inhibitory effects at 32h compared with the VEGF165 alone control. (B) CV (5mg/ml) significantly (P=0.009) inhibited HuDMEC migration at 32h compared with the $VEGF_{165}$ alone control.

Data is presented as mean±SEM (% gap closure compared with the $VEGF_{165}$ control; n=3). Statistical analysis was performed using a t-test (Sigmaplot 11 software).

Low doses of Bz (Bz 0.125 and 0.25 and 0.5mg/ml) exerted no inhibitory effects on $VEGF_{165}$ HuDMEC migration. However, a stimulatory trend was observed with all three doses compared with the $VEGF_{165}$ alone control (mean±SEM; Bz 0.125 and 0.25 and 0.5mg/ml versus $VEGF_{165;}$ 137±50% and 149±28% and 184±32% versus 100±0%; n=3, NS) (**Figure 3.12a**), this was not significant (*P = 0.499, 0.151 and 0.059* respectively). In contrast, CV, at an equivalent volume (0.25mg/ml and 0.5mg/ml) significantly inhibited HuDMEC migration *in vitro* at 32h compared with the $VEGF_{165}$ alone control (mean±SEM; CV 0.25 and 0.5mg/ml versus $VEGF_{165;}$ 78±3% and 61±1% vs. 100±0%; n=3, *P* =0.002 and <0.001) (**Figure 3.12b).**

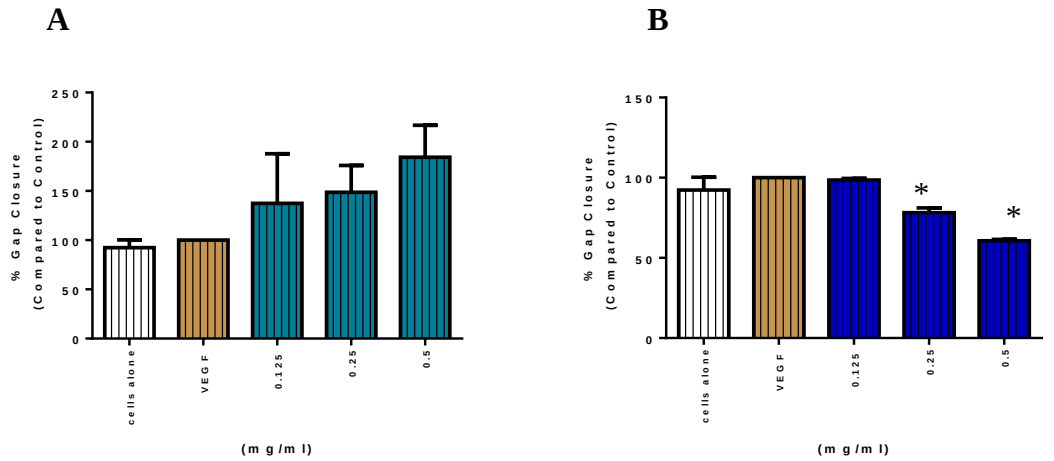

Figure 3.12 ***Effects of Low Doses of Bz and CV on HuDMEC Migration***:
In the presence of $VEGF_{165}$, plus varying doses of (**A**) Bz, no significant effects were observed on HuDMEC cell migration *in vitro* when expressed as % gap closure compared with the $VEGF_{165}$ control at 32h. **B**) With the addition of CV (0.25mg/ml and 0.5mg/ml), significant *(P= 0.002 and P= < 0.001* respectively) inhibitory effects on HuDMEC cell migration *in vitro* was observed when expressed as % gap closure compared with the $VEGF_{165}$ alone control at 32h.

Data is presented as mean±SEM (% gap closure compared with $VEGF_{165}$; n=3). Statistical analysis was performed using a t-test (Sigmaplot 11 software).

3.2.3 Effects of the Np1 peptides on HuDMEC Function

The Np1 peptides have previously been tested for the ability to bind the human Np1 receptor *in vitro* (***Cebe-Suarez et al, 2008***). However, the effect on functional activity associated with these Np1 peptides has not previously been evaluated. The table below (**Table 3.2**) summarises the different properties of the four peptides used in this project. The peptides used in this project are designed primarily to bind Np1 and block the interaction with functional $VEGF_{165}$. Np1 was the primary focus of the current project, as, to date (*Sept 2013*), the majority of research on the neuropilin receptors in breast cancer, was being carried out on Np1. In addition, substantially less was known about the role of Np2 in tumour angiogenesis and tumour progression. The affinity of these peptides were tested in a competitive binding assay with radiolabelled $VEGF_{165}$, and it was observed that, a RPPR sequence demonstrated high affinity to Np1, and inhibited almost entirely binding of exogenous $VEGF_{165}$. In contrast, a DKPRR sequence, displayed intermediate ability (***Cebe-Suarez et al, 2008***).

PEPTIDE	ORIGIN	SEQUENCE	NP1 BINDING
1	Viral VEGF-E protein	GSGST**RPPR**	Yes
2	Human VEGF-A protein (control)	GSGST**EPPR**	No
7b	Human VEGF-A protein	GSGST**DKPRR**	Yes
10	Viral VEGF-E protein	GSGST**RPPR**RRR	Yes and potentially Np2

Table 3.2 ***Properties of the Four Np1 Peptides***:
The differences present in the sequence of the four Np1 peptides used during this project are outlined in the table. The RPPR sequence is thought to exhibit higher binding affinity to human Np1. Peptide 2 was used in the presents as a control peptide, as this peptide lacked Np1 binding affinity

Differentiation

Matrigel Assay

Peptide 1 (p1), significantly inhibited HuDMEC differentiation when measured as cord formation at the 10µM and 50µM concentration compared with the $VEGF_{165}$ alone control (mean±SEM; p1 10µM and 50µM vs. $VEGF_{165}$; 87±5% and 78±3% vs. 100±0%; n=4, *P = 0.029*) (**Figure 3.13a**). The complexity of the network formed when measured as the number of branch points formed was not inhibited by p1 (**Figure 3.13b**). Surprisingly, peptide 2 (p2), which is a control peptide that does not bind to Np1 *in vitro*, also significantly inhibited HuDMEC differentiation when measured as cord formation at the 10µM and 50µM concentration compared with the $VEGF_{165}$ alone control (mean±SEM; p2 10µM and 50µM vs. $VEGF_{165}$; 57±10% and 54±15% vs. 100±0%; n=4, *P = 0.029*) (**Figure 3.14a**). Similar to p1, no significant inhibitory effects were observed on the complexity of the network in the presence in p2 (**Figure 3.14b**). The addition of peptide 7b (p7b), significantly inhibited cord formation at 1µM and 10µM compared with the $VEGF_{165}$ alone control (mean±SEM; p7b 1µM and 10µM vs. $VEGF_{165}$; 54±11% and 85±5% vs. 100±0%; n=4, *P = 0.029*) (**Figure 3.15a**). No effect on network complexity was observed with p7b (**Figure 3.15b**). Peptide 10 (p10) is thought to bind both Np1 and Np2 (although this has not been confirmed). The addition of p10, significantly inhibited cord formation at the 10µM and 50µM concentration compared with the $VEGF_{165}$ alone control (mean±SEM; p10 10µM and 50µM vs. $VEGF_{165}$; 63±10% and 44±12% vs. 100±0%; n=4, *P = 0.029*; **Figure 3.16a**) but no significant effects on network complexity was observed (**Figure 3.16b**).

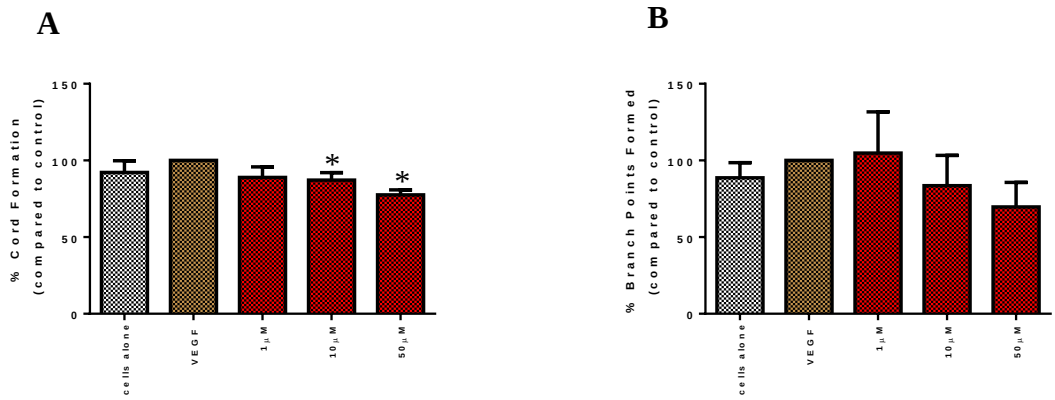

Figure 3.13 ***Effects of P1 on HuDMEC Differentiation***:
In the presence of recombinant $VEGF_{165}$, plus p1 (10 and 50μM) a significant (*P=0.029*) effect was observed on (**A**) cord formation when expressed as a percentage of the $VEGF_{165}$ alone control**. (B**) No significant effects were observed on branch point formation when expressed as a percentage of the $VEGF_{165}$ alone control.

Data is presented as mean±SEM (% cord or branch point formation compared to $VEGF_{165}$; n=4, p=0.029). Statistical analysis was performed using the Mann-Whitney U test (Sigmaplot 11 software).

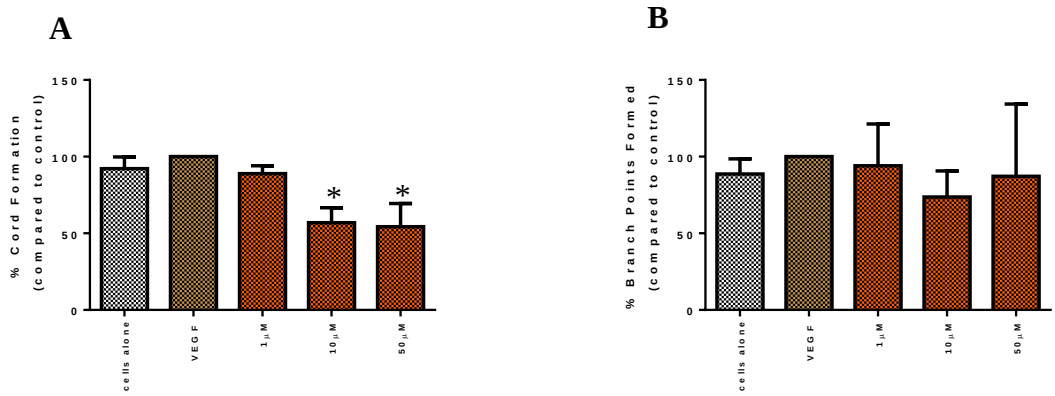

Figure 3.14 ***Effects of P2 on HuDMEC Differentiation***:
In the presence of recombinant $VEGF_{165}$,, p2 at 10 and 50μM exerted significant (*P=0.029*) effects on (**A**) cord formation when expressed as a % of the $VEGF_{165}$ alone control **(B**) No significant effects were observed on branch point formation when expressed as a % of the $VEGF_{165}$ alone control.

Data is presented as mean±SEM (% cord or branch point formation compared with $VEGF_{165}$; n=4, P = 0.029). Statistical analysis was performed using the Mann-Whitney U test (Sigmaplot 11 software).

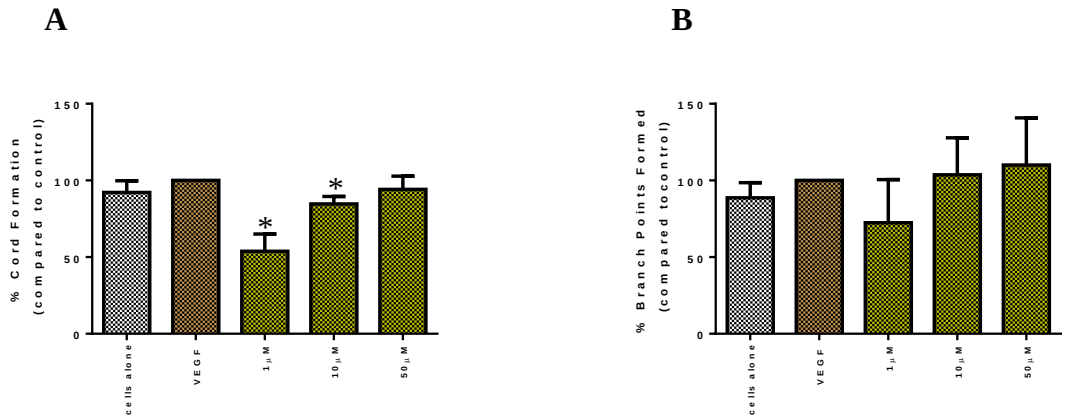

Figure 3.15 ***Effects of P7b on HuDMEC Differentiation***:
In the presence of recombinant $VEGF_{165}$, p7b at 1µM and 10µM exerted significant (*P=0.029*) effects on (**A**) HuDMEC cord formation when expressed as a % of the $VEGF_{165}$ alone control. **(B**) No significant effects were observed on branch point formation when expressed as a % of the $VEGF_{165}$ control.

Data is presented as mean±SEM (% cord or branch point formation compared with $VEGF_{165}$; n=4, P = 0.029). Statistical analysis was performed using the Mann-Whitney U test (Sigmaplot 11 software).

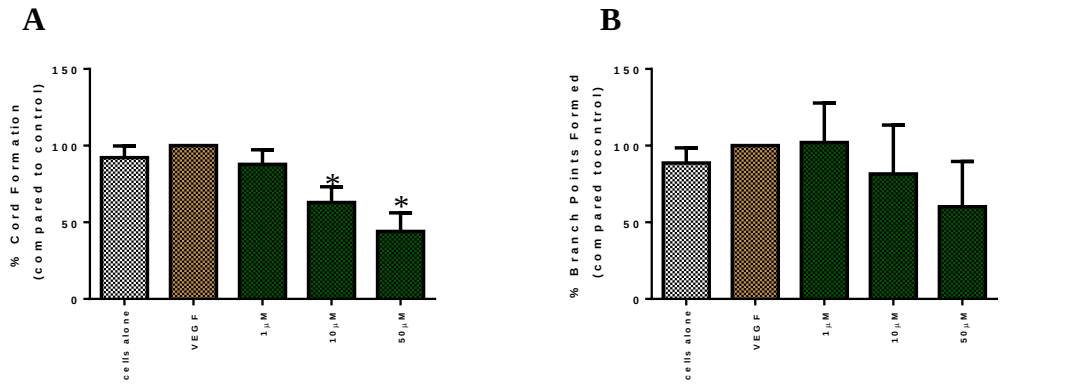

Figure 3.16 ***Effects of P10 on HuDMEC Differentiation***:
In the presence of recombinant $VEGF_{165}$, p10 at 10µM and 50µM exerted significant (*P=0.029*) effects on (**A**) HuDMEC cord formation when expressed as a % of the $VEGF_{165}$ alone control. **(B**) No significant effects were observed on branch point formation when expressed as a % of the $VEGF_{165}$ alone control.

Data is presented as mean±SEM (% cord or branch point formation compared with the $VEGF_{165}$ control; n=4, P = 0.029). Statistical analysis was performed using the Mann-Whitney U test (Sigmaplot 11 software).

3D Sprouting Angiogenesis Assay

The 3D angiogenesis assay (PromoCell) utilises endothelial cell spheroids that are embedded in a collagen matrix and simulates the entire process of vessel formation; proteolytic activity, migration, proliferation and lumen formation. In this assay a significant stimulatory effect on percentage sprout formation was observed in the presence of $VEGF_{165}$ compared with cells alone (mean±SEM; $VEGF_{165}$ versus cells alone; 100±0% versus 31±5%; n=3, P <0.001) (**Figure 3.17b**). Peptide 2 and p10 both exerted significant inhibitory effects on percentage sprout formation compared with the $VEGF_{165}$ alone control (mean±SEM; p2 and p10 versus $VEGF_{165}$; 80±6% and 60±11% versus 100±0%; n=3, *P = 0.027 and 0.022*) (**Figure 3.17b**). Although peptide 7b apparently reduced the percentage sprout formation compared with the $VEGF_{165}$ alone control (mean±SEM; p7b versus $VEGF_{165;}$ 82±20% versus 100±0%; n=3, ns), however, this was not significant (*P = 0.402*) (**Figure 3.17b**). It is important to note, that although statistical significance was observed between treatments in this assay, the sprout formation was poor, even in the presence of VEGF (**Figure 3.17**), suggesting that the 3D angiogenesis assay may not be a reliable assay especially if the data produced is not biologically relevant.

A

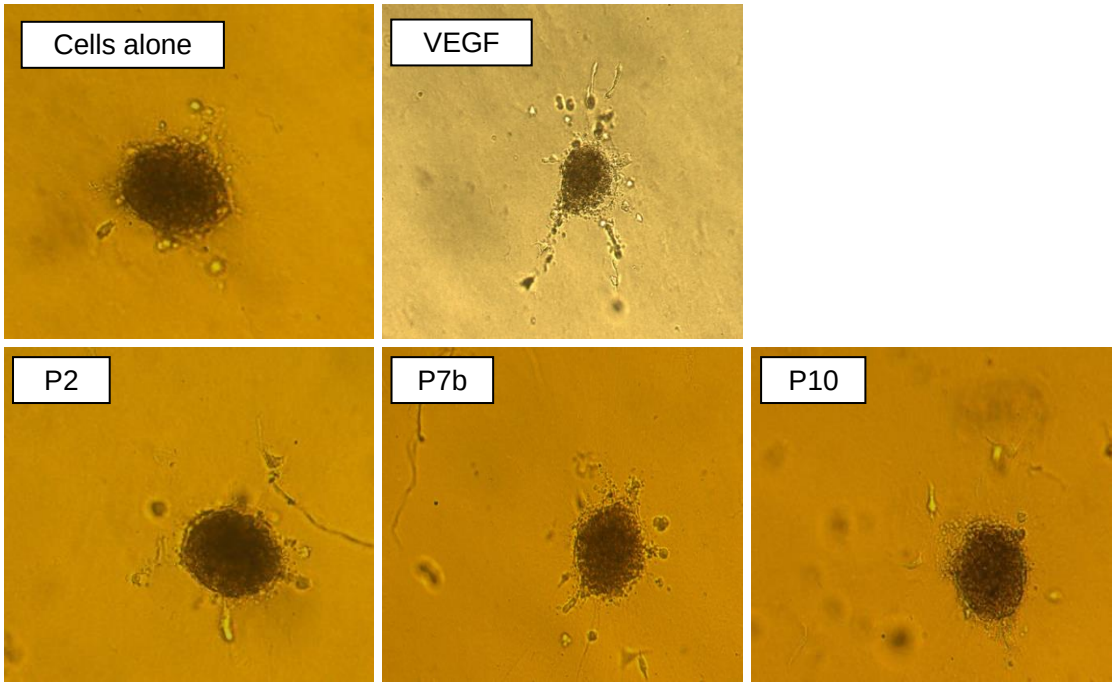

B

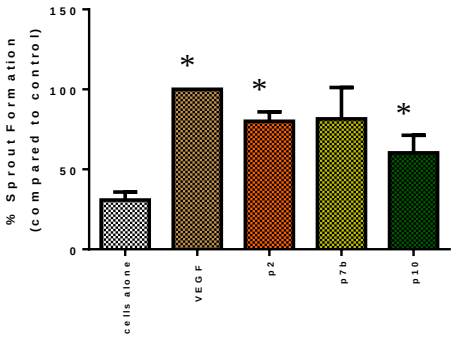

Figure 3.17 ***Effects of Np1 Peptides on 3D HuDMEC Sprout Formation***:
(**A**) Representative images of the sprouts formed in the 3D angiogenesis assay in the presence of $VEGF_{165}$ and the Np1 binding peptides (**B**) P2 and p10 significantly (*P=0.027 and P=0.022*), inhibited HuDMEC sprout formation when expressed as a % of the $VEGF_{165}$ alone control. No inhibitory effects were observed in the presence of p7b.

Data is presented as mean±SEM (% sprout formation compared with $VEGF_{165}$; n=3, p<0.001). Statistical analysis was performed using a t-test (Sigmaplot 11 software).

Proliferation

When cells were plated directly in media containing Np1 peptides, no effects on HuDMEC cell proliferation was observed in the presence of any of the peptides (**Figure 3.18a-d**). A second MTS experiment was set up, whereby the peptides were pre-incubated for 2h with the HuDMECs prior to adding $VEGF_{165}$, to determine if this exerted an inhibitory effect on HuDMEC cell proliferation (**Figure 3.19a-d**). Pre-incubating p1 (50µM) (**Figure 3.19a**) and p10 (50µM) (**Figure 3.19d**) appeared to inhibit HuDMEC cell proliferation at 48h, however, these experiments were only carried out twice, therefore a trend can be suggested, but no significant analysis or conclusions can made as to whether pre-incubating the Np1 peptides inhibit HuDMEC cell proliferation.

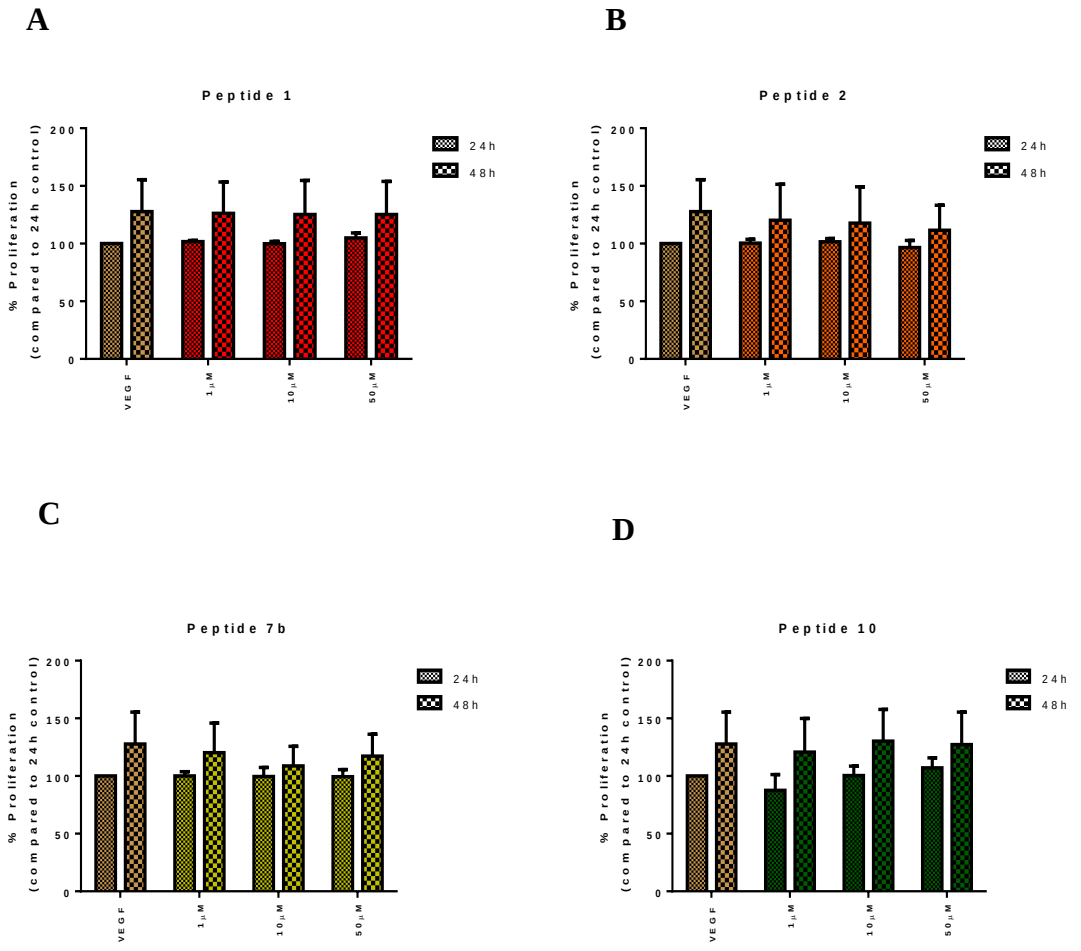

Figure 3.18 ***Effects of Np1 Peptides on HuDMEC Proliferation***:
In the presence of recombinant $VEGF_{165}$ plus varying doses of the four Np1 peptides, no inhibitory effects were observed on HuDMEC cell proliferation with (**A**) peptide 1 (**B**) peptide 2 (**C**) peptide 7b and (**D**) peptide 10 compared with the $VEGF_{165}$ alone control.

Data is presented as mean±SEM (% proliferation compared with $VEGF_{165}$ alone at 24h; n=3). Statistical analysis was performed using a t-test (Sigmaplot 11 software).

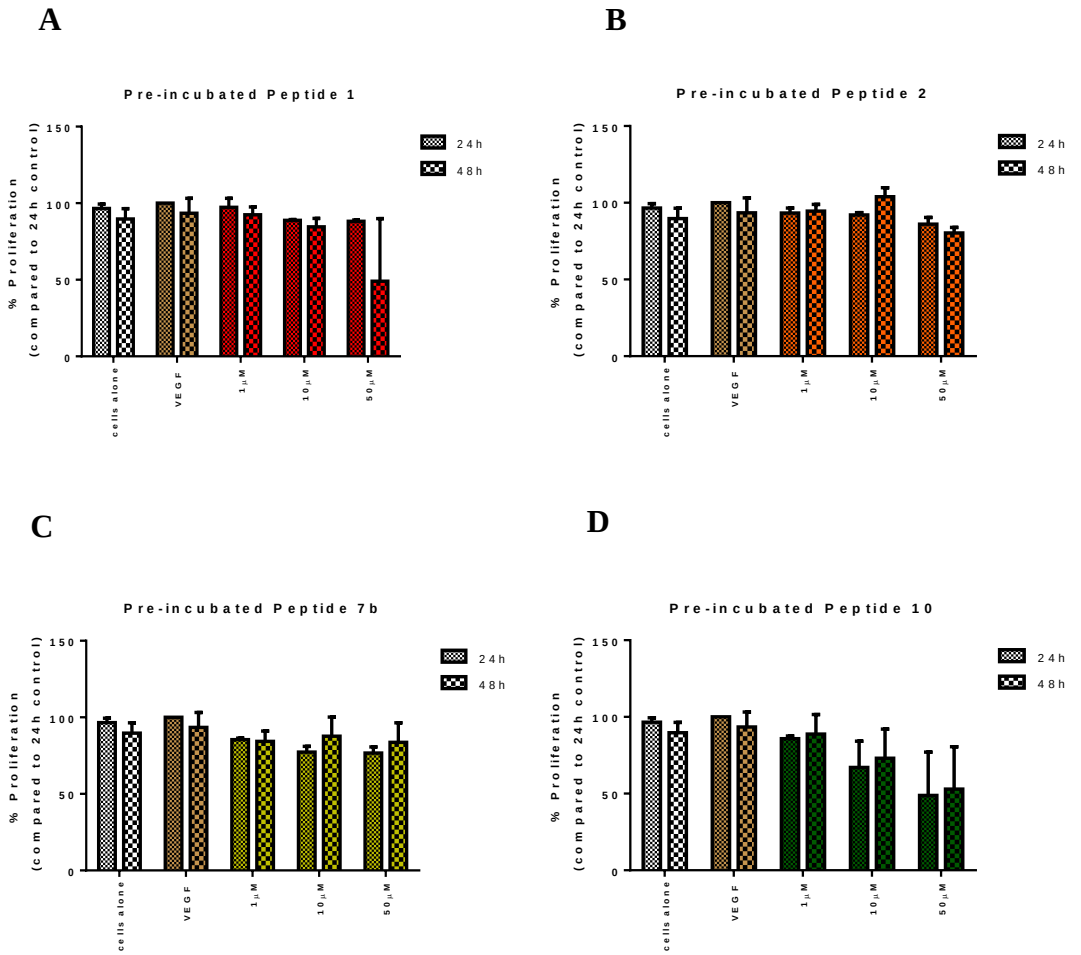

Figure 3.19 ***Effects of Pre-incubating the Np1 Peptides on HuDMEC Proliferation***:
Pre-incubating the Np1 peptides 2h prior to adding recombinant $VEGF_{165,}$ resulted an inhibitory trend with p1 and p10. However, since the experiment was only carried out twice, a conclusion cannot be made as to the effects of pre-incubating the peptides on HuDMEC cell proliferation, due to the lack to statistical analysis.

Data is presented as mean±SEM (% proliferation compared with $VEGF_{165}$ alone at 24h; n=2).

Migration

In the scratch assay, the presence of peptide 1, p2 and p7b all inhibited HuDMEC migration. However, this did not reach statistical significance (**Figure 3.20a-c**). Peptide 10 stimulated HuDMEC migration *in vitro*; however, this did not reach statistical significance (**Figure 3.20d**). It is possible that the nature of the scratch assay increased the variability of the data observed as mitomycin C was added to minimise the proliferation activity to ensure that the closure of the gap was a result of migration alone. It was thus decided that a Boyden chamber assay should be performed to observe whether a chemotactic assay that created a VEGF gradient was more relevant when measuring HuDMEC cell migration *in vitro*. Peptide 7b was

used in the Boyden assay as it demonstrated a inhibitory trend in HuDMEC migration in the scratch assay. Peptide 10 was also chosen as it was the only Np1 peptide to display a trend towards stimulatory effects on HuDMEC migration and it was important to assess, if consistent results could be obtained using different migration assays. In the Boyden chamber assay, as expected, $VEGF_{165}$ alone significantly (*P = 0.010*) increased HuDMEC cell migration compared with cells alone (mean±SEM; $VEGF_{165}$ vs. cells alone; 100±% vs. 61±9%; n=3, p=0.010) (**Figure 3.21**). The presence of p7b significantly (*P < 0.001*) inhibited HuDMEC cell migration compared with the $VEGF_{165}$ alone control (mean±SEM; p7b vs.$VEGF_{165}$; 33±5% vs. 100±0%; n=3, p<0.001) (**Figure 3.21**). Unlike in the scratch assay, p10 exerted an inhibitory effect on HuDMEC cell migration compared with the $VEGF_{165}$ alone control ((mean±SEM; p710 vs.$VEGF_{165}$; 57±38% vs. 100±0%; n=3, NS), however this inhibition failed to reach statistical significance (*P = 0.552*).

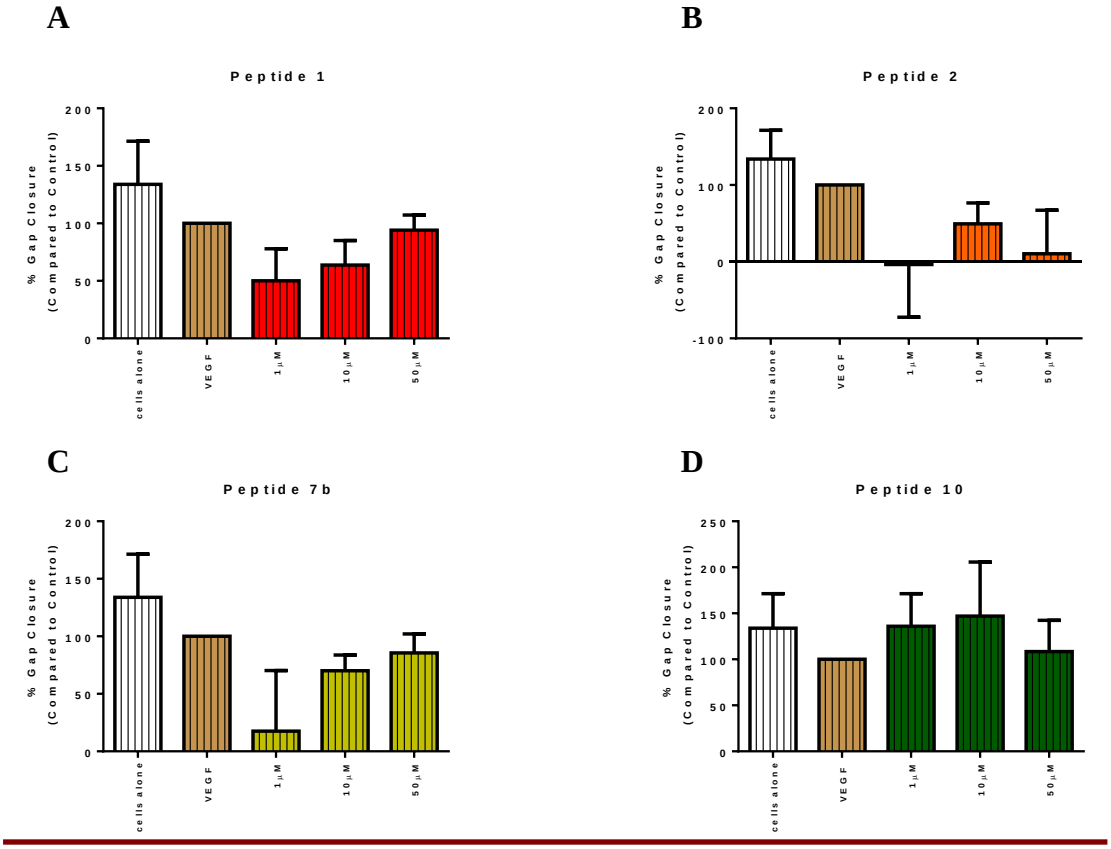

Figure 3.20 ***Effects of Np1 Peptides on HuDMEC Migration***:
In the presence of $VEGF_{165}$, plus varying doses of the Np1 peptides, no significant effects were observed on HuDMEC cell migration *in vitro*; (**A**) peptide 1 (**B**) peptide 2 (**C**) peptide 7b and (**D**) peptide 10 when expressed as % gap closure compared with the $VEGF_{165}$ alone control

Data is presented as mean±SEM (% gap closure compared with $VEGF_{165}$; n=3. Statistical analysis was performed using a t-test (Sigmaplot II software).

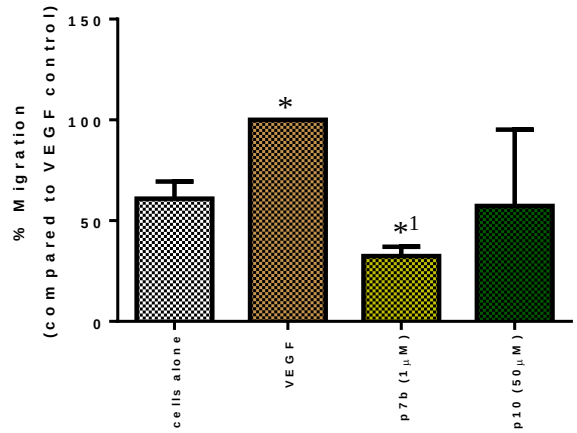

Figure 3.21 ***Effects of the 7b and p10 on HuDMEC Migration; Boyden Chamber:***
In the presence of recombinant $VEGF_{165}$, peptide 7b significantly (*P <0.001*) inhibited migration in the Boyden chamber, after 4 hours compared with the $VEGF_{165}$ alone control. In contrast to the scratch assay, p10 reduced HuDMEC migration but this was not significant.

Data is presented as mean±SEM (% Migration compared with $VEGF_{165}$; n=3, $*_1$ p<0.001). Statistical analysis was performed using a t-test (Sigmaplot 11 software).

3.2.4 Combining Bz with the Np1 peptides on HuDMEC Function

Differentiation

In previous experiments p1, p2, p7b and p10 all showed a significant inhibition in HuDMEC differentiation, however only p2, p7b and p10 exerted a reduction of approximately 50% HuDMEC cord formation when compared with the $VEGF_{165}$ alone control (**Figure 3.13-3.16)**. Thus, it was decided that p2, p7b and p10 would be used in combination with Bz at the following doses; 50μM, 1μM and 50μM respectively.

As expected the addition of Bz (5mg/ml) significantly (*P=0.029*) inhibited HuDMEC cell differentiation when measured as cord formation compared with the $VEGF_{165}$ alone control (mean±SEM; Bz 5mg/ml vs. $VEGF_{165}$; 75±89% vs. 100±0%; n=4, p=0.029) (**Figure 3.22a**). However, the extent to which Bz inhibited cord formation was less compared with what was previously observed. Similarly, the level of inhibition previously observed with the addition of p2, was not evident in the combination experiments (54% vs, 94% cord formation). When Bz was combined with p2, a significant inhibition was observed (*P = 0.029*), however the efficacy of this inhibition was not greater than the inhibition observed with Bz alone (81% vs. 75%) (**Figure 3.22a**). Bz alone, significantly (*P=0.029*) inhibited the network complexity compared with the $VEGF_{165}$ alone control (mean±SEM; Bz 5mg/ml vs. $VEGF_{165}$; 73±9% vs. 100±0%; n=4, p=0.029). This inhibition, however was lost when Bz was combined with p2

(mean±SEM; Bz/p2; 92±28%) (**Figure 3.22b**). No significant effects on HuDMEC cord formation or branch point formation were observed in the presence of CV alone or in combination with p2 (**Figure 3.23**).

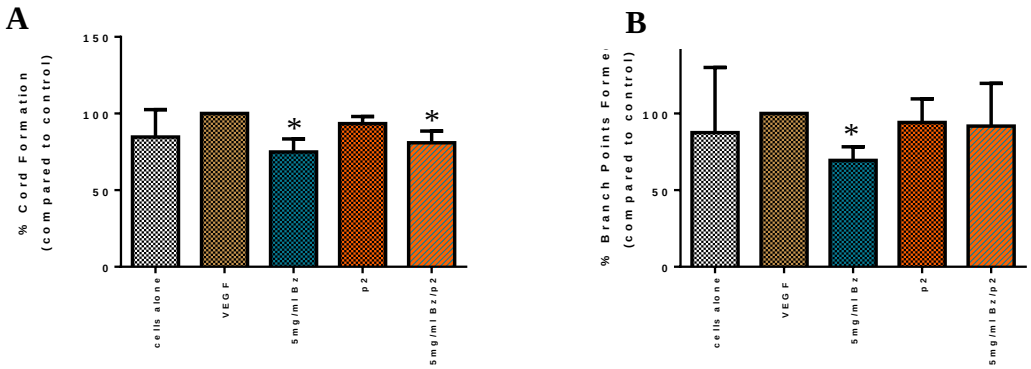

Figure 3.22 ***Effects of Combining Bz and P2 on HuDMEC Differentiation***:
(**A**) In the presence of recombinant $VEGF_{165}$, no additive inhibitory effects were observed on HuDMEC differentiation when Bz was combined with P2 on (**A**) cord formation and (**B**) branch point formation in the presence of Bz and p2 together compared with Bz alone.

Data is presented as mean±SEM (% cord or branch point formation compared with $VEGF_{165}$; n=4, *p=0.029). Statistical analysis was performed using the Mann-Whitney U Test (Sigmaplot 11 software)

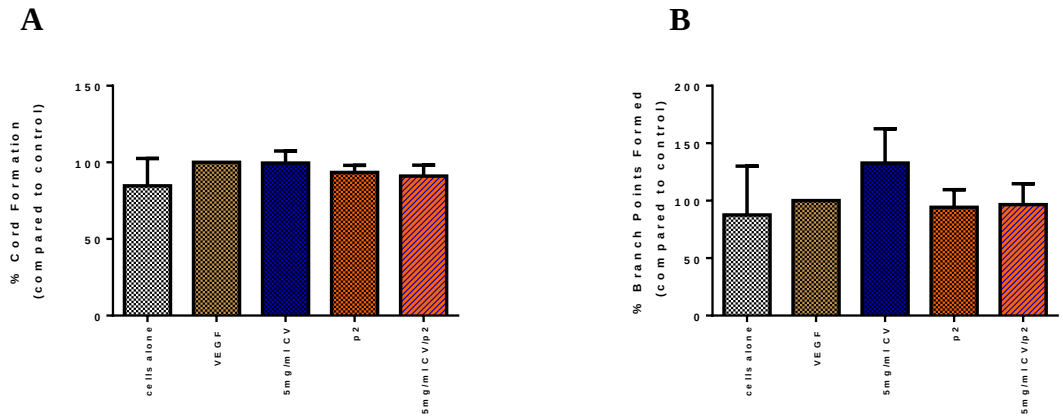

Figure 3.23 ***Effects of Combining CV and P2 on HuDMEC Differentiation***:
In the presence of recombinant $VEGF_{165}$, no effects on HuDMEC cell differentiation were observed when CV and p2 were combined when measured as (**B**) cord and (**C**) branch point formation compared to Bz alone.

Data is presented as mean±SEM (% cord or branch point formation compared with $VEGF_{165}$; n=4, NS). Statistical analysis was performed using the Mann-Whitney U Test (Sigmaplot 11 software)

Similarly, the inhibition previously observed with p10 on HuDMEC cord formation was not evident in these experiments (44% vs. 90%) (**Figure 3.24**). Combining p10 with Bz, resulted in a significant (*P=0.029*) inhibition in cord formation. However, the combined inhibition was not much greater than that observed with Bz alone (73% vs. 75% respectively) (**Figure 3.24a**). However, unlike p2 when combined with Bz, p10 did not reduce the efficacy of Bz alone. Combining Bz with p10 resulted in significant (*P = 0.029*) inhibition in branch point formation, this combined effect was greater than that observed with Bz alone (mean±SEM; Bz/p10 vs. Bz alone; 63±7% vs. 70±9%; n=4, NS). However this did not reach statistical significance (*P = 0.686*) (**Figure 3.24b**). When p10 was combined with CV a significant (p=0.029) inhibition in HuDMEC cord formation was observed when compared with the $VEGF_{165}$ alone control (71% vs. 100% respectively) (**Figure 3.25a**). This was not expected, as neither p10 nor CV alone, exerted any inhibitory effects on cord formation in these experiments.

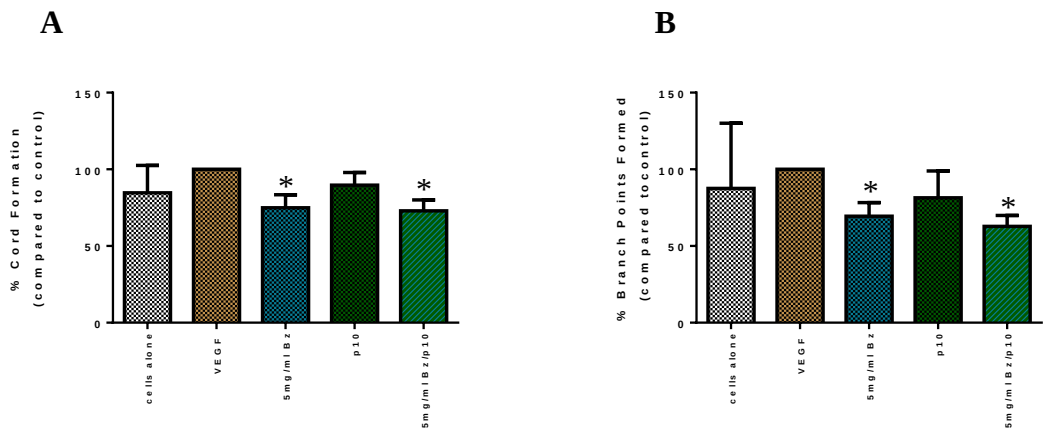

Figure 3.24 ***Effects of Combining Bz and P10 on HuDMEC Differentiation***:
In the presence of recombinant $VEGF_{165}$, no significant (*P=0.686*) additive effect were observed on HuDMEC differentiation when Bz was combined with p10, when measured as (**A**) cord formation and (**B**) branch point formation compared to Bz alone.

Data is presented as mean±SEM (% cord or branch point formation compared with $VEGF_{165}$; n=4, *p=0.029). Statistical analysis was performed using the Mann-Whitney U Test (Sigmaplot 11 software)

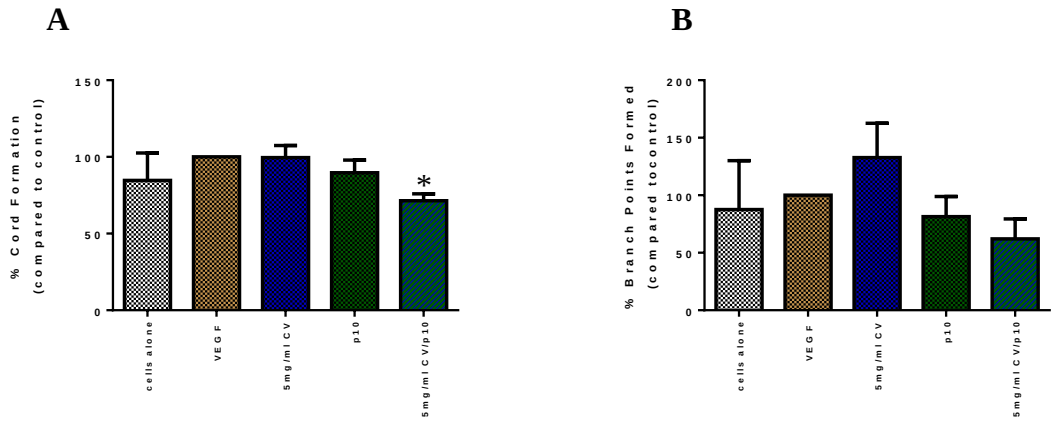

Figure 3.25 ***Effects of Combining CV and P10 on HuDMEC Differentiation***:
In the presence of recombinant $VEGF_{165,}$ combining CV with p10 exerted a significant (*P=0.029*) inhibitory effect on HuDMEC differentiation when measured as (**A**) cord formation when compared with CV control. No significant inhibition was observed on (**B**) branch point formation.

Data is presented as mean±SEM (% cord or branch point formation compared with $VEGF_{165}$; n=4, *p=0.029). Statistical analysis was performed using the Mann-Whitney U Test (Sigmaplot 11 software)

Combining p7b with Bz, resulted in significant (*P=0.002*) inhibition in cord formation when compared with the $VEGF_{165}$ alone control. However, this combined inhibition was not greater than that observed with Bz alone (87% vs. 83% respectively) (**Figure 3.26a**). In the p7b experiments, Bz and p7b alone failed to exert a significant (*p=0.079 and p=0.942* respectively) inhibitory effect on HuDMEC branch point formation compared with the $VEGF_{165}$ control (mean±SEM; Bz alone and p7b alone vs. $VEGF_{165}$; 72±10% and 102±20% vs. 100±0%; n=3, NS). However, combining Bz with p7b resulted in significant (*P=0.002*) inhibition in network complexity when compared with the $VEGF_{165}$ alone control (mean±SEM; Bz/p7b vs. $VEGF_{165;}$ 71±7% vs. 100±0%; n=3, p=0.002) (**Figure 3.26b**). Combining p7b with CV resulted in a significant (*P=0.012*) inhibitory effect on HuDMEC cord formation (**Figure 3.27a**) compared with the $VEGF_{165}$ alone control (mean±SEM; CV/p7b alone vs. $VEGF_{165}$; 90±1% vs. 100±0%; n=3, p=0.012). No significant effects on HuDMEC branch point formation were observed with either the CV or p7b compared with the $VEGF_{165}$ control (mean±SEM; CV alone and p7b alone vs. $VEGF_{165}$; 103±6% and 102±20% vs. 100±0%; n=3, NS). However, combining the two significantly (*P=0.022*) inhibited HuDMEC branch point formation compared with the $VEGF_{165}$ alone control (85±10% vs. 100±0% respectively) (**Figure 3.27b**). In the combination experiments even though some of the treatments exerted significant inhibitory effects on HuDMEC

differentiation, this was minimal compared with previous experiments observed during this study and could be due to batch to batch variation in the HuDMECs. This batch variation, may also explain the increased level of proliferating islands compared with previous Matrigel experiments, suggesting that the cells are not responding to stimuli as efficiently as previously observed.

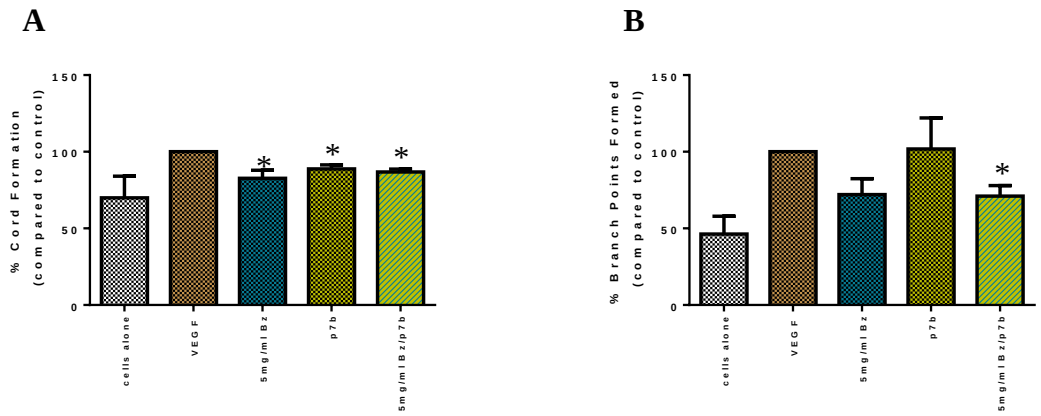

Figure 3.26 ***Effects of Combining Bz and P7b on HuDMEC Differentiation***:
In the presence of recombinant $VEGF_{165}$, although significant (*P=0.002*) reductions were observed when Bz was combined with P7b, this inhibition had no additive inhibitory effects in (**B**) cord and (**C**) branch point formation compared to Bz alone.

Data is presented as mean±SEM (% cord or branch point formation compared with $VEGF_{165}$; n3,* p<0.05). Statistical analysis was performed using a t-test (Sigmaplot 11 software)

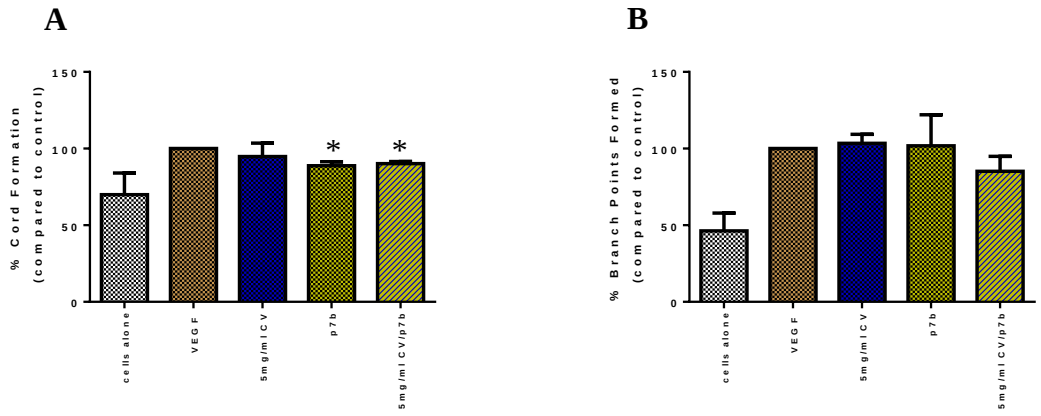

Figure 3.27 ***Effects of Combining CV and P7b on HuDMEC Differentiation***:
In the presence of $VEGF_{165}$, although a significant (*P=0.012*) combined effect was observed on cord formation, no additive inhibitory effects were displayed on HuDMEC differentiation, when measured as (**A**) cord formation when compared with p7b alone. (**C**) No inhibitory effects on branch point formation were observed compared with p7b alone.

Data is presented as mean±SEM (% cord or branch point formation compared with $VEGF_{165}$; n=3,* p<0.05). Statistical analysis was performed using a t-test (Sigmaplot 11 software)

Proliferation

Since there were no inhibitory effect observed on HuDMEC cell proliferation in the presence of any of the four Np1 peptides alone or Bz, a combination MTS assay was not deemed relevant.

Migration

Similar to previous experiments, both Bz and CV (5mg/ml) significantly (*P=<0.001*) inhibited HuDMEC migration i*n vitro* compared with the $VEGF_{165}$ alone control (9.8% SEM± and -1.2% SEM± vs. 100% respectively). However, the level of inhibition appeared to be much greater in the combination experiments, with CV alone resulting in regression of HuDMEC cells, from the area where the monolayer of cells were 'wounded' (**Figure 3.29**). The presence of p7b (1μM) significantly (*P=<0.001)* inhibited HuDMEC migration compared with the $VEGF_{165}$ alone control (52% SEM± vs. 100% respectively) (**Figure 3.28a & 3.29a**). Combining p7b, with both Bz and CV, resulted in a additive effect on HuDMEC migration inhibition, which resulted in regression of the gap closure. However, this did not reach statistical significance (**Figure 3.28a & 3.29a**). Combining p10, with Bz exerted no additive inhibitory effects on HuDMEC cell migration *in vitro* compared with Bz or CV alone (**Figure 3.28b & 3.29b**).

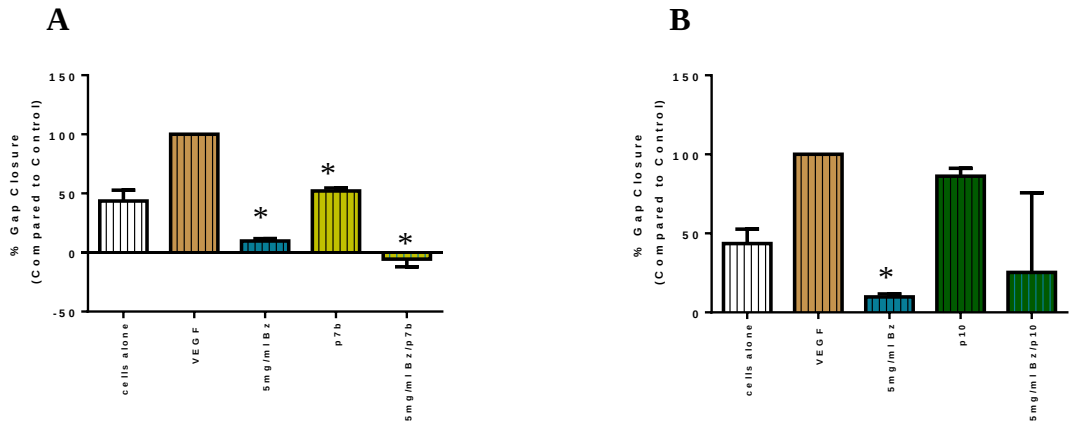

Figure 3.28 ***Effects of Combining Bz with P7b and P10 on HuDMEC Migration***:
In the presence of recombinant $VEGF_{165}$ (**A**) no significant additive effects on HuDMEC migration were observed when p7b was combined with Bz compared to Bz alone. Similarly, (**C**) no significant effects on HuDMEC migration were observed when p10 was combined with Bz

Data is presented as mean±SEM (%gap closure compared with $VEGF_{165}$; n=3, *p<0.001). Statistical analysis was performed using a t-test (Sigmaplot 11 software)

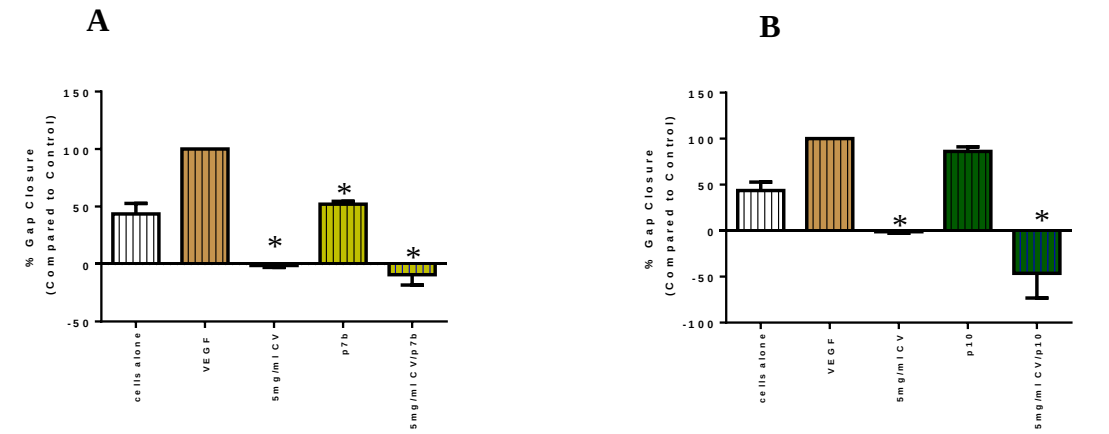

Figure 3.29 ***Effects of Combining CV with P7B and P10 on HuDMEC Migration***:
In the presence of recombinant $VEGF_{165}$ (**A**) no additive effects on HuDMEC cell migration were observed when p7b or (**B**) p10 was combined CV compared to CV alone.

Data is presented as mean±SEM (%gap closure compared to $VEGF_{165}$; n=3, *p<0.001). Statistical analysis was performed using a t-test (Sigmaplot 11 software)

3.2.5 Effects of Np1 and Np2 antibodies on HuDMEC Function

As the Np1 peptides used in this study are small in nature and the efficacy of these peptides as biological inhibitors of Np1 and $VEGF_{165}$ interactions are being tested for the first time, it was deemed important that an antibody against the neuropilin receptors also be tested. At the time of these experiments the only commercially available antibodies were from R&D systems (these antibodies have been tested for blocking ability in an ELISA based assay). The Np1 and Np2 antibodies were thus purchased and utilised in subsequent experiments.

Differentiation

The Np1 antibody (5µg/ml and 10µg/ml) significantly inhibited HuDMEC differentiation when measured as cord formation compared with the $VEGF_{165}$ alone control (mean±SEM; Np1 antibody 5 and 10µg/ml vs. $VEGF_{165;}$ 93±2 and 94±3% vs. 100±0%; n=3, p=0.008 and p=0.028) (**Figure 3.30a**). No significant effects were observed on HuDMEC branch point formation in the presence of the Np1 antibody when compared with the $VEGF_{165}$ alone control (**Figure 3.30b**). The addition of an Np2 antibody (20µg/ml) also significantly (*P=0.004*) inhibited HuDMEC cord formation compared with the $VEGF_{165}$ alone control (mean±SEM; Np2 20µg/ml vs. $VEGF_{165;}$ 89±3% vs. 100±0%) (**Figure 3.31a**). Similar to the Np1 antibody, no significant effects on the complexity of the network was observed with the Np2 antibody (**Figure 3.31b**). The inhibition in cord formation observed with the Np1 and Np2 antibodies was less then that observed with the Np1 peptides suggesting that at the concentrations used, the peptides appear to display greater biological activity.

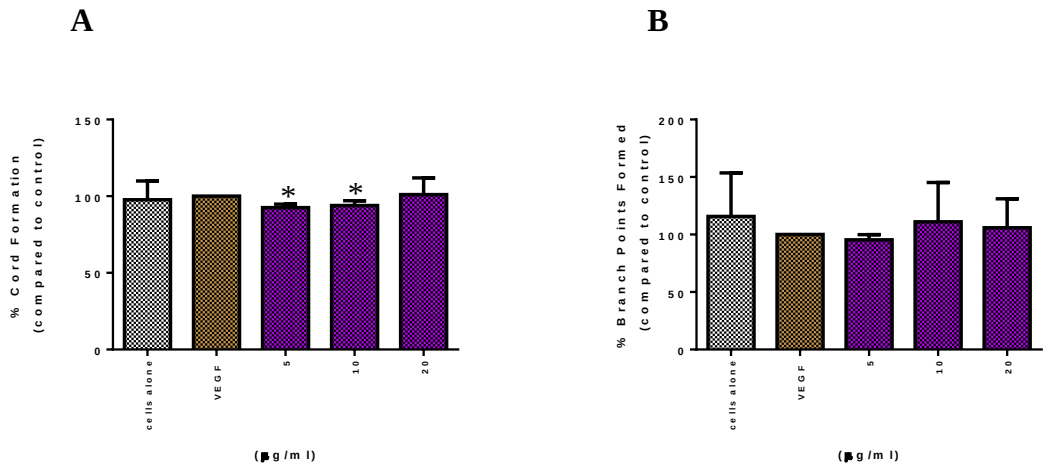

Figure 3.30 ***Effects of Np1 antibody on HuDMEC Differentiation***:
In the presence of recombinant $VEGF_{165}$ plus varying doses of an Np1 antibody (**A**) a significant (*P=0.008 and P=0.028*, respectively) inhibitory effect on cord formation, was observed at 5µg/ml and 10µg/ml when expressed as a percentage of the $VEGF_{165}$ alone control. (**B**) No significant effects on branch point formation were observed in the presence of the Np1 antibody when expressed as a % of the $VEGF_{165}$ control.

Data is presented as mean±SEM (% cord or branch point formation compared with $VEGF_{165}$; n=3, *p<0.05). Statistical analysis was performed using a t-test (Sigmaplot 11 software).

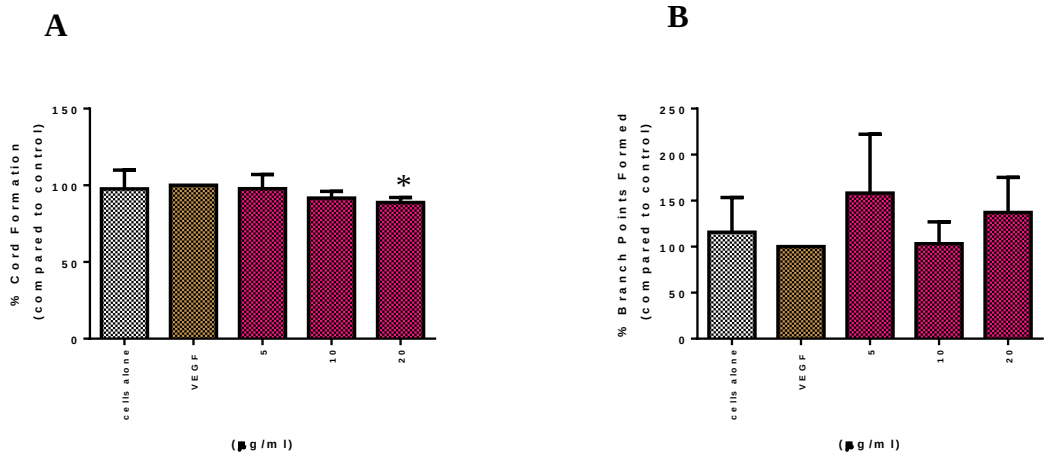

Figure 3.31 ***Effects of Np2 antibody on HuDMEC Differentiation***:
In the presence of recombinant $VEGF_{165}$ plus varying doses of an Np2 antibody (**A**) a significant (*P=0.004*) inhibition in cord formation was observed with 20µg/ml of the Np2 antibody when expressed as a percentage of the $VEGF_{165}$ alone control. (**B**) No effects on HuDMEC branch point formation were observed.

Data is presented as mean±SEM (% cord or branch point formation compared with $VEGF_{165}$; n=3, p<0.004). Statistical analysis was performed using a t-test (Sigmaplot 11 software)

Migration

The presence of the Np1 antibody appeared to have no inhibitory effect on HuDMEC migration *in vitro* (**Figure 3.32a**). In contrast, the Np2 antibody appeared to have a plausible inhibitory effect on HuDMEC cell migration at 10µg/ml, whereby regression of the gap was observed (**Figure 3.32b**). However, since these experiments were only carried out twice, due to time constraints, no conclusive deduction can be made as to the effect of the Np1 and Np2 antibodies on HuDMEC cell migration *in vitro* and would require further analysis.

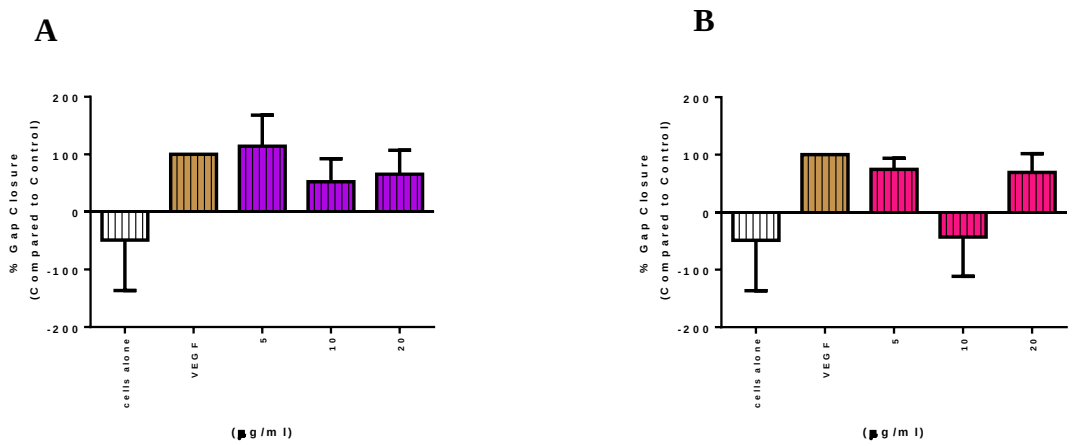

Figure 3.32 ***Effects of the Np1 and Np2 antibody on HuDMEC Migration***:
In the presence of recombinant $VEGF_{165}$ plus varying doses of the Np1 antibody (**A**) no inhibitory effects were observed on HuDMEC migration after 32h compared with the $VEGF_{165}$ alone control. In contrast, (**B**) Np2, 10µg/ml caused regression of the gap created, however without statistical analysis, conclusions can not be made.

Data is presented as mean±SEM (% gap closure compared with $VEGF_{165}$; n=2)
Statistical analysis was not carried out due to the lack of adequate experimental replicates.

KEYPOINT
In vitro results that represent 'true' activity of Bz on HuDMEC activity include inhibitory effects on endothelial cell cord formation and network complexity

3.3 DISCUSSION

3.3.1 Characterisation of Factors

VEGF

VEGF is a multi-functional molecule that is critical to tumour growth and as mentioned is a potent pro-angiogenic factor. The role of VEGF on endothelial cell biology is crucial, with a number of processes involved in the angiogenic process being regulated by VEGF, such as endothelial cell survival, migration, differentiation and proliferation (***Byrne et al, 2005***).

VEGF protein expression was detected in the cell lysate of HuDMEC cells cultures *in vitro*, with a range of bands being observed between 42-50kDa in size. Several bands were expected as these represent the different VEGF isoforms that exist. Interestingly, only the dimeric forms of VEGF were detected, suggesting that the VEGF produced by the HuDMECs is functional since VEGF can only active receptor signalling when present as a dimer. This is important and should ideally be measured, since the level of dimeric VEGF present in 'resting' endothelial cells forms the baseline for VEGF expression. If baseline expression is relatively high, then the presence of exogenous VEGF may saturate the system, thus leading to no further stimulation by additional VEGF. Interestingly; no VEGF was detected in the media fraction, however it is possible that the levels were too low to detect using western blot methods, thus an ELISA assay would have been useful to measure the levels of VEGF released into the media. An ELISA assay would also have proved useful in potentially measuring the different levels of VEGF isoforms present. This is important as the different isoforms have differential receptor expression profiles with regards to the neuropilin receptors and thus the levels of each individual isoform is potentially important in the response to targeted therapy.

$VEGF_{165b}$

The discovery of $VEGF_{165b}$ and the suggestion that these isoforms are anti-angiogenic implies a potentially important role in the efficacy of VEGF targeted therapy.

$VEGF_{165b}$ protein expression remained undetected in the cell lysate and media fractions of the cultured HuDMEC cells *in vitro*. This finding was unexpected, as the $VEGF_{165b}$ protein is thought to be a negative regulator of angiogenesis, thus would be expected to be present in 'resting' or inactivated endothelial cells. The cells were serum starved prior to protein extraction, as this process is thought to increase protein expression, and therefore it is possible that a stress response was activated as a result of the serum starvation thus activated the

HuDMECs, and reduced the levels of $VEGF_{165b}$. A PCR experiment was carried out to determine, if the lack of $VEGF_{165b}$ expression was due to the antibody not working or if the absence of expression was a true reflection. However, the quality of the DNA extracted was poor as there was evidence of smearing on agarose gel and therefore may be masking the presence or the absence of $VEGF_{165b}$. The expression of $VEGF_{165b}$ can not be completely ignored in this instance.

VEGF Receptors

Protein expression of all four VEGF receptors was observed in the cell lysate fractions of the HuDMEC cells suggesting that targeting the VEGF pathway via these receptors is feasible.
In hindsight however it would have been useful to measure the levels of receptor expression both on the surface of the HuDMECs and internally using flow cytometry. Measuring the different levels of receptor expression could aid in identifying which cell types are likely to respond to a treatment that is either targeting the classical VEGF receptors or the alternative newly identified, neuropilin receptors, as the levels of surface receptor expression are extremely important. Additionally it would have been useful to measure the levels of VEGF receptors under both normoxic and hypoxic conditions especially since within the tumour microenvironment, the microvascular endothelial cells, along with other cells are subjected to low oxygen. The low oxygen tension could potentially result in a different VEGF receptor expression profile in the HuDMEC cells resulting in different levels of sensitivity of HuDMECs to VEGF receptor targeted therapy such as Bz. VEGF-R1 mRNA expression has been observed to be greatly up-regulated under different hypoxic conditions (***Barleon et al, 1997 & Gerber et al, 1997***). These studies also observed an increase in soluble VEGF-R1 mRNA expression. Whereas VEGF-R2 mRNA expression under hypoxia is variable with some studies showing no detectable increase in VEGF-R2 expression in HuVEC cells under hypoxic conditions (***Barleon et al, 1997 & Gerber et al, 1997***) whereas other have observed increased up-regulation of VEGF-R2 (***Waltenberger et al, & Brogi et al, 1996***). The presence of hypoxia appears to reduce or diminish Np1 protein expression by HuVEC cells *in vitro* (***Bae et al, 2008***) whereas Np2 expression appears to be unaffected (***Bae et al, 2008***).

It is important to note that although the protein expression data is based on triplicate results, the western blot experiments were carried out a number of times, as variable results with the VEGF receptors was observed. This variability in protein expression of all four VEGF receptors may be representative of the mixed endothelial cell populations present in the different batches of cultured HuDMECs utilised in these experiments.

3.3.2 Functional Activity

Bz

The extent to which Bz inhibited HuDMEC differentiation, varied across Matrigel experiments during this current project. It is possible that the variation in response to Bz treatment, is due to fluctuations in the level of VEGF-R1 and VEGF-R2 surface expression. Additionally, the HuDMECs used in these experiments are isolated from the dermis thus are a mixture of both vascular and lymphatic endothelial cells (Promocell). Lymphatic endothelial cells predominantly express VEGF-R3 and may not respond to Bz treatment as effectively as vascular endothelial cells and since Bz only inhibits VEGF isoforms from binding to VEGF-R1 and VEGF-R2, the ratio of vascular versus lymphatic endothelial cells present in the HuDMEC culture is important.

It has previously been observed that treatment of serum-starved HuVECs with exogenous VEGF for 24h resulted in reduced (upto 66%) levels of VEGF-R1 and VEGF-R2 cell surface expression *in vitro*. This loss in cell surface expression was quickly reversed with the removal of exogenous VEGF (***Wang et al, 2000***). This observation may in part explain why there was little stimulation in HuDMEC activity in the presence of recombinant $VEGF_{165}$ compared with the cells alone, in the majority of experiments carried out during this PhD project. The group also observed that although exogenous VEGF treatment reduced VEGF receptor cell surface expression, mRNA of both receptors was increased in the presence of VEGF in conditioned media (24h- from tumour cells), suggesting that the exogenous VEGF regulates a compensatory modulation of VEGF receptor production when cell surface expression is lost. Interestingly, treating the HuVECs (that were exposed to conditioned media) with A4.6.1 (Bz) for 2h decreased the mRNA production of VEGF-R1 and VEGF-R2. This suggests that pre-treating the HuDMECs in the current set experiments with exogenous $VEGF_{165}$ followed by Bz treatment, could potentially increase or improve the inhibitory effects observed on HuDMEC cell activity *in vitro*, in response to $VEGF_{165}$ stimulation. Additionally a $VEGF_{165}$ rescue experiment could have proved useful in establishing the effectiveness and duration of Bz treatment in maintaining an inhibitory effect on HuDMEC cell function *in vitro*.

Unfortunately the control vehicle (CV) in which Bz is re-suspended also exerted similar effects on HuDMEC differentiation *in vitro*. The majority of other studies that measure the effects of Bz use either a human IgG1 (***Hoang et al, 2012***) or do not describe the nature of the control used. The only study that used the same control vehicle used in this current study, did not observe any effects with the vehicle on HuVEC activity, however, the volumes at which the vehicle was used was not stated (***Carneiro et al, 2009***). It was initially thought that the

presence of the control vehicle might be causing the media in which Bz was added to the cells to change, however this was tested and was found not to be any different between the different treatment groups.

The effects of Bz on cell differentiation of pre-screened HuDMECs were also tested, with the thought that, if the cells have previously been tested for the response to VEGF treatment, these cells in theory would respond to anti-VEGF targeted therapy to a greater extent and thus would allow for a more reliable assessment of the hypothesis which was proved to be the case, as the pre-screened HuDMECs responded to a much greater extent to Bz treatment in the cell differentiation assay, suggesting that if the level of VEGF-R1 and VEGF-R2 is adequate and available on the cell surface, targeting these receptors is an effective means for targeting the tumour vasculature (data not shown).

High doses of Bz exerted no inhibitory effects on HuDMEC proliferation *in vitro* during this study, this differs to what has been observed in the literature, whereby the presence of Bz resulted in inhibition of HuDMEC cell proliferation (***Li et al, 2007).*** However in the ***Li et al, 2007*** study the HuDMECs were incubated with Bz (10μg/ml) for 72h therefore it is possible that the proliferation assay carried out in this project was not long enough to observe inhibitory effects on proliferation as the latest time point observed was 48hours. Bz also significantly inhibited HuDMEC migration, this was expected since it has previously been shown that VEGF-R2 is important in $VEGF_{165}$ induced EC migration and when blocking the interactions of VEGF-R2 with VEGF with Bz inhibits HuDMEC migration *in vitro* (***Costa et al, 2009***). Unfortunately the control vehicle also exerted similar effects on HuDMEC migration, the reason why the control vehicle is acting as an anti-angiogenic agent *in vitro* has yet to be determined and is a cause for concern as the extent to which the control vehicle is inhibiting HuDMEC function *in vitro* is similar to that observed with Bz.

Np1 Peptides

The Np1 peptides exerted inhibitory effects on HuDMEC differentiation and migration, suggesting that Np1 plays an important role in some key steps of the angiogenic process. However these inhibitory effects were variable over the course of the *in vitro* experiments. As mentioned previously, the HuDMEC cells utilised in these experiments were a mixture of both venous and lymphatic ECs. These two endothelial cell types observe differential expression of Np1 with venous ECs expressing Np1 to a greater extent and lymphatic ECs expressing pre-dominantly Np2. Thus if the ratio of lymphatic ECs to venous ECs was greater in the HuDMEC cultures used in different experiments, it is possible that the response to the

Np1 peptides would be greatly reduced or diminished due to the lack of Np1 receptor expression.

Peptide 1, 7b and 10 all exerted inhibitory effects on HuDMEC differentiation, and was expected as it has previously been observed that Np1 plays a role in EC differentiation *in vitro* (***Uniewicz et al, 2011***). Peptide 2, which is a control peptide that does not bind Np1, also exerted significant inhibitory effects on HuDMEC *in vitro* activity. There is a lot of controversy surrounding the ability of $VEGF_{121}$ to bind Np1, with some studies showing that even though $VEGF_{121}$ does not bind Np1 directly, yet it is still capable of transducing downstream signalling that results in EC biological activity. However, it is possible that the peptides are having a toxic effect on the cells, which may explain the effects observed with the control peptide (p2). A toxicity assay would have been useful to assess this, prior to commencing functional assay analysis.

No inhibitory effects on HuDMEC cell proliferation were observed with any of the four Np1 peptides, again this may be a result of the experimental time points measuring the effects on cell proliferation being too short, thus longer time point beyond 72h may prove more useful.

Migration

Although no significant effects were observed on HuDMEC migration with the Np1 peptides in the scratch assay, there was an obvious inhibitory trend present, and the fact that no significance was reached may be due to the nature of the technique. In hindsight, the scratch assay may not be the ideal assay to measure cell migration, since mitomycin C pre-treatment may have caused the cells added stress during the process of making a 'wound', thus rendering the cells less efficient in terms of migration and partly for this reason the boyden chamber was carried out to assess the effects of p7b and p10 on HuDMEC cell migration. It is also important to note that the Boyden chamber induces chemotactic migration towards a VEGF gradient, this gradient may be important in the response of HuDMECs to VEGF. Interestingly, it appears that the gradient formed by VEGF in a chemotactic assay such as the boyden chamber is important, as the HuDMECs appeared to migrate more readily in this assay. Interestingly, it is important to note that results obtained on a particular effect on one function can not necessarily be compared over different techniques for that function, since in these experiments, the boyden chamber and scratch assay resulted in different observations. At least in relation to p10, whereby a trend suggesting stimulatory effect was observed with the scratch assay with the opposite being observed in the boyden assay. This emphasises that

when comparing data in the literature, the technique used is important. The observation that the Np1 peptides alone inhibit HuDMEC differentiation and migration (Boyden chamber) suggests that the peptides potentially display biological activity.

Combination

Combining p2, p7b or p10 with Bz resulted in no additive inhibitory effects on HuDMEC cell differentiation when compared with Bz alone. However, in the combination experiments all three Np1 peptides tested failed to inhibit HuDMEC differentiation when added alone, compared with previous experiments carried out, where a minimum of a 50% reduction in cord formation was observed with all three peptides. Again, it is possible that the extent, to which the HuDMECs responded to anti-Np1 treatment, is all dependent on the level of Np1 available on the cell surface. As mentioned with VEFG-R1 and VEGF-R2 previously, the addition of exogenous VEGF results in down-regulation of the receptors on the surface of the cell. This may also be the case with Np1, which could be tested using flow cytometry to measure the level of surface Np1 that present, in the presence and absence of exogenous VEGF over a time course and whether the Np1 expression profile changes after the removal of excess VEGF. Since there were no inhibitory effects observed with the three peptides alone, an additive effect could not be expected.

Interestingly, when p2 was combined with Bz, the significant inhibitory effect that was observed with Bz alone on branch point formation was lost. This suggests that p2 and Bz are interacting in some way and subsequently impacting on HuDMEC activity *in vitro*. It is also possible that the peptides (p2 and p7b) are promoting angiogenesis to a certain extent by inducing signalling via Np1 rather than blocking it, which might explain why p2 caused the efficacy of Bz in inhibiting HuDMEC differentiation to be reduced somewhat. Therefore measuring the level of receptor activation in the presence and absence of the Np1 peptides would prove useful in establishing if the process of angiogenesis is being promoted. It is also possible that the blockade of the VEGF pathway through inhibiting interactions with both receptor families causes a compensatory effect via the up-regulation of alternative pro-angiogenic factors such as FGF, thus any additive effects expected are lost. Additionally, the peptides used in these experiments are Np1 targeting and Np2 binding has not been reported (although p10 is thought to potentially also bind Np2, but this has not been confirmed). Since the peptides are confirmed to bind Np1 only, it is possible that Np2 signalling may compensate for the loss of Np1. Treating the cells with a peptide that effectively blocks both Np1 and Np2 could prove useful. Additionally, pre-treating the HuDMECs with Bz followed

by treatment with the Np1 peptides may prove a more useful regime in inhibiting the VEGF pathway.

Similar to the differentiation assay, no significant additive inhibitory effects on HuDMEC cell migration were observed when p7b and p10 were combined with Bz, compared with Bz alone. However, there was a trend that suggested the p7b might have additive effects with Bz and the control vehicle, this was not significant but may be a result of the nature of the scratch assay. With this in mind, the transwell or Boyden chamber would prove to be a more useful method for measuring cell migration for future experiments.

Np1 and Np2 antibodies

Interestingly, the commercially available Np1 antibody (R&D Systems) inhibited HuDMEC differentiation to a lesser extent then any of the four Np1 peptides as observed in the primary experiments. The antibody available at the time, has been tested for receptor-ligand blockade in an ELISA assay using immobilised human Np1. It is therefore possible, that the level of Np1 expressed on the cell surface of the HuDMECs in the Matrigel assay was higher than that tested in the ELISA assay, thus suggesting the use of higher doses of both neuropilin receptor antibodies in future experiments to allow for more effective blocking of the receptor.

Interestingly, the Np2 antibody inhibited HuDMEC differentiation to a slightly greater extent then the Np1 antibody, however this was still considerably lower then the inhibition observed with the Np1 peptides. This suggests that Np2 is also important in endothelial cell biology and could prove a useful anti-angiogenic target, thus it would have been interesting to test the Np1 and Np2 antibodies alone and in combination with one another to assess if inhibiting both neuropilin receptors is more effective at inhibiting and maintaining inhibitory actions of HuDMEC function *in vitro*.

3.4 CHAPTER CONCLUSION

The data from the *in vitro* experiments carried out, provide further evidence for the importance of VEGF and the VEGF receptors on microvascular endothelial cell activity *in vitro*. Additionally, the data shows that not only is Np1 protein expressed on human microvascular endothelial cells but also plays a functional role in endothelial cell biology (*in vitro)*. The inhibition in HuDMEC cell differentiation and migration observed in the assays suggest that the Np1 peptides are biologically active as inhibitors of $VEGF_{165}$ and Np1 interactions on microvascular endothelial cells *in vitro*.

The peptides have shown that they are potentially capable of acting as anti-angiogenic agents in the *in vitro* setting. However, since Np1 is also thought to be expressed on breast cancer cells, it is also important to assess if these peptides have the potential to act as dual targeting agents. If this is the case, the use of Np1 targeting agents, could lead to more effective inhibition of tumour progression, as these peptides may be capable of targeting tumour progression via indirect (endothelial cells) and direct (tumour cells) mechanisms. The next chapter investigates the role that Np1 plays on breast cancer cell activity *in vitro* and whether this can be blocked with the Np1 peptides.

Chapter Four

In Vitro Results
Targeting the Breast Cancer Cells

4. INTRODUCTION

For a tumour to progress, breast cancer cells must exhibit a versatile phenotype whereby, they are able to effectively migrate and proliferate at both the primary tumour site and, the secondary metastatic niche.

The expression and functional role of VEGF-R1 and VEGF-R2 with regards to endothelial cells, is relatively well established. However, the expression and function of these two receptors in conducting autocrine VEGF signalling in breast cancer cells is less defined. The expression of VEGF-R1 and VEGF-R2 on breast cancer cells is controversial with some studies observing expression whilst others, detect no expression at all. However, when the receptors are present they do appear to play a functional role on breast cancer cell activity. VEGF-R1 exerts a survival effect on MDA-MB-231 breast cancer cells (***Lee et al, 2007***). Suggesting that anti-angiogenic agents that target VEGF signalling, such as Bz may in fact be acting on both the tumour vasculature and the breast cancer cells.

The more recent identification of Np1 and Np2 as VEGF receptors further suggests an autocrine role for VEGF in breast cancer cells activity. To date (*Sept 2014*), Np1 has been show to play an important role in VEGF signalling, involved in breast cancer progression. Np1 acts as both a survival factor for breast cancer cells *in vitro* (***Bachelder et al, 2001 and Barr et al, 2008***) and has been implicated in promoting the breast cancer cell invasion, (***Bachelder et al, 2002***), migrate (***Nasarre et al, 2003)*** and metastasis (***Wanami et al, 2008***). Thus inhibiting both the classical VEGF receptors and Np1 appears to be an interesting target.

$VEGF_{165b}$ is thought to exhibit anti-angiogenic properties (***Qiu et al, 2009)*** and is down regulated in other cancer cells such as renal cell carcinoma (***Bates et al, 2002***). The presence or absence of the suggested anti-angiogenic isoform has potential implications on the efficacy of VEGF targeted therapy and therefore, it was important to assess the expression profile of $VEGF_{165b}$ in the breast cancer cells.

4.1 MATERIALS & METHODS

The MDA-MB-231 and MDA-MB-436 breast cancer cells are triple negative cells lines that resemble basal like breast cancer (***Kao et al, 2009***). Bz was approved for metastatic breast cancer and with the increased interest in personalised therapy, the use of two metastatic breast cancer cell lines with relatively similar profiles was deemed important in this current project.

Western blot analysis was carried out, to characterise protein expression of VEGF and its receptors, VEGF-R1, VEGF-R2, Np1 and Np2, as well as the anti-angiogenic isoform, $VEGF_{165b}$ (**section 2.2**). Once the expression of the receptors was established, functional assays were performed.

The MTS assay was used to measure the effects of Bz and the four Np1 peptides on breast cancer cell proliferation *in vitro*. For the MDA-MB-231 and MDA-MB-436 breast cancer cells, the proliferation assay was carried out in the absence of exogenous $VEGF_{165}$ ($rhVEGF_{165}$) since optimisation of the MTS assay observed non-significant stimulatory effects of $rhVEGF_{165}$ (20ng/ml) on these two metastatic breast cancer cells lines in comparison to cells alone in 1% serum media (**section 2.5.2**).

The Scratch/wound healing assay was used to measure the effects of the above treatment groups on breast cancer cell migration *in vitro*. Similar to the MTS assay, the scratch assay was carried out in the absence of $rhVEGF_{165}$ as optimisation of the assay observed non-significant stimulatory effects of $rhVEGF_{165}$ on MDA-MB-231 and MDA-MB-436 breast cancer cell migration compared with the cells alone in 1% serum media (**2.6.1**).

The Boyden chamber was used to measure the effects of the Np1 peptides on directional migration of the breast cancer cells *in vitro*. Unlike the scratch assay, the Boyden chamber with the breast cancer cells was carried out in the presence of $rhVEGF_{165}$ (50ng/ml) (**section 2.6.2**), as initial experiments using this assay demonstrated the requirement of exogenous $VEGF_{165}$ for sufficient migration of the breast cancer cells.

Similar to the HuDMEC experiments (Chapter 3), all *in vitro* functional assays measuring the effects of Bz, were carried out in the presence of a control vehicle (CV) at equivalent volumes as those used for the Bz treatment wells. All experiments were carried out in triplicate and the graphs are a representative mean of the 3 separate experiments, allowing for statistical analysis to be carried out on the data using Sigmaplot software. Following assessment of normality, a t-test or a Mann-Whitney U Test was performed using Sigmaplot 11 software. Significance was considered at $P = 0.05$.

4.2 RESULTS

4.2.1 Characterisation of Factors

Characterisation of all VEGF related proteins, was carried out using MDA-MB-231 and MDA-MB-436 cell lines to establish, which of these breast cancer cell lines would be most appropriate to utilise in the *in vivo* experiments.

Protein expression of different VEGF isoforms was detected in both MDA-MB-231 and MDA-MB-436 breast cancer cell lysates as represented by several bands ranging from ~ 30-50kDa (**Figure 4.1a**). VEGF protein expression was not detected in the conditioned media from either cell line. The anti-angiogenic isoform of VEGF, $VEGF_{165b}$, was not detected in the cell lysates or conditioned media of either MDA-MB-231 or MDA-MB-436 breast cancer cells (**Figure 4.1b**).

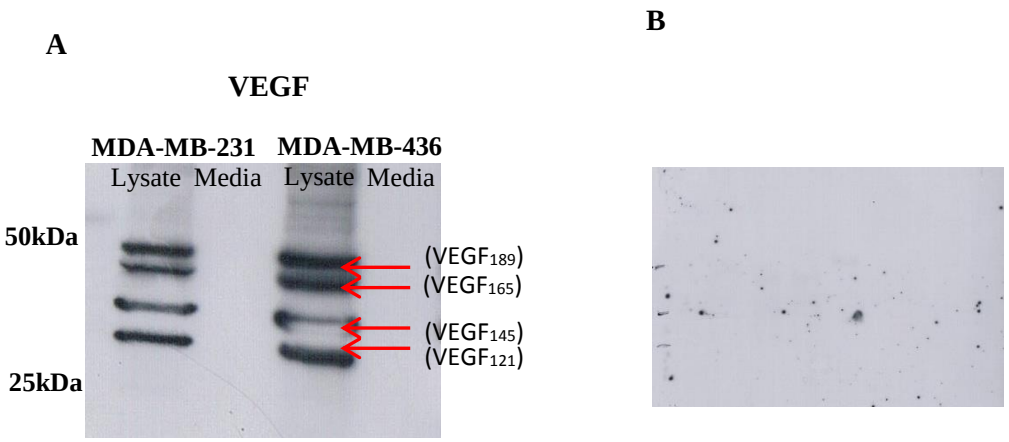

Figure 4.1 ***VEGF is Expressed by Breast Cancer Cells:***
(**A**)The active form of VEGF is secreted as a dimer and from the western blot above it is evident that the various VEGF isoforms are expressed by both MDA-MB-231 and MDA-MB-436 breast cancer cells. (**B**) No $VEGF_{165b}$ was detected in the breast cancer cell lines.

Images are representative of protein expression detected in triplicate experiments

VEGF-R1 protein expression was detected in the cell lysates of both MDA-MB-231 and MDA-MB-436 breast cancer cells (**Figure 4.2a**). A band was observed at ~180kDa in the MDA-MB-436 cells and to a lesser extent in the MDA-MB-231 cells, although flow cytometry would be required to more accurately compare the levels of VEGF-R1 between the two breast cancer cells. VEGF-R1 was not detected in the conditioned media of either MDA-MB-231 or MDA-MB-436 breast cancer cells.

VEGF-R2 protein expression was detected in the cell lysates of both the MDA-MB-231 and MDA-MB-436 breast cancer cells (**Figure 4.2b**). Interestingly, different forms of VEGF-R2 were detected in the two breast cancer cells. In the MDA-MB-231 cell lysates, two bands were detected, one at ~200/230kDa, representing the mature glycosylated form of VEGF-R2 (***Takahashi et al, 1996***) and the other at ~ 80kDa, representing a product of partial degradation of the receptor (***cell signalling antibody datasheet)***. The MDA-MB-436 breast cancer cells also expressed both these forms of VEGF-R2, and an additional band at ~ 150kDa, thought to represent the immature form of VEGF-R2 (***Takahashi et al, 1996***). VEGF-R2 protein expression was not detected in the conditioned media of either breast cancer cell line.

Np1 protein expression was detected in the cell lysates of both MDA-MB-231 and MDA-MB-436 breast cancer cells (**Figure 4.2c**). A single band at ~130kDa, representing full length Np1 was observed. No Np1 protein expression was detected in the conditioned media of either breast cancer cell line. Full length Np2 protein expression was also detected in the cell lysate of both MDA-MB-231 and MDA-MB-436 breast cancer cells (band at ~135kDa), (**Figure 4.2d**) although from the Western blot, the levels of Np2 protein expression in the cell lysate fraction appears to be greater in the MDA-MB-436 breast cancer cells compared with the MDA-MB-231 cells. However, overall protein expression of Np2 appears to be greater in the cultured HuDMECs cells (**Figure 3.2D**) compared with the breast cancer cell lines, although flow cytometry would be required to confirm this. No protein expression of Np1 or Np2 was detected in the conditioned media of either the MDA-MB-231 or MDA-MB-436 breast cancer cells. In contrast to the MDA-MB-231 cells, two prominent bands were detected in the cell lysate of the MDA-MB-436 breast cancer cells, one at ~135kDa and the other at ~75kDa, with the latter band thought to correspond to the soluble form of Np2.

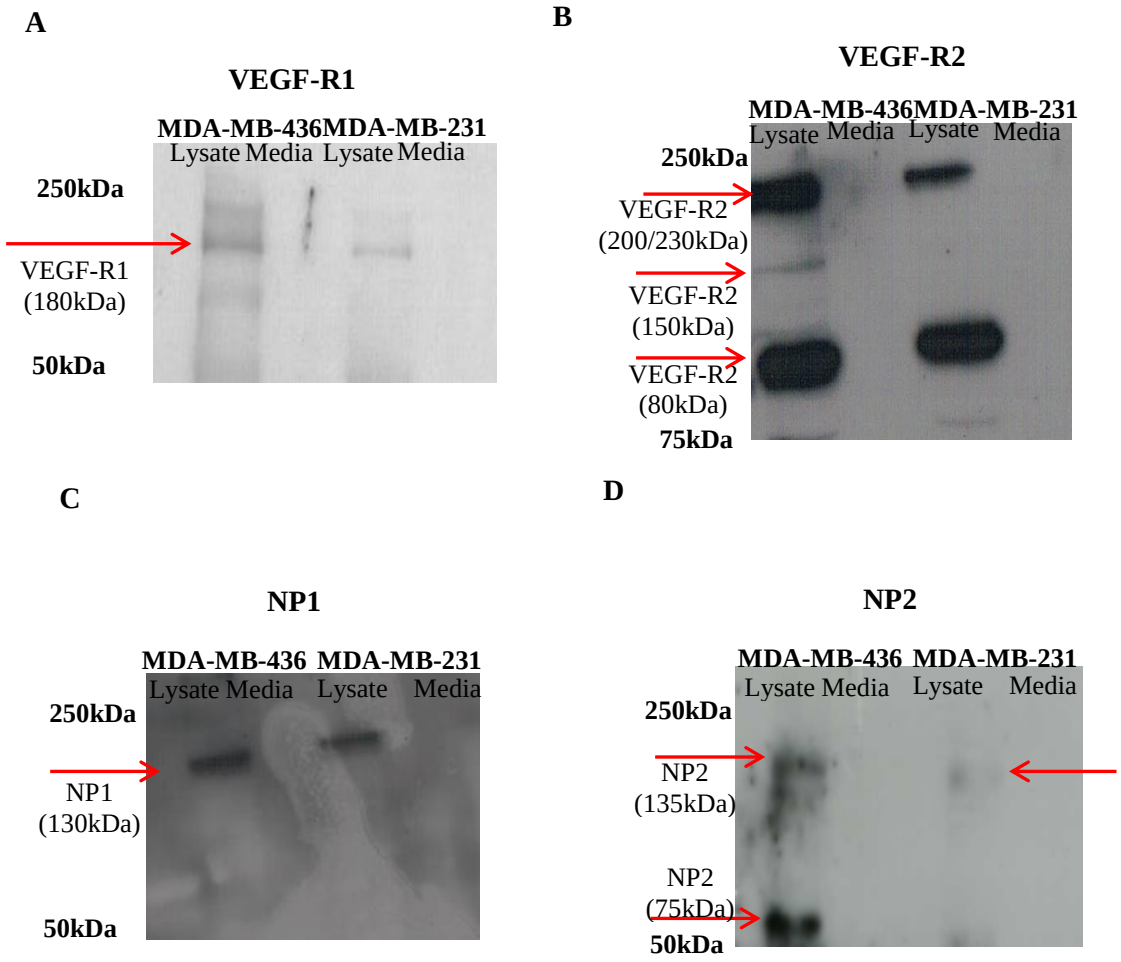

Figure 4.2 ***VEGF Receptors are Expressed on Breast Cancer Cells:***
(**A**) VEGF-R1 protein expression was detected in both MDA-MB-231 and MDA-MB-436 cell lysates. (**B**) Various forms of the VEGF-R2 receptor was detected in both cell lines (**C**) Np1 was largely evident in both cell lines (**D**) Np2 appears to be expressed to a lesser extent then Np1 but was detected in MDA-MB-436 cells and very slightly in the MD-MB-231 breast cancer cells.

Images are representative of protein expression detected in triplicate experiments

4.2.2 Effects of Bz on breast cancer cell function

Bz is thought to primarily inhibit tumour growth indirectly via its effects on ECs. However, expression of both VEGF-R1 and VEGF-R2 was observed on the two metastatic breast cancer cell lines (MDA-MB-231 & MDA-MB-436) investigated in this study (**Figure 4.2a&b**) and increasing evidence in the literature supports a direct functional role of VEGF-R1 and VEGF-R2 on breast cancer cells (***Liang et al, 2006; Lee at al, 2007***). Therefore, it was important to assess the effects of Bz on breast cancer cell function *in vitro*.

Proliferation

Bz treatment (0.25, 1 & 2.5mg/ml) significantly increased MDA-MB-231 breast cancer cell proliferation (0.25, 1 and 2.5 mg/ml Bz vs. cells alone control; 12 SEM±3.5%, 13 SEM±4.8 and 20% SEM±2.2 vs. 100% SEM±0; n=3; p=0.029, 0.049, 0.001 respectively) compared with the cells alone control at 24 hours (**Figure 4.3a**). However, this significant increase was lost by the 48h time point, although the trend remained. Furthermore, there was also a significant increase (*P=0.032*) observed when the MDA-MB-231 cells were treated with CV (at the equivocal dose of 1mg/ml) (**Figure 4.3b**) at 24 hours compared with the cells alone control (14% increase SEM±4.2). However, this inhibition was lost due by 48h.

No inhibitory effects on MDA-MB-436 breast cancer cell proliferation (**Figure 4.3c)** were observed, in the presence of increasing doses of Bz, at both 24 and 48h. Furthermore no effects on MDA-MB-436 breast cancer cell proliferation were observed with the addition of equivalent doses of CV (**Figure 4.3d**).

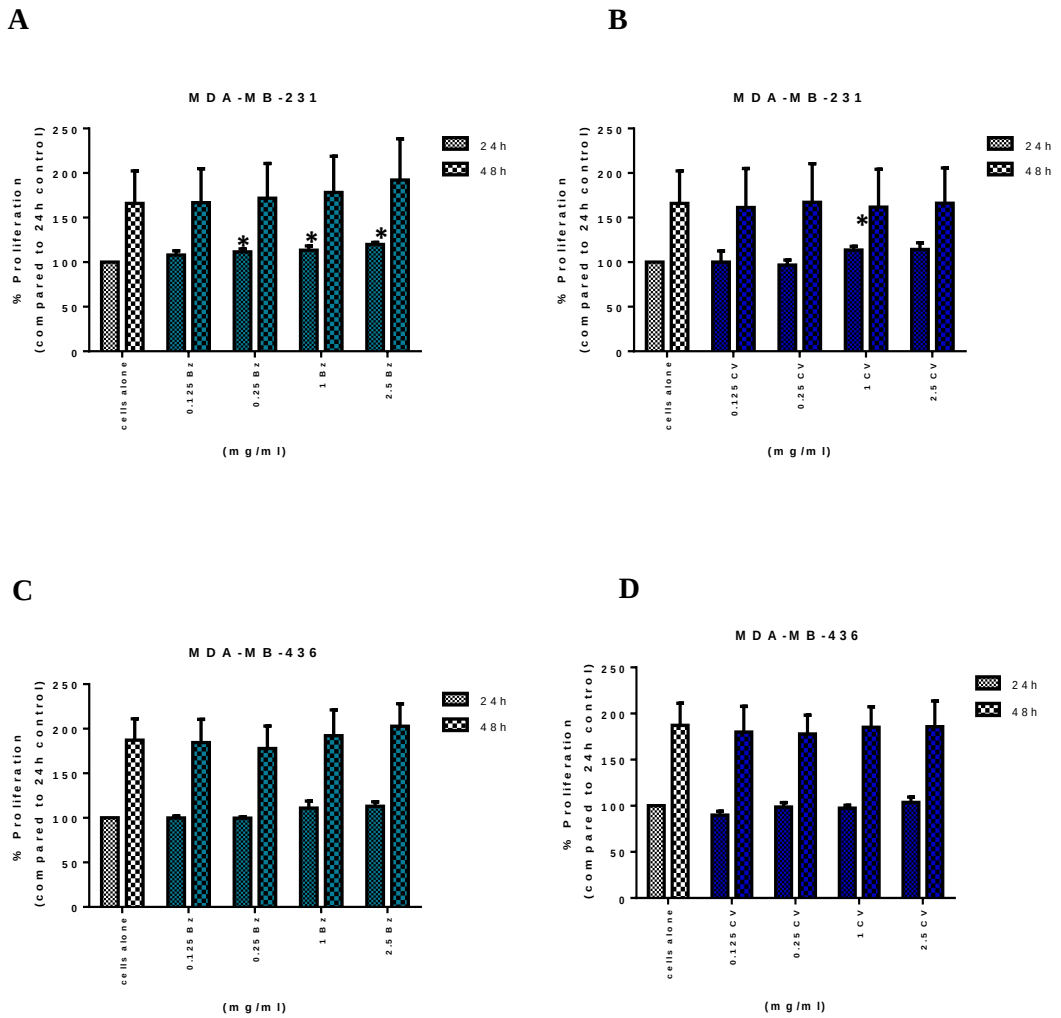

Figure 4.3 ***Effects of Bz on Breast Cancer Cell Proliferation:***
In the absence of recombinant $VEGF_{165}$, (**A**) treatment of MDA-MB-231 breast cancer cells with Bz resulted in an initial dose dependent increase in cell proliferation at 24h when expressed as a % of the cells alone control at 24h which was significant (*P= 0.029,P=0.049 and P=0.001*). However, this was not maintained. (**B**) CV (1mg/ml) also significantly (*P=0.032*) stimulated MDA-MB-231 breast cancer cell proliferation at 24h but again was lost b 48h. In contrast (**C**) Bz or the (**D**) CV exerted no significant effects on MDA-MB-436 breast cancer cells proliferation.

Data is presented as mean±SEM (% proliferation compared with cells alone; n=3, *p<0.05). Statistical analysis was performed using a t-test (Sigmaplot 11 software).

Migration

Bz displayed no inhibitory effects on MDA-MB-231 breast cancer cell migration compared with the cell alone control at 24 or 48h (**Figure 4.4a&b**). Similarly, no inhibitory effects were observed on MDA-MB-231 cell migration in response to CV (**Figure 4.4c**). In contrast, MDA-MB-436 breast cancer cell migration was significantly (*P=0.044 and P=0.003*) inhibited in the presence of Bz at 0.125 and 1mg/ml compared with the cells alone

control at 24h (mean±SEM; Bz 0.125 and 1mg/ml vs. cells alone; 86±5% and 75±4% vs. 100±0%; n=3, p=0.044 and p=0.003) (**Figure 4.5a**). However, the significant inhibitory effects were not maintained after 48h. The CV at the 0.125mg/ml dose also displayed a significant (*P=0.004*) inhibitory effect on MDA-MB-436 breast cancer cell migration compared with the cells alone control at 24h (mean±SEM; CV 0.125mg/ml vs. cells alone; 67±5% vs. 100±0%; n=3, p=0.004) (**Figure 4.5b**). Similar to Bz, the significant inhibitory effect observed with the control vehicle was not maintained after 48h.

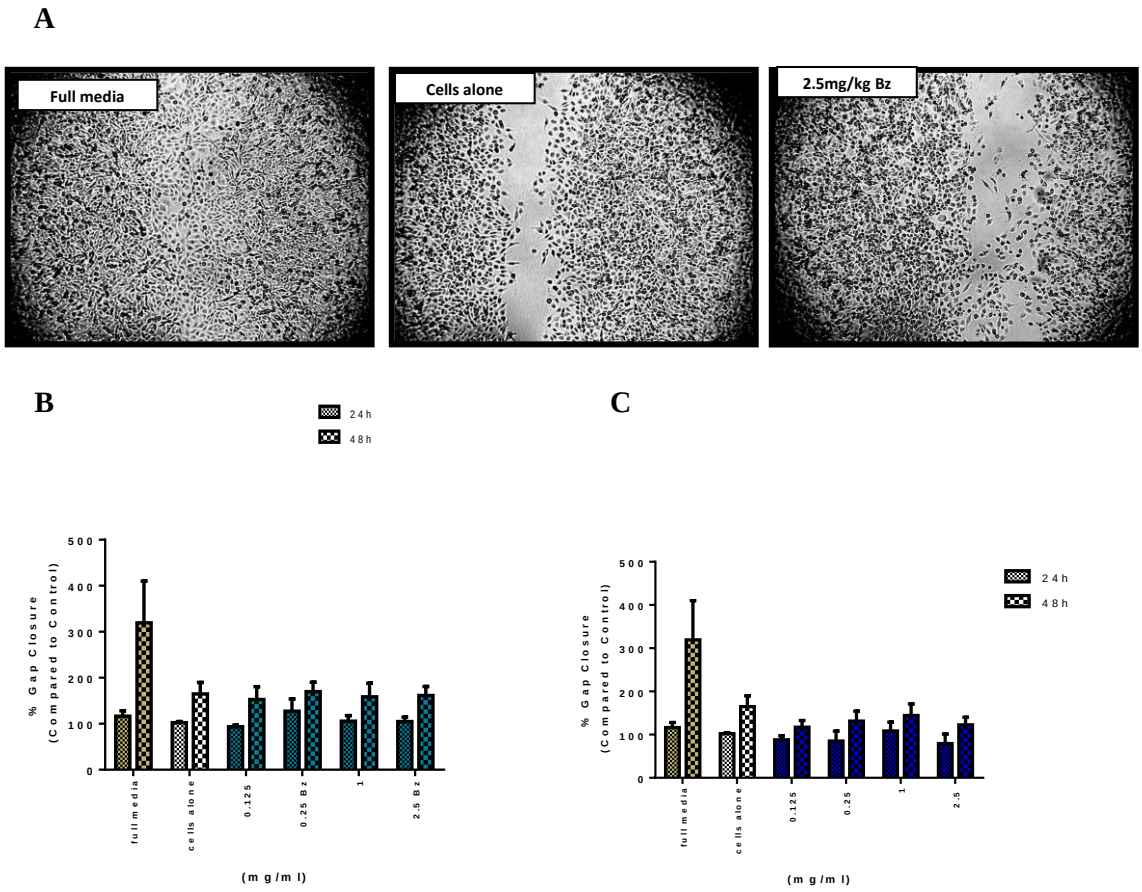

Figure 4.4 ***Effects of Bz and CV on MDA-MB-231 Breast Cancer Cell Migration***:
(**A**) Representative images of MDA-MB-231 gap closure 48h after creating a scratch in the presence of cells alone or Bz. In the absence of recombinant $VEGF_{165}$, no inhibitory effects on MDA-MB-231 breast cancer cell migration was observed with the addition of (**B**) Bz or (**C**) CV, when expressed as the % gap closure compared with the cells alone control at 24h.

Data is presented as mean±SEM (% gap closure compared with cells alone at 24h; n=3, NS). Statistical analysis was performed using a t-test (Sigmaplot 11 software).

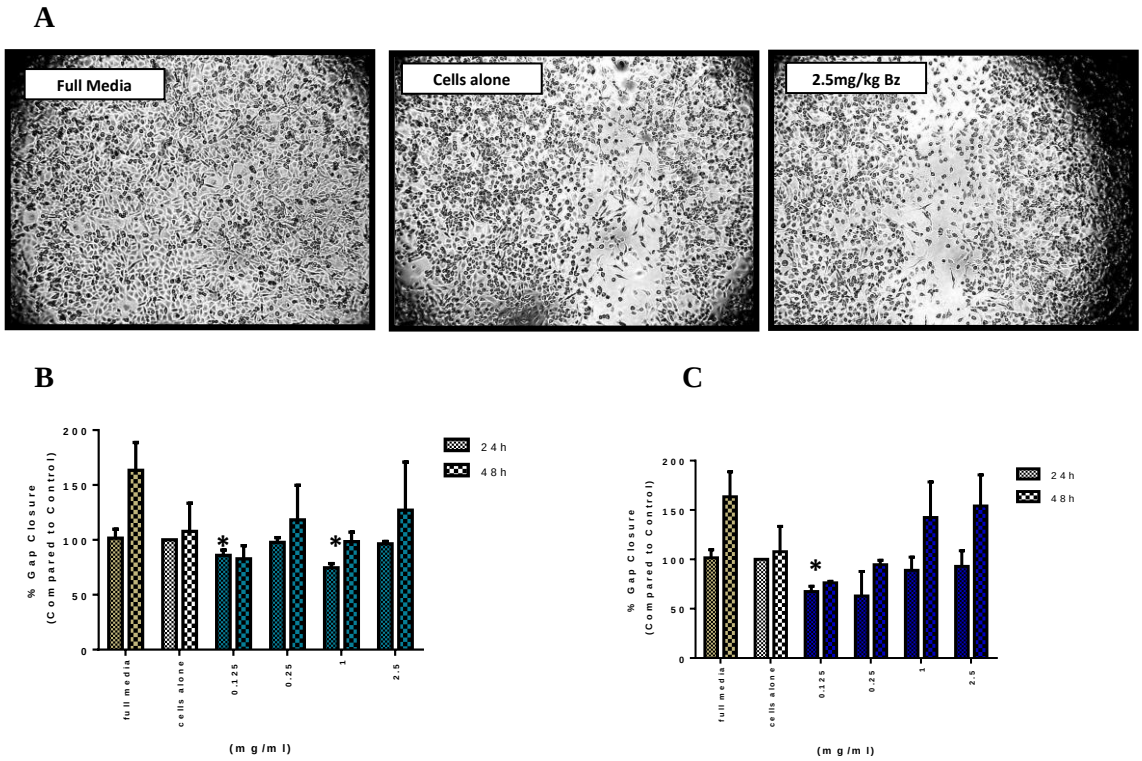

Figure 4.5 ***Effects of the Bz and CV on MDA-MB-436 Breast Cancer Cell Migration***:
(**A**) Representative images of MDA-MB-436 gap closure 48h after creating a scratch in the presence of cells alone or Bz In the absence of recombinant $VEGF_{165}$, (**B**) MDA-MB-436 breast cancer cell proliferation was significantly (*P= 0.044 and P=0.003)* inhibited at 24h in response to Bz treatment (0.125 & 1mg/ml) compared with the cells alone control. However, this was lost by 48h. (**C**) CV at 0.125mg/ml significantly (*P=0.004*) inhibited

Data is presented as mean±SEM (% gap closure compared with cells alone; n=3, p<0.05). Statistical analysis was performed using a t-test (Sigmaplot 11 software).

KEYPOINT

The effects of Bz on breast cancer cell activity compared with the control vehicle (CV) could not be differentiated.

4.2.3 Effects of the four Np1 Peptides on Breast Cancer Cell Function

In order to assess, whether the Np1 peptides detailed in Chapter 3 had a direct effect on breast cancer cells, their efficacy was tested in the *in vitro* functional assays.

Proliferation

None of the, Np1 peptides had any effect on MDA-MB-231 breast cancer cell proliferation *in vitro* after 24 or 48h of treatment (**Figure 4.6**).

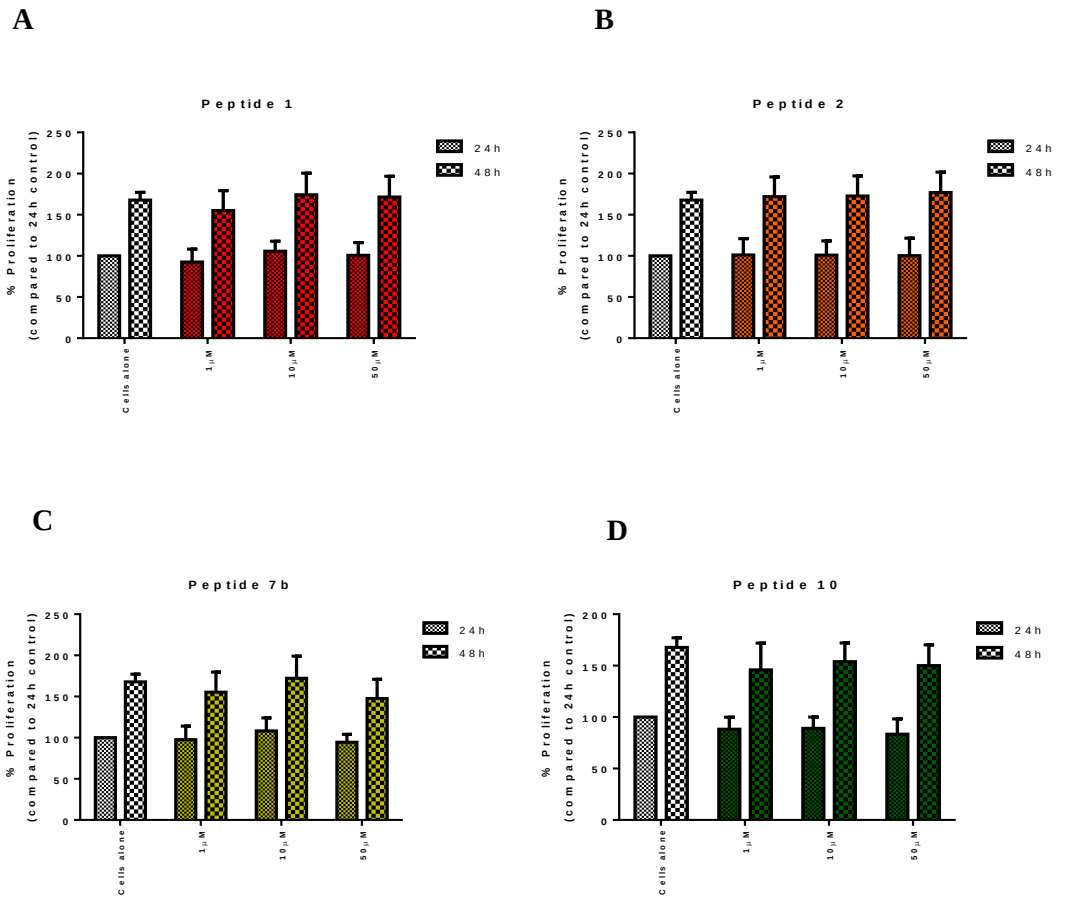

Figure 4.6 ***Effects of the Np1 Peptides on MDA-MB-231 Proliferation*** No inhibitory effects on MDA-MB-231 breast cancer cell proliferation was observed in the presence of any of the four Np1 peptides (**A**) P1 (**B**) P2 **C**) P7b or (**D**) P10

Data is presented as mean±SEM (% proliferation compared with the cells alone; n=3, NS). Statistical analysis was carried out using a t-test (Sigmaplot 11 software).

Peptide 1 and p2 had no significant effects (**Figure 4.7a&b**), whereas Peptide 7b at the highest dose (50μM) significantly inhibited (*P=0.021*), MDA-MB-436 breast cancer cell proliferation (**Figure 4.7c**) after 48h compared with the 48h cells alone control (31±5% decrease). Similarly, peptide 10, which is thought to bind both Np1 and Np2, significantly inhibited (*P=0.021*) MDA-MB-436 breast cancer cell proliferation (**Figure 4.7d**) compared with the cells alone control at 24h (mean±SEM; 11±5%; 11±3% and 17±1% decrease respectively). However, only the 1μM dose of Peptide 10 significantly (*P=0.021*) maintained an inhibitory effect on MDA-MB-436 breast cancer cell proliferation after 48h when compared with the 48h cells alone control (mean±SEM; 32±4% decrease).

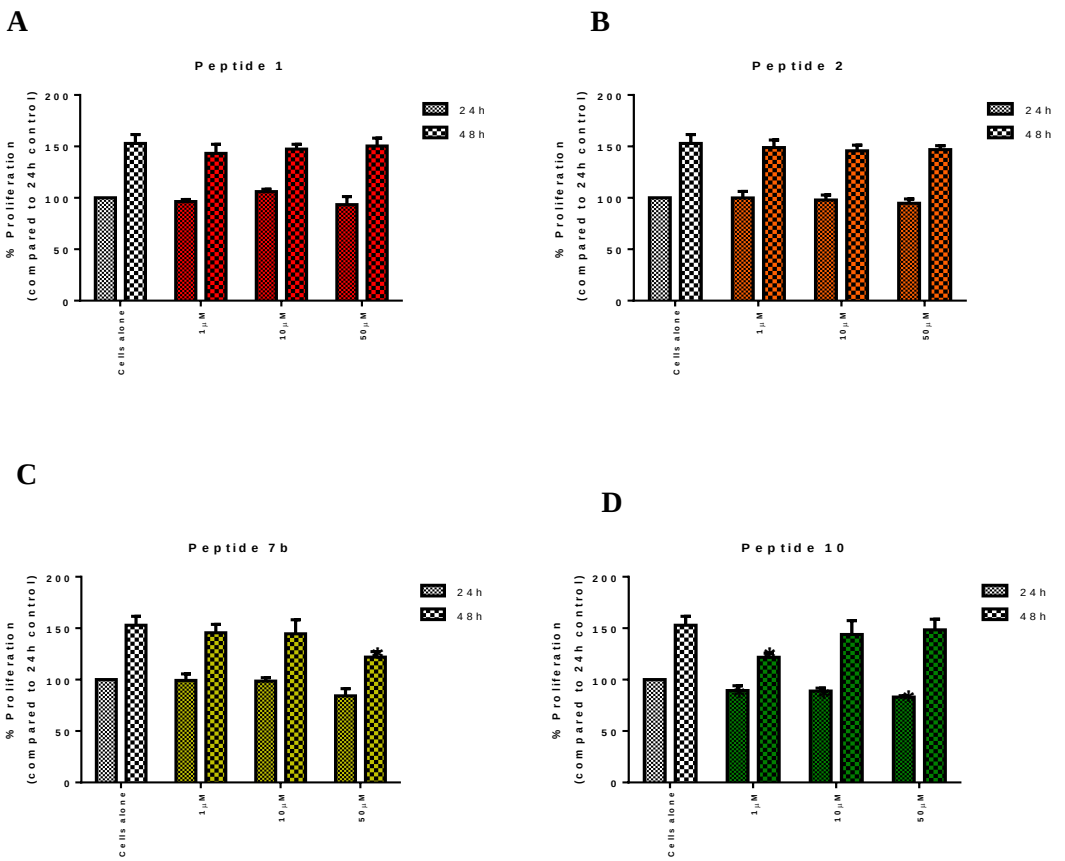

Figure 4.7 ***Effects of the Np1 peptide on MDA-MB-436 Breast Cancer Cell Proliferation:***
In the absence of recombinant $VEGF_{165}$, (**A**) P1and (**B**) p 2 exerted no inhibitory effects on MDA-MB-436 breast cancer cell proliferation. Whereas both (**C**) p7b and (**D**) p10 significantly inhibited MDA-MB-436 breast cancer cell proliferation *in vitro*.

Data is presented as mean±SEM (% gap closure compared with cells alone; n=4, *p=0.021). Statistical analysis was performed using the Mann-Whitney U Test (Sigmaplot 11 software).

Migration

Scratch Assay

In the Np1 migration experiments, MDA-MB-231 breast cancer cells treated with the full media control displayed a significantly lower rate of migration after 24h compared with the cells alone grown in low serum media (mean±SEM; full media vs. low serum; 52±16% vs. 100±0%; n=3, p=0.037) (**Figure 4.8a-d**). However by 48h, there was no significant difference in the rate of MDA-MB-231 breast cancer cell migration when treated with full media or low serum (cells alone control). No significant effects were observed on MDA-MB-231 breast cancer cell migration *in vitro*, in the presence of any of the Np1 peptides compared with the cells alone control at either 24 or 48h (**Figure 4.8a-d**). Similarly, no

significant effects were observed on MDA-MB-436 breast cancer cell migration, in the presence of any of the Np1 peptides (**Figure 4.9a-d**).

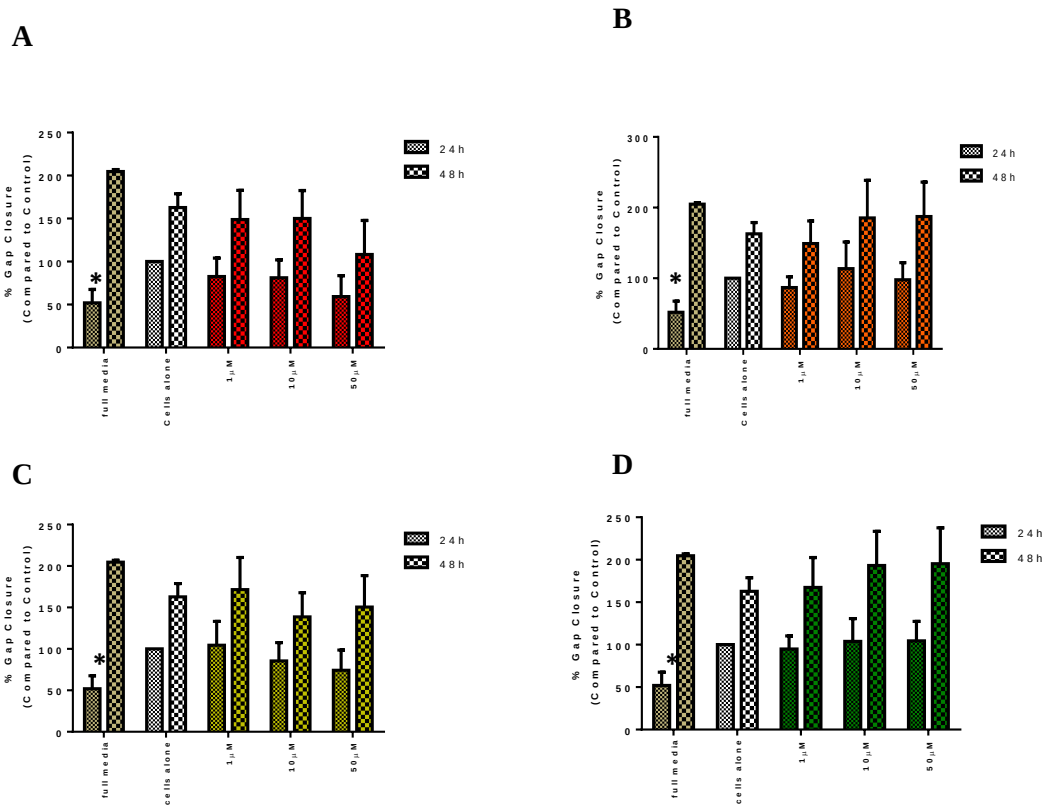

Figure 4.8 ***Effects of Np1 Peptides on MDA-MB-231 Breast Cancer Cell Migration:***
In the absence of recombinant $VEGF_{165}$, neither, (**A**) p1, (**B**) p2, (**C**) p7b or (**D**) p10 exerted any significant inhibitory effects on MDA-MB-231 breast cancer cell migration *in vitro* when expressed as a % of the cells alone control

Data is presented as mean±SEM (% gap closure compared with cells alone; n=3, *p=0.037). Statistical analysis was performed using t-test (Sigmaplot 11 software).

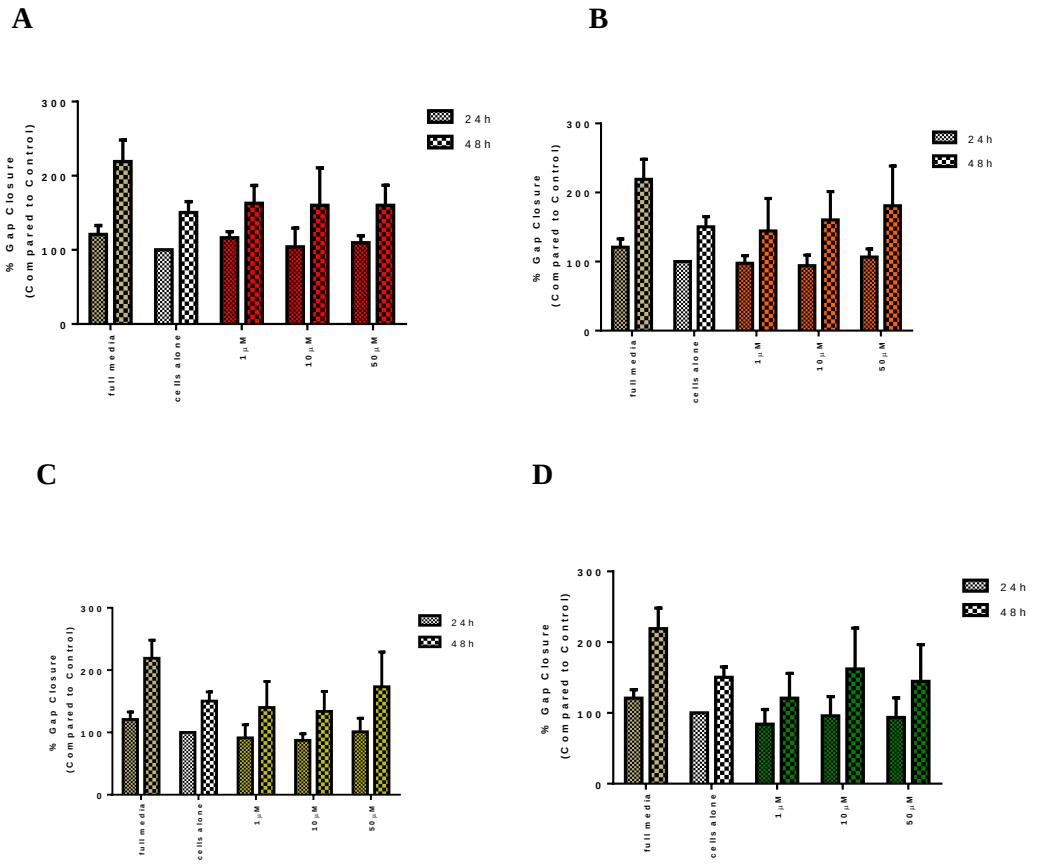

Figure 4.9 ***Effects of Np1 Peptides on MDA-MB-436 Breast Cancer Cell Migration:***
In the absence of recombinant $VEGF_{165}$, neither, (**A**) p1, (**B**) p2, (**C**) p7b or (**D**) p10 exerted any significant inhibitory effects on MDA-MB-231 breast cancer cell migration *in vitro* when expressed as a % of the cells alone control

Data is presented as mean±SEM (% gap closure compared with cells alone; n=3, NS). Statistical analysis was performed using t-test (Sigmaplot 11 software).

Boyden Chamber

The Boyden chamber assay measures directional migration and potentially is a better method for assessing the effects of drugs on breast cancer migration. Recombinant $VEGF_{165}$ was added to the breast cancer cells in the Boyden chamber assay, as an initial experiment prior to treating with the peptides demonstrated that insufficient breast cancer chemotaxis occurred in the absence of exogenous $VEGF_{165}$. However, in these Boyden experiments, VEGF did not significantly increase migration of MDA-MB-231 breast cancer cells, suggesting that there is a high level of heterogeneity in the response to VEGF by the cultured breast cancer cells. Since, no inhibitory effects on breast cancer cell migration were observed with any of the peptides in the scratch assay, one human derived peptides (p7b)

and the other peptide with potential Np1 and Np2 binding (p10) were chosen to measure the effects on breast cancer cell migration, in the chemotactic migration assay.

There was a trend that suggested that the presence of p7b and p10 stimulated MDA-MB-231 breast cancer migration *in vitro* compared with the $VEGF_{165}$ alone control (mean±SEM; p7b and p10 vs. $VEGF_{165}$; 410±287% and 363±262% vs. 100±0%; n=3, NS). (**Figure 4.10a**) However, this trend was not significant (p= 0.341 and p=0.372 respectively). In the Boyden chamber assay, the addition of $VEGF_{165}$ (50ng/ml) significantly (*P=0.013*) increased MDA-MB-436 breast cancer migration compared with the cells alone control (mean±SEM; $VEGF_{165}$ vs. cells alone; 100±0% vs. 53±11%, n=3, p=0.013) (**Figure 4.10b**). Similar to the MDA-MB-231 breast cancer cells, p7b and p10 both increased MDA-MB-436 breast cancer cell migration compared with the $VEGF_{165}$ alone control (mean±SEM; p7b and p10 vs. $VEGF_{165}$; 272±40% and 211±37% vs. 100±0%; n=3, p= 0.013 and p=0.039), this however was significant (*P=0.013 and P=0.039*) (**Figure 4.10b**).

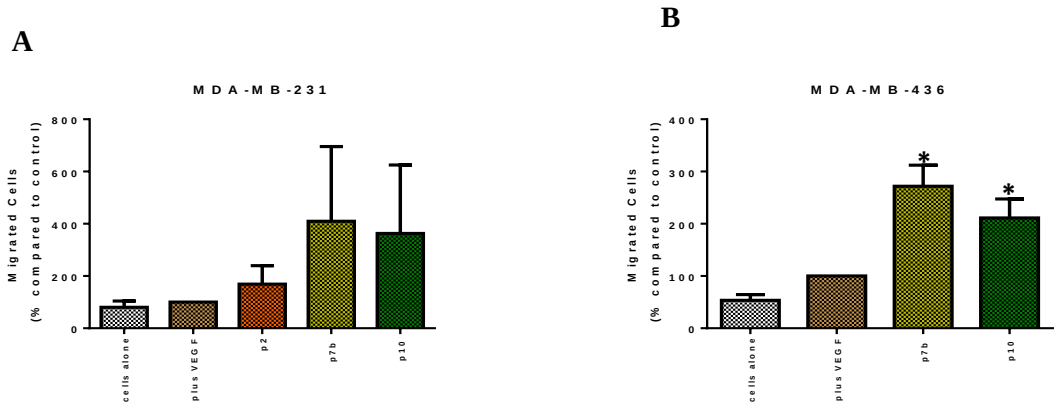

Figure 4.10 ***Effects the Np1 Peptides on Breast Cancer Cell Migration; Boyden Chamber:***
In the presence of recombinant $VEGF_{165}$, (**A**) P7b and p10 stimulated MDA-MB-231breast cancer cell migration. However this increase was not significant. (**B**) In contrast significant (*P=0.013 and P=0.039*) stimulatory effects were observed on MDA-MB-436 breast cancer cell migration in the presence of p7b and p10 respectively.

Data is presented as mean±SEM (% gap closure compared with cells alone; n=3, p<0.05). Statistical analysis was performed using the t-test (Sigmaplot 11 software).

4.2.4 Effects of combining Bz with Np1 Peptides on Breast Cancer Cell Function

As no inhibitory effects on MDA-MB-231 breast cancer cell proliferation or migration were observed in the presence of Bz or any of the four Np1 peptides, a combination experiment was deemed irrelevant. Similarly, as no overall inhibitory effect with Bz or any of the four Np1 peptides was observed, on MDA-MB-436 breast cancer cell migration, a combination experiment was not carried out. Peptide7b and p10 alone, both significantly inhibited MDA-

MB-436 breast cancer cell proliferation in previous experiments; therefore the effects of combining Bz with p7b and p10 on MDA-MB-436 breast cancer cell proliferation were assessed.

No significant inhibition on MDA-MB-436 proliferation was observed when the cells were treated with 5mg/ml Bz at 24 and 48h compared with the relevant cells alone control. This is consistent with the previous results looking at the effects of varying doses of Bz on MDA-MB-436 proliferation (**section 4.2.1**). There was a significant (*P< 0.001*) reduction (34%) in MDA-MB-436 proliferation at 24h in the presence of CV (5mg/ml) compared with the 24h cells alone control. However, this inhibition was lost by the 48h time point (**Figure 4.11**). There was also a significant (*P<0.001*) inhibitory effect (42%) on MDA-MB-436 proliferation when the cells were treated with a combination of CV and p7b (5mg/ml and 50µM respectively) compared with the 24h cells alone control which was maintained at the 48h time point (*P=0.029*). However, there was no significant additive effect of the combination compared with CV alone (*P=0.159*) at 48h (**Figure 4.11**).

At the 24h time point, combining Bz (5mg/ml) with p10 (1µM) resulted in a significant (*P=0.011*) inhibitory effect in MDA-MB-436 proliferation (23% decrease) compared with the 24h cells alone control (**Figure 4.12**). However, this combined inhibition was not significantly different when compared with Bz alone (*P=0.925*), despite the fact that there was no inhibition observed in the presence of Bz alone at either concentration. Unfortunately, the inhibition observed at 24h was not maintained at 48h. Combining CV with p10 demonstrated no additive effects in MDA-MB-436 cell proliferation (**Figure 4.12**).

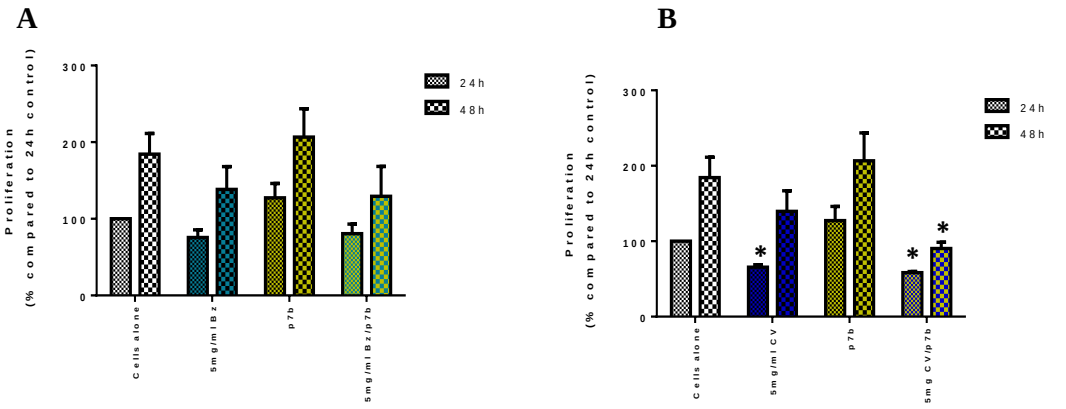

Figure 4.11 ***Effects of Combining Bz and CV with P7b on MDA-MB-436 Breast Cancer Cell Proliferation:*** In the absence of recombinant $VEGF_{165}$, combining (**A**) p7b with Bz exerted no additive effects on MDA-MB-436 breast cancer cell proliferation *in vitro* when compared with Bz alone. (**B**) Combining p7b with CV, displayed no significant additive effects on MDA-MB-436 breast cancer cell proliferation *in vitro* when compared to the CV alone

Data is presented as mean±SEM (% gap closure compared with cells alone; n=3, *p<0.001). Statistical analysis was performed using a t-test (Sigmaplot 11 software).

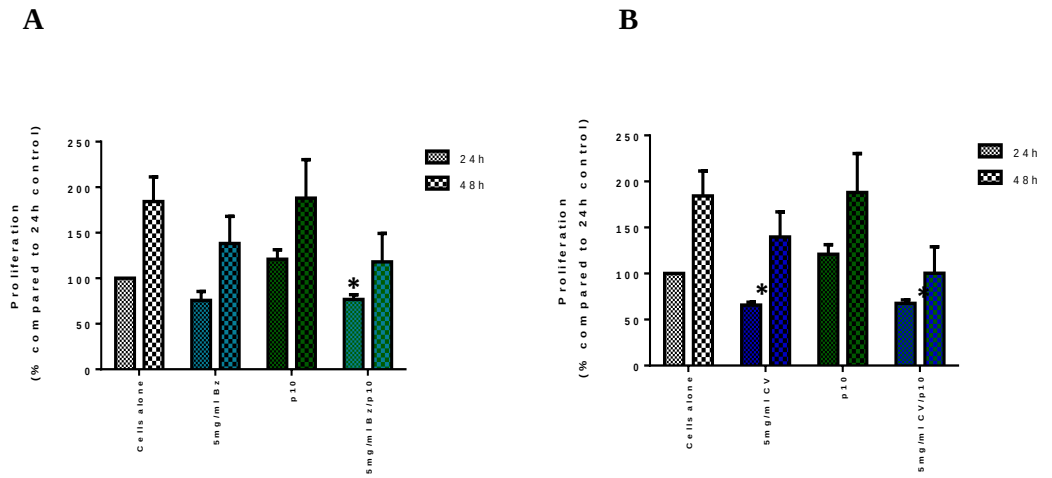

Figure 4.12 ***Effects of Combining Bz and CV with P10 on MDA-MB-436 Breast Cancer Cell Proliferation:***
In the absence of recombinant $VEGF_{165}$, combining (**A**) p10 with Bz exerted no additive effects on MDA-MB-436 breast cancer cell proliferation when compared with Bz alone. (**B**) Combining p10 with CV displayed no significant additive effects on MDA-MB-436 breast cancer cell proliferation when compared with CV alone.

Data is presented as mean±SEM (% gap closure compared with cells alone; n=3, *p<0.05). Statistical analysis was performed using a t-test (Sigmaplot 11 software).

4.2.5 Effects of a Np1 and Np2 Antibody on Breast Cancer Function

Migration

It was thought that looking at the effects of Np2 along with Np1 was also important, so a Np1 and Np2 blocking antibody (R&D Systems) that blocks $VEGF_{165}$ binding to Np1 or Np2, was used to assess if an antibody against Np1 or Np2 had greater inhibitory effects than those observed with the peptides. The addition of the Np1 or Np2 antibody exerted no inhibitory effects on MDA-MB-231 breast cancer cell migration (**Figure 4.13**), whereas, the Np1 antibody at 5µg/ml significantly (*P=0.001*) inhibited MDA-MB-436 breast cancer cell migration compared with the cells alone control at 24h (mean±SEM; Np1 antibody 5µg/ml vs. cells alone; 97±0.4% vs. 100±0%; n=3, p=0.001) (**Figure 4.14a**). However, although the trend remained, the inhibition with this dose of the Np1 antibody, compared with the cells alone control at 48h (mean±SEM; Np1 antibody 5µg/ml vs. cells alone; 110±13% vs. 132±8%; n=3, NS) did not reach statistical significance (*P=0.414*). The addition of the Np2 antibody to the MDA-MB-436 breast cancer cells, did not significantly (P=0.062 and P=0.161) inhibit cell migration at either, 24h (mean±SEM; Np2 antibody 10µg/ml vs. cells alone; 87±5% vs. 100±0%; n=3, NS) or 48h (mean±SEM; Np2 antibody 10µg/ml vs. cells alone; 103±15% vs. 132±8%; n=3, NS) (**Figure 4.14b**).

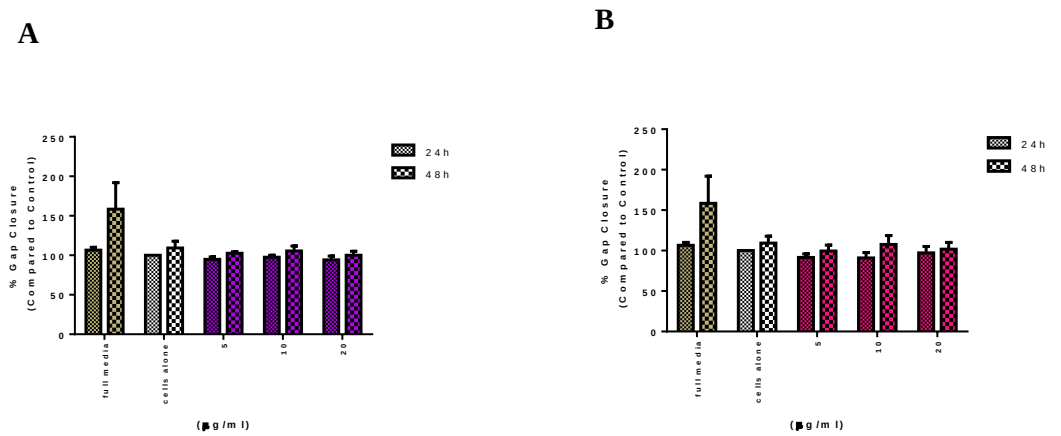

Figure 4.13 ***Effects of the Np1 and Np2 Antibody on MDA-MB-231 Breast Cancer Cell Migration:***
In the absence of recombinant $VEGF_{165}$, **(A)** the Np1 antibody exerted no significant effects on MDA-MB-231 breast cancer migration *in vitro* when expressed as a % of the cells alone control. (**B**) Neither did the Np2 antibody exert any inhibitory effects on breast cancer cell migration.

Data is presented as mean±SEM (% gap closure compared with cells alone; n=3, NS). Statistical analysis was carried out using the t-test (Sigmaplot 11 software).

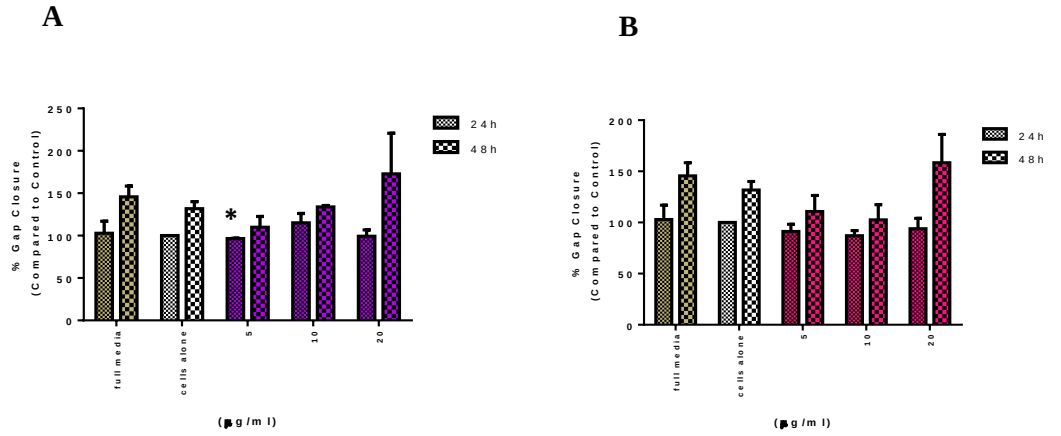

Figure 4.14 ***Effects of the Np1 and Np2 Antibody on MDA-MB-436 Breast Cancer Cell Migration:***
In the absence of recombinant $VEGF_{165}$, **(A)** the Np1 antibody exerted significant (*P=0.001*) inhibitory effects on MDA-MB-436 breast cancer migration when expressed as a % of the cells alone control at 24h. However, this inhibition was not maintained at 48h. (**B**) The Np2 antibody did not exert significant inhibitory effects on breast cancer cell migration.

Data is presented as mean±SEM (% gap closure compared with cells alone; n=3, p=0.001). Statistical analysis was carried out using the t-test (Sigmaplot 11 software).

4.3 CHAPTER DISCUSSION

4.3.1 Characterisation of VEGF Related Proteins

VEGF and $VEGF_{165b}$

VEGF protein expression was detected in both MDA-MB-231 and MDA-MB-436 breast cancer cell lysates, with a number of bands being observed, which corresponds to the presence of the various VEGF isoforms produced. However no expression was observed in the conditioned medium of either cell line, which was surprising as VEGF is secreted and would be expected to be present in the medium. It is possible that western blotting techniques are not sensitive enough to detect secreted VEGF, thus an ELISA assay may prove useful in determining the levels of VEGF that are secreted by the breast cancer cells *in vitro*.

$VEGF_{165b}$ protein expression was not detected in the cell lysate or the conditioned medium of either the MDA-MB-231 or MDA-MB-436 breast cancer cells. Initially, this was not surprising as $VEGF_{165b}$ is thought to be an endogenous regulator of VEGF activity, thus potentially displaying anti-angiogenic activity (***Qiu et al, 2009***) and the levels of this anti-angiogenic isoform are thought to be markedly decreased in tumours such as renal carcinoma (***Bates et al, 2002***) and prostate cancer (***Woolard et al, 2004***). Therefore it could be assumed that aggressive breast cancer cells such as MDA-MB-231 and MDA-MB-436 cells would down-regulate $VEGF_{165b}$ expression. However, more recently it has been observed that $VEGF_{165b}$ is in fact up-regulated in malignant breast tissue compared with normal breast epithelium (***Catena et al, 2010),*** although there are no reports in the literature of $VEGF_{xxxb}$ being detected in the breast cancer cell lines, the role of $VEGF_{165b}$ as a negative regulator of $VEGF_{165}$ activity and the role, if any, that this isoform plays in breast cancer progression needs further investigation.

VEGF Receptors

Assessment of VEGF receptor expression in breast cancer cells in the literature is mostly measured by mRNA levels; however protein expression is a better reflection of functional relevance of the receptors. VEGF-R1 and VEGF-R2 protein expression was observed on both breast cancer cells lines. The presence of a partially degraded product of VEGF-R2 in the breast cancer cells suggests that the breast cancer cells were activated in culture in a autocrine manner, as degradation of tyrosine kinase receptors is thought to occur upon ligand binding (***Grunewald et al 2010 & Goh et al, 2013***) and the presence of the immature form of VEGF-R2 may be indicative of newly synthesised VEGF-R2. The observation of a partial degradation product and the immature form of VEGF-R2, suggests that the

expression of cell surface VEGF-R2 is transient, and therefore, recycling, degradation and synthesis of VEGF-R2 could potentially occur in breast cancer cells as a result of autocrine VEGF signalling. No VEGF-R1 and VEGF-R2 protein expression was detected in the conditioned medium of both breast cancer cells despite soluble forms of both receptors existing. As with VEGF, it is possible that an ELISA assay may prove more sensitive in detecting soluble VEGF receptor expression.

Np1 and Np2 protein expression were detected in both breast cancer cell lines, although to varying degrees, with Np2 expression appearing to be greater in the MDA-MB-436 breast cancer cells as only a faint band was observed in the MDA-MB-231 cells, although flow cytometry would be required to confirm this. The MDA-MB-436 cells, similar to the HuDMECs, also appear to express soluble form of Np2. The expression of all four VEGF receptors on the breast cancer cell lines, suggested that targeting both VEGF receptor families is a feasible therapeutic measure. Np1 protein expression in the MDA-MB-231 cells has been previously observed (***Barr et al, 2005; Lee et al, 2007***), and Np2 mRNA (***Timoshenko et al, 2007***) whereas Np1 and Np2 expression on MDA-MB-436 breast cancer cells has not been investigated (PubMed).

As with the HuDMEC receptor expression discussion (3.3.2), analysis of cell surface receptor expression using flow cytometry would prove useful in determining the levels of different receptor expression and would allow for direct comparison on the levels of receptors that are present on the two different breast cancer cell lines. Also as suggested for the HuDMEC cells, receptor expression under normoxic and hypoxic conditions would be useful, as hypoxia can affect the level of receptors present on the cell surface of breast cancer cells. Differential receptor expression has been observed by MDA-MB-231 breast cancer cells under stress conditions such as hypoxia, although the observations varied, with one group observing an increase in Np1 expression in MDA-MB-231 under hypoxic conditions (***Barr et al, 2008***), whereas, another study observed, a slight decrease in Np1 protein expression in these cells under hypoxic conditions (***Bae et al, 2008***).

4.3.2 Effects of Bz on Breast Cancer Cell Function *In Vitro*

Since VEGF-R1 and VEGF-R2 protein expression was observed on both MDA-MB-231 and MDA-MB-436 breast cancer cells, assessing the direct effects that Bz had on these breast cancer cells *in vitro* was important prior to commencing any *in vivo* experimentation.

Proliferation

Overall, longer experimental time points for assessing effects on cell proliferation may prove more informative, especially to establish if the stimulatory effects observed on MDA-MB-231 breast cancer cell proliferation in the presence of Bz are maintained over time. The results in this current study differ from those previously observed, where no effects on MDA-MB-231 breast cancer cell proliferation, in response to Bz treatment have been noted (***Roland et al, 2009 & Ortholan et al, 2010***).

In the current studies the control vehicle for Bz at the 1mg/ml dose also exerted a stimulatory effect on MDA-MB-231 breast cancer cell proliferation in a similar manner to the equivalent dose of Bz. Therefore the effects seen with Bz, that are mirrored by the CV, can not be taken as positive data, as these are not a reflection of 'true' Bz activity. There is very little literature that investigates the effects of the vehicle in which Bz is re-suspended, and studies that contain a control treatment group generally use PBS or saline as a control. The Bz vehicle and therefore the control vehicle used in this study consists of sodium salts and tween, thus we initially thought that CV alone may cause a change in pH in the medium. However, we tested this, and there was no difference in pH, between the medium containing CV alone or Bz. It is important to further determine why CV, itself appears to exhibit effects on breast cancer function, which was at times comparable to the effects observed with Bz. More recently, there have been some studies investigating the effects of tween20 (which is in the CV) on cell activity, including breast cancer cells (***Yamagata et al, 2009, Yang et al, 2012 & Eskandani et al, 2013***). These studies suggest that the tween20 present in CV may partly be responsible for the *in vitro* activity observed on the breast cancer cells.

The MDA-MB-231 and MDA-MB-436 cell lines phenotypically appear very similar, in that both are ER/PR/HER receptor negative, and both are aggressive cell lines that show metastatic capability *in vivo* (***Iorns et al, 2012***). However, the two cell lines responded differently to Bz treatment, as no significant effects were observed on MDA-MB-436 breast cancer cell proliferation. It is possible that, the levels of VEGF-R1 and VEGF-R2 expression differ between the two metastatic breast cancer cells, resulting in differences in the response to VEGF receptor targeted therapy, such as Bz. It is thought that VEGF-R1 expression in breast cancer cells is detected mostly on the nuclear envelope rather then the cell surface (***Lee et al, 2007***), thus inhibitors that are unable to penetrate into the nucleus may not be able to maintain VEGF-R1 signalling inhibition. Therefore the location of the VEGF receptors and ability of subsequent inhibitors to penetrate into the nucleus could prove crucial in designing effective inhibitors.

Migration

No inhibitory effects on breast cancer cell migration were observed in response to Bz treatment *in vitro* in the scratch assay. These finding differ to what has been observed in the literature, whereby Bz inhibited MDA-MB-231 breast cancer migration (***Roland et al, 2009 and Prager et al, 2010***). In the above studies, different formats of the transwell assay were used to assess the effects of Bz on MDA-MB-231 cell migration. In the ***Prager et al*** study MDA-MB-231 breast cancer cells were seeded on a monolayer of endothelial cells in the upper chamber of a transwell assay. It is possible that, differences in migration assays used (scratch vs. transwell in the presence of endothelial cells or a Matrigel monolayer), may explain why the results from the current study differ from previous publications as the scratch assay measures unidirectional migration and the transwell and Boyden chamber both measure directional chemotaxis. The various VEGF isoforms, *in vivo*, create a VEGF gradient that is important for appropriate VEGF signalling and orchestrating the formation of the vasculature, with this in mind, it may have proved more informative to have carried out transwell assays to measure the effects of Bz on breast cancer cell migration *in vitro*, however, time constraints prevented this.

Overall, Bz displayed no inhibitory effects on MDA-MB-231 or MDA-MB-436 breast cancer cell proliferation or migration *in vitro*. As both the breast cancer cell lines used in these experiments exhibit an aggressive phenotype, it is possible that these cells are less dependent on the VEGF signalling pathway. It is also possible that upon VEGF blockade, these aggressive cells are capable of up-regulating factors that will compensate for the loss of VEGF. The presence of $VEGF_{165b}$ renders Bz treatment ineffective as unlike other tumour types, it has been observed that $VEGF_{165b}$ is up-regulated in breast cancer (***Catena et al, 2010***) and since $VEGF_{165b}$ also binds Bz (***Varey et al, 2008***) it is possible that $VEGF_{165b}$ sequesters Bz, making the more pro- active form of VEGF available to maintain tumour growth. However, as $VEGF_{165b}$ was not detected in these cell lines this makes it less likely, although it is possible that the antibody used in the Western blot analysis was not sensitive enough to detect $VEGF_{165b}$ levels.

4.3.3 Effects of the Np1 Peptides on Breast Cancer Function *In Vitro*

Since Np1 and Np2 protein expression was observed on both MDA-MB-231 and MDA-MB-436 breast cancer cells and as previous studies suggest Np1, at least is involved in prevention of breast cancer cell apoptosis (***Bachelder et al, 2001 and Barr et al***, ***2008***), it is possible that Np1 and Np2 are feasible targets for breast cancer therapy. As previously stated

there appears to very little difference in phenotype between the MDA-MB-231 and MDA-MB-436 cells, however the two cell lines responded differently to treatment with the Np1 peptides.

Proliferation

Treatment with the four Np1 peptides exerted no inhibitory effects on MDA-MB-231 breast cancer cell proliferation. The Np1 peptides exerted significant inhibitory effects on MDA-MB-436 breast cancer cell proliferation *in vitro.* The inhibitory effects on MDA-MB-436 breast cancer cell proliferation in the presence of the peptides, although minimal, differ to that observed with Bz treatment. Suggesting that not only does Np1 play a vital role in VEGF autocrine signalling, but it may also act as the primary receptor for VEGF induced activity on breast cancer cells, at least in relation to breast cancer cell proliferation *in vitro.* The differences observed in the response to Np1 treatment by the MDA-MB-231 and MDA-MB-436 breast cancer cells, may be a result of higher Np1 expression by the MDA-MB-436 breast cancer cells, which thus respond better to Np1 targeted therapy. Although from the Western blotting techniques, there were no obvious differences (quantification would confirm this). Alternatively, the levels of other angiogenic factors expressed by the two breast cancer cells, may allow the MDA-MB-231 cells to elicit a stronger compensatory response *in vitro,* thus flow cytometry and a cytokine array would be useful to test these potential hypotheses. The use of peptides in inhibiting neuropilin interactions with VEGF *in vitro,* have previously has been investigated (***Barr et al, 2005***) and this study demonstrated significant apoptotic activity when MDA-MB-231 cells were treated with a 24-mer anti-Np1 peptide (***Barr et al, 2005***). Although this study was investigating the effects on the peptide on MDA-MB-231 breast cancer apoptosis, it is important to note that the level of biological activity was similar in the ***Barr et al, 2005*** study, to the peptides used in this current study in the MDA-MB-436 proliferation assay. Overall, the MTS assays, as a measure of proliferation may not have been the most appropriate assay. As dying cells, also require energy, which is the indirect parameter that is the principle behind the MTS assay. Thus, no differentiation was made in these assays, which would allow determination of whether the effects observed with the peptides was a consequence of toxic effects of the peptides or a true anti-proliferative effect.

Migration

No significant effects on MDA-MB-231 or MDA-MB-436 breast cancer cell migration were observed in the presence of any of the four Np1 peptides, when assessed using the scratch assay. However, the Boyden chamber assay resulted in a trend that suggested p7b and p10 exert stimulatory effects on breast cancer cell migration *in vitro,* with significant stimulatory

effects being observed on the MDA-MB-436 breast cancer cells. This has previously been observed in the literature, whereby treatment with an anti-Np1 antibody caused a stimulatory effect on MDA-MB-231 migration *in vitro* (***Bachelder et al, 2003***). The group suggested that the reason for this stimulatory effect may be due to the VEGF/SEMA ratio present in the breast cancer cells. The binding site for the SEMA proteins lies within the a1/a2 domain of Np1, with the VEGF binding site lying within the b1/b2 domain. However, there is thought to be some over-lap in binding, suggesting that the SEMA proteins may act as antagonists. The group therefore suggested that the anti-Np1 and anti-Np2 antibody might also block the SEMA binding site, thus potentially decreasing the regulatory role that the SEMA proteins may play.

It is not known if these peptides are capable of simultaneously inhibiting the other isoforms of VEGF, as the other VEGF isoforms, are also capable of transducing alternative VEGF signals via Np1. $VEGF_{189}$ has been observed to induce apoptosis of breast cancer cells via Np1 (***Vintonenko et al, 2011***) thus if the peptides also inhibit $VEGF_{189}$ from binding Np1, the apoptotic activity that $VEGF_{189}$ induces on the MDA-MB-231 breast cancer cells *in vitro* may potentially be lost, thus maintaining breast cancer activity.

4.3.4 Effects of Combining Bz with the Np1 Peptides on Breast Cancer Function

As MDA-MB-436 breast cancer cell proliferation was the only breast cancer activity that was significantly inhibited in the presence of the Np1 peptides, a combination assay was only carried out. However, no additive effects were observed on MDA-MB-436 breast cancer cell proliferation *in vitro* when compared with the peptides alone. This, however could be expected as no inhibitory effects on breast cancer cell activity was observed with Bz alone, thus it would perhaps have been useful to carry out co-culture experiments whereby the breast cancer cells were cultured with the HuDMECs and then the effects of combining the peptides with Bz compared with Bz alone be evaluated. Since the two different cell types responded differently to Bz and Np1 peptide treatment, a co-culture assay may have proved more informative when trying to establish whether blocking both VEGF receptor families limits the resistance to therapy by targeting both the endothelial and the cancer cells.

In the combination experiments, the initial inhibitory effect displayed with p7b and p10 on MDA-MB-436 breast cancer cell proliferation was not observed, this inconsistency in response is potentially due to trafficking and recycling of the Np1 receptors on the cell surface of the MDA-MB-436 breast cancer cells. Subtle changes in the microenvironment,

stress, or over confluency of cells may have affects on the levels of Np1 present on the surface, thus altering the response of these breast cancer cells to the peptides, although further work is needed to confirm this.

4.3.5 Effects of a Np1 and Np2 Antibody on Breast Cancer Cell Function

When commercially available antibodies against Np1 and Np2 were used in the scratch assay, no inhibitory effects were observed on MDA-MB-231 breast cancer cell migration. Similarly, no effects on MDA-MB-231 breast cancer cell migration were observed in the presence of the Np2 antibody. An inhibitory effect on MDA-MB-231 breast cancer cell migration was not necessarily expected as in the literature the presence of an anti-Np1 antibody displayed stimulatory effects on MDA-MB-231 migration (***Bachelder et al, 2003***). Furthermore, the MDA-MB-231 cells had minimal Np2 expression. In contrast, the MDA-MB-436 cells, which did express Np2, demonstrated an inhibitory trend which suggests that Np2 may play an important role in MDA-MB-436 breast cancer cell migration. However, additional repeats would be required to confirm the initial trend observed.

Overall, the use of the scratch assay to measure migration may not be the best technique as although a number of trends were observed, no statistical significance was reached due to variability. When inhibiting receptor-ligand interactions, a certain amount of variability can be expected, especially since the expression of cell surface receptors can be transient and can change under various environmental conditions. However, it seems that the variability in the scratch assay may be partly due to the nature of the technique itself. The addition of MITC to limit cell proliferation, thus ensuring gap closure is due to cell movement. The 'wound' itself may have stressed the breast cancer cells, causing them to release factors that may affect breast cancer cell migration, thus changing or affecting the response of the breast cancer cells to Bz or anti-Np1 treatment.

4.4 CHAPTER CONCLUSION

The *in vitro* functional assays carried out, suggest that the Np1 peptides used in this study could potentially have some limited anti-tumourgenic effects on some breast cancer cell lines. However, VEGF is not the main cytokine involved in breast cancer cell function, thus blocking the VEGF system alone may not be the most effective method, especially when targeting the breast cancer cells. The nature of the neuropilin receptors, acting as both co-receptors and independent receptors, suggest that they exert wide spread function and that the neuropilin receptors are a feasible target. However, blocking the interactions of Np1 and/or Np2 with other cytokines as well as or instead of VEGF may prove more beneficial and effective at inducing or maintaining an inhibitory effect on breast cancer cell activity.

When aiming to improve the efficacy of Bz in breast cancer treatment, having a secondary treatment that blocks Np1 interactions with a number of ligands, that are up-regulated in response to VEGF inhibition, such as FGF and TGF-β may prove more efficacious.

The differences that exist between the two breast cancer cell lines tested, need to be investigated further as the differential response to the Np1 peptides may prove to be very important in mirroring differences that are apparent in individual breast cancer patients. This also highlights the importance of finding biomarkers that will allow identification of individuals that will respond to Np1 therapies. At first glance, there appears to be very little difference in the phenotype between the MDA-MB-231 and MDA-MB-436; however analysis carried out more recently has identified the presence of different mutations in the two cell lines (***Lehmann et al, 2011***). Further analysis, using microarrays, on these supposedly similar breast cancer cell lines may enable identification of downstream events that may be responsible for differential responses to Bz and the Np1 peptides.

4.5 *IN VITRO* RESULTS CONCLUSION

From the *in vitro* experiments performed in Chapters 3 and 4, it is confirmed that Bz primarily inhibits tumour growth via its effects on the endothelial cells. As the *in vitro* data observed no significant effects on breast cancer cell proliferation or migration in the presence of Bz. The role of Np1, however, appears to be widespread across the two cell types, as the Np1 peptides significantly inhibited both microvascular endothelial and breast cancer cell activity *in vitro* albeit to a limited extent. The interplay between the microvascular and breast cancer cells is important in cancer progression and the communication between these two cell types is vitally important especially when assessing the effects of treatments such the Bz and anti-Np1 targeting agents.

From the *in vitro* data it was decided that the MDA-MB-436 cells would be the most appropriate to follow up in the *in vivo* experiments, as expression of all four receptors appeared to be greater in these cells compared with the MDA-MB-231 cells. In terms of the Np1 peptides, both p7b and p10 exerted significant inhibitory effects on both the HuDMECs (differentiation and migration) and MDA-MB-436 (proliferation) breast cancer cells *in vitro*. This suggested that combining either of these two peptides with Bz may allow for a dual targeting approach *in vivo*, thus enhancing tumour inhibition and potentially overcoming resistance to Bz therapy.

Chapter Five

In Vivo Results
Effects on Primary Breast Cancer Growth

5. INTRODUCTION

The *in vitro* experiments allowed for direct investigation of the interaction of $VEGF_{165}$ with the Np1 receptor and the potential role that this interaction has on breast cancer progression and resistance to Bz therapy. However, to assess if the Np1 peptides can be developed into clinically or biologically relevant targets for breast cancer therapy the evaluation of *in vivo* models was essential. The initiation of tumour development and metastasis is a dynamic process involving a number of other cell types that reside within the tumour microenvironment such as ECs, fibroblasts and macrophages. These different cell types produce and release a variety of growth factors and cytokines that can have various effects on the tumour cells. The relevance of blocking the interaction between $VEGF_{165}$ and Np1 *in vivo* in both the primary and metastatic setting is important to assess.

Bz was granted accelerated approval by the FDA in 2008 for use in the clinic in treatment of mBC. The clinical trial that lead to the approval of Bz in mBC resulted in an significant increase in PFS but with no additive effect on OS in the Bz containing arm compared with the paclitaxel alone (***Miller et al, 2008***). However, since FDA approval combination therapy with Bz has mostly resulted in modest effects in mBC, with no reported increase in OS. A retrospective study reported that several compensatory factors were up-regulated in response to Bz treatment, with potential impact on response to Bz therapy (***Jubb et al, 2011***), Np1 was amongst these factors. This suggests that Np1 may play an important role in providing an alternative signalling pathway for VEGF, thus enabling tumours to escape therapy.

The majority of preclinical data available using Bz in breast cancer treatment is limited mostly to adjuvant therapy which investigates combining Bz with standard chemotherapeutic agents or radiotherapy. This is due to the proposed vascular mechanism of action for Bz, which is thought to primarily act on the endothelial compartment, thus exerting indirect effects on the breast cancer cells. The emerging role of Np1 in breast cancer progression via actions on both the angiogenic pathway and the breast cancer cells directly, suggests that targeting Np1 alongside the classical VEGF receptors is a feasible approach that may have more wide-spread effects on the tumour micro-environment. In addition to this, there are also indications that lower tumour Np1 expression favours a positive Bz response in breast cancer patients (***Jubb et al, 2011***) suggesting that combing Bz with agents that target the Np1 receptor may potentially overcome the problem of resistance that is now apparent in a proportion of some Bz treated mBC patients. Thus, Bz was combined with two neuropilin peptides (p7b or p10) to achieve both an anti-angiogenic and an anti-tumourgenic effect in the combination groups, thus increasing tumour inhibition.

5.1 MATERIALS & METHODS

5.1.1 Cell Lines

In the current project two human metastatic breast cancer cells were utilised (MDA-MB-231 and MDA-MB-436) to test the hypothesis that combination treatment targeting the VEGF pathway in metastatic breast cancer, demonstrates enhanced efficacy. Additionally, with the increased interest in personalised medicine, the use of two metastatic cell lines may prove more informative and allow identification of downstream effectors that might be responsible for any differential responses observed to therapy in the clinical setting.

Both cell lines are identified as representing triple negative breast cancer (TNBC) with a Basal B phenotype and both display a histology that is reflective of invasive ductal carcinoma (***Lehmann et al, 2011***). The two cell lines display a similar morphology in culture, are known to form tumours *in vivo* and display metastatic potential when implanted in a murine model. However, although both are metastatic, the MDA-MB-436 are thought to be moderately metastatic compared with MDA-MB-231 cells, which are known to be highly metastatic (***Tu et al, 2011***). In addition, molecular analysis has brought to light a number of mutational differences that are present between the two cell lines (***Lehmann et al, 2011***), with some of these mutations having various potential effects on the VEGF pathway.

5.1.2 Sub-Cutaneous Murine Breast Cancer Model

Growth Kinetics

A GFP-labelled MDA-MB-436 cell line had been previously generated in the laboratory for use *in vivo*. GFP-labelled human MDA-MB-436 breast cancer cells were implanted into the flank region of anaesthetised (isofloarine) athymic CD1 nude female mice (4–5weeks old) at three different cell densities ($1x10^5$, $1x10^6$ and $5x10^6$; administered in a total volume of 100µl). The three different densities were used to establish growth kinetics and the minimum treatment window. Once a palpable tumour had developed ($100mm^3$), tumour growth was measured twice weekly using callipers. At the end of the study (4 weeks post development of a treatable tumour) tumours were excised and wax embedded to allow optimisation of staining protocols.

Combination Studies

For the treatment experiments, $1x10^6$ GFP-labelled human MDA-MB-436 breast cancer cells were injected via a sub-cutaneous (s.c.) injection into the left flank of anaesthetised (isofloarine) CD1 nude female mice (4-5weeks old). Tumours were measured using callipers twice weekly and treatment with either Bz, CV, p7b, p10, Bz/p7b, Bz/p10 or saline began

when tumours reached a tumour volume of 100mm$^{3.}$ (**Table 5.1-5.3**). The 5mg/kg dose of Bz used in the initial *in vivo* studies was chosen as a result of a literature search (PubMed) that demonstrated several breast cancer *in vivo* experiments administered the same dose with tumour growth delays (***Higgins et al, 2007; Xue et al, 2008; Borgan et al, 2012; Conley et al, 2012***). In addition this dose was chosen due to results obtained from the *in vitro* studies (see section 3.2.2). During combination experiments animals received both Bz and one of the Np1 peptides on the same day; the peptides were administered one hour after the Bz injection. The end of the experiment was determined when either 1) the Home Office (HO) tumour diameter limit was reached (15mm), (2) the tumour ulcerated or (3) the animals lost greater than 10% body weight due to tumour development. Following cull, tumours were excised, divided in two and either frozen or formalin fixed prior to wax-embedding. Tumour sections were cut (5μM from the blocks) and stained with H&E for measuring tumour necrosis. CD34, Ki67 and Caspase 3 staining was carried out to assess the formation of new vessels, proliferation and apoptosis respectively. Normal tissues were also resected (liver, lungs, kidney and spleen) divided in two and frozen or formalin fixed to allow for further analysis to determine drug 'off-target' effects.

5.1.3 Tumour Analysis

Assessment of tumour necrosis was carried out on H&E stained tumour sections, using the chalkley grid (section 2.8.2), whereby the entire tumour section scored for positive and negative areas of necrosis allowed for the overall percentage necrosis to be calculated. Assessment of Ki67, Caspase 3 and CD34 staining was carried out by quantifying the mean number of positive cells or vessels present in 5 random fields of view. This methodology and analysis was used in all *in vivo* subcutaneous experiments described in the following results section.

Treatment	Dose	Frequency of Injection	Route of Administration	Volume of Injection	n= (injected)
Saline	Not applicable	Each time a Bz/peptide treatment was administered	i.p.	100µl	5
Bz	5mg/kg	Twice weekly	i.p.	100µl	5
CV	Equivalent volume to Bz at 5mg/kg	Twice weekly	i.p.	100µl	5
p7b	1µM	Twice weekly	i.p.	100µl	5
p10	50µM	Twice weekly	i.p.	100µl	5
Bz/p7b	Bz: 5mg/kg p7b: 1µM	Both twice weekly	i.p. (p7b administered 1hour after Bz injection)	100µl	5
Bz/p10	Bz: 5mg/kg p10: 50µM	Both twice weekly	i.p. (p10 administered 1hour after Bz injection)	100µl	5

Table 5.1 ***Dosing regimens for Experiment One:*** Outlines the dosing regimen for the initial Bz and peptide combination study detailed in section 5.2.2.1–5.2.2.3.

Treatment	Dose	Frequency of Injection	Route of Administration	Volume of Injection	n= (injected)
Saline	Not applicable	Each time a Bz/peptide treatment was administered	i.p.	100µl	6
Bz	5mg/kg	Twice weekly	i.p.	100µl	6
CV	Equivalent volume to Bz at 5mg/kg	Twice weekly	i.p.	100µl	6
Bz	2.5mg/kg	Twice weekly	i.p.	100µl	6
CV	Equivalent volume to Bz at 2.5mg/kg	Twice weekly	i.p.	100µl	6
Bz	1mg/kg	Twice weekly	i.p.	100µl	6
CV	Equivalent volume to Bz at 1mg/kg	Twice weekly	i.p.	100µl	6
Bz	0.5mg/kg	Twice weekly	i.p.	100µl	6
Bz	0.1mg/kg	Twice weekly	i.p.	100µl	6

Table 5.2 ***Dosing regimens for the Bz Dose Study:*** Outlines the dosing regimen for the Bz dose study detailed in section 5.2.2.4.

Treatment	Dose	Frequency of Injection	Route of Administration	Volume of Injection	n=
Saline	Not applicable	Each time a Bz/peptide treatment was administered	i.p.	100µl	5
Bz	0.1mg/kg	Twice weekly	i.p.	100µl	5
Bz/p7b	Bz: 0.1mg/kg P7b: 1µM	Twice weekly Three times a week	i.p. (p7b administered 1hour after Bz injection)	100µl	5

Table 5.3 ***Dosing regimens for Experiment Three:*** Outlines the dosing regimen for the second Bz combination study (with low doses of Bz) detailed in **section** 5.2.2.5.

5.1.4 Statistical Analysis

Following assessment of normality statistical analysis was performed using the Mann-Whitney U Test or a student's t test. When comparing multiple groups the One Way ANOVA, followed by the Holm-Sidak's post-hoc test or the Kruskal-Wallis was used (Sigmaplot 11 software). Statistical significance was considered at $P = 0.05$.

5.2 RESULTS

5.2.1 Optimisation of Cell Density for s.c MDA-MB-436 Implantation

The optimal cell density required for s.c. tumour implantation was initially assessed. Implantation of $5x10^5$ MDA-MB-436 GFP labelled breast cancer cells into the left flank resulted in 50% tumour uptake in athymic CD1 nude females (n=4), with two animals demonstrating small palpable tumour growth at 21 days and treatable tumours ($100mm^3$) within 4.5 weeks post injection (**Figure 5.1**), however two animals had no detectable tumours. One animal with tumour growth demonstrated ulceration five days after reaching treatable tumour volume, thus had to be culled. In contrast, implantation of $1x10^6$ MDA-MB-436 GFP labelled breast cancer cells (n=3) resulted in 100% tumour take. Tumour growth was observed at 6 days post injection and treatable tumours ($100mm^3$) within four weeks post injection (**Figure 5.1**). Implantation of $5x10^6$ MDA-MB-436 breast cancer cells resulted in 67% tumour uptake (n=3), with two animals developing a palpable tumour (**Figure 5.1**). All three cell densities tested resulted in a tumour treatment window of approximately 4 weeks, before the end of procedure (EOP) was reached. All tumours from this study were excised and wax embedded to allow for optimisation of staining protocols for the IHC studies. This initial pilot study demonstrated that the optimal cell density for subcutaneous tumour implantation was $1x10^6$ when taking into account the growth kinetics and volume ($100mm^3$) required for the commencement of treatment.

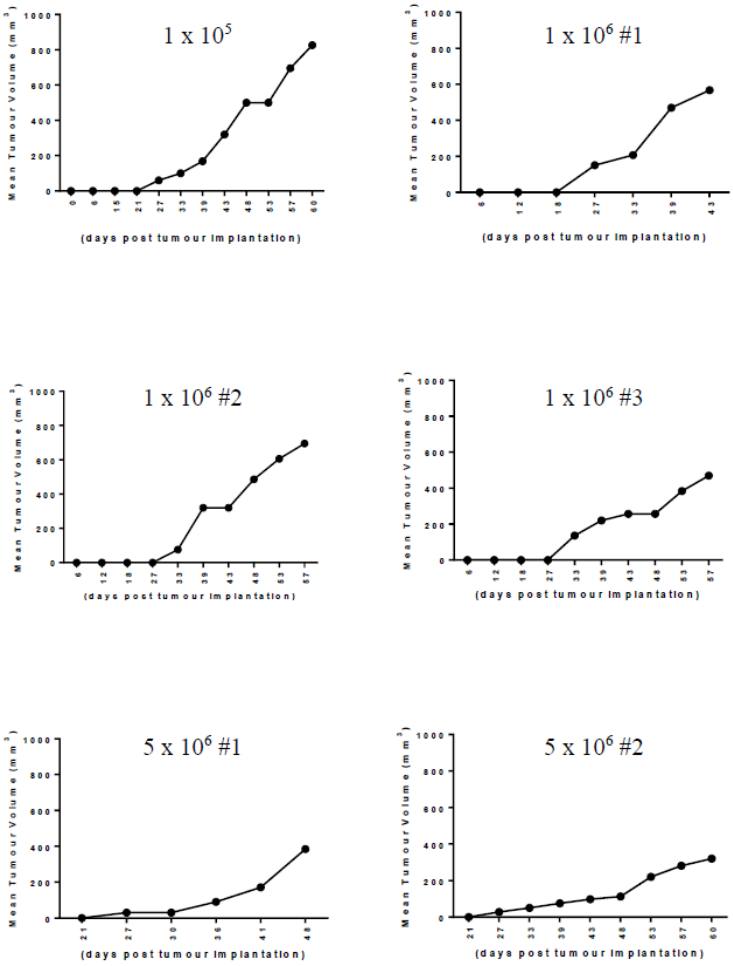

Figure 5.1 ***Optimising MDA-MB-436 Breast Cancer Cell Density:*** MDA-MB-436 GFP breast cancer cells were implanted at varying concentrations into the left flank of CD1 nude female mice under anaesthesia (isoflurane). $5x10^5$, (n=1) $1x10^6$ (n=3) and $5x10^6$ (n=2)

# denotes individual animals that developed tumours

5.2.2 Primary Tumour Growth

5.2.3 Effects of Bz on Subcutaneous Breast Cancer Growth

Bz

Having established the concentration of cells required to induce s.c. primary tumour growth a therapeutic intervention study was planned with Bz alone, the control vehicle for Bz (CV), p7b alone, p10 alone and Bz in combination with p7b and p10. Peptide 7b and p10 were chosen as the most efficacious neuropilin peptides from the *in vitro* study (see chapter 3&4). The EOP for individual animals was determined by one of the following criteria (1) once tumour diameter reached 15mm as measured by callipers (2) if the tumour ulcerated or (3) if greater than 10% body weight was lost due to tumour development. When EOP was reached for each individual animal, both tumour and normal organs (lung, liver, kidney and spleen) were excised, divided into two and frozen or formalin fixed to allow for subsequent *ex vivo* analysis.

Control

Following tumour implantation (MDA-MB-436; $1x10^6$), an equal number of animals were randomly assigned to each treatment group (n=5/group). On the day treatment commenced, all five animals assigned to the saline control group had palpable tumours. Twenty-nine days post initial injection of saline treatment; two of the five animals were culled due to tumours reaching the maximum tumour size permitted by the Home Office and NCRI guidelines (15mm diameter) (***Workman et al, 2010***). By day forty-two post initial injection, all remaining animals (n=3) in the saline treated group were culled, due to tumour volume being reached or tumour ulceration (792.7±319.9mm^3). In the Bz (5mg/kg) alone group, three of the five animals implanted with MDA-MB-436 breast cancer cells developed palpable tumours and were treated with Bz twice weekly via i.p injection, as one animal was culled prior to the start of treatment due to ulceration of the tumour and the second failed to develop a palpable tumour. By day twenty-one post initial injection, one of three remaining animals treated with Bz alone was culled due to tumour ulceration (864mm^3). The remaining two animals continued to be treated until the end of the experiment (day 42). At the end of the experiment, treatment with Bz (n=2) resulted in inhibition of tumour growth compared with the saline (n=3) group (mean±SEM; Bz vs. saline control; 184±0mm^3 vs. 793±320mm^3; n=2/3) (**Figure 5.2**), however statistical analysis was not possible due to numbers. Therefore an earlier time point (day seventeen) was chosen for statistical analysis. It is important to note that throughout the Bz treatment period, a relatively cytostatic effect on tumour growth was observed (**Figure 5.2**). At day seventeen, Bz (n=3) inhibited tumour growth compared with the saline control (n=5) group (mean±SEM; Bz vs. saline control; 164±47mm^3 vs.

406±103mm^3; n=3/5, ns), this was not significant (*P = 0.970*) (**Figure 5.2**). In the group treated with the control vehicle for Bz (CV) at an equivocal volume of animals receiving 5mg/kg Bz, four of the five animals implanted with MDA-MB-436 breast cancer cells developed palpable tumours and were treated with CV twice weekly via i.p. injection. By day thirty-five, post initial injection, one of the four animals treated with CV was culled due to tumour ulceration (900mm^3). The remaining three animals continued to be treated with CV until the end of experiment (day 42). At day seventeen, when statistical analysis was performed, CV (n=4) resulted in inhibition in tumour growth compared with the saline (n=5) group (mean±SEM; CV vs. saline control; 212±60mm^3 vs. 406±103mm^3; n=4/5, ns), this was not significant (*P = 0.173*) (**Figure 5.2**).

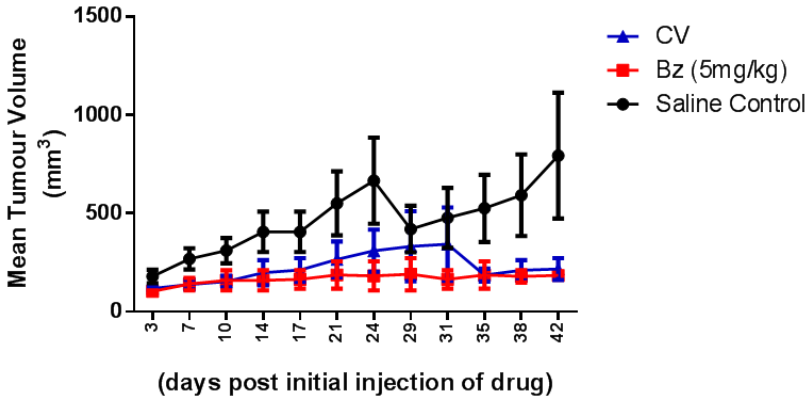

Figure 5.2 Effects of Bz and CV on Breast Cancer Growth In Vivo.: Administration of Bz (5mg/kg) and CV; twice weekly (i.p.) reduced tumour growth compared with the saline control group.

Data is presented as mean±SEM tumour volume (mm^3); n=3-5, NS. Statistical analysis was performed on day seventeen using the One Way ANOVA (Sigmaplot 11 software).

5.2.4 Tumour Histology and Immunohistochemistry

Due to the inhibitory trend observed with Bz and CV on of tumour growth *in vivo*, it was important to establish if there were any differences in tumour morphology or histology between experimental groups. Normal tissue was harvested from each animal at the EOP however; histology was only carried out on the tumour tissue. Wax embedded blocks and frozen sections for normal tissue are available for any further analysis required, especially to establish, if any effects observed with the treatment groups are tumour specific or more wide-spread.

VEGF and VEGF Receptor Expression in MDA-MB-436 Tumours *In Vivo*

From the *in vitro* experiments (**section 4.2.1**) it was evident that VEGF, VEGF-R1, VEGF-R2, Np1 and Np2 were all expressed by MDA-MB-436 breast cancer cells in culture. However it was important to determine the *in vivo* expression of these molecules.

VEGF expression was observed in the tumours from all the different treatment groups with a diffuse distribution being observed across the tumour tissue (**Figure 5.3**). The Bz treated tumours observed the weakest intensity of VEGF expression (**Figure 5.3**). In general VEGF-R1 staining was observed across the tumour tissue, however, interestingly, stronger staining was evident within the necrotic areas of the tumour tissue (**Figure 5.4**). In the saline, Bz alone and Bz/p7b treated tumours VEGF-R1 expression was mostly weak to moderate in 75% of the cells that expressed the receptor. In contrast, CV and Bz/p10 treated tumours expressed moderate to strong VEGF-R1 staining (**Figure 5.8a**).

VEGF-R2 staining was observed in the tumours and displayed a wide-spread distribution pattern (**Figure 5.5**). The saline control, Bz/p7b and Bz/p10 treated tumours VEGF-R2 staining was weak to moderate, whereas both CV and Bz treated displayed moderate to strong VEGF-R2 expression (**Figure 5.8b**)

Np1expression was observed in the tumours but in contrast to the other VEGF receptor it was neither as wide-spread nor as strong (**Figure 5.6**), with the different treatment groups observing mostly weak staining (**Figure 5.8c**). Np2 expression was only observed in the control and Bz/p7b treated tumours (**Figure 5.7** and **Figure 5.8d**). However, as the tumours were resected at different time-points an accurate endpoint comparison can not be made between the different treatment groups.

VEGF

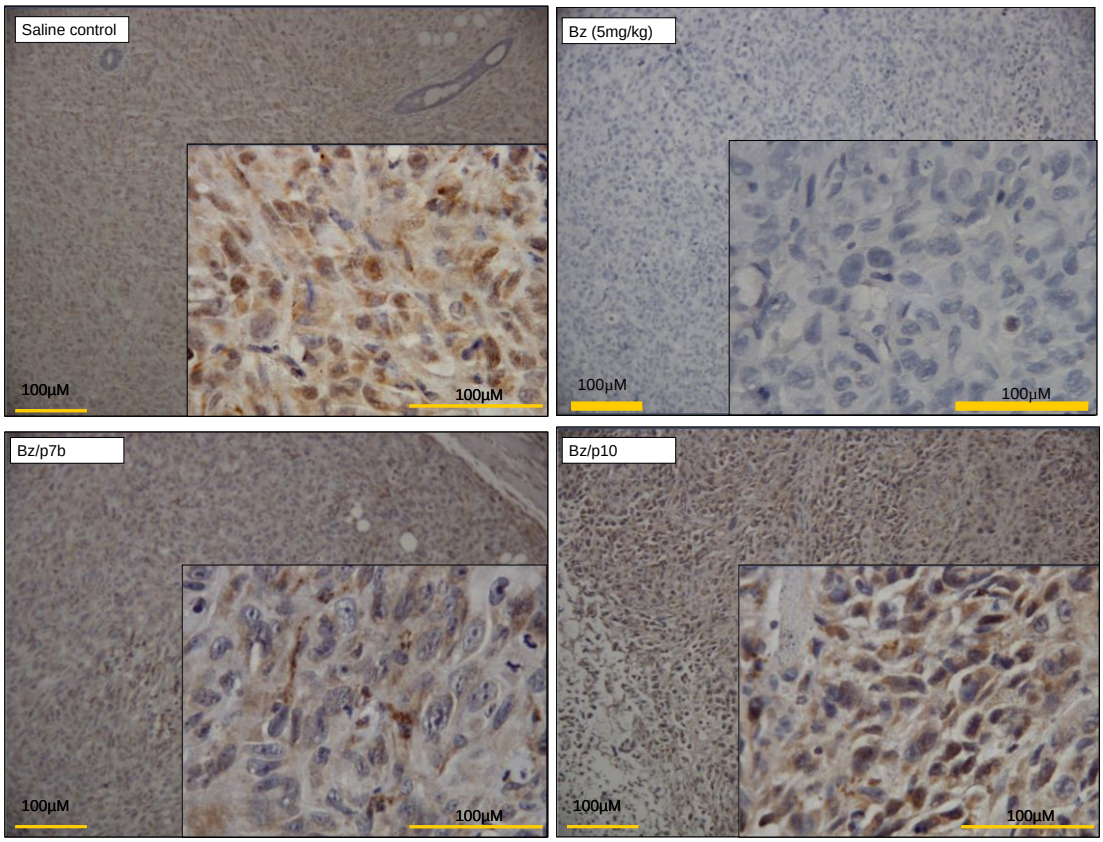

Figure 5.3 ***Expression of VEGF by MDA-MB-436 Breast Cancer Tumours:***
Representative images to that demonstrate the presence of VEGF expression in the tumours. Diffuse, cytoplasmic VEGF staining was observed in all the tumours from the different treatment groups. Images were taken at x10 (main panel) and x60 (insert panel) magnification to visualise the pattern of VEGF staining.

NB: It is important to note that VEGF staining was carried out using tumours taken at different experimental time-points, and therefore are not completely comparable.

VEGF-R1

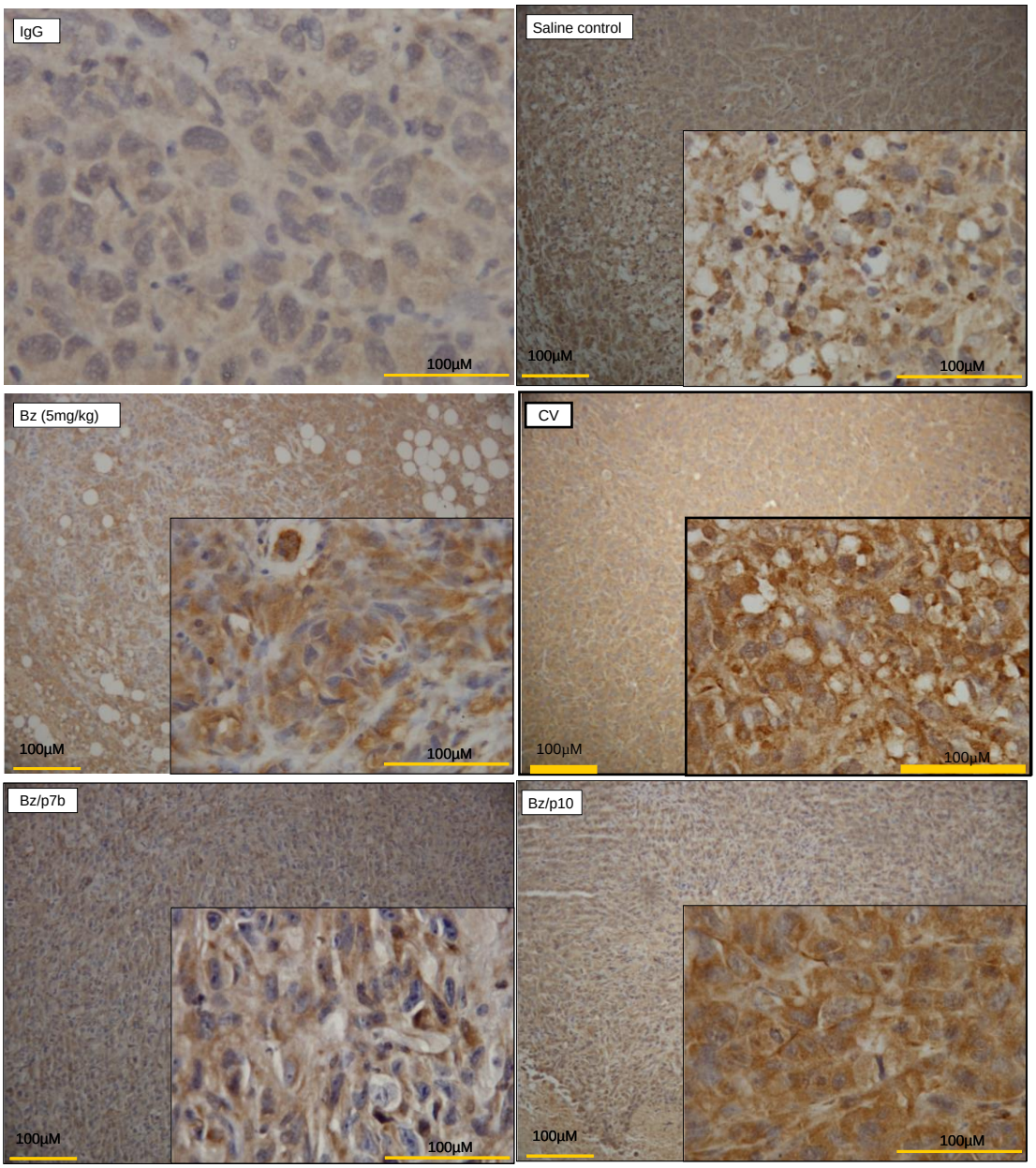

Figure 5.4 ***Expression of VEGF Receptor 1 by MDA-MB-436 Breast Cancer Tumours:***
Representative images to that demonstrate the presence of VEGF expression in the tumours. VEGF-R1 staining was observed in all the tumours from the different treatment groups. Images were taken at x10 (main panel) and x60 (insert panel) magnification to visualise the pattern of VEGF staining.

NB: It is important to note that VEGF-R1 staining was carried out using tumours taken at different experimental time-points, and therefore are not completely comparable.

VEGFR2

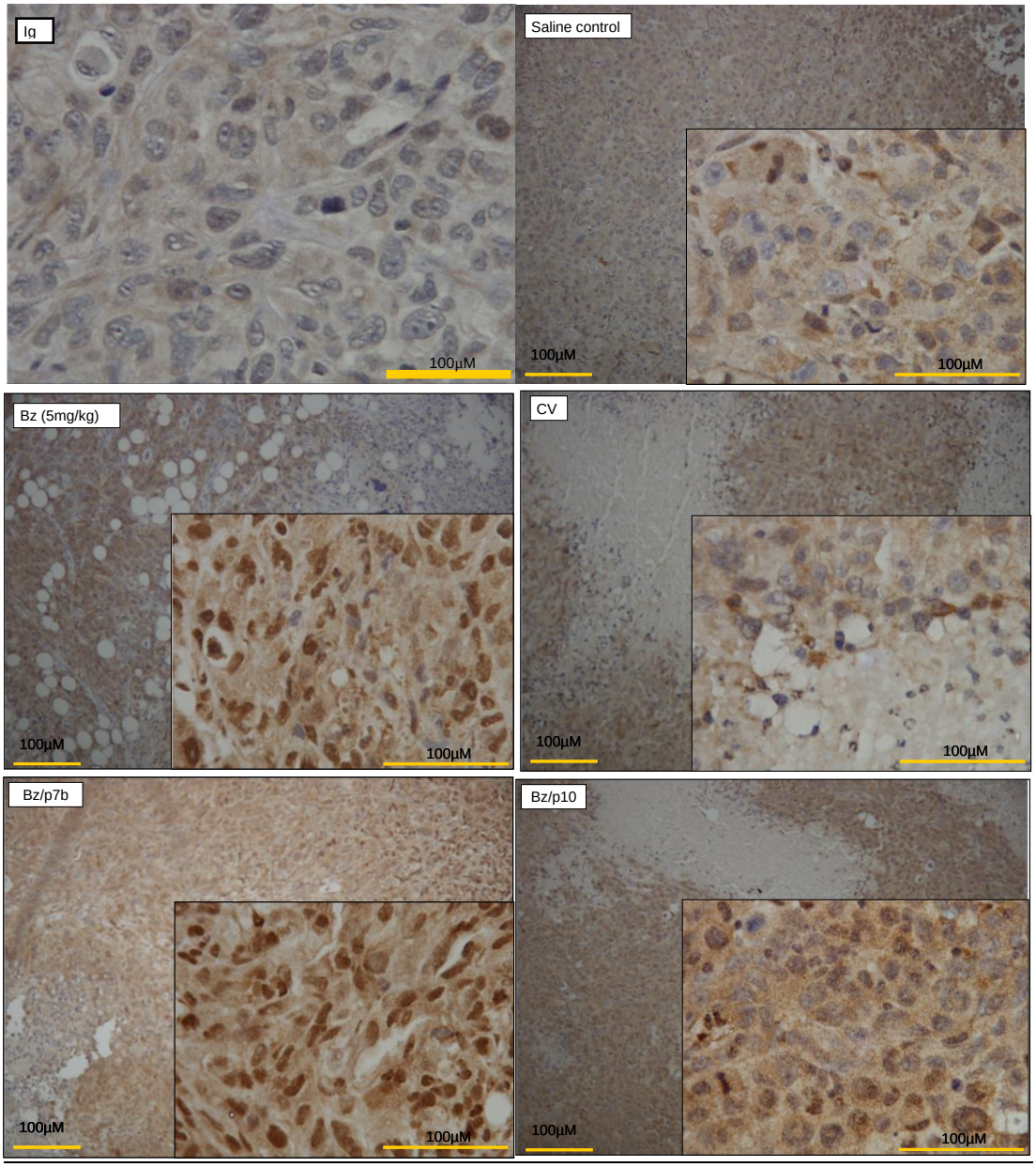

Figure 5.5 ***Expression of VEGF Receptor 2 by MDA-MB-436 Breast Cancer Tumours:***
Representative images to that demonstrate the presence of VEGF-R2 expression in the tumours. VEGF-R2 staining was observed in all the tumours from the different treatment groups. Images were taken at x10 (main panel) and x60 (insert panel) magnification to visualise the pattern of VEGF –R2 staining.

NB: It is important to note that VEGF-R2 staining was carried out using tumours taken at different experimental time-points, and therefore are not completely comparable.

NP1

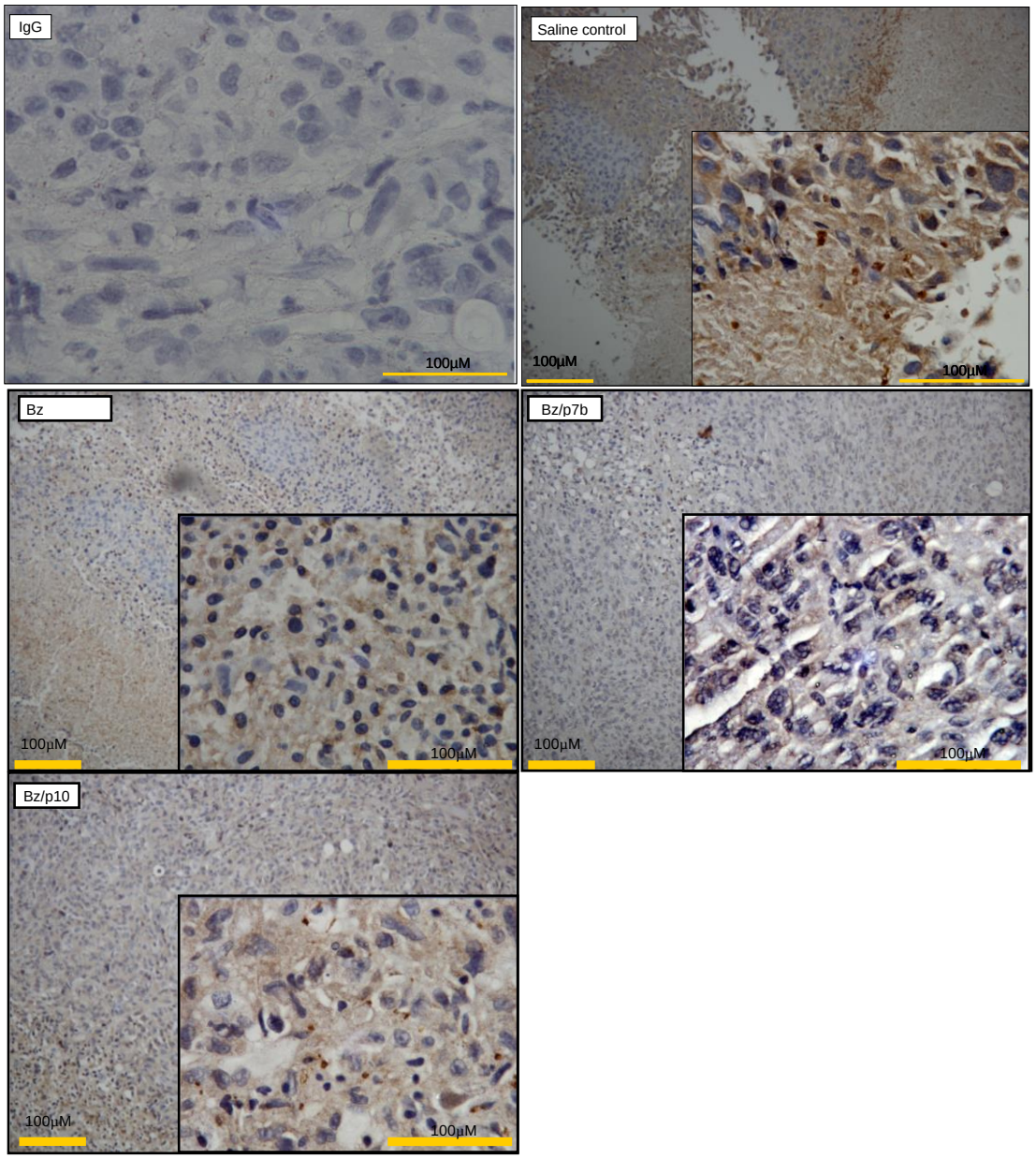

Figure 5.6 ***Expression of NP1 by MDA-MB-436 Breast Cancer Tumours:***
Representative images to that demonstrate the presence of Np1expression in the tumours. Np1 staining was observed in all the tumours from the different treatment groups but was much weaker compared to the other VEGF receptors. Images were taken at x10 (main panel) and x60 (insert panel) magnification to visualise the pattern of Np1 staining.

NB: It is important to note that Np1 staining was carried out using tumours taken at different experimental time-points, and therefore are not completely comparable.

NP2

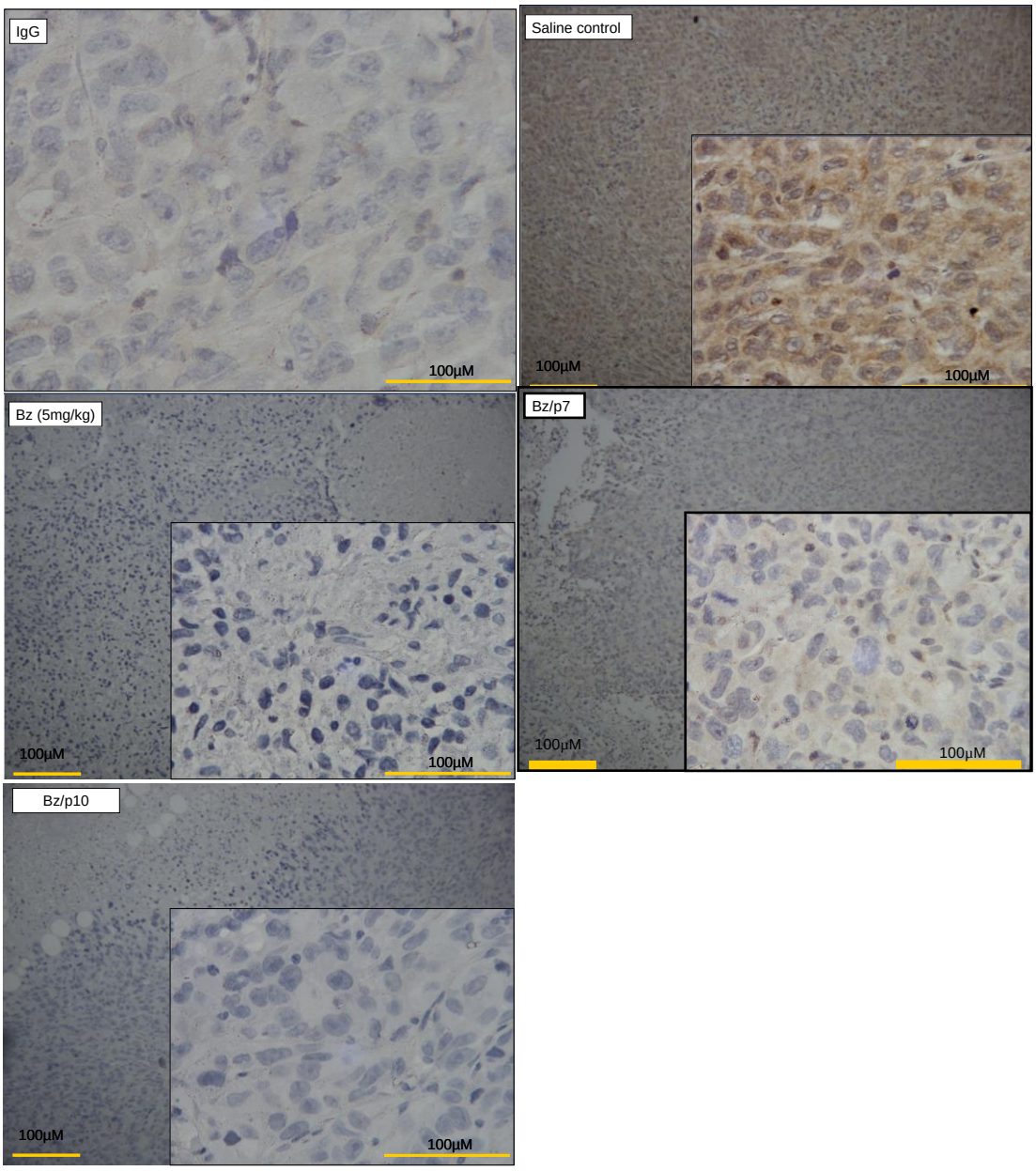

Figure 5.7 ***Expression of NP2 by MDA-MB-436 Breast Cancer Tumours:***
Representative images to that demonstrate the presence of Np2 expression in the tumours. Np2 staining was observed in the saline control tumours, with very little expression observed in the drug treatment groups. Over-all expression of Np2 was much weaker compared with the classical VEGF receptors. Images were taken at x10 (main panel) and x60 (insert panel) magnification to visualise the pattern of Np2 staining.

NB: It is important to note that Np2 staining was carried out using tumours taken at different experimental time-points, and therefore are not completely comparable.

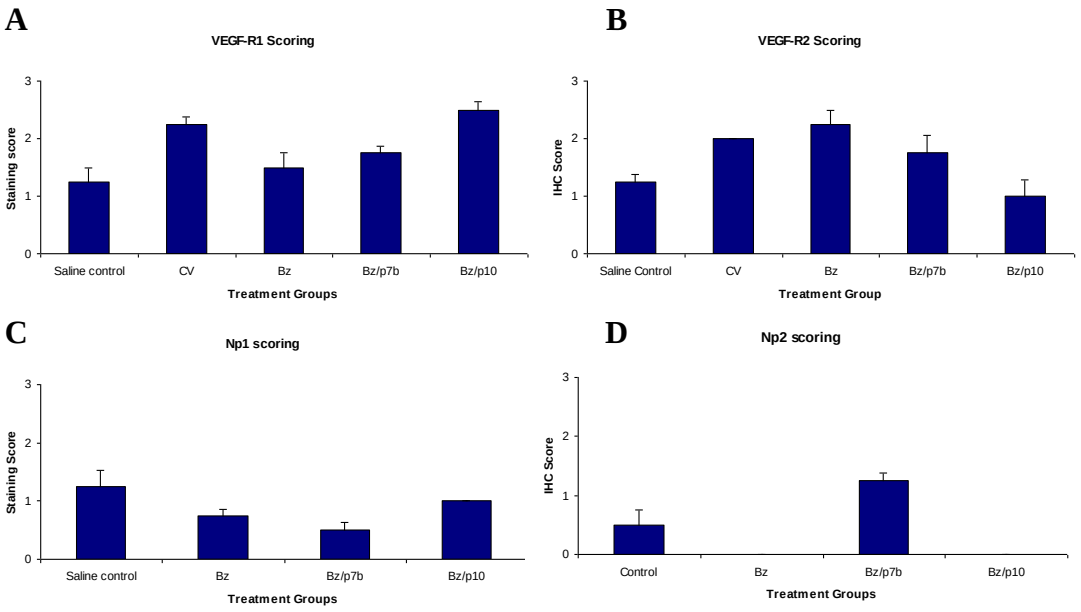

IHC Score:
0–1: no to weak staining;
1–2: weak to moderate staining
2–3: moderate to strong staining

Figure 5.8*IHC Scoring of VEGF Receptor in Treated Tumours:*
VEGF receptor IHC staining was scored by the intensity of staining observed within the tumour of the different treatment groups.

***NB: It is important to note that staining was carried out using tumours taken at different experimental time-points, and therefore are not completely comparable*.**

5.2.4 Breast Tumour Histology Evaluation

Following tumour histological analysis was carried out to investigate the mechanism of action of the various drug treatments. Due to the pharmacological action of the agents used, a number of markers were identified. Ki67 is a nuclear marker that detects cell proliferation. In addition, the use of an anti-human antibody allowed assessment of treatment effects on the breast cancer cells directly (**Figure 5.9**).

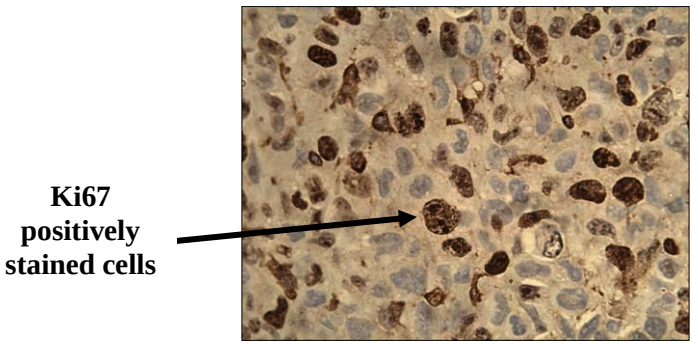

Figure 5.9 Nuclear staining of Ki67 positive breast cancer cells from a control tumour tissue fixed with formalin and wax embedded.

Caspase 3 is an important marker for measuring tumour apoptosis. Caspase 3 can be observed in both cytoplasmic and membranous locations, with the location of staining indicating the stage of apoptosis. The caspase 3 antibody reacts with both human and murine, therefore the direct effects on breast cancer cells as a result of different treatments could not be determined (**Figure 5.10**).

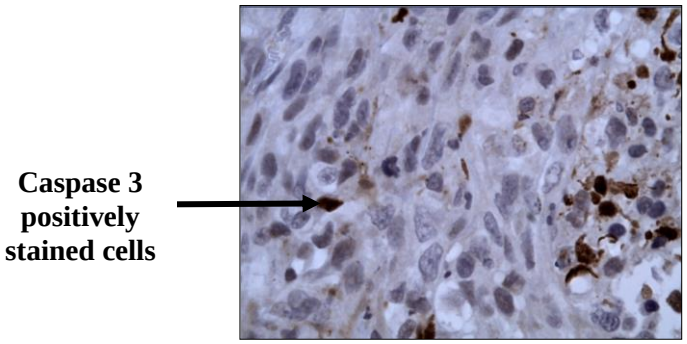

Figure 5.10 Cytoplasmic and membranous staining of Caspase 3 positive cells from a Bz treated breast xenograft tumour tissue fixed with formalin and wax embedded.

CD34, an endothelial marker is important for assessing the effects of anti-angiogenic agents such as Bz, as it identifies newly formed vessels and also haematopoietic progenitor cells (**Figure 5.11**).

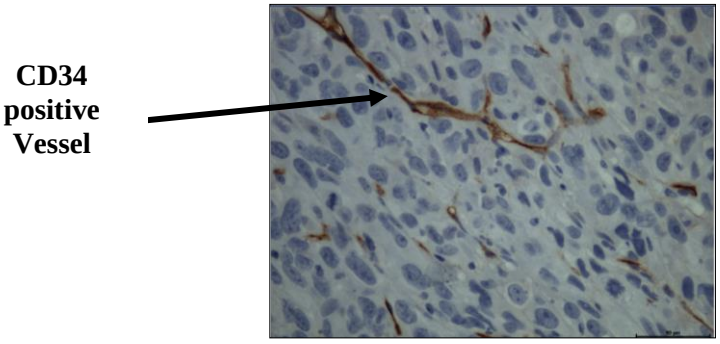

Figure 5.11 Positive CD34 vessels staining from a p10 treated breast xenograft tumour tissue fixed with formalin and wax embedded.

The tumours when resected at the end of the experiment demonstrated more than 60% necrosis in all experimental groups. However, no significant effects on tumour necrosis were observed when comparing tumours treated with Bz (5mg/kg), the CV or the saline control (mean±SEM; Bz (5mg/kg) and CV vs. saline control; 73±5% and 66±6% vs. 66±9%; n=3, ns (**Figure 5.12).** The number of proliferating breast cancer cells in the Bz treated tumours compared with saline control tumours, when measured as the number of Ki67 positive cells was not significantly (*P = 0.086*) different (mean±SEM; Bz 5mg./kg vs. saline control; 110±11 vs. 133±2; n=3, ns) (**Figure 5.13**). Treatment with CV significantly increased the number of proliferating tumour cells compared with the saline control (mean±SEM; CV vs. saline control; 160±8 vs. 133±2; n=3, *P = 0.030*) (**Figure 5.13**).

Bz significantly increased the number of apoptotic cells compared with tumours from the saline control group (mean±SEM; Bz vs. saline control; 33±2 vs. 21±1; n=3, *P = 0.008*) (**Figure 5.14**). A significant increase in caspase 3 positive cells was also observed in the CV treated tumours compared with the saline control group (mean±SEM; CV vs. saline control; 30±46 vs. 21±1; n=3, *P = 0.031*) (**Figure 5.14**).

Treatment with Bz (5mg/kg) resulted in a reduction in the number of CD34 positive vessels compared with the saline control group (±SEM; Bz vs. saline control; 9±3 vs. 19±7; n=3, ns), however this reduction did not reach statistical significance (*P = 0.311*) (**Figure 5.15**). Interestingly, the pattern of CD34 staining in the CV treated tumours differed to that observed with Bz treatment, whereby a mix of CD34 vessels were detected in addition to individual cells CD34 positive cells that were present in clusters (**Figure 5.15**).

A

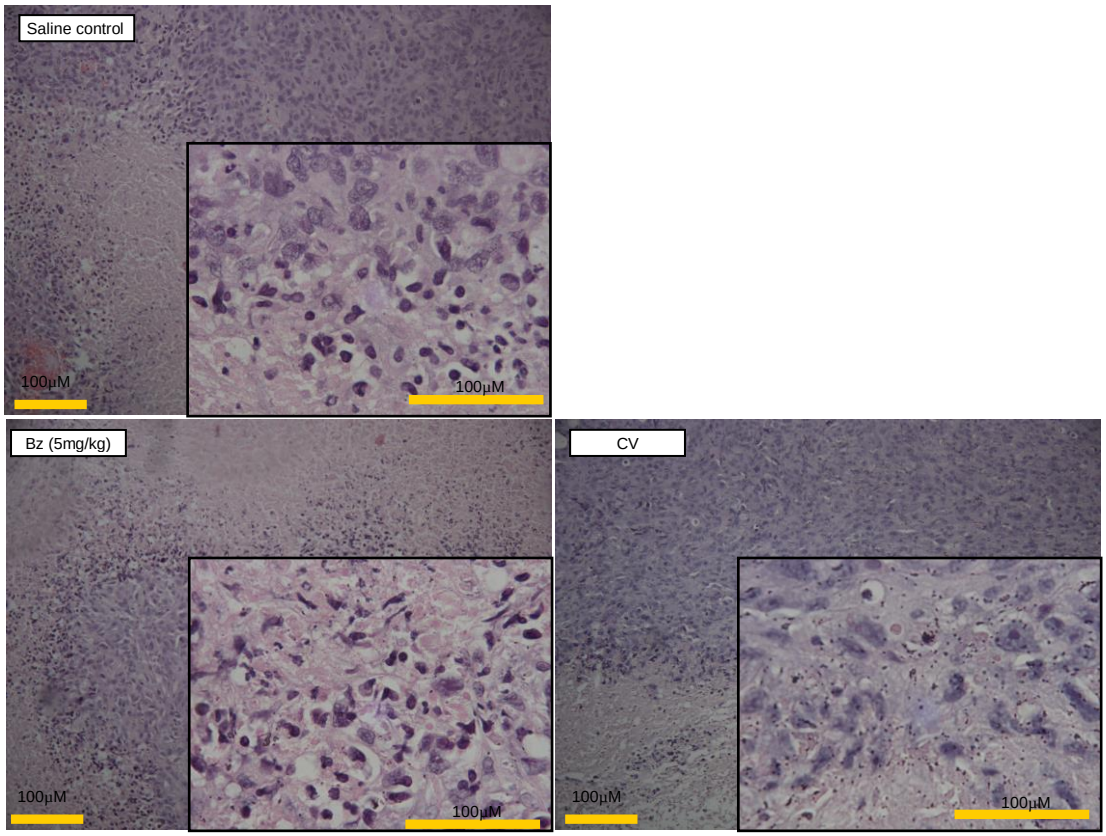

B

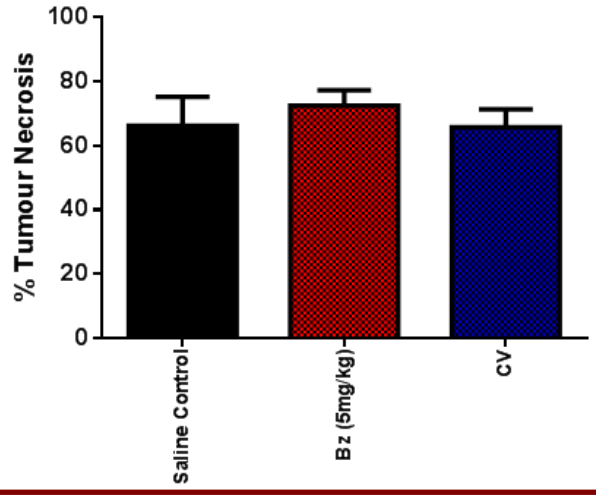

Figure 5.12 Effects of Bz and the CV on Tumour Necrosis:
(**A**) Representative images taken at x10 and x60 magnification, illustrate an area of necrosis within the MDA-MB-436 tumour tissue. (**B**) A high level of necrosis was present in the MDA-MB-436 tumours (~60%) and remained unchanged after treatment with both Bz (5mg/kg) and the CV.

Data is presented at mean±SEM (% tumour necrosis); n=3, NS. Statistical analysis was performed on using a t-test (Sigmaplot 11 software).

NB: It is important to note that analysis of tumour necrosis was carried out using tumours taken at different experimental time-points.

A

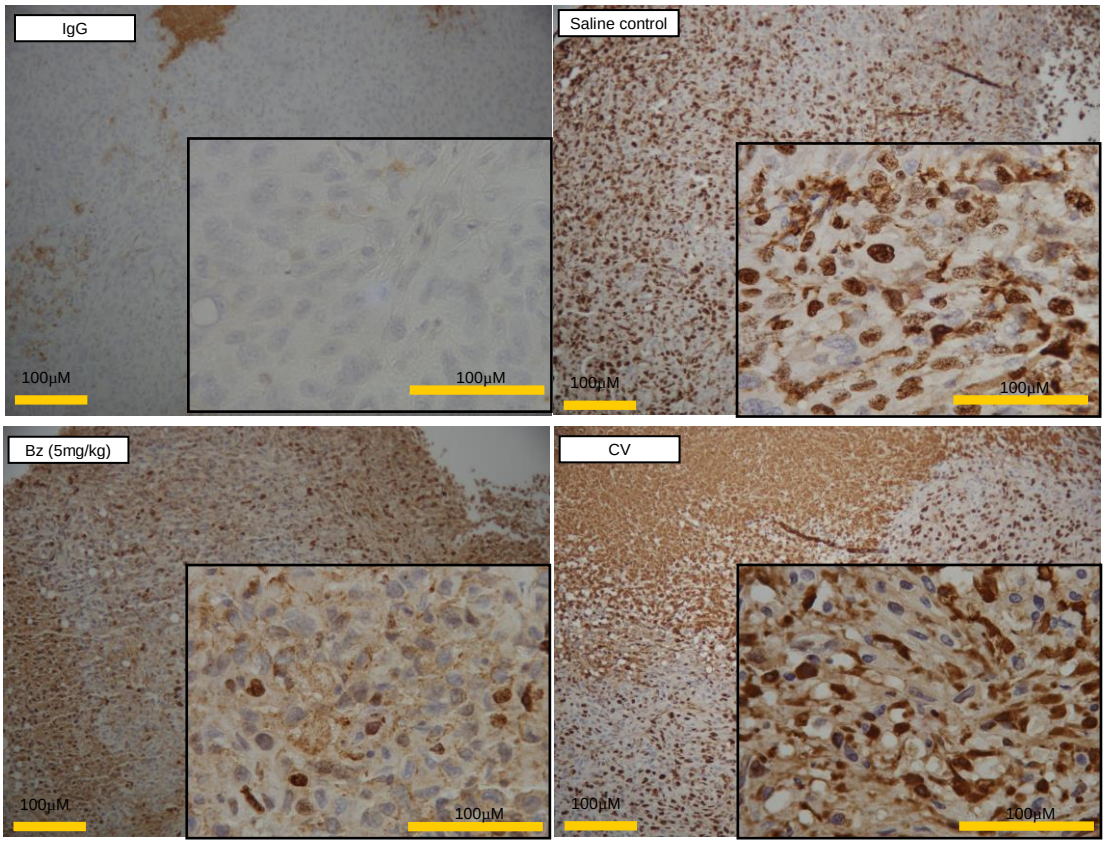

B

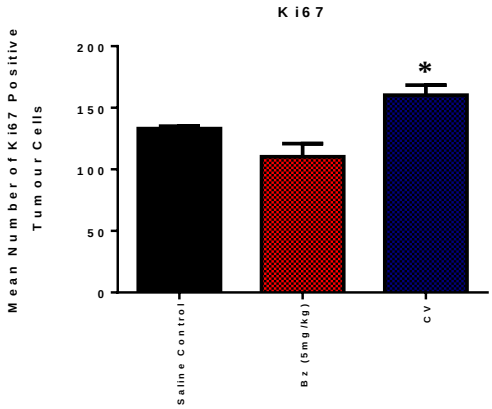

Figure 5.13 ***Effects of Bz and the Control Vehicle on Tumour Proliferation***
(A) Representative images taken at x 10 and x 60 magnification, illustrating Ki67 positive staining. (**B**) The level of breast cancer cell proliferation remained unchanged after treatment with Bz (5mg/kg) twice weekly (i.p.). In contrast, treatment with CV twice weekly (i.p.) significantly (*P = 0.030*) increased proliferation of the tumour cells.

Data is presented as mean±SEM (Ki67+ cells); n=3, p=0.030 w.r.t to saline control. Statistical analysis was performed using the One Way ANOVA, followed by the Holm-Sidak post hoc test (Sigmaplot 11 software).

NB: It is important to note that analysis of tumour necrosis was carried out using tumours taken at different experimental time-points.

A

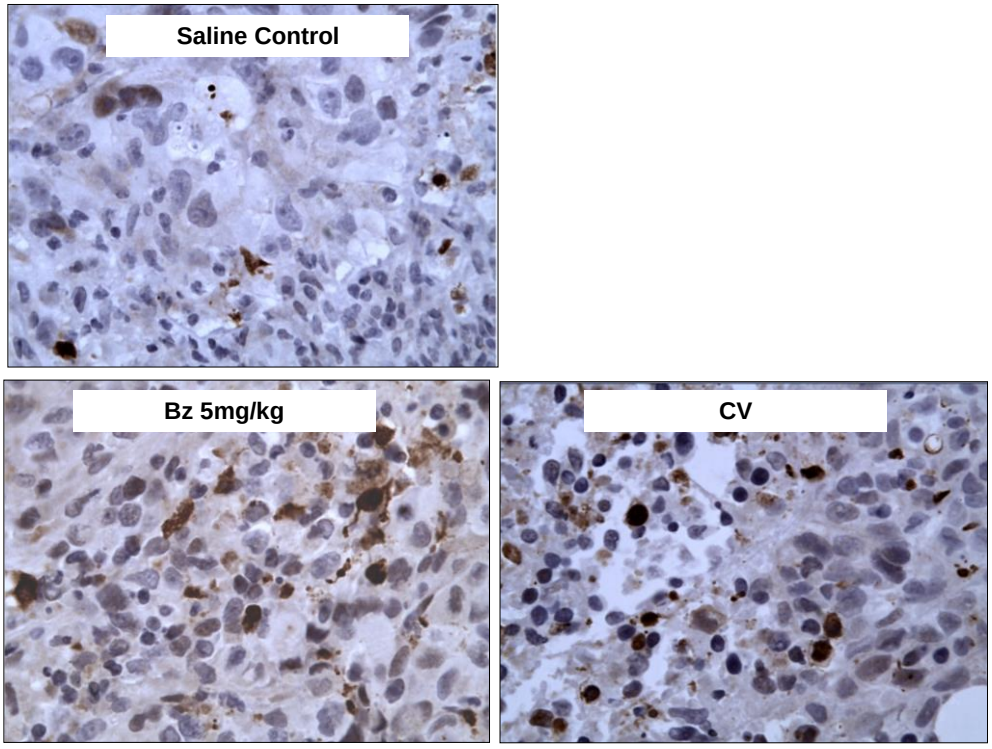

B

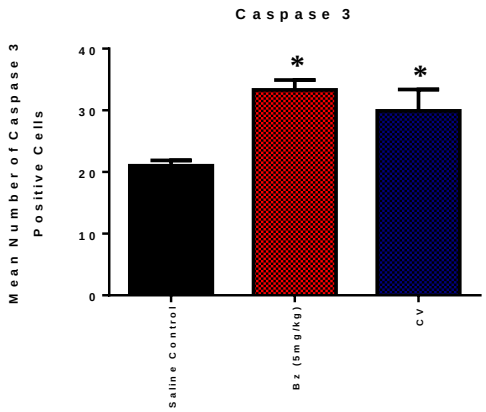

Figure 5.14 ***Effects of Bz and CV on Apoptosis:***
(A) Representative images of caspase 3 staining taken at x 10 and x 60 magnification. (**B**) Bz (5mg/kg) and CV significantly (*P = 0.008 and P = 0.031* respectively) increased the level of apoptosis within the tumour tissue compared with the saline control group.

Data is presented as mean±SEM (Caspase 3+ cells); n=3, p<0.05 w.r.t saline control. Statistical analysis was performed using the One Way ANOVA followed by the Holm-Sidak post hoc test (Sigmaplot 11 software).

NB: It is important to note that analysis of tumour necrosis was carried out using tumours taken at different experimental time-points.

A

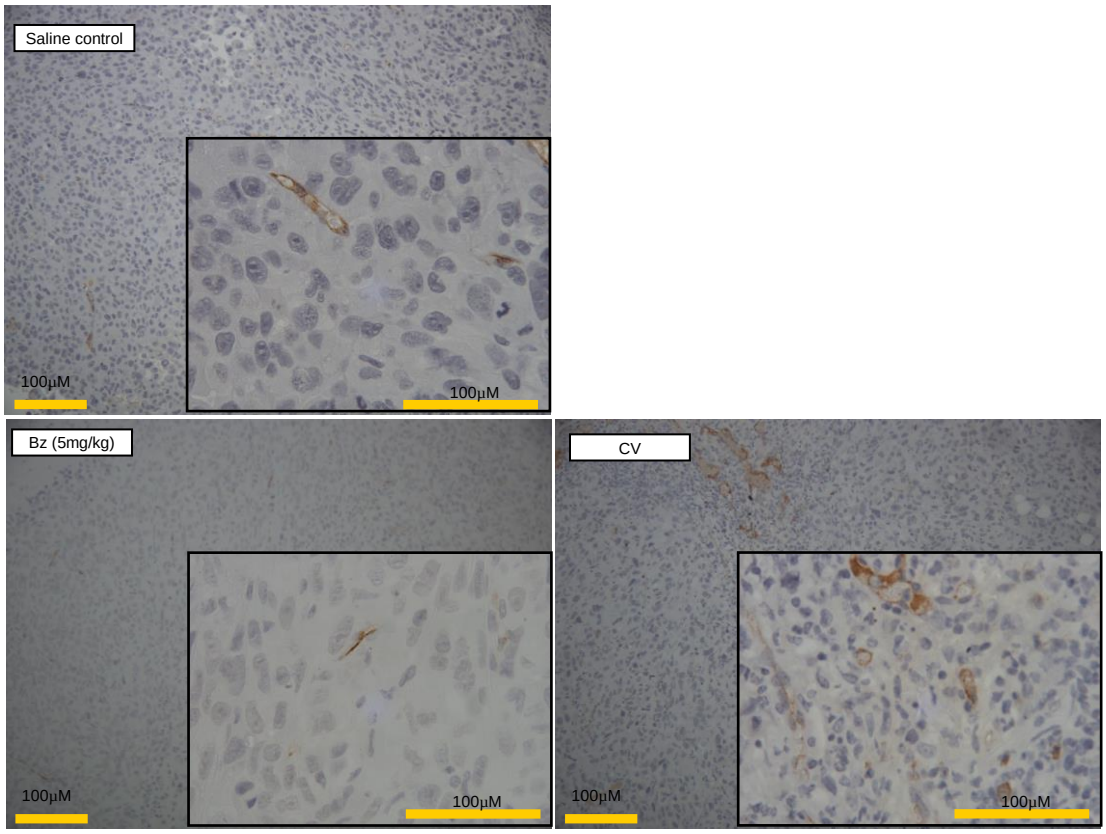

B

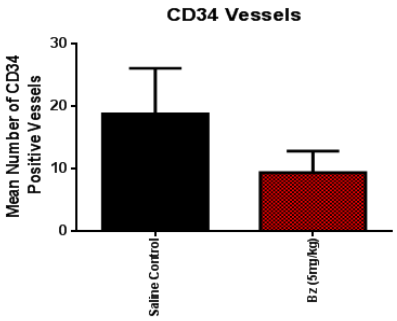

Figure 5.15 Effects of Bz and CV on CD34 Vessel Formation:
(**A**) Representative images of CD34 positive vessels taken at x 10 and x 60 magnification. (**B**) Bz (5mg/kg) reduced the formation of new vessels in the tumour tissue compared with the saline control; however this was not significant (***P 0.311***). As the CV treated tumours had a mix of CD34+ vessels and individual cells, comparing between groups was difficult.

Data is presented as mean±SEM (CD34+ vessels); n=3, NS. Statistical analysis was performed using a t-test (Sigmaplot 11 software).

NB: It is important to note that analysis of CD34 was carried out using tumours taken at different experimental time-points

5.2.5 Effects of the Np1 Peptides on Subcutaneous Breast Cancer Growth

Peptide 7b

Following tumour implantation, an equal number of animals were assigned to each treatment group (n=5/group). All five animals developed palpable tumours and were subsequently treated with two weekly injections of p7b (1μM). On day twenty-one post initial injection of p7b, two of the animals were culled due to tumour ulceration (with tumour volumes of 525mm^3 and 817mm^3) , with the remaining three continuing treatment until the end of experiment (day 31). However, as only 2 animals remained in the saline control group on day thirty-one, statistical analysis was performed on day twenty-one. At this time point p7b alone (n=5) had no inhibitory effects on tumour growth when compared with the saline (n=3) treated group (mean±SEM; p7b vs. saline control; 422±133mm^3 vs. 467±138mm^3; n=5/4, ns) (**Figure 5.16**).

Peptide 10

In the p10 treated group, four of the five animals implanted with MDA-MB-436 breast cancer cells developed palpable tumours and were treated with p10 (50μM) twice weekly via i.p injection. On day seventeen post initial injection of p10 alone, one animal was culled due to maximum tumour growth (1688mm^3) with the remaining three animals continuing treatment with p10 until the end of experiment (day 42). At the end of the experiment, treatment with p10 alone (n=3) reduced tumour growth compared with the saline (n=3) group (mean±SEM; p10 vs. saline control; 329±111mm^3 vs. 793±320mm^3; n=3, ns) (**Figure 5.17**), however this inhibition did not reach statistical significance (*P = 0.242*).

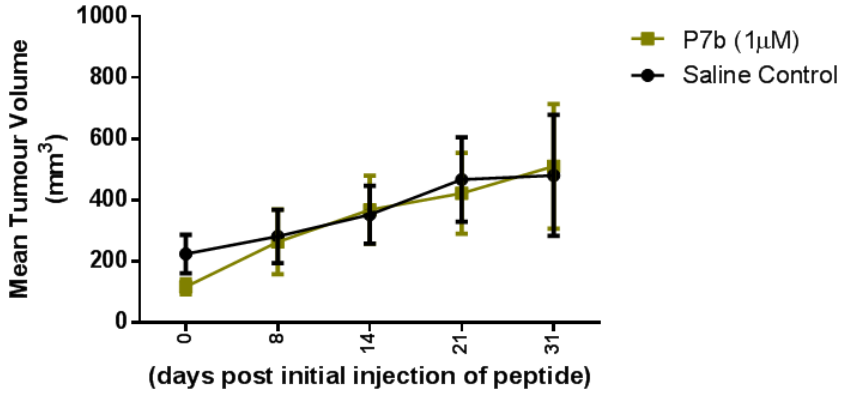

Figure 5.16 Effects of P7b MDA-MB-436 Breast Cancer Growth In Vivo:
Twice weekly injections with peptide 7b (1μM) alone (i.p.) displayed no inhibitory effects on MDA-MB-436 breast cancer growth *in vivo* compared with the saline control group when analysed at day 21. Data points for the saline group, post day 21 are representative of the two remaining animals in this treatment group.

Data is presented as mean±SEM tumour volume (mm^3); n=4/5, NS. Statistical analysis was performed on Day 21 using the One Way ANOVA

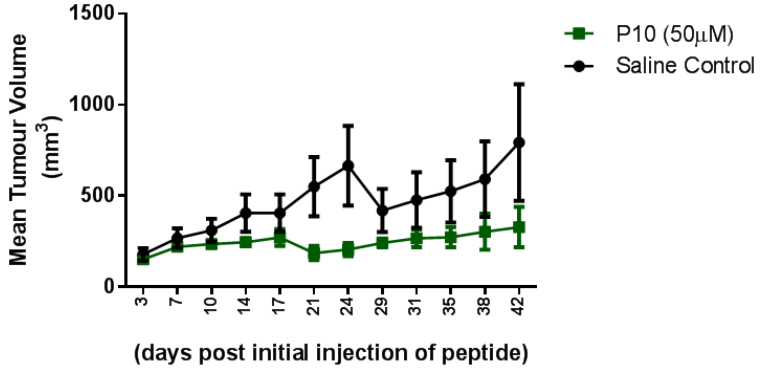

Figure 5.17 Effects of P10 on Breast Cancer Growth In Vivo:
Treatment with p10 (50μM) alone when administered twice weekly (i.p.) exerted no significant inhibitory effects on MDA-MB-436 breast cancer growth *in vivo* compared with the saline control when analysed at day 42.

Data is presented as mean±SEM tumour volume (mm^3); n=3, NS. Statistical analysis was performed on Day 42 using the One Way ANOVA (Sigmaplot 11 software).

Histology and Morphology

Similar to the Bz treated tumours, a high level of tumour necrosis was present in the p7b treated tumours. However, no significant (*P= 0.571)* difference was observed when compared with the saline treated tumours (mean±SEM; p7b vs. saline control; 72±3% vs. 65±11%; n=3, ns) (**Figure 5.18**). Treatment with p7b did not significantly (*P = 0.432*) effect the number of proliferating breast cancer cells compared with the saline control (mean±SEM; p7b vs. saline control; 48±18 vs. 31±7; n=3, ns) (**Figure 5.19**). Peptide 7b reduced the number of caspase 3 positive cells within the tumour compared with the saline control (mean±SEM; p7b vs. saline control; 8±4 vs. 16±0.4; n=3, ns) (**Figure 5.21**). However, this reduction did not reach statistical significance (*P= 0.127*). Interestingly, p7b alone treated tumours resulted in a different CD34 staining pattern then that observed with the other treatment groups. The staining pattern for p7b treated tumours displayed CD34 positive single cells rather then vessel structures, much like that observed with the CV treated tumours (**Figure 5.23**).

Treatment with p10 alone reduced tumour necrosis (mean±SEM; p10 vs. saline control; 45±9% vs. 66%±9%; n=3, ns) (**Figure 5.18**) however, this was not significant (*P = 0.160*). Breast cancer cell proliferation remained similar in p10 treated tumours compared with the saline control group (mean±SEM; p10 vs. saline control; 145±13 vs. 133±2; n=3, ns) (**Figure 5.20**). Similarly, no effect on apoptosis was observed after p10 treatment compared with the saline control group (mean±SEM; p10 vs. saline control; 18±4 vs. 21±1; n=3, ns) (**Figure 5.22**). The number of CD34 positive vessels remained the same after p10 treatment compared with the saline control (mean±SEM; p10 vs. saline control; 23±1 vs. 19±7; n=3, ns) (**Figure 5.24**).

A

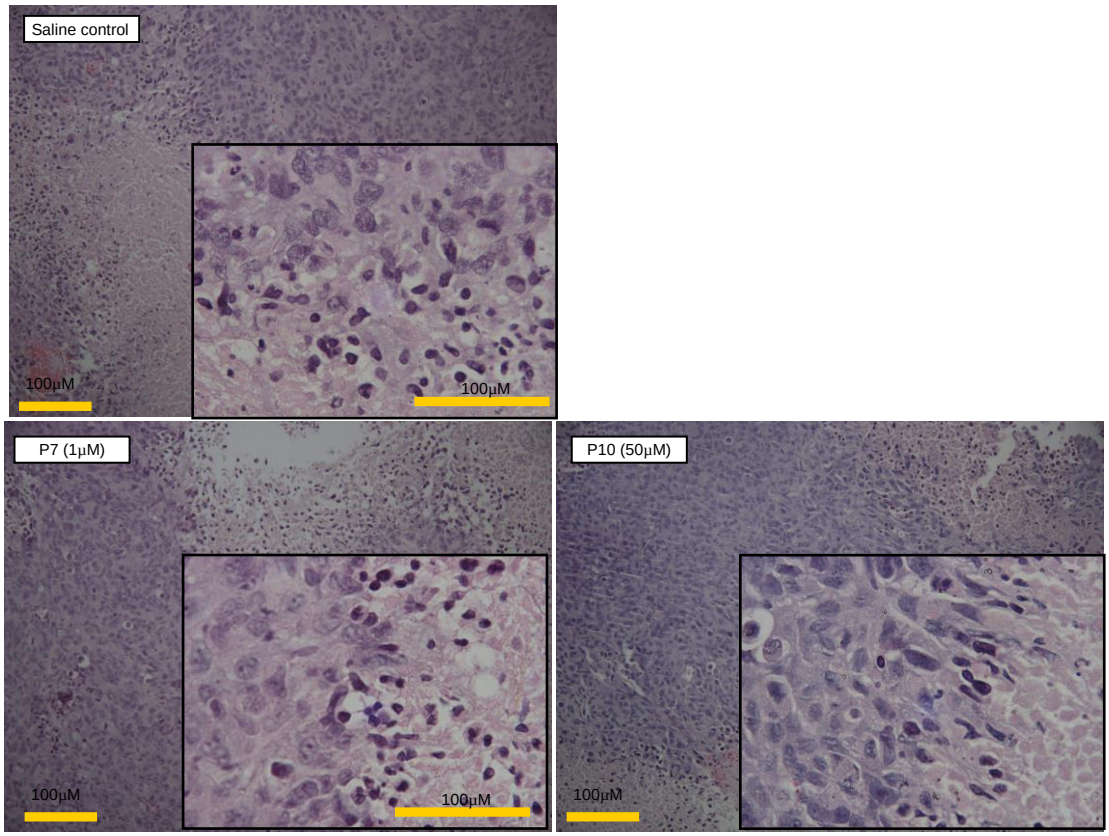

B

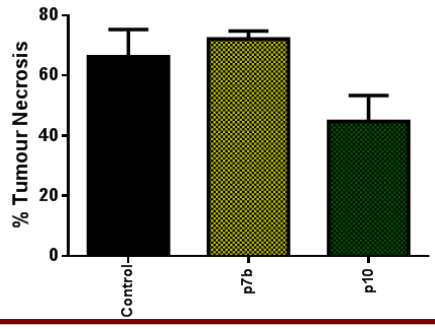

Figure 5.18 ***Effects of P7b and P10 on Tumour Necrosis*** (**A**) Representative image of an area of necrosis within the MDA-MB-436 tumour tissue taken at x10 (main panel) and x60 (insert panel) magnification (**B**) Treatment with p7b (1µM) did not alter the level of tumour necrosis present. Whereas, p10 (50µM) reduced the level of tumour necrosis within the tumour tissue, however this was not significant (NS) (*p=0.160*).

Data is represented as mean±SEM (% tumour necrosis); n=3, NS. Statistical analysis was performed using the One Way ANOVA (Sigmaplot 11 software).

NB: It is important to note that analysis of tumour necrosis was carried out using tumours taken at different experimental time-points

A

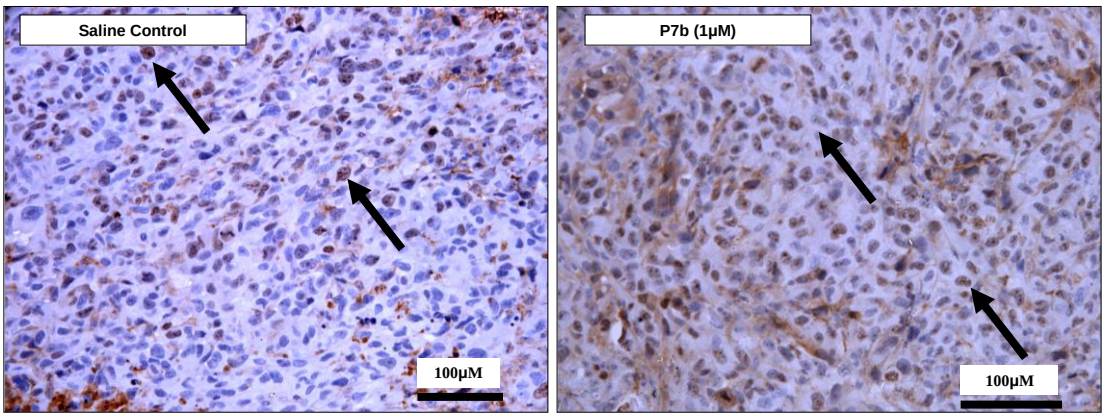

B

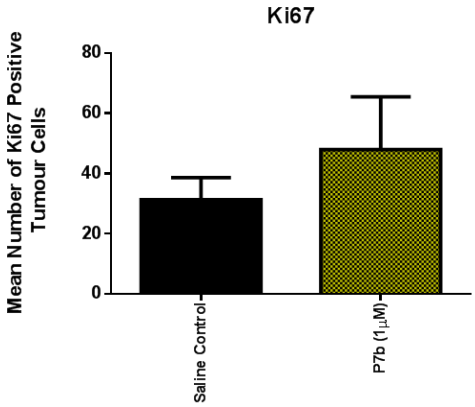

Figure 5.19 ***Effects of P7b on Tumour Cell Proliferation In Vivo***
(**A**)Representative images of Ki67 staining taken at X40 magnification (**B**) Treatment with two weekly injections (i.p.) of p7b (1µM) did not significantly affect the level of breast cancer proliferation occurring within the tumour tissue compared with the saline control

Data is presented as mean±SEM (Ki67 positive cells); n=3, NS. Statistical analysis was performed using the One Way ANOVA (Sigmaplot 11 software).

NB: It is important to note that analysis of Ki67 staining was carried out using tumours taken at different experimental time-points

A

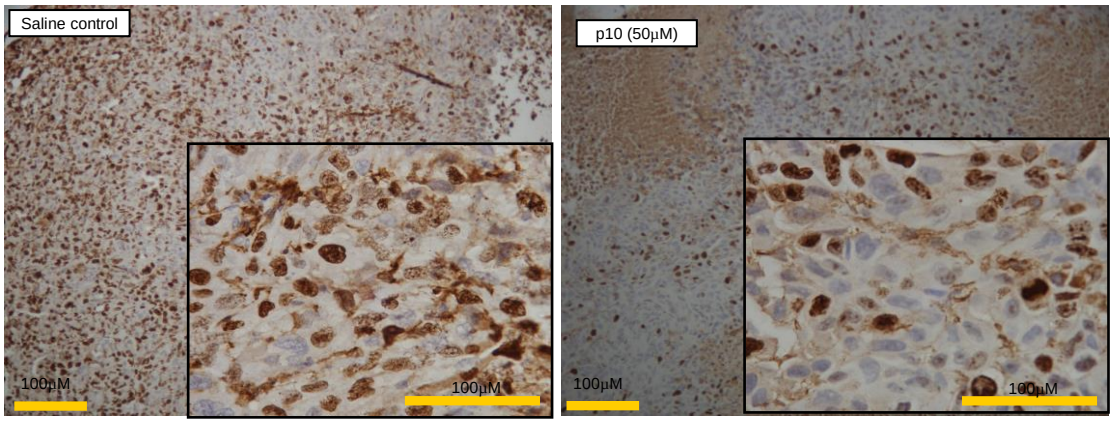

B

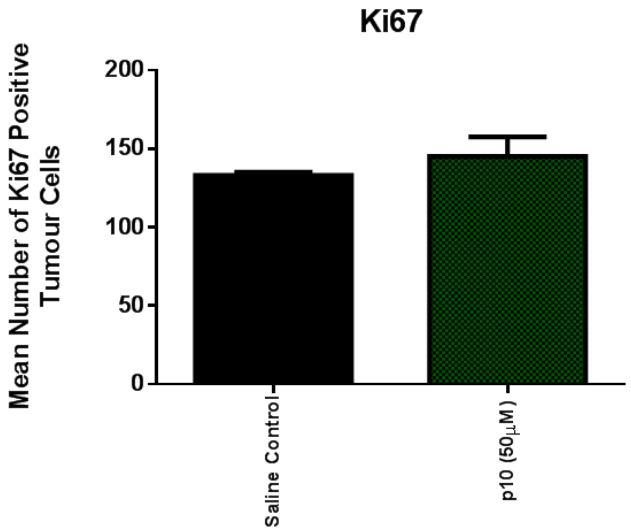

Figure 5.20*Effects of P10 on Tumour Cell Proliferation In Vivo:*
(**A**) Representative images of Ki67 staining taken at x40 magnification (**B**) Treatment with two weekly injections (i.p.) of p10 (50µM) did not alter the level of breast cancer proliferation occurring within the tumour tissue compared with the saline control.

Data is presented at mean±SEM (Ki67 positive cells); n=3, NS. Statistical analysis was performed using the Kruskal Wallis One Way ANOVA on Ranks (Sigmaplot 11 software).

NB: It is important to note that analysis of Ki67 staining was carried out using tumours taken at different experimental time-points

A

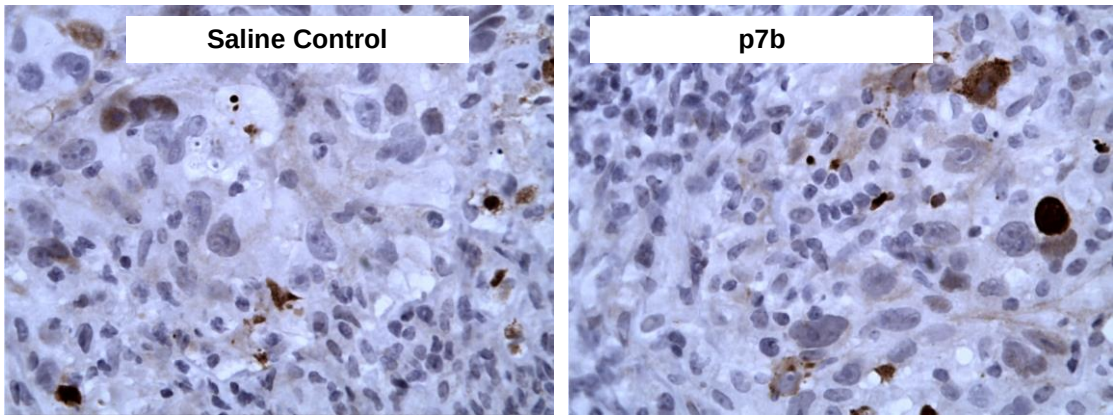

B

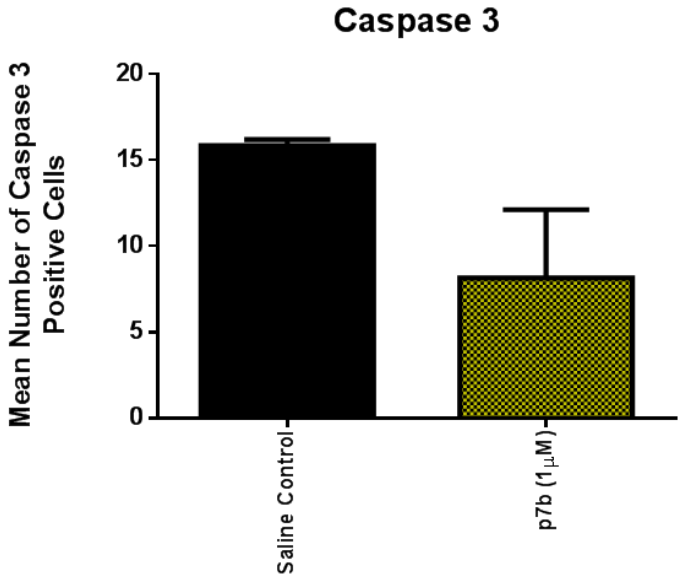

Figure 5.21 ***Effects of P7b on Tumour Apoptosis***
(**A**) Representative images of Caspase 3staining taken at x40 magnification (**B**) Treatment with p7b twice weekly (i.p.) demonstrated no significant effects on the level of apoptosis occurring in the tumour tissue

Data is presented as mean±SEM (Caspase 3+ cells); n=3, NS. Statistical analysis was performed using the One Way ANOVA (Sigmaplot 11 software).

NB: It is important to note that analysis of tumour apoptosis was carried out using tumours taken at different experimental time-points

A

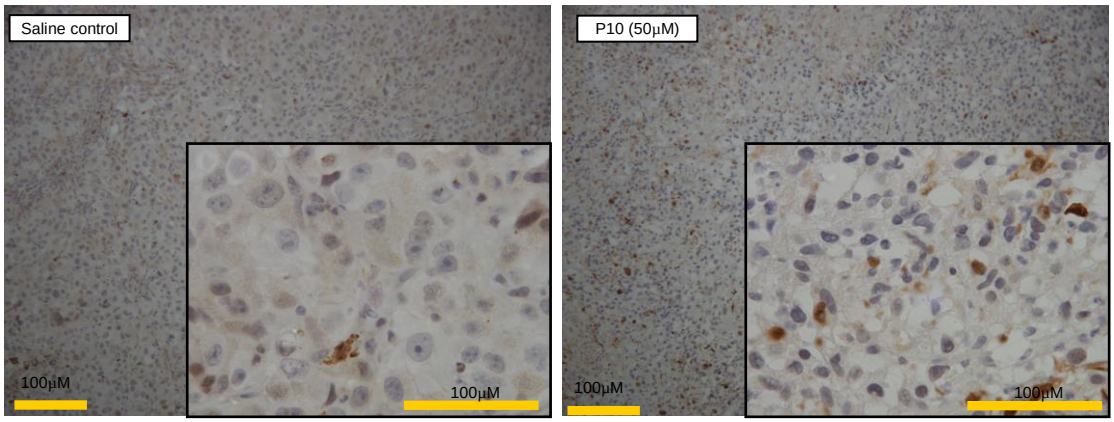

B

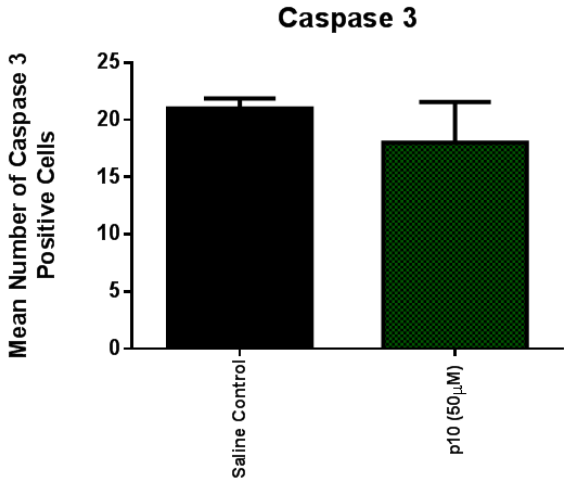

Figure 5.22 ***Effects of P10 on Tumour Apoptosis***
(**A**) Representative images of Caspase 3staining taken at x10 (main panel) and x60 (insert) magnification (**B**) Treatment with p10 twice weekly (i.p.) demonstrated no significant effects on the level of apoptosis occurring in the tumour tissue

Data is presented as mean±SEM (Caspase 3+ cells); n=3, NS. Statistical analysis was performed using the One Way ANOVA (Sigmaplot 11 software).

NB: It is important to note that analysis of tumour apoptosis was carried out using tumours taken at different experimental time-points

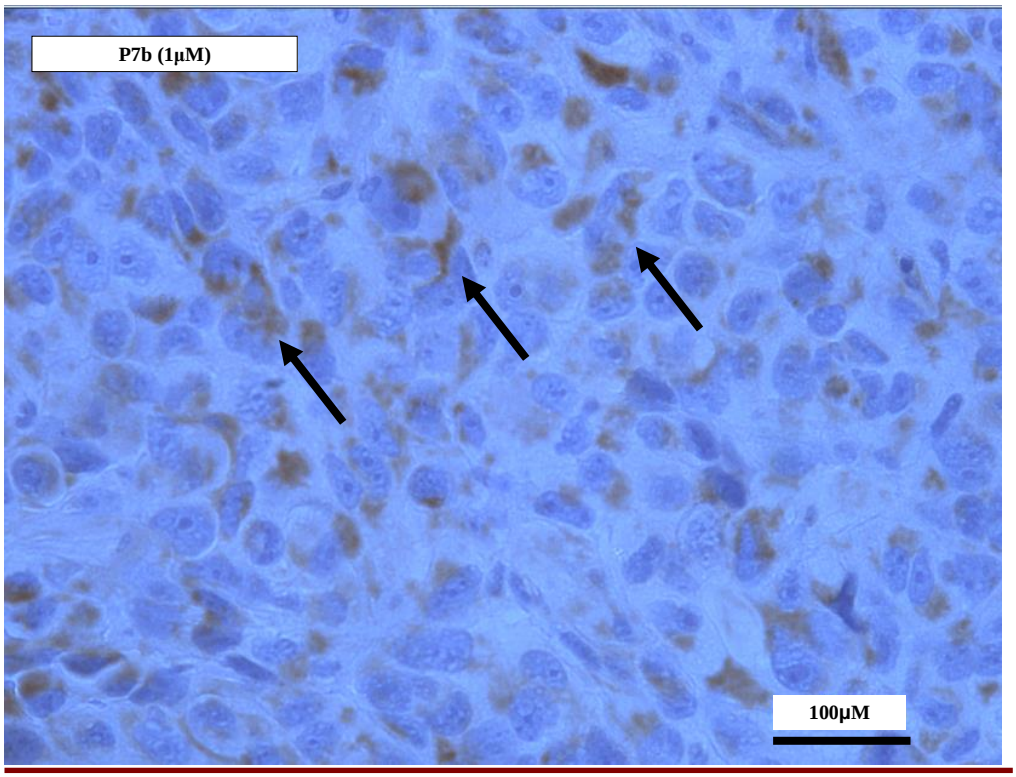

Figure 5.23 ***Effects of P7b on Micro-Vessel Density***
(***A***) Representative images of CD34 staining taken at x magnification (**B**) Treatment with two weekly (i.p.) injections of p7b (1µM) demonstrates an uncharacteristic staining pattern for CD34; rather than vessel, CD34 positive cells were present in clusters in the tumour tissue.

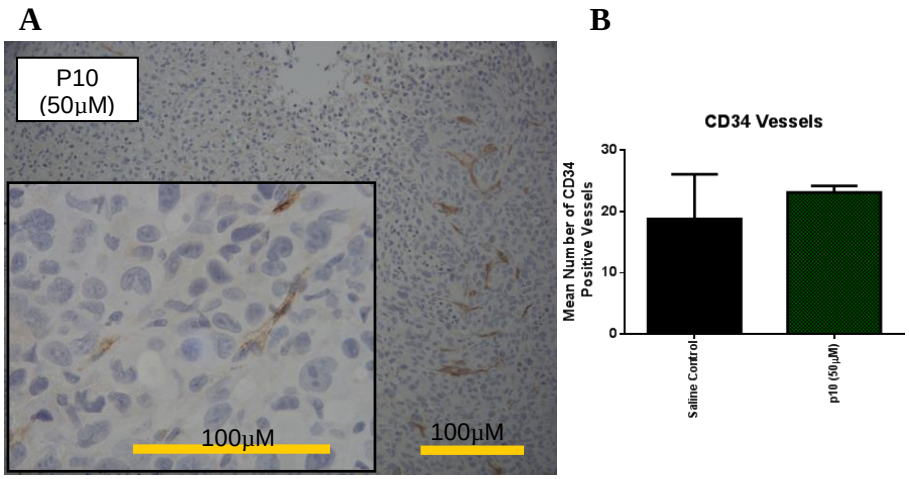

Figure 5.24 ***Effects of P10 on Micro-Vessel Density***
(***A***) Representative images of CD34 staining taken at x 60 magnification (**B**) Treatment with two weekly (i.p.) injections of p10 (50µM) demonstrates an uncharacteristic staining pattern for CD34; rather than vessel, CD34 positive cells were present in clusters in the tumour tissue.

Data is presented at mean±SEM (CD34 positive vessels); n=3, NS. Statistical analysis was performed using the Kruskal Wallis One Way ANOVA on Ranks (Sigmaplot 11 software).

NB: It is important to note that analysis of tumour apoptosis was carried out using tumours taken at different experimental time-points

5.2.6 Combined Effects of the Np1 Peptides with Bz on Breast Cancer Growth *In Vivo*

Bz/ p7b

Following tumour implantation of MDA-MB-436 ($1x10^6$ cells), an equal number of animals were assigned to each treatment group (n=5/group). In the Bz/p7b combination group all five animals developed palpable tumours and were subsequently treated with Bz (5mg/kg) and p7b (1μM) twice weekly via i.p. injection with Bz being administered 1 hour prior to p7b injection. Ten days post initial administration of Bz/p7b one animal was culled due to tumour ulceration (239.1mm^3) with the remaining four animals continuing treatment with Bz/p7b until the end of the experiment (day 42). At the end of the experiment combining p7b with Bz (n=4) reduced MDA-MB-436 tumour growth *in vivo* compared with the saline control group (mean±SEM; Bz/p7b vs saline control; 227±61mm^3 vs. 726±313mm^3) however this inhibition did not reach statistical significance (*p=0.229*), due to the wide variation in the treatment group. However, the combination of p7b with Bz (n=4) exerted no additive inhibitory effects on tumour growth when compared with Bz alone (n=2) treated group (mean±SEM; Bz/p7b vs. Bz; 227±61mm^3 vs. 184±0mm^3) (**Figure 5.25**). As only n=2 remained in the Bz treatment group at the end of the experiment, an earlier time point at day seventeen post initial injection of Bz, was used to carry out statistical analysis. At this time point combining p7b with Bz (n=4) displayed no significant additive effects on tumour growth *in vivo* when compared with the Bz alone (n=3) group (mean±SEM; Bz/p7b vs. Bz 189±66mm^3 vs. 164±47mm^3).

Bz/ p10

In the Bz/p10 combination group, all five animals that underwent tumour implantation developed palpable tumours and were treated with Bz (5mg/kg) and p10 (50μM) twice weekly via i.p injection. Bz was administered 1 hour prior to p10 injection. All five animals continued to receive Bz/p10 treatment until the end of the experiment (day 42), with treatment resulting in a reduction in tumour growth *in vivo* compared with the saline (n=3) treated group (mean±SEM; Bz/p10 vs. saline control; 299±70mm^3 vs. 726±313mm^3) (**Figure 5.26**). However, this reduction did not reach statistical significance (*p=0.393*), again due to wide variation in the control treatment group. The combination displayed no additive inhibitory effects on tumour growth when compared with the Bz alone (n=2) group (mean±SEM; Bz/p10 vs. Bz; 299±70mm^3 vs. 184±0mm^3) (**Figure 5.26**). Again, statistical analysis was carried out on day seventeen post initial injection when comparing the effects of Bz alone versus Bz/p10 as at day forty-two, only n=2 remained in the Bz group. At day seventeen, Bz/p10 (n=5) resulted in a reduction in efficacy in inhibiting tumour growth *in*

vivo compared with the Bz (n=3) alone group (mean±SEM; Bz/p10 vs. Bz; 320±69mm^3 vs. 164±47mm^3; n=5/3, NS) (**Figure 5.26**) however this reduction did not reach statistical significance (*p=0.704*).

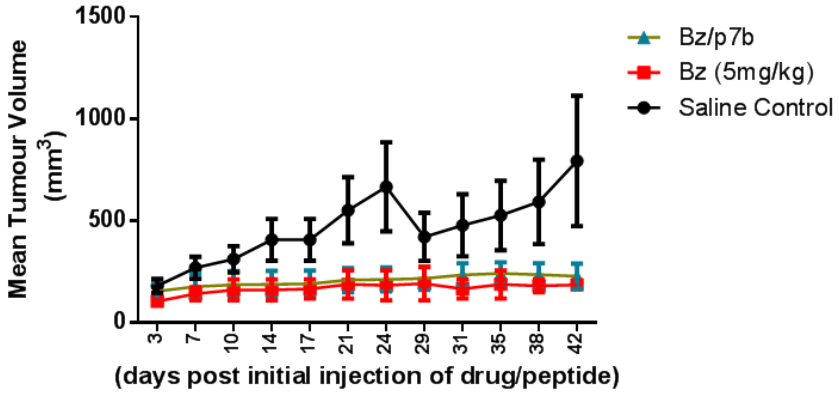

Figure 5.25 ***Effects of Combining Bz with P7b MDA-MB-436 Breast Cancer In Vivo.***
Combined treatment of Bz (5mg/kg) with p7b (1µM) twice weekly (i.p.) displayed no additive effects on tumour growth *in vivo* compared to the Bz (5mg/kg) alone treated group. In the combination group, p7b was administered 1 hour after Bz injection.

Data is presented as mean±SEM tumour volume (mm^3); n=3-5, NS. Statistical analysis was performed on day 17 using the One Way ANOVA (Sigmaplot 11 software).

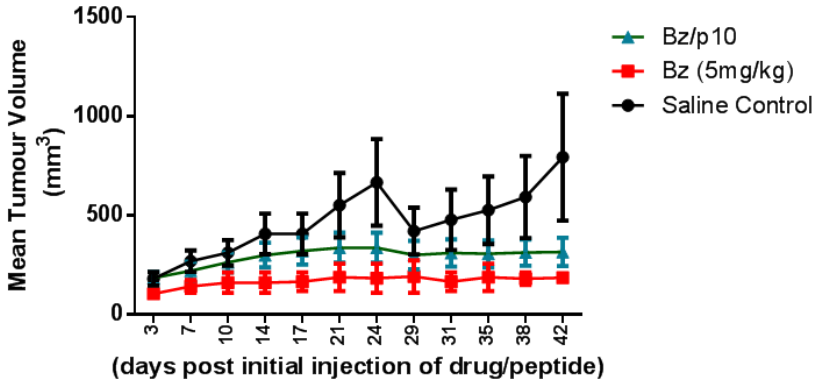

Figure 5.26 ***Effects of Combining Bz with P10 MDA-MB-436 Breast Cancer In Vivo.***
Combined treatment of Bz (5mg/kg) with p10 (50µM) twice weekly (i.p.) displayed no additive effects on tumour growth *in vivo* compared to the Bz (5mg/kg) alone treated group. In the combination group, p10 was administered 1 hour after Bz injection.

Data is presented as mean±SEM tumour volume (mm^3); n=, NS. Statistical analysis was performed on day 17 using the One Way ANOVA (Sigmaplot 11 software).

Histology
Bz/p7b

Treatment with a combination of Bz/7b resulted in high level of tumour necrosis, however no additive effects were observed on the level of necrosis when compared with the Bz alone treated tumours (mean±SEM; Bz/p7b vs. Bz; 71±16 vs. 72±5%; n=3, ns) (**Figure 5.27**). Combined Bz with p7b significantly inhibited the number of Ki67 positive proliferating breast cancer cells compared with the saline control (mean±SEM; Bz/p7b vs. saline control; 101±10 vs. 133±2; n=3, *p=0.031*) (**Figure 5.28**). However, the inhibitory effect observed with Bz/p7b exerted no significant (p=0.544) additive effect when compared with Bz alone treated tumours (mean±SEM; Bz/p7b vs. Bz (5mg/kg); 101±10 vs. 110±11; n=3, ns). Treatment with Bz/p7b resulted in an increase in apoptotic activity compared with the saline control group (mean±SEM; Bz/p7b vs. saline control; 32±6 vs. 21±1; n=3, ns) when measured as the number of Caspase 3 positive cells (**Figure 5.29**) however this increase did not reach statistical significance (*p=0.132*). In addition, treatment with Bz/p7b displayed no additive effects on apoptotic activity compared with the Bz alone treated tumours (mean±SEM; Bz/p7b vs. Bz (5mg/kg; 32±6 vs. 33±2; n=3, ns). Combining Bz with p7b resulted in a decrease in the number of CD34 positive vessels compared with the saline treated tumours (mean±SEM; Bz/p7b vs. saline control; 8±3 vs. 19±7; n=3, ns) (**Figure 5.30**) however this did not reach significance (p=0.262). Additionally, treatment with Bz/p7b did not exert an additive inhibitory effect on vessel formation, when compared with the Bz alone treated tumours (mean±SEM; Bz/p7b vs. Bz (5mg/kg); 8±3 vs. 9±3; n=3, ns) (**Figure 5.30**).

Bz/p10

Combining Bz with p10 reduced the levels of tumour necrosis compared with the Bz alone, treated tumours (66.7±4.5% vs. 72.5±4.8% respectively) (**Figure 5.27**) however this did not reach statistical significance (p=0.432). Combining p10 with Bz displayed no significant (p=0.238) effects on tumour breast cancer proliferation compared with the saline control (mean±SEM; Bz/p10 vs. saline control; 125±5 vs. 133±2; n=3, NS) when measured as the mean number of Ki67 positive cells (**Figure 5.28**). In addition there were no additive effects on breast cancer proliferation when Bz was combined with p10 compared with Bz alone (mean±SEM; Bz/p10 vs. Bz (5mg/kg); 125±5 vs. 110±11; n=3, NS). Combination treatment of p10/Bz displayed no further apoptotic effects compared with the saline control (mean±SEM; Bz/p10 vs. saline control; 21±2 vs. 21±1; n=3, NS) (**Figure 5.29**). However, combining p10 with Bz caused a significant loss in the apoptotic activity observed with Bz

alone (mean±SEM; Bz/p10 vs. Bz (5mg/kg); 21±2 vs. 33±2; n=3, p=0.008) (**Figure 5.29**). Combining p10 with Bz resulted in abnormal vessel formation (**Figure 5.31**).

A

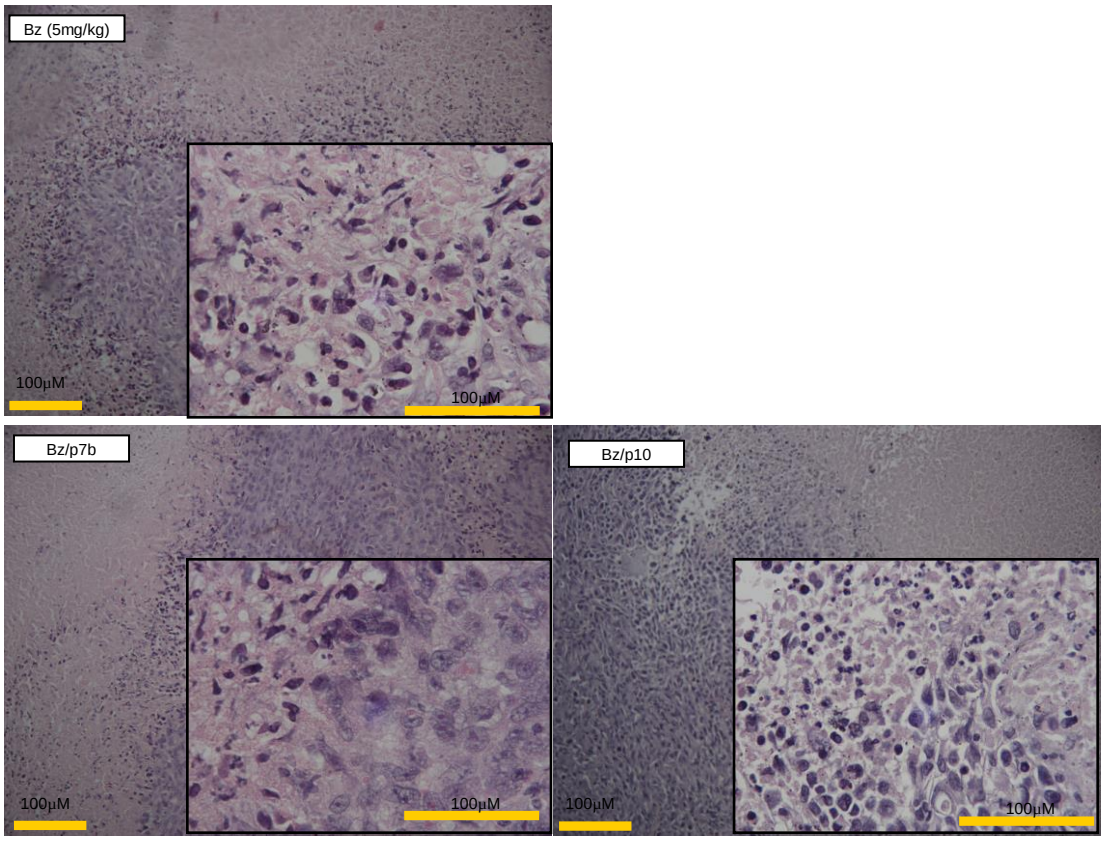

B

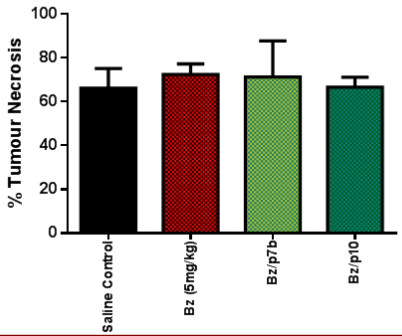

Figure 5.27 ***Effects of Combining Bz with P7b and P10 on Tumour Necrosis***
(**A**)Representative images taken at x10 (main panels) and x60 (insert) magnification, of necrotic areas within the MDA-MB-436 tumour tissue. (**B**) No effects on tumour necrosis were observed with any of the treatment**.**

Data is presented as mean±SEM (% tumour necrosis); n=3, NS.
Statistical analysis was performed using the One Way ANOVA (Sigmaplot 11 software).

NB: It is important to note that analysis of tumour necrosis was carried out using tumours taken at different experimental time-points

A

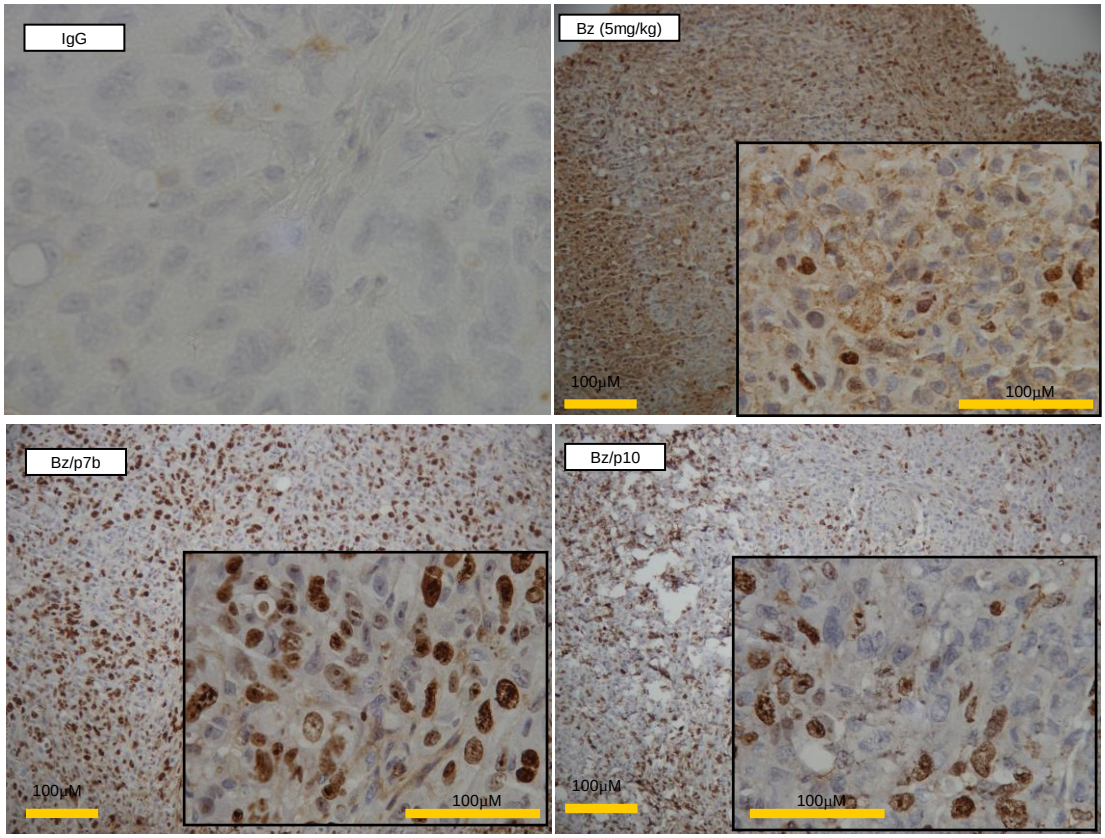

B

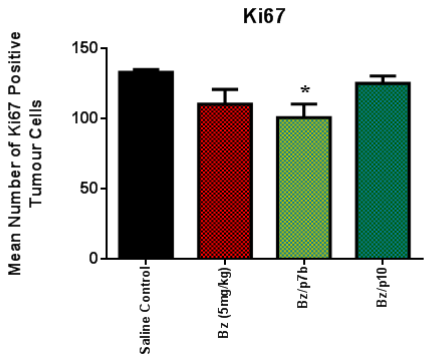

Figure 5.28 ***Effects of Combining Bz with P7b and P10 on Tumour Cell Proliferation In Vivo***
(**A**)Representative images of Ki67staining taken at x10 (main panel) and x60 (insert) magnification (**B**) Combined treatment with Bz/p7b twice weekly (i.p.) significantly inhibited the level of breast cancer proliferation occurring within the tumour compared to the saline control. However, no additive effects on tumour proliferation in either Bz/p7b or Bz/p10 combined group compared to Bz alone (5mg/kg).

Data is presented as mean±SEM; n=3, p=0.031 w.r.t the saline control. Statistical analysis was performed using the One Way ANOVA followed by Holm-Sidak post-hoc test (Sigmaplot 11 software). NB: It is important to note that analysis of tumour necrosis was carried out using

A

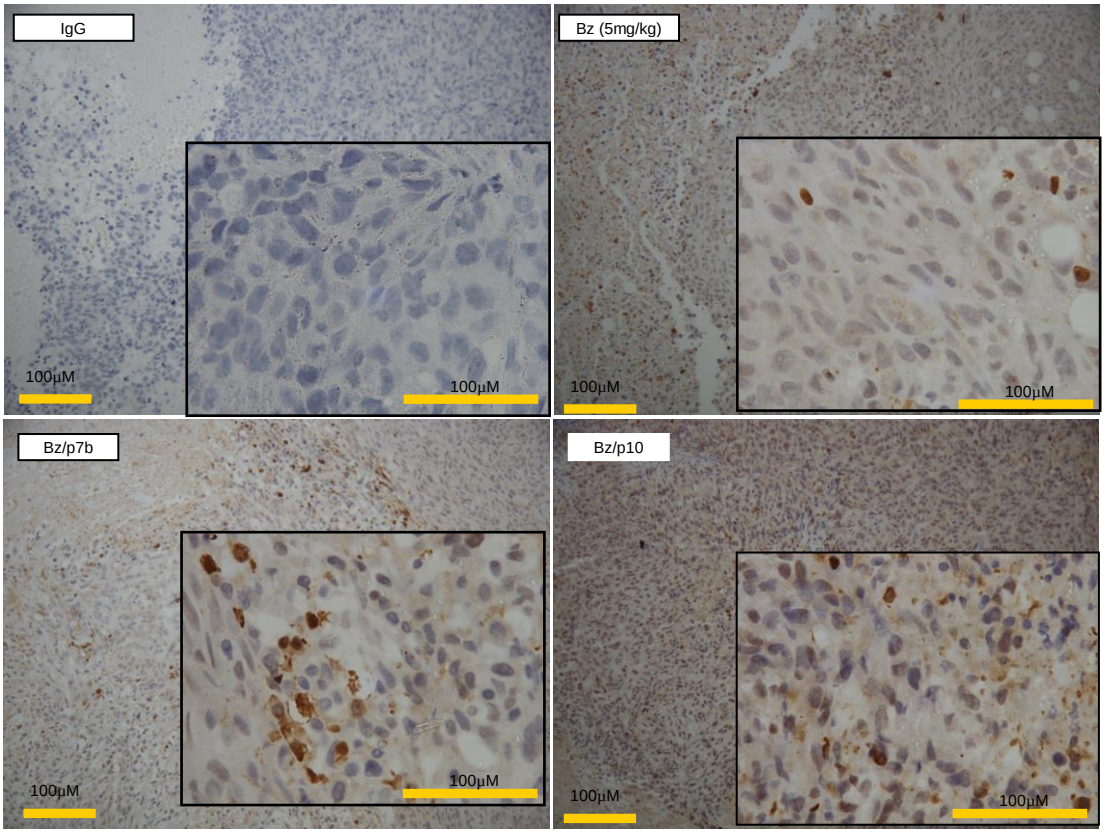

B

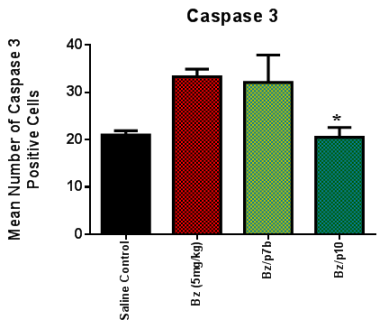

Figure 5.29 ***Effects of Combining Bz with P7b and P10 on Tumour Apoptosis***
(**A**)Representative images of Caspase 3 staining taken at x10 (main panel) and x60 (insert) magnification (**B**) Combining Bz with p10 caused a significant decrease in apoptotic activity associated with Bz (5mg/kg) alone.

Data is presented as mean±SEM (Caspase 3+ cells); n=3, p=0.008.
Statistical analysis was performed using (Sigmaplot 11 software).
NB: It is important to note that analysis of tumour necrosis was carried out using tumours taken at different experimental time-points

A

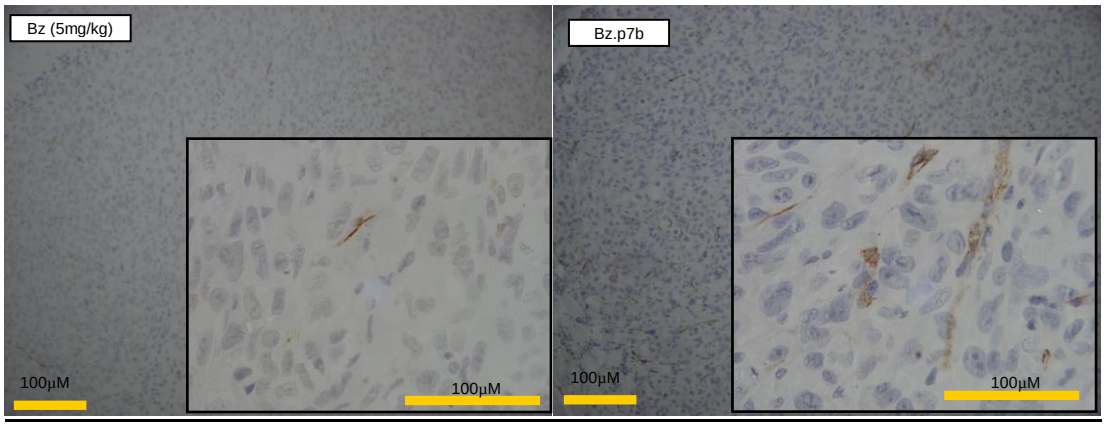

B

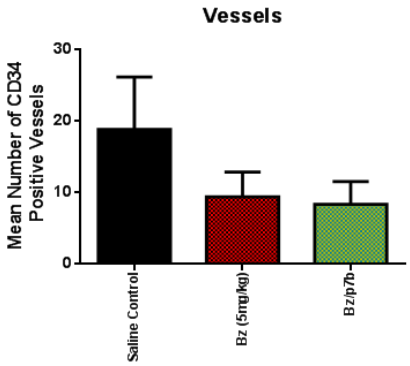

Figure 5.30 ***Effects of Combining Bz with P7b on CD34 Vessel Formation***
(**A**)Representative images taken at x10 (main panel) and x60 (insert) magnification of CD34positive vessels (**B**) No additive effects were observed on inhibiting CD34 positive vessel formation after combined treatment of Bz/p7b (5mg/kg and 1µM) twice weekly (i.p.) compared to Bz alone (5mg/kg) twice weekly (i.p.)

Data is presented as mean±SEM (CD34+ vessels); n=3, NS. Statistical analysis was performed using the One Way ANOVA (Sigmaplot 11 software).

NB: It is important to note that analysis of tumour necrosis was carried out using tumours taken at different experimental time-points

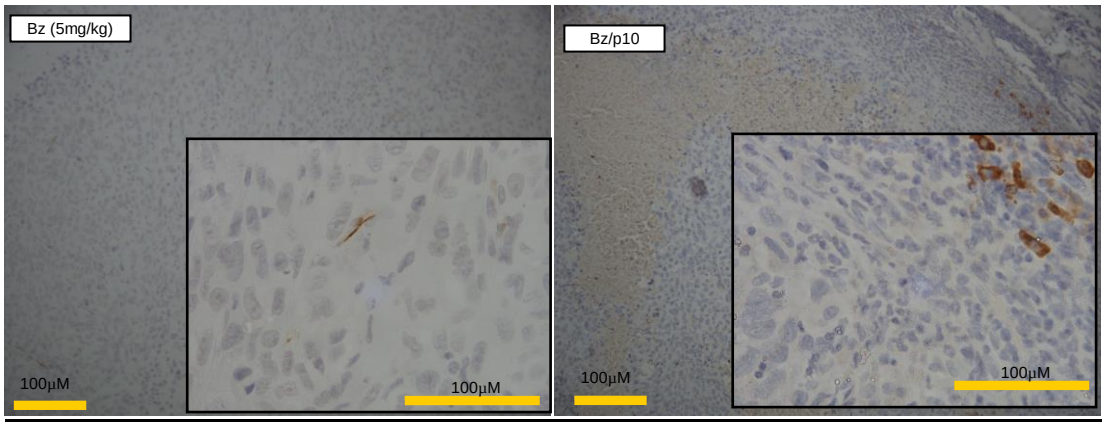

Figure 5.31 ***Effects of Combining Bz with P10 on CD34 Vessel Formation***
Representative images taken at x10 (main panel) and x60 (insert) magnification. (Bz/p10 combination) demonstrates to distinct staining patterns for CD34. The Bz alone treated tumours demonstrate CD34 positive staining for newly formed vessels within the tumour. However, combined treatment of Bz/p10 (5mg/kg and 50µM) twice weekly (i.p.) demonstrates a more individual CD34 positive staining pattern. Due to this irregular pattern of CD34 staining in the combination treated tumour, comparison of MVD was not possible.

5.2.7 Dose Response Study

In the previous studies conducted during this project, Bz (5mg/kg) displayed an inhibitory trend on MDA-MB-436 tumour growth *in vivo*. Thus, a potential additive effect in the presence of the neuropilin peptides may have been masked due to the efficacy of Bz treatment. It was therefore decided, that a dose response study was required to evaluate the tumour responses to Bz alone and determine a sub-optimal Bz dose to assess the effects of combining Bz with the Np1 peptides. Since CV also displayed an inhibitory trend this was added for each of the equivalent doses of Bz.

Following tumour implantation ($1x10^6$) an equal number of animals were assigned to each treatment group (n=6/group). In the saline treated group four of the six animals developed palpable tumours and were treated with saline. Twenty-four days post initial injection of the saline control, one animal was culled due to reaching maximum tumour burden ($1276mm^3$). The remaining three animals continued treatment with saline until the end of the experiment where the animals were culled due to tumour ulceration (Day 59). However, as only one animal remained in the saline control group ay Day 59, statistical analysis was carried out on Day 42. In the Bz group, four of the six animals implanted with MDA-MB-436 breast cancer cells were treated with Bz (5mg/kg) twice weekly via i.p injection, with the remaining two animals failing to develop palpable tumours. On day forty-two, one animal was culled due to tumour ulceration (1140.75 mm^3) with the remaining three animals continuing with Bz

treatment until the end of the experiment (day 59). However, as all but one animal in the saline control group were culled at day forty-two statistical analysis was carried at this time point (Day 42). Bz at 5mg/kg (n=3) significantly inhibited the tumour growth *in vivo* compared with the saline (n=3) control group (mean±SEM; Bz 0.5mg/kg vs. saline control; 198±22mm^3 vs. 713±82mm^3; n=3, *p<0.001*) (**Figure 5.32**).

In the CV group, five of the six animals implanted with MDA-MB-436 (1x10^6) breast cancer cells developed palpable tumours and were injected with CV at the appropriate volume. On day fifteen post initial administration of CV, one animal was culled due to tumour ulceration (650mm^3), with a second animal culled nineteen days after initial injection of CV due to tumour ulceration (786.5mm^3). The remaining three animals continued treatment with CV until the end of the experiment (day 59). Similar to Bz, statistical analysis was carried out on day forty-two. At day forty-two CV also (n=3) significantly inhibited tumour growth when compared with the saline control (n=3) group (mean±SEM; CV vs. saline control; 249±31mm^3 vs. 713±82mm^3; n=3, *p<0.001*) (**Figure 5.32**). No significant (*p=0.243*) differences were observed in tumour growth between Bz and the CV.

In the second Bz treated group, four of the six animals that underwent tumour implantation developed palpable tumours and were treated with Bz (2.5mg/kg) twice weekly via i.p injection with all four animals continuing treatment until the end of the experiment (day 59). Again statistical analysis was carried out on day forty-two. Bz, 2.5mg/kg (n=4) also significantly inhibited tumour growth compared with the saline control (n=3) group (mean±SEM; Bz 2.5mg/kg vs. saline control; 213±26mm^3 vs. 713±82mm^3; n=4/3, *p<0.001*) (**Figure 5.32**). In the second CV treated group, five of the six animals that underwent tumour implantation developed palpable tumours and were injected with CV at an equal volume to that used with Bz 2.5mg/kg. On day eight post initial CV administration, one animal was culled due to tumour ulceration (171.5mm^3), with a second being culled forty-two days after starting treatment with CV due to maximum tumour burden (1140.75mm^3). The remaining three animals continued treatment with CV until the end of experiment (day 59). At day forty-two, CV (2.5) also significantly inhibited tumour growth *in vivo* when compared with the saline control group (mean±SEM; CV vs. saline control; 184±9mm^3 vs. 713±82mm^3; n=3, *p<0.001*) (**Figure 5.32**). No significant (*p=0.559*) differences on tumour growth were observed between Bz and the CV.

In the third Bz treated group, five of the six animals implanted with MDA-MB-436 tumour cells developed palpable tumours and were treated with a lower dose of Bz (1mg/kg) twice weekly via i.p injection. On day forty-two post initial injection of Bz, one animal was culled due to (288mm^3), with a second being culled on day fifty-two (171.5mm^3) due to the animal looking weak and generally unhealthy. The remaining three animals continued treatment with Bz until the end of the experiment (day 59). Again, statistical analysis was performed at day forty-two. Bz, 1mg/kg (n=4) significantly inhibited tumour growth *in vivo* compared with the saline control (n=3) group (mean±SEM; Bz 1mg/kg vs. saline control; 405±55mm^3 vs. 713±82mm^3; n=4/3, p<0.001) (**Figure 5.32**). In the equivalent CV treated group, five of the six animals that underwent tumour implantation developed palpable tumours and were treated with CV at the appropriate equivalent volume. On day forty-two post initial treatment with CV, two animals were culled due to tumour ulceration with the remaining three continuing treatment with CV until the end of experiment (day 59). On day forty-two the CV (n=3) also significantly inhibited tumour growth *in vivo* when compared with the saline control (n=3) group (mean±SEM; CV vs. saline control; 256±42mm^3 vs. 713±82mm^3; n=3, p=0.001). Again, there was no significant (P=0.527) difference between Bz at the 1mg/kg dose and the CV (**Figure 5.32**).

In the Bz 0.5mg/kg treated group, four of the five animals implanted with MDA-MB-436 breast cancer cells developed palpable tumours and were injected with Bz (0.5mg/kg) twice weekly via i.p. injection. On day twenty-four all animals in the saline control group were culled due to maximum tumour burden and tumour ulceration. Four of the five animals in the treatment group developed palpable tumours and were administered with Bz (0.5mg/kg twice weekly via i.p. injection). On day twenty-four, Bz (0.5mg/kg) (n=4) inhibited tumour growth *in vivo* compared with the saline control (n=3) group (mean±SEM; Bz 0.5mg/kg vs. saline control; 195±53mm^3 vs. 1022±220mm^3; n=4/3, ns), this was not significant (*p=0.057*) (**Figure 5.32**). In contrast the lowest dose of Bz (0.1mg/kg) tested did not display tumour growth inhibition (mean±SEM; Bz 0.1mg/kg vs. saline control; 213±30 vs. 467±138; n=5/4, NS) (**Figure 5.32**). In these 0.5mg/kg and 0.1mg/kg Bz dosing experiments a CV group was not added as at this point a sub-optimal dose of Bz was required rather than assessment of differences between Bz and the CV. Therefore, with this and the HO 3R guidance in mind a CV treatment control was not added.

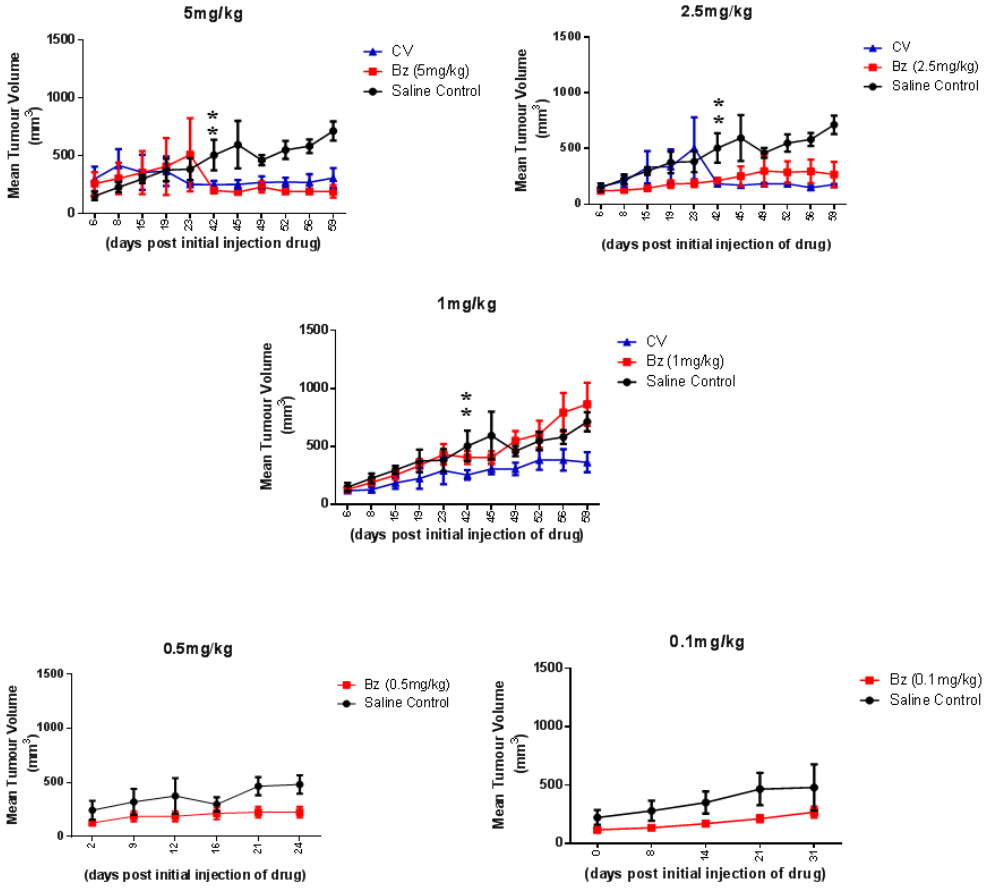

Figure 5.32 Dose Curve (Bz 0.1-5mg/kg)

Bz effectively inhibits MDA-MB-436 tumour growth *in vivo* at a number of doses. A relatively cytostatic effect on tumour growth is observed in all treatment groups, with only the 0.1mg/kg dose beginning to lose this cytostatic effect.

For 5-1mg/kg graphs, data is presented at mean±SEM tumour volume (mm^3); n=3/4, p=<0.001) w.r.t saline control. Statistical analysis on Day 42 was performed using the One way ANOVA followed by the Holm-Sidak post hoc test for multiple comparisons

For the 0.5mg/kg graph, data is presented at mean±SEM tumour volume (mm^3); n=3/4, NS) w.r.t saline control. Statistical analysis was performed on Day 24 using the Kruskal-Wallis One way ANOVA on ranks.

The tumour growth after Day 42 for the control group is representative of one animal. The time points past Day 42 were left to allow visualisation of the tumour growth in the tumours in animals that continued to receive Bz treatment.

** ***Indicates both Bz and CV as being significant compared with the saline group***

5.2.8 Effects of Combining P7b with Lower Doses of Bz on Tumour Growth *In Vivo*

From the Bz dose-response studies it was decided that Bz 0.1mg/kg dose would be used in the final combination experiment. Due to time constraints it was decided that p7b would be used in the combination study with Bz. Due to time constraints a pre-determined treatment period of thirty-one days was set as the final end point.

In the group treated with saline four of the five animals implanted with MDA-MB-436 ($1x10^6$) breast cancer cells developed palpable tumours. On day twenty-one post initial injection of saline, two animals were culled due to tumour ulceration. At the end of the experiment (day 31) there were still two animals remaining that had not reached the EOP criteria. In the Bz treated group, all five animals that underwent tumour implantation developed palpable tumours and were treated with a lower dose of Bz (0.1mg/kg) twice weekly via i.p injection. At the end of the experiment (day 31) all five animals in the Bz treated group had not reached EOP criteria. However, as only two animals in the saline treated group remained at day thirty-one, statistical analysis was performed at day twenty-one post initial injection. At this time point Bz (n=5) reduced tumour growth compared with the saline (n=4) group (mean±SEM; Bz 0.1 vs. saline control; 213±30mm^3 vs. 467±138mm^3; n=5/4, ns) however, again due to variability this reduction did not reach statistical significance (*p=0.084*) (**Figure 5.33**).

In the Bz/p7b combination group, all five animals that were implanted with tumour cells developed palpable tumours and were treated with a combination of Bz (0.1mg/kg) twice weekly and p7b (1μM) three times a week via i.p. injection. At the end of the experiment (day 31), similar to the Bz alone treated group, all five animals had not reached EOP criteria. Again, end point statistical analysis was carried out at day twenty-one. At this time point combined Bz/p7b treatment (n=5) reduced tumour growth compared with the saline (n=4) treated animals (mean±SEM; Bz/p7b vs. saline control; 286±101mm^3 vs. 467±138mm^3; n=5/4, ns) but again did not reach statistical significance (*p=0.316*) (**Figure 5.33**). However, although combining lower doses of Bz with p7b resulted in a trend that displayed reduced tumour growth, no additive effects were observed when compared with Bz alone (mean±SEM; Bz/p7b vs. Bz; 287±101mm^3 vs. 213±30mm^3; n=5, ns). This suggests Bz (0.1mg/kg) was not masking any inhibitory effects of p7b.

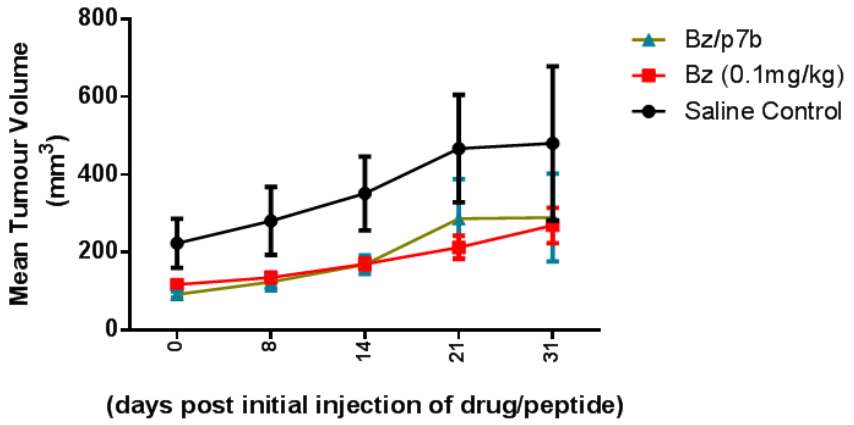

Figure 5.33 ***Effects of Combining Lower Dose of Bz with p7b:***
No additive effects on tumour growth *in vivo* were observed when p7b was combined with lower doses of Bz.

Data is presented as mean±SEM tumour volume (mm3); n=4/5, NS.
Statistical analysis was performed using a One Way ANOVA (Sigmaplot 11 software).

Histology

The tumours that were treated with Bz (0.1mg/kg) were necrotic as seen with previous doses of Bz in the earlier experiments. However, no differences were observed between the Bz (0.1mg/kg) and saline treated tumours (mean±SEM; Bz vs. saline control; 68±15% vs. 65±11%; n=3, ns) (**Figure 5.34**). No additive effects were observed on tumour necrosis when tumours were treated with Bz/p7b compared with Bz alone (mean±SEM; 65±9% vs. 68±15%; n=3, ns) (**Figure 5.34**).

Bz (0.1mg/kg) exerted a proliferative effect on primary tumour growth, as a statistical increase (*p=0.044*) in the number of Ki67 positive cells was observed in the Bz treated group compared with the saline control (mean±SEM; Bz vs. saline control; 73±13 vs. 31±7; n=3, *p=0.044*) (**Figure 5.35**). Combining Bz with p7b displayed no additional effects on tumour proliferation compared with the Bz alone treated tumours (mean±SEM; Bz/p7b vs. Bz; 72±11 vs. 74±13; n=3, ns). The level of apoptosis occurring was significantly *(p=0.017*) lower in the Bz treated tumours compared with the saline control tumours (mean±SEM; Bz vs. saline control; 9±0.4 vs. 16±0.4; n=3, *p=0.017*) (**Figure 5.36**). This is in contrast to what was observed with the higher dose of Bz (5mg/kg).
Interestingly, the CD34 staining pattern in this final cohort was similar to that observed with treatment with CV, Bz/p10 and p7b alone in previous experiments, whereby single cells

stained positively for CD34 rather than the vessels (**Figure 5.37**). However combining Bz with p7b resulted in a loss of inhibitory effects observed on CD34 positive cells compared with the Bz alone tumours (mean±SEM; Bz/p7b vs. Bz; 12±1 vs. 9±3; n=3, ns) (**Figure 5.37**), which was not statistically significant (*p=0.700*).

A

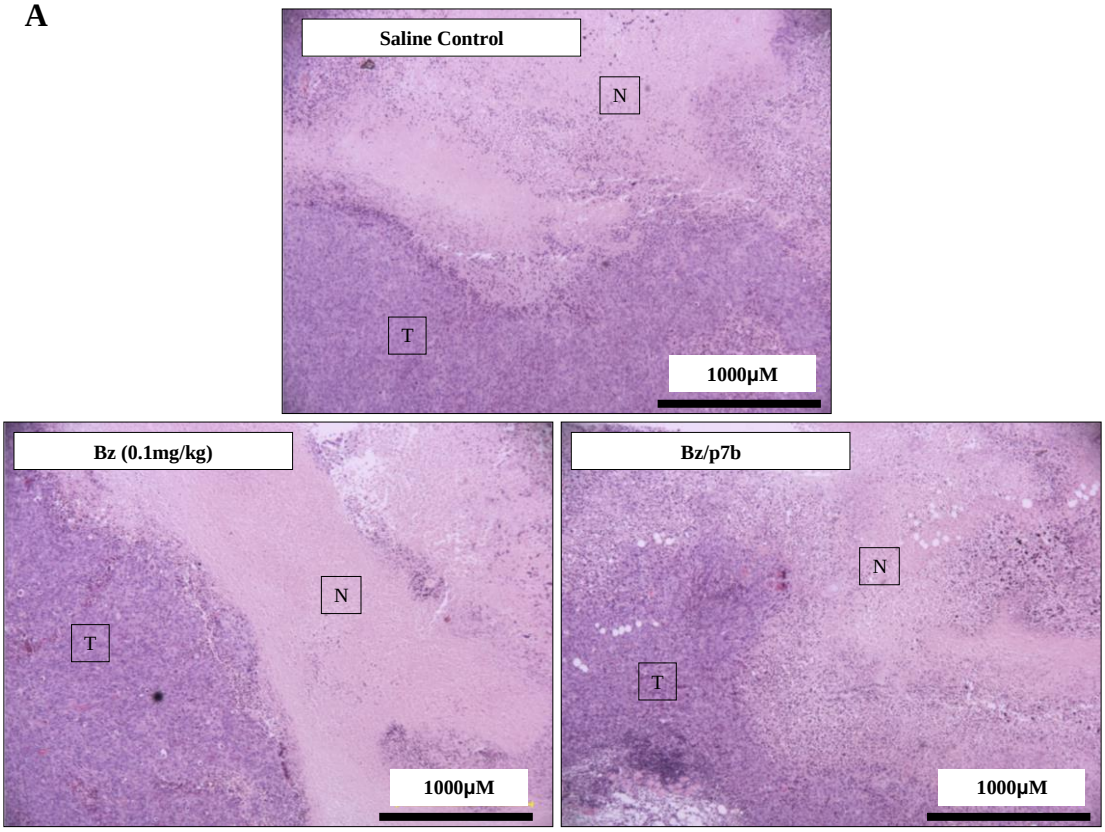

B

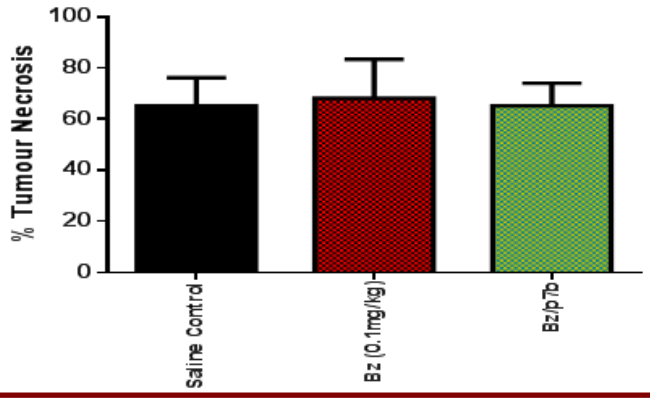

Figure 5.34 ***Effects of Combining Low Doses of Bz with p7b on Tumour Necrosis*** (**A**) Representative images at x4 magnification of necrotic areas (N) within the MDA-MB-436 tumour tissue (T) (**B**) No additive effects on tumour necrosis were observed when Bz was combined with p7b (1µM) compared to Bz alone (0.1mg/kg)

Data is presented as mean±SEM (%tumour necrosis); n=3; NS. Statistical analysis was performed using test (Sigmaplot 11 software).

A

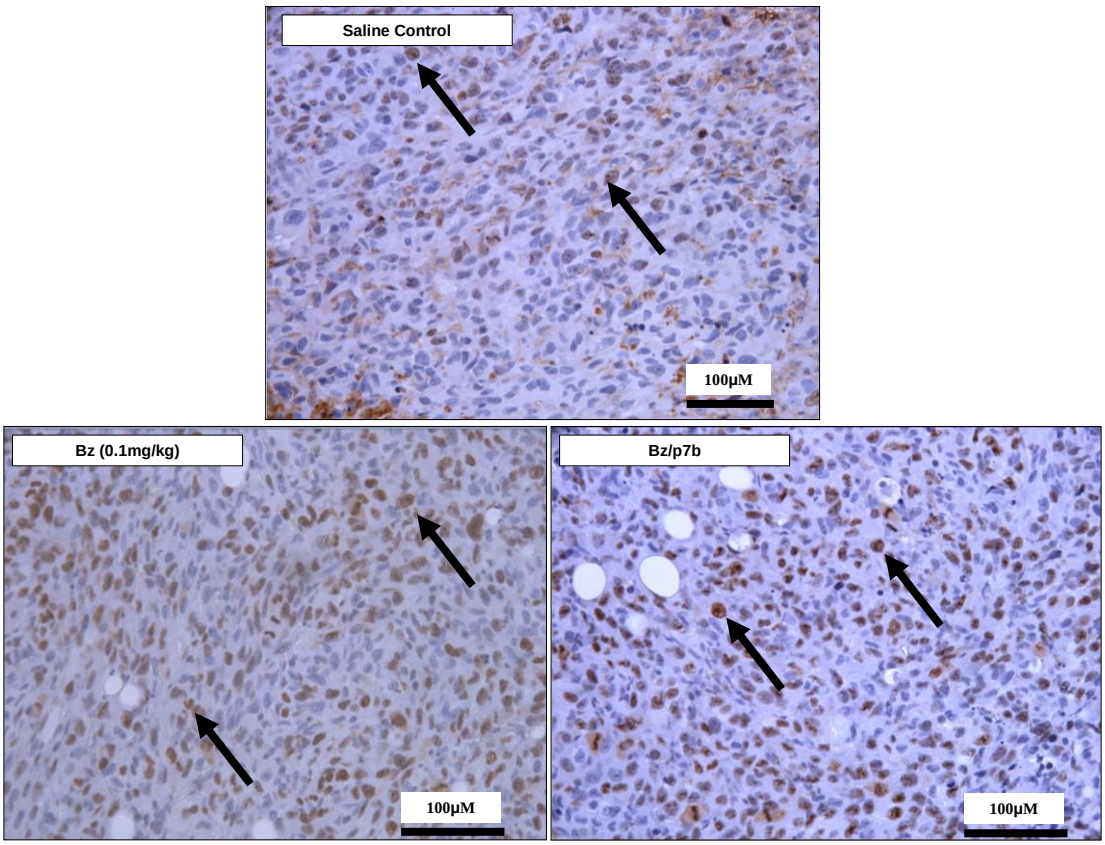

B

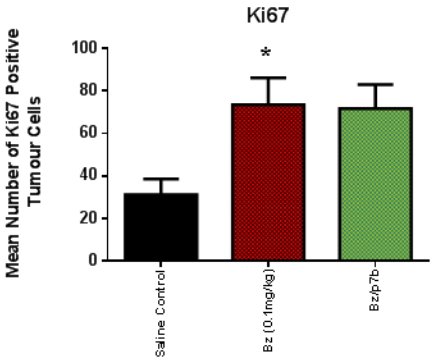

Figure 5.35 ***Effects of Combining Low Doses of Bz with p7b on Tumour Cell Proliferation*** (**A**) Representative images of Ki67 staining taken at x20 magnification (**B**) No additive effects on tumour cell proliferation was observed when Bz was combined with p7b compared with Bz alone

Data is presented as mean±SEM Ki67 positive cells; n=3; p=0.044. Statistical analysis was performed using a t-test (Sigmaplot software).

A

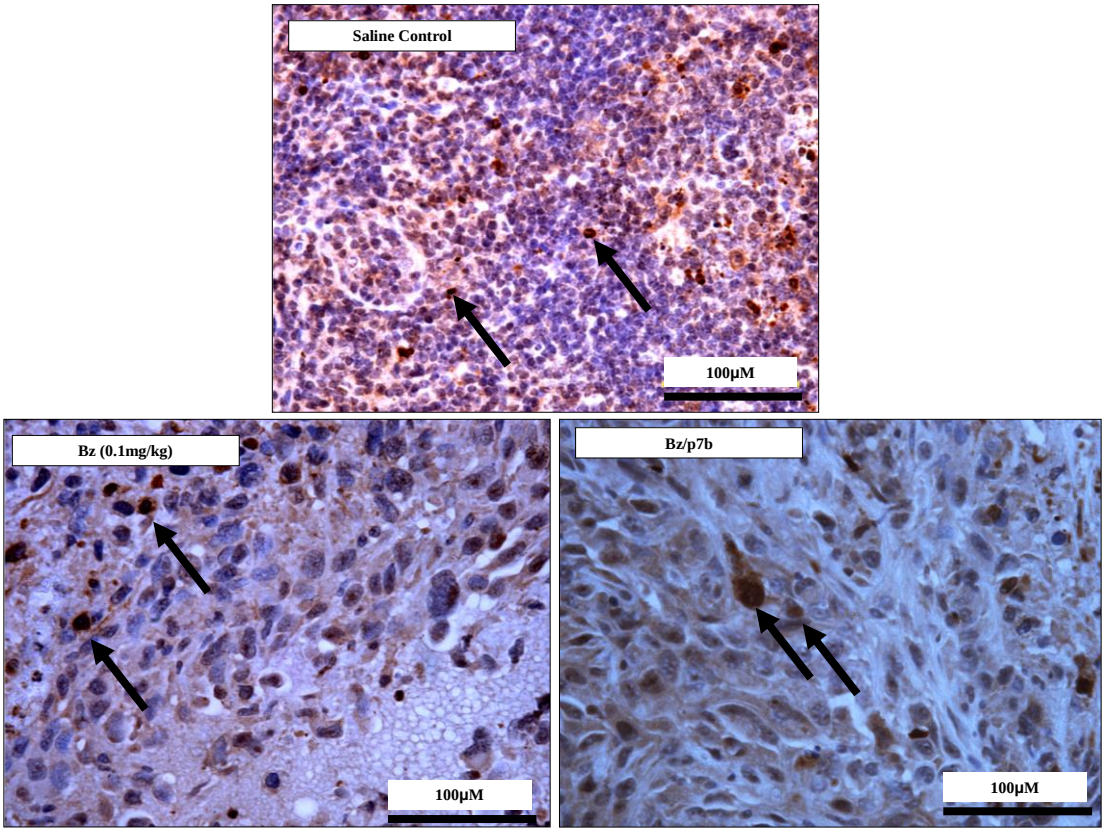

B

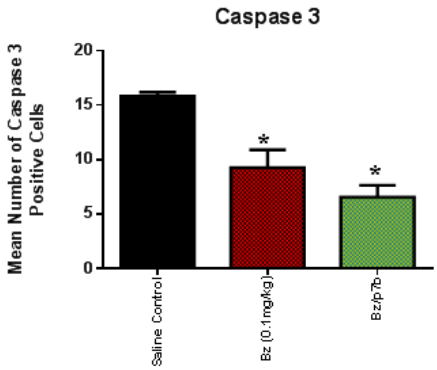

Figure 5.36 ***Effects of Combining Low Doses of Bz with p7b on Tumour Apoptosis***
(**A**) Representative images of Caspase 3 staining taken at X40 (**B**) No additive effects on tumour apoptosis was observed when Bz was combined with p7b compared to Bz alone. However Bz (0.1mg/kg) significantly reduced the number of apoptotic events occurring within the tumour tissue.

Data is presented as mean±SEM positive Caspase 3 cells; n=3; p=0.017w.r.t saline control. Statistical analysis was performed using a t-test (Sigmaplot software)

A

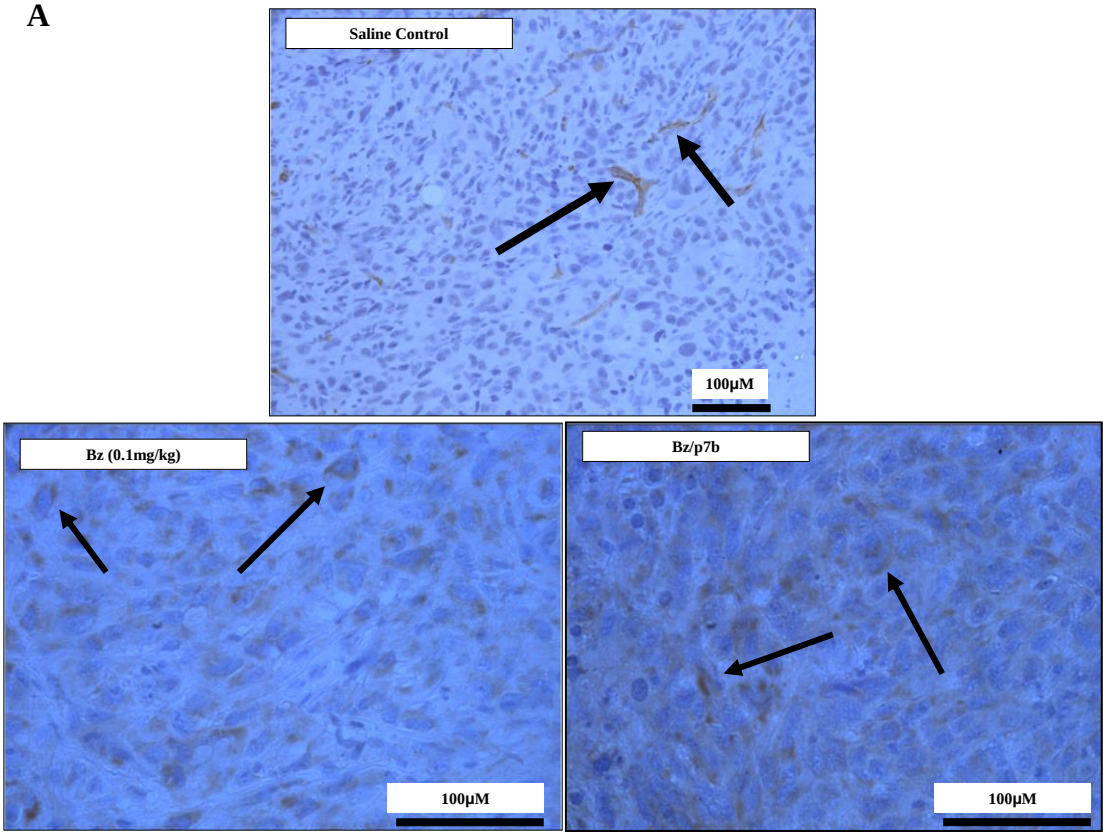

B

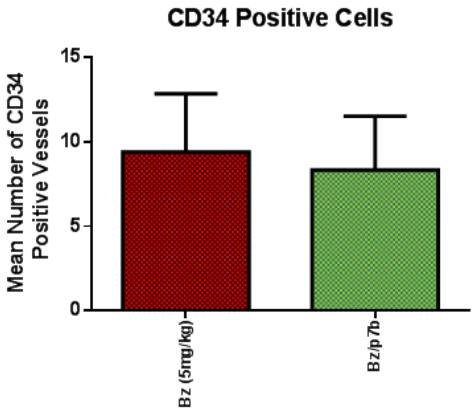

Figure 5.37 ***Effects of Combining Low Doses of Bz with p7b on CD34 Positive Cells*** (**A**) Representative images of CD34 positive staining taken at X60 (**B**) No additive effects on CD34 positive cells reduction was observed when Bz was combined with p7b compared to Bz alone

Data is presented as mean±SEM CD34 positive cells; n=3 NS.

5.3 DISCUSSION

5.3.1 VEGF and VEGF Receptor Protein Expression

VEGF and all four VEGF receptors were expressed by MDA-MB-436 tumours *in vivo*. The diffuse staining pattern for VEGF has previously been observed in breast xenograft tumour tissue (***Banerjee et al, 2011 & Chougule et al, 2011***). VEGF appeared to be localised within the cytoplasmic regions, with some membranous staining. It is possible that this membranous staining is representative of secreted VEGF.

Expression of VEGF-R1 was wide-spread through-out the tumour but moderate in intensity in the viable regions of the tumour, which has previously been observed in both breast cancer patient samples (***Schmidt et al, 2008***) and in breast xenograft tissue (***Wu et al, 2006***). The stronger expression in the necrotic areas of the tumour tissue appeared associated with macrophages. VEGF-R1 expression has previously been observed on macrophages (***Muramatsu et al, 2010***). The role of macrophages in breast cancer progression is contradictory; with as some studies suggesting anti-tumour effects whereas, others have shown that macrophages act in a pro-tumourgenic manner. Macrophages are also known to be a rich source of angiogenic cytokines and induce increased tumour vessel formation. It is thought that the tumour associated macrophages can shift from a anti-tumourgenic to a tumour promoting phenotype depending on the cytokines released by the tumour (***Biswas et al, 2010 & Zamarron et al, 2011***). Therefore F4/80 staining on frozen tumour sections would be interesting to perform to any altered levels of F4/80 macrophages infiltrating into the tumour, in the treatment groups especially. Bz has been shown to alter the levels of macrophage infiltration into breast tumours (***Roland et al, 2009***). More recently the use of F4/80 as a macrophage specific marker has been questioned, as neutrophils also express this marker. Therefore double staining with a neutrophils marker on frozen sections to identify which immune cells are reduced and which are increased and what implications this may have on breast cancer progression would be informative.

Np1 expression was weak and not as widely distributed as the other VEGF receptors, suggesting that within the tumour, Np1 expression appears to be restricted to specific clones of cells, identification of which requires double staining using confocal microscopy. Np2 expression was in the MDA-MB-436 tumours. Previously Np2 expression has been observed in tissue from breast cancer patients with strong Np2 staining observed in both the blood and lymph vessels and all invasive breast cancer cells (***Yasuoka et al, 2009***). A similar staining

pattern for Np2 in murine mammary tumours (TBP) thought to develop a phenotype similar to TNBC has also been observed (***Goel et al, 2013***).

Generally the level of VEGF and VEGF receptor expression was relatively similar between the different treatment groups. Although analysis of the intensity of staining was carried out, the data is not comparable as staining was carried out on tumour tissue that was taken at different experimental time-points. The primary aim was to assess tumour growth and observe is any added effects on growth were observed in the combination experiments, therefore the studies were designed to assess if resistance was observed and causes tumour re-growth. Going forward analysis of tumour activity would require all tumours to be removed at the same time-point. In addition, although IHC is a good technique for assessing the location of expression of different factors within the context of the tumour as a whole and provides useful information regarding the morphology of the tumour, flow cytometry is an alternative technique that may have been more useful. Flow cytometry more accurately measuring changes in receptor expression with the added advantage of allowing identification of which cell types are expressing VEGF and the VEGF receptors in the tumour tissue.

5.3.2 Bz alone

We tried to source murine/human Bz derivative from Genentech but this was not possible thus the humanised monoclonal VEGF antibody Bz, was used in all studies. Bz alone at a dose-range of (5mg/kg-0.5mg/kg) significantly inhibited MDA-MB-436 breast cancer growth *in vivo* compared with the saline treated group with a cytostatic effect on tumour growth being observed. This cytostatic effect is typical of anti-angiogenic agents such as Bz, (***Loges et al, 2009***). In contrast to chemotherapeutics, Bz primarily acts on the ECs thus inhibiting the availability of essential nutrients. This mechanism is the main reasoning for combining anti-angiogenic agents such as Bz with chemotherapy or radiotherapy which target the tumour cells. In the current study Bz inhibited tumour growth which confirms the previously reported data in an orthotopic model of breast cancer (***Roland et al, 2009***). Consequently, the Bz dose-response study should have been carried out prior to starting the combination *in vivo* experiments to ensure that the *in vitro* doses translated to the *in vivo* experiments. The dramatic inhibitory effects on breast cancer growth *in vivo* by Bz in the current study, along with previous literature suggests that tumour derived VEGF plays an extremely important role on breast cancer progression. This maybe more than effects on stromal derived VEGF at least in a animal model, as Bz only inhibits human VEGF isoforms from binding VEGF-R1 and VEGF-R2, therefore only inhibits tumour derived VEGF in

murine models. This notion that the tumour derived VEGF drives primary tumour growth is further supported by ***Roland et al, 2009***, whereby MDA-MB-231 tumours treated with Bz or an antibody that inhibits both human and murine VEGF from binding VEGF-R2 (r84) had similar final tumour volumes after 4 weeks of treatment. The anti-apoptotic effects observed in response to Bz (5mg/kg) treatment in the MDA-MB-436 tumours may be a result of apoptotic activity in either the breast cancer cells, the endothelial cells or other cell types that have infiltrated into the tumour micro-environment. VEGF is a survival factor for vascular endothelial cells, and Bz appears to inhibit the pro-survival effect of VEGF on newly formed vessels and by maintaining the integrity of existing vasculature (***Fujii et al, 2009***). Therefore it is most likely that the apoptotic effect observed in the current study is a result of endothelial cell death, for which there was some evidence in the tumour sections, however there were other cell types present that were positive for CD34, which would be worth investigating.

To date the majority of clinical studies in mBC combine Bz with a number of different targeting agents, particularly chemotherapeutic agents with eventual escape from treatment. Although a dramatic inhibition was observed on primary tumour growth with Bz alone in this current study, resistance to Bz is ultimately inevitable as targeting one signalling pathway alone is insufficient, particularly in metastatic disease as the metastatic cells are thought to be phenotypically more aggressive.

The control vehicle for Bz (CV) also exerted effects *in vivo* similar to Bz efficacy, however in the previously published studies saline is used as a control. The control vehicle consists mainly of sodium salts with a low level of the detergent tween20. Cells are sensitive to high levels of detergent and changes in pH. Additionally during the *in vitro* the pH of CV and media were tested and no differences were detected. However, accumulation of the CV over time in the *in vivo* studies may have resulted in changes in pH within the microenvironment, leading to cell death and the reduced tumour growth observed, resulting in the similar histological changes observed in tumours treated with the CV or Bz. In addition there are some recent studies that access the anti-tumour effects of tween20, and it appears that the effects observed with the control vehicle for Bz, may not be due to changes in micro-environmental alone, but due to activation of downstream signalling events that are activated by tween20 (***Yamagata et al, 2009, Yang et al, 2012 & Eskandani et al, 2013***).

5.3.3 Np1 Peptides

Pre-clinical data using Bz provided encouraging results however in the clinic, Bz failed to increase OS in breast cancer patients with metastatic disease (***Miller et al, 2007***). Retrospective biomarker analysis suggested that the presence of Np1 in breast cancer patients post Bz therapy, indicates a poor prognosis (***Jubb et al, 2011***). Additionally, over recent years there is ample data to suggest that the neuropilins are important VEGF receptors that play an important role in breast cancer cell activity (***Bachelder et al, 2001, 2003 and Barr et al, 2005***). The binding site for the neuropilin receptors lies downstream of the binding site for the classic VEGF receptors thus when Bz binds to VEGF the neuropilin binding site remains un-inhibited, suggesting that these receptors may provide VEGF with an alternative signalling pathway. This alternative signalling pathway may allow escape from Bz therapy and therefore based on this argeting the neuropilin receptors both alone and in combination with the classical VEGF receptors (VEGF-R1 and VEFG-R2) is a feasible target.

The neuropilin peptides (p7b and p10) used in the current *in vivo* studies had previously been tested for binding ability to Np1 in vitro (***Cebe-Suarez et al, 2008***). However, no previous *in vivo* studies have been performed using these peptides. The two peptides demonstrate different binding affinities to the Np1 receptor with p10 (RPPR) displaying a higher binding affinity then that observed with p7b (DKPRR) (***Cebe-Suarez et al, 2008***).

Based on the literature available on inhibiting neuropilin 1 in breast cancer tumour growth (***Lee et al, 2013 & Starzec et al, 2006***) it was assumed that treatment with p7b and p10 would induce some inhibitory effects on breast cancer growth *in vivo*, especially since both peptides displayed both anti-angiogenic and minimal anti-tumourgenic activity *in vitro* (Chapter 3 & 4). However, neither p7b nor p10 alone exerted any significant inhibitory effects on MDA-MB-436 breast cancer growth *in vivo* compared with the saline control treated tumours although p10 alone did reduce tumour volume but was reduction did not reach significance. A reduction in tumour growth despite not being significant suggested that p10 at least was reaching the tumour. As p10 is thought to bind both Np1 and Np2, it is possible that this dual inhibition resulted in p10 alone exerted more of an inhibitory effect on tumour growth then that observed with p7b alone. Additionally, the dose administered for p7b was much lower then that of p10, therefore it is possible that the peptides were degraded rapidly and therefore insufficient amounts of the peptide reached the tumour and the surrounding vasculature. Np1 expression is wide-spread in other healthy organs such as liver, lungs and kidneys, therefore is it possible that the peptides were directed in high

amounts to the healthy organs rather then the tumour itself. This has recently been investigated, whereby the distribution of an anti-Np1 antibody was measured in non-tumour bearing mice and tumour bearing mice to assess how much of the antibody (after i.v injection) is cleared (***Bambaca et al, 2012***). The group found that non-tumour Np1 'sinks' required saturating before sufficient amounts of the Np1 antibody was delivered to the tumour and that delivery to the healthy organs was greater possibly due to the fact these tissues are better perfused then the tumour tissue (***Bambaca et al, 2012***). This is an important observation, as the group found that relatively high concentrations of the Np1 antibody were required to achieve adequate tumour levels. It is therefore possible that the peptides were sequestered within these non-tumour 'sinks' and higher doses of both peptides would be required in order to observe any significant inhibitory effects on tumour growth *in vivo.* It would therefore be informative and useful to tag the peptides to monitor the distribution to the tumour and other tissues following *in vivo* administration.

The literature available that investigates the effects of blocking VEGF-Np1 interactions, utilise peptides that are designed to bind VEGF which leads to subsequent inhibition of Np1 receptor activation (***Starzec et al, 2006***) or inhibit both neuropilin receptors (***Lee et al, 2013***). The peptides used in the current study are derived from the human VEGF sequence, which bind Np1 and are thought to block functional VEGF from interacting with the Np1 receptor. However, as the peptides are derived from the VEGF sequence it is possible that both *in vitro* and *in vivo* these peptides are activating Np1 rather then blocking downstream signalling, therefore designing peptides that bind VEGF may prove more effective in blocking VEGF-Np1 signalling. Additionally blocking only Np1 may lead to compensatory up-regulation of the Np2 receptor and therefore negate any inhibitory effects exerted with a Np1 targeting peptide only, such as p7b. Neuropilin 2 is thought to be involved in lymph-angiogenesis and subsequent metastatic events (***Yasuoka et al, 2009***). This potentially suggests that Np2 may induce a more aggressive phenotype in breast cancer cells in order to allow them to metastasis to distant sites, thus up-regulating Np2 as a compensatory mechanism, may result in a more aggressive response to treatment with p7b in particular, as this peptide is thought to bind Np1 only.

Additionally Np1 also exists as a soluble form (***Cackowski et al, 2004***) and it is therefore possible that the peptides are also binding this inactive form of the receptor, thereby increasing the availability of the 'active' receptor. Therefore the ratio of soluble versus membrane bound Np1 is potentially important in determining the response to p7b/p10 treatment *in vivo*.

It is also possible that *in vivo* the effects of the Np1 peptides alone displayed no inhibitory effects on MDA-MB-436 breast cancer growth due to the lack of Np1 expression on both the tumour and endothelial cells, as it has been shown that both HuVECs and MDA-MB-231 breast cancer cell protein expression of Np1 is down-regulated in the presence of hypoxia (***Bae et al, 2008***). A key characteristic of solid tumours such as breast carcinomas is the presence of hypoxic regions. Interestingly, it has been observed that in contrast to Np1, expression of Np2 is maintained over long periods of exposure to hypoxia (up to 5 days) (***Bae et al, 2008***). This also suggests that a therapy that targets both neuropilin receptors may prove more effective in inhibiting tumour progression and may explain why p7b and p10 failed to effectively inhibit breast cancer growth *in vivo*. Interestingly, the MDA-MB-436 breast cancer cell line is thought to predominantly express $VEGF_{121}$ mRNA compared with the other VEGF isoforms (***Stimpfl et al, 2002***). The Np1 peptides used in the experiments were derived from the $VEGF_{165}$ sequence, if the affinity of $VEGF_{121}$ in the MDA-MB-436 breast cancer cells is higher for Np1 compared with $VEGF_{165}$; it is therefore possible that endogenous levels of $VEGF_{121}$ displaced the peptides therefore rendering them ineffective.

Histological analysis of the tumour tissue after treatment with p7b or p10 observed some interesting changes in some of the different parameters measured, however these changes did not reach statistical significance but do suggest an interesting trend. Interestingly, p10 but not p7b reduced tumour necrosis; however this reduction was not significant. Necrosis is cell death that occurs as a result of micro-environmental changes, thus the reduction in tumour necrosis in the p10 alone treated tumours (despite not reaching statistical significance) suggests that treatment with p10 is in some manner changing the micro-environment within the tumour. A decrease in tumour necrosis is potentially favourable as extensive necrosis is thought to indicate rapid growth in breast cancer patients (***Santamaria et al, 2010***). Neither peptide displayed any inhibitory effects on breast cancer cell proliferation when measured as the number of positively stained Ki67 cells; this was not surprising for p10, as in the *in vitro* MTS assay no inhibitory effects on MDA-MB-436 breast cancer cell proliferation were maintained at the p10 dose (50μM) used in the *in vivo* experiments. However, p7b *in vitro* significantly inhibited MDA-MB-436 breast cancer cell proliferation, however the MTS assay measured effects on proliferation up to 48h, therefore it is possible that p7b *in vitro* did not maintain inhibitory effects of breast cancer cell proliferation, which is what was observed *in vivo*. Caspase 3 staining suggested that p7b alone reduced the level of apoptosis occurring within the tumour tissue, which may in part explain why p7b alone exerted no inhibitory effects on MDA-MB-436 tumour growth, this observation however was surprising as *in vitro*, Np1 has been shown to be an autocrine survival factor for breast cancer cells

(***Barr et al, 2005***). The peptides designed for use in this project are derived from the human $VEGF_{165}$ protein sequence and are designed to bind to Np1 or potentially both Np1 and Np2 (in terms of p10), it is therefore possible that the peptides are activating the receptor signalling pathway instead of inhibiting it, thus peptides designed to bind VEGF and inhibit VEGF from binding to the neuropilin receptors may be more effective in blocking VEGF induced signals. No effects on CD34 positively stained cells or vessels were observed with either p7b or p10.

Abnormal Vasculature

Abnormal vasculature appeared to be formed in the MDA-MB-436 breast tumours, whereby clusters of single cell CD34 staining were present in the tumours from some of the treatment groups rather then the typical vessel structure. CD34 is expressed by other cells types in addition to endothelial cells, such as haematopoietic stem cells and mesenchymal cells. The antibody purchased from Abcam used in the current studies detects CD34 on murine endothelial cells and murine leukocytes (monocytes and granulocytes). Co-staining on frozen sections would be useful in identifying which cells are being detected in the MDA-MB-436 treated tumours. Additionally, two markers would prove useful for determining vessel counts in these tumours. In addition, CD31 staining would be informative in terms of assessing of the different treatments are able to exert effects on the more mature vessels. Initially when the project began, a CD31 antibody for use on formalin fixed tissue was not available therefore CD31 staining on the formalin fixed tumour tissue could not be carried out. However, more recently, a CD31 specific antibody is now commercially available for use on formalin fixed tissue, thus could be used on the remaining tumours to assess if the different treatments have any vascular disrupting effects

Overall the differences observed between treatment with p7b and p10 *in vivo* may be due to lack of delivery of p7b, which may be a result of rapid degradation, especially since p7b (1μM), was administered at a much lower dose compared with p10 (50μM) based on the *in vitro* studies (see chapter 3&4). Additionally, the affinity of p7b for Np1 *in vitro* has been shown to be less then that observed with p10. Peptide 10 in a competitive binding assay almost completely inhibited labelled VEGF from binding Np1 whereas p7b displayed intermediate effects therefore it is possible that p7b is easily displaced *in vivo* by tumour derived VEGF, thus resulting in little inhibition in tumour growth. This may also explain why the inhibitory effects observed in vitro with p7b on both microvascular endothelial cells and the breast cancer cells did not translate to the *in vivo* setting.

5.3.4 Combination

Previously combining Bz with an antibody targeting Np1 observed an additive effect on lung tumour growth *in vivo* compared with Bz alone (***Pan et al, 2007***). However there are no studies that look at the combination in breast cancer *in vivo* (PubMed).

Bz/p7b

Although combining either p7b or p10 with Bz displayed no additive effects *in vitro* on the endothelial cells or the breast cancer cells, a potential additive effect *in vivo* was not dismissed as it was thought that treating the breast cancer cells separately to the endothelial cells in the *in vitro* studies may not have represented the interaction between these two cell types accurately. However, similar to what was observed *in vitro*; combining Bz with p7b exerted no additive effects on MDA-MB-436 breast cancer growth *in vivo* or on the tumour histology when compared with Bz alone. Since no inhibitory effects were observed with p7b alone *in vivo* an additive effect could not be expected. As previously mentioned it is possible that the dose of p7b required to be delivered to the tumour required to exert a biological effect was not adequate in these current experiments, especially if the p7b is being delivered to other organs that also express Np1.

Bz/p10

Although p10 alone did not exert a significant inhibitory effect on breast cancer growth *in vivo*, a reduction in tumour volume was observed when compared with the saline treated tumours, therefore when combining Bz with p10 as additive effect on tumour growth was expected. However, combining Bz with p10 resulted in reduced efficacy of Bz on inhibiting MDA-MB-436 breast cancer growth. However, from the histology is appears that the loss of Bz efficacy when Bz is combined with p10 is not a result of changes in necrosis, tumour cell proliferation, apoptosis or vessel formation as these parameters remained similar in the combination and Bz alone group. It is also possible that downstream activation of the Np1 receptor occurs upon peptide binding. Since p10 is thought to bind both Np1 and Np2 it is possible that when p10 binds the neuropilin receptors in this model, the activation of these two receptors compensates for the inhibitory effects observed with Bz alone. This is feasible as it has been shown that treatment of tumours with Bz up-regulates the expression of Np1 and Np2 and if p10 is activating rather then inhibiting neuropilin receptor signalling this may abolish Bz induced inhibitory effects as observed in the current experiments. What external factors might be determining whether the peptides inhibit or activate neuropilin receptor signalling is yet unclear.

It is also possible that the order in which Bz and the peptide are injected plays an important role in the response of tumours to combination therapy, therefore further work into the drug regime may prove more effective (***Ottewell et al, 2010***). Also heavily pre-treating one group with Bz prior to introducing the peptides, might also prove useful, as administering both treatments at the same time may result in resistance to the VEGF pathway at a much quicker rate, therefore rendering the combination therapy ineffective.

2.3.5 Models of Primary Breast Cancer Growth

In this project a subcutaneous model was used to test the effects of Bz and the neuropilin peptides on breast cancer growth *in vivo*. Mammary fat pad tumour implantation represents an orthotopic model of breast cancer, as injection of human breast cancer cells into the mammary fat pad allows the cells to grow and establish within a micro-environment that would be reflective of the human disease. The subcutaneous model was used to initially allow for optimisation of drug doses and combinations *in vivo*, prior to mammary fat pad studies, as the subcutaneous model would allow for a greater 'treatment window' as stated by HO regulations . However due to time constraints, the mammary fat pad studies were not carried out, as treatment with the peptides, in particular have not been concluded in the sub-cutaneous model therefore an optimal treatment combination was not feasible to take forward into an orthotopic model.

Although a number of questions are still unanswered with regards to inhibiting the neuropilin receptors during primary breast cancer growth, it was deemed important that analysis of the metastatic process also be investigated as currently, there is a lack of preventative therapy for breast cancer induce bone metastasis and since the secondary disease accounts for a high morbidity rate in breast cancer patients, the bone metastasis model was essential to investigate. Since the efficacy of the peptide design and general dosing issues were raised at the end of the sub-cutaneous experiments, it was deemed sensible to take only Bz forward to the metastasis experiments. As Bz effectively inhibited primary tumour growth at a number of doses, two low doses of Bz were used to assess if low doses could inhibit both primary and secondary tumour growth. The MDA-MB-231 breast cancer cells are known to 'home' to the bone after intra-cardiac injection and unfortunately due to time constraints, we did not have time to first test the homing ability of the MDA-MB-436 breast cancer cells to the bone, therefore the metastasis model was carried out with the MDA-MB-231 breast cancer cells.

Chapter Six

In Vivo Results
Effects on Breast Cancer-Induced Bone Metastasis

6.1 INTRODUCTION

6.1.1 Breast Cancer Induced Metastasis

Breast cancer metastasis is a major clinical problem, with the secondary disease accounting for approximately 90% of the mortality rates (***Suva et al, 2009***). The prognosis of patients with mBC is poor, as the median survival time from diagnosis from the metastatic disease is between 24-48 months (***Gennan et al, 2005***). The major sites of breast cancer metastases are to the bone, lungs and liver, with bone being the primary site for metastasis for approximately 25% of breast cancer patients, for which there is currently no curative treatment.

6.1.2 The Process of Metastasis

The process of metastasis involves a number of key steps which must be successfully completed in order to establish metastasis in a distant tissue. According to Paget's 'seed and soil' hypothesis (**section 6.1.3**), the first step involved in metastasis is the formation of a pre-metastatic niche, whereby tumour cells prepare a specific tissue to colonise. Secondly, once an efficient vasculature (tumour angiogenesis) has formed within the primary tumour mass, the tumour cells must detach from the primary site (***Weilbaecher et al, 2011***). Thirdly, tumour cells must be able to invade into the surrounding ECM, via the process of proteolysis, which is aided by MMPs. Once the ECM has been degraded intravasation of the tumour cells into the newly formed tumour vasculature allows for migration of tumour cells via capillaries, venules or lymphatic vessels (***Langley & Fidler, 2011; Talmadge & Fidler et al, 2010***). The fourth step in the metastatic process requires tumour cells forming aggregates with other cells such as the hematopoietic cells that are present in the circulation. The fifth and crucial step requires the tumour aggregates to be able to survive, evade immune detection and successfully migrate through the circulatory system. After which the tumour aggregates, arrests in a capillary bed and undergo extravasation into the surrounding tissue. Finally, once the tumour cells have 'homed' to the secondary site, the cells must be able to colonise and proliferate in the secondary site in order for metastasis to be successfully established. Once a tumour metastasis has formed in the secondary site, a new vasculature is formed to maintain tumour growth and to allow further disseminate to distant sites (***Langley & Fidler, 2011; Mathot & Stenninger, 2012***; ***Talmadge & Fidler et al, 2010***) (**Figure 6.1**).

6.1.3 'Seed and Soil' Hypothesis

The 'homing' of tumour cells to the secondary site is thought to be a specific process whereby the tumour cells migrate towards a specific tissue in a pre-determined manner, this is known at Paget's 'Seed and Soil' hypothesis. Paget's 'seed and soil' hypothesis has three main principles, the first principle states, the tumour mass contains both tumour and host cells (including ECs, fibroblast and infiltrating leukocytes) and that not all tumour cells possess the ability to successfully establish secondary disease. The second principle states that early identification of the cells that possess the ability to metastasise is crucial, with the third principle stating that metastasis only occurs in specific tissues (***Talmadge & Fidler et al, 2010***). These principles are derived from initial observations that demonstrated preferential spread of breast cancer cells to the liver and not the spleen. Paget stated that tumour cells will only metastasise to specific tissues that possess an optimal micro-environment in which the tumour cells will be able to survive and proliferate. To support this theory, studies looking at the expression profile of certain host cells demonstrated differences in cell surface expression of receptors on ECs residing in different tissues (***Langley & Fidler, 2011; Talmadge & Fidler et al, 2010***).

In light of Paget's hypothesis, there is evidence that suggests that the tumour cells that establish distant metastasis acquire a phenotype that allows for successful completion of the metastatic process (***Yokota et al, 2000***), thus making these tumours cells more difficult to treat using conventional therapy. The process of metastasis appears to select aggressive tumour cells with metastatic capacities that have acquired many mechanisms to survive, proliferate, evade and resist anti-cancer therapy. Studies assessing marker profiles to identify 'metastatic' tumour cells could prove beneficial in treating and preventing bone metastasis. Research into these metastatic-initiating cells is currently under investigation with the suggestion that these cells have self-renewal properties and give rise to phenotypically diverse tumour cell population that are efficient in evading therapy and survival in hostile environments once de-attached from the primary tumour site (***Mimeault and Batra, 2010).***

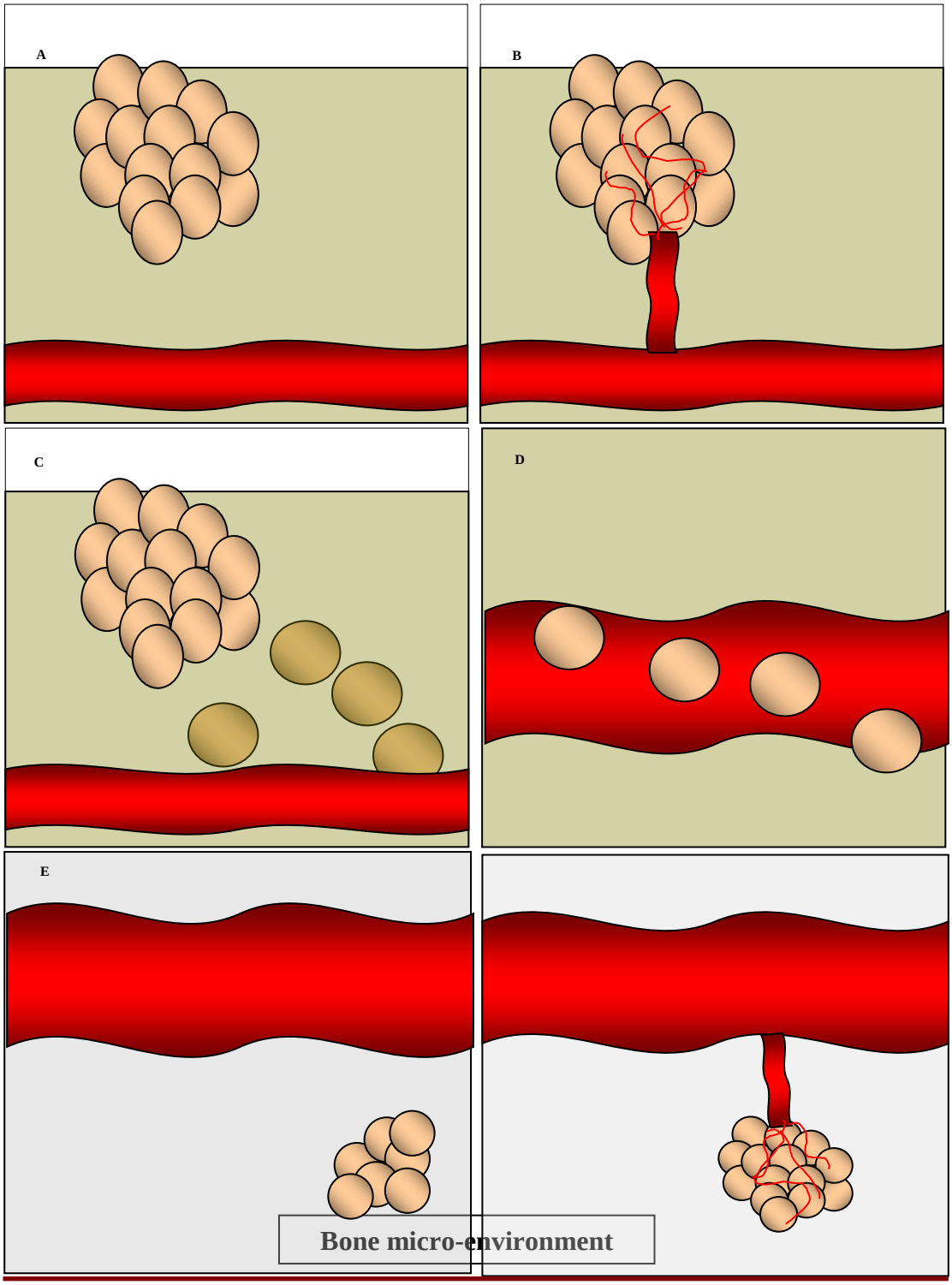

Figure 6.1 ***The Metastatic Cascade*** (**A**) Once a tumour reached a diameter of 1-2mm, it can no longer obtain nutrients via diffusion, there the process of (**B**) tumour angiogenesis is initiated primarily through the actions of VEGF. (**C**) Once a tumour vasculature has established, tumour cell must detach from the primary tumour and invade the surrounding ECM. (**D**) Entry into the vasculature and extravasation precedes (**E**) entry into the secondary site of metastasis (e.g. bone). (**F**) Lastly, once the tumour cells have colonised the secondary tissue, process of tumour angiogenesis is re-initiated to allow further dissemination of the tumour cells.
Adapted from Mathot & Stenninger, 2012. Behaviour of seeds and soil in the mechanism of metastasis: A deeper understanding

6.1.4 Breast Cancer Induced Bone Metastasis

Post mortem examinations of breast cancer patients demonstrate approximately 70% of all patients have evidence of bone metastasis (***Suva et al, 2009***). Understanding the mechanism by which breast cancer cells metastases to and survive within the new bone environment will allow for a more effective means of treatment and potential preventative measures. Bone metastasis associated with breast cancer has a higher mortality rate than the primary disease as the metastatic tumour cells affect the health of the bone both via direct effects of the tumour cells and indirect effects of treatment, which may lead to rapid loss of bone. Symptoms associated with bone metastasis include, hypocalcaemia, bone pain, fractures and nerve compressions (***Korzlow et al, 2005***).There are two types of bone metastasis; osteolytic and osteoblastic. Osteolytic metastasis results in bone destruction whereas osteoblastic activity is associated with new bone formation (***Rose & Siegel, 2006***). Although there is evidence of both types of bone metastasis occurring, breast cancer patients commonly develop osteolytic lesions (***Zhang et al, 2009***).

The bone offers a favourable micro-environment for breast cancer metastasis due to a variety of growth factors and cytokines present in the bone matrix. Bone tissue is constantly undergoing remodelling during development, physiological adult skeletal remodelling and during trauma repair. The process of bone remodelling requires vascularisation thus the network formed between these two processes indicates an important link between factors that drive both vascularisation and bone remodelling, such as VEGF.

Under physiological conditions the direct communication between osteoclasts and osteoblasts through cytokine signalling is important in maintaining bone turnover events, as the ratio of these two cell types is required to maintain bone homeostasis (***Yang et al, 2012***). In the case of breast cancer-induced bone metastasis, excessive bone destruction is demonstrated as a result of increased osteoclast numbers. It is thought that the increase in osteoclast numbers present in bone metastasis is a result of indirect or direct effects of the tumour cells on osteoclast activity. Excessive bone destruction leads to an increase in cytokines and growth factors released from the bone matrix, which subsequently leads to the process known as the 'vicious cycle', as increased cytokine release from the matrix leads to further bone destruction (***Guise, 2002***). In addition osteoblasts demonstrate a regulatory role in osteoclast differentiation (***Yang et al, 2012***) therefore suggesting that treatments that alter either of the two cell types involved in bone remodelling must take into account the link that exists between osteoblasts and osteoclasts.

Bisphosphonates

Current treatment of bone metastasis for breast cancer patients is the use of bisphosphonate drugs (BPs), which are anti-resorptive agents that primarily target the bone osteoclasts (**Figure 6.2A&B**). Nitrogen-containing bisphosphonates (N-BPs) such as Risedronate and Zoledronic acid, are routinely used for treatment of lytic metastatic bone disease and are thought to elicit an anti-resorptive effect by altering bone metabolism (***Fournier et al, 2010***). Inhibition of key enzymes in the mevalonate pathway is thought to be the mechanism by which N-BPs modulate bone turnover activity, which leads to an improvement in bone health in patients with bone metastasis (***Fournier et al, 2010***). Generally BPs are known more for the palliative effects that they induce as they reduce bone loss, thus reducing the number of skeletal complications observed in breast cancer patients with bone metastasis. However, more recently, the effects of BPs on tumour cell activity are being investigated with evidence both *in vitro* and *in vivo* that suggests that BP display a level of anti-tumour activity (***Fournier et al, 2010***). Risedronate displays anti-proliferative activity on a range of breast cancer cell lines *in vitro*, including the highly metastatic MDA-MB-231 cells (***Fournier et al, 2010***). In addition daily injection of Risedronate also reduced the size of bone metastasis formed in the hind limbs of BALB/c nude mice that were injected with human B02 breast cancer cells (MDA-MB-231-BO2) via tail vein injection (***Fournier et al, 2010***). In the ***Fournier et al*** study, risedronate treatment commenced on the same day that the tumours were injected, however the majority of breast cancer patients already have signs of metastasis when diagnosed, therefore investigating whether N-BPs are able to reduce tumour burden once the breast cancer cells have colonised the secondary site of metastasis may be more relevant to the clinical settings.

A 1 to 6% incident rate of osteonecrosis of the bone has been reported with the use of BPs alone in the clinic (***Guarneri et al, 2010***). In a high portion of the *in vitro* and pre-clinical studies, anti-tumour activity associated with BPs is a result of high doses that are not clinically relevant (***Fournier et al, 2010***) There are other studies that combine clinically relevant doses of Zoledronic acid with chemotherapeutic agents (such as doxorubin) that have shown synergistic effects of combining N-BPs with standard anti-tumour therapy (***Ottewell et al, 2009***). However the use of BPs as anti-tumour agents is still being investigation.

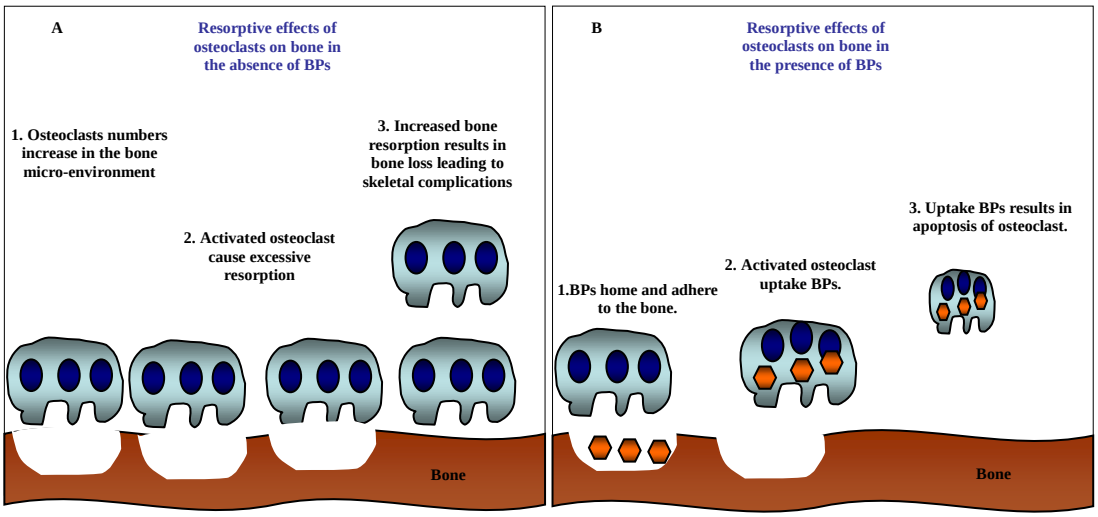

Figure 6.2 ***Effects of Bisphosphonates***:
(**A**) In the absence of BPs, increased osteoclast numbers recruited by tumour cells results in excessive bone destruction which is the primary cause of morbidity in patients with bone metastasis (**B**) BPs, have high affinity for bone , therefore rapidly 'home' to the bone and are taken up by osteoclasts. The presence of BPs in osteoclasts causes apoptosis of osteoclasts by inhibiting key enzymes involved in the metabolism of these cells (via the mevalonate pathway).

Adapted from Drake &Cremers, 2010. Bisphosphonates Therapeutic in Bone: the Hard and SOFT Data on Osteoclast Inhibition.

6.1.5 Role of VEGF in Bone Metastasis

The literature available concerning the role of VEGF in tumour progression is vast and supports the importance of VEGF in many aspects of tumour progression, including both primary and secondary metastatic disease as serum levels of $VEGF_{165}$ and $VEGF_{121}$ in breast cancer patients demonstrate a positive association with bone metastasis (***Voorzanger-Rousselot et al, 2006***), with increased plasma VEGF levels being observed in many patients with metastasis compared with patients that do not have metastasis. The evidence from the literature suggests that VEGF is a feasible target for treating the metastatic disease (***Pluijm et al, 2001***). In addition targeting bone metastasis specifically is justified as breast cancer cells expression of VEGF mRNA is thought to be significantly up-regulated in bone metastasis compared with soft tissue metastasis in experimental models (***Pluijm et al, 2001***).

VEGF although originally identified as an angiogenic mitogen for vascular endothelial cells, is a multi-functional molecule that exerts effects on a variety of different cell types. VEGF receptors have been identified on the surface of osteoclast and osteoblast cells in the bone matrix and thus suggest a role for VEGF in bone remodelling. The role of VEGF in bone metastasis is two-fold, (1) as an angiogenic factor and (2) via effects on osteoclasts and

osteoblasts. Osteoblasts and osteoclasts are located in close proximity to ECs, haemopoietic cells and stromal cells in the bone micro-environment and the concordant actions of these different cell types is important in maintaining healthy bone tissue (***Deckers et al, 2000 & Street et al, 2009***).

The Effects of VEGF on Osteoblasts

VEGF-R1 and VEGF-R2 are both expressed on human osteoblasts, however functional activity of VEGF on osteoblasts is thought to be via VEGF-R1, as an *in vitro* kinase assay failed to demonstrate activation of VEGF-R2 after stimulation with VEGF (***Yang et al, 2012***). VEGF regulates differentiation of primary human osteoblasts (***Yang et al, 2012***) and osteoblast cell survival *in vitro* (***Street & Lenehan, 2009***). In addition to expressing VEGF receptors, osteoblasts are also known to produce VEGF under certain conditions, including hypoxia (***Street & Lenehan, 2009***) suggesting both a paracrine and autocrine role for VEGF in osteoblast activity.

The Effects of VEGF on Osteoclasts

VEGF receptor protein expression is detected on isolated osteoclasts (***Nakagawa et al, 2000; Street & Lenehan, 2009***). VEGF demonstrates a pro-survival activity on mature osteoclasts isolated from rabbits bones *in vitro* as well as increasing the level of bone resorption (***Nakagawa et al, 2000***) suggesting that the increased osteoclast resorption induced by VEGF, is potentially due to increased osteoclast survival.

VEGF also regulates osteoclast invasion as the addition of exogenous human VEGF increased osteoclast invasion *in vitro* by approximately 40 to 50% compared with non-stimulated controls (***Henriksen et al, 2003***). Two forms of VEGF inhibition were utilised in this study, (1) addition of soluble VEGF-R1 and (2) treatment of cells with endostatin. Endostatin is an endogenous C-terminal fragment derived from type XVIII collagen and demonstrates anti-VEGF effects by blocking VEGF from binding VEGF-R2 and subsequent activation of ERK and p38 MAPK (***Kim et al, 2002***). The addition of soluble VEGF-R1 resulted in inhibition of VEGF mediated osteoclast invasion. The presence of endostatin had a similar effect on osteoclast invasion. However, this was only observed when the osteoclasts were pre-incubated with endostatin for 30 minutes (***Henriksen et al, 2003***). VEGF is also involved in osteoclast recruitment (***Yang et al, 2012***) which is important in breast cancer-induced bone metastasis, where an increase in osteoclast number is observed.

These functional studies and the clinical assessment of VEGF expression in patients with bone metastasis, provide evidence and rationale for targeting the VEGF pathway as an approach to inhibit or reduce breast cancer-induced bone metastasis. There is also evidence suggesting a link between tumour angiogenesis and metastasis (***Weidner et al, 1991***) which suggests the potential for anti-VEGF treatment to target both primary tumour angiogenesis and bone remodelling process that occur during bone metastasis.

6.2 MATERIALS & METHODS

6.2 Bone Metastasis Model

6.2.1 Luciferin Imaging

The luciferin is a bioluminescence *in vivo* imaging system that allows for non-invasive tumour monitoring over time. D-Luciferin is a low molecular weight organic compound that freely diffuses across membranes. In the *in vivo* system, animals are injected with tumour cells that are tagged with luciferase. When injected, luciferase catalyses the oxidisation of D-luciferin to oxyluciferin in the presence of oxygen, and the co-factors, ATP and Mg^{2+}. This oxidisation reaction produces a yellow/green light which *in vivo* at 37^{o}C is visualised at 560nm. Since ATP is required for the reaction to occur, the imaging can also be used as an indicator of live/dead tumour staining.

6.2.2 Protocol

Luciferase labelled MDA-MB-231 ($1x10^5$) breast cancer cells were injected via intra-cardiac injection into the left ventricle of anesthetised (isoflurane) 6 week old BALB/C nude female mice (performed by Dr Kim Reeves, University of Sheffield). BALB/C nude mice were used as previously, studies comparing that 'homing' of MDA-MB-231 breast cancer to the tibia in three different nude mouse strains (1) nude SCIDs, (2) CD1 and (3) BALB/C observed that a higher incidence of breast cancer metastasis to the bone was observed in the BALB/C nude mice compared with the other two strains (***Dr Holen group, Sheffield, data not published***).

Mice were imaged twice weekly using the IVIS Lumina II bioluminescence system for the presence of tumours by injecting (150mg/kg) of D-luciferin (potassium salt) via i.p. injection (200µl) 15 minutes prior to imaging. Once a bioluminescence signal was detected in the bone, treatment with Bz (0.5mg/kg), Bz (0.1mg/kg) and the control vehicle (0.5mg/kg) commenced. The control vehicle was deemed a relevant control for these experiments as the control vehicle displayed similar inhibitory effects on primary tumour growth as those observed with Bz. Tumours were monitored for approximately 5 week, twice weekly by

IVIS imaging. The end of procedure (EOP) was marked as no more then six weeks after administration of the first treatment, as at this time point, increased tumour burden could lead to morbidity. Animals were culled prior to this if required. All animals were culled at the same time point (56 days post injection of the MDA-MB-231 Luciferase labelled cells). Hind limbs were removed, decalcified and processed (**2.8.4**) for micro-CT analysis and bone histomorphometry. Following micro-CT analysis bones were wax embedded and sectioned to allow for Tartrate-resistant acid phosphatase (TRAP) staining in osteoclasts to assess bone cell turnover events.

6.2.3 Analysis

Analysis of the IVIS data was carried out using the IVIS software (Caliper Life Sciences, UK). Images observed were loaded and regions of interest (ROIs) drawn around each individual metastasis, present in individual animals. The total flux measured as radiance was then calculated for each individual animal from the signal obtained from the ventral side (**section 2.8.4**).

Micro-computed tomography (μ-CT) analysis was carried out using a Skyscan 1172 X-ray-computed micro-tomograph (Skyscan) on representative animals (n=3) from each treatment group (Bz 0.1mg/kg, Bz 0.5mg/kg and CV). Imaging was carried out at a voltage of 49kV and a current of 200μA, an aluminium filter of 0.5mm and a pixel size was set to a dimension of 4.3μm. Scanning was initiated from the growth plate and images were reconstructed with NRecon software. The volume of interest was specified by drawing on the two-dimensional (2D) acquisition images from which trabecular bone mineral density was calculated. In addition other trabecular bone morphometric analysis was calculated using the SkyScan software including trabecular thickness, trabecular bone volume and trabecular number.

Bone Turnover Analysis

Osteoclasts and osteoblasts are the two main cell types involved in bone remodelling and the ratio of these two cells present in bone is crucial for maintaining 'healthy' bone. An increase in osteoclast number is usually associated with breast cancer-induced bone metastasis and therefore these cells are the main target for reducing bone loss in metastatic disease. TRAP staining measured the number of osteoclasts present in the bone sections whereas osteoblast numbers were measured based on morphological identification of the cells in the bone sections (**Figure 6.3**). In this project, osteoclast and osteoblast that were not in direct contact with the tumour were quantified.

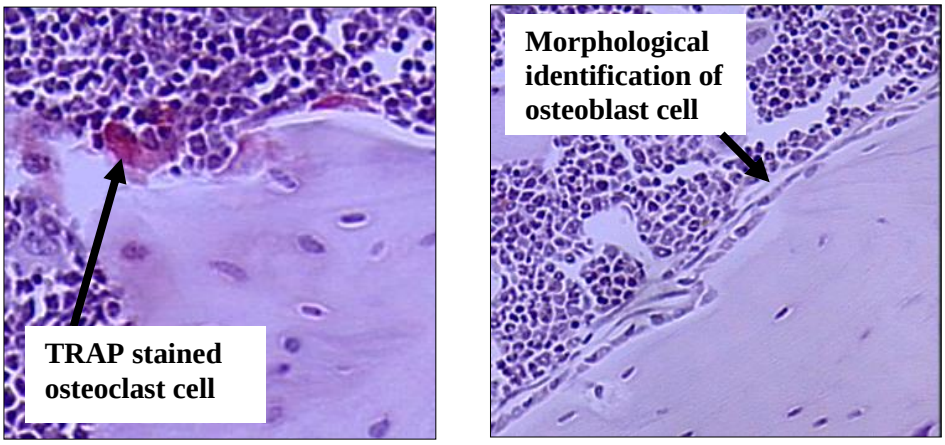

Figure 6.3 (A) Example of TRAP staining: identifying osteoclasts present in a wax-embedded bone section from a control treated animal. (B) Osteoblast quantification was carried out on the same sections that were stained for TRAP. Osteoblasts were identified from the unique morphology.

6.2.4 Statistical Analysis

Following assessment of normality statistical analysis was performed using the non-parametric test, Mann-Whitney U Test or a student's t test. When comparing multiple groups the One Way ANOVA, followed by the Dunn's post-hoc test was used to determine any differences between groups. Data is presented as mean±SEM and statistical significance was considered at $p=0.05$. All statistical analysis was performed using the Sigmaplot package (version 11).

6.3 RESULTS

6.3.1 Effects of Bz on Breast Cancer Induced Bone Metastasis

Due to time constraints and resources and since no inhibition on primary tumour growth were observed with either neuropilin binding peptide it was decided that the preliminary bone metastasis experiments be carried out with Bz alone and the control vehicle. In these experiments, the MDA-MB-231 breast cancer cells rather then the MDA-MB-436 breast cancer cells were utilised, as they have previously been shown to migrate to the bone following intra-cardiac injection.

At the end of the experiment (day 56 post injection of MDA-MB-231 Luciferase cells), treatment with Bz (n=4) at 0.1mg/kg reduced the total bone tumour burden (hind limbs, jaw, shoulders and rib cage) present compared with the CV (n=8) control group (**Figure 6.4** and

Figure 6.5a), when measured as the total bioluminescence signal produced from the IVIS LuminaII software (mean±SEM total flux; Bz (0.1mg/kg) vs. CV; 2264563±747005 vs. 9154359±7344633; n=4/8, NS) which did not reach statistical significance (*p=0.808*). Additionally Bz (n=4) at 0.1mg/kg also reduced tumour burden present in the hind limbs only compared with the CV (n=5) control group (mean±SEM total flux; Bz (0.1mg/kg) vs. CV; 1921925±623456 vs. 4373306±36684411; n=4/5, ns) (**Figure 6.6a**), but again this did not reach statistical significance (*p=0.413*).

In contrast, treatment with Bz (n=4) at 0.5mg/kg increased the total tumour burden present when compared with the CV (n=8) control group (mean±SEM total flux; Bz (0.5mg/kg) vs. CV; 17591394±11493360 vs. 9154359±734463; n=4/8, ns) (**Figure 6.5b**) but this was not significant (*p=0.808*). Similarly, the total tumour burden present in the hind limbs after treatment with Bz (0.5mg/kg) (n=3) also demonstrated an increase compared with the CV (n=5) control group (mean±SEM total flux; Bz (0.5mg/kg) vs. CV; 22660207±14051318 vs. 4373306±36684411; n=3/5, ns), which was not significant (**Figure 6.6b**).

Interestingly, the number of metastasis present in each individual animal at the end of the experiment (day 56) was lower in both of the Bz treated groups (0.1mg/kg n=4 & 0.5mg/kg n=4) compared with the CV (n=8) control group (mean±SEM; Bz (0.1mg/kg) and Bz (0.5mg/kg) vs. CV; 2.8±0.5 and 2.3±1.3 vs. 4.3±0.6; n=4/8, ns) (**Figure 6.7**), but this was not statistically significant (*p=0.164* and *p=0.170* respectively), potentially due to low numbers. This trend observed with Bz (0.1mg/kg) treatment suggests both a reduction in the number of bone metastasis and the overall bone tumour burden.

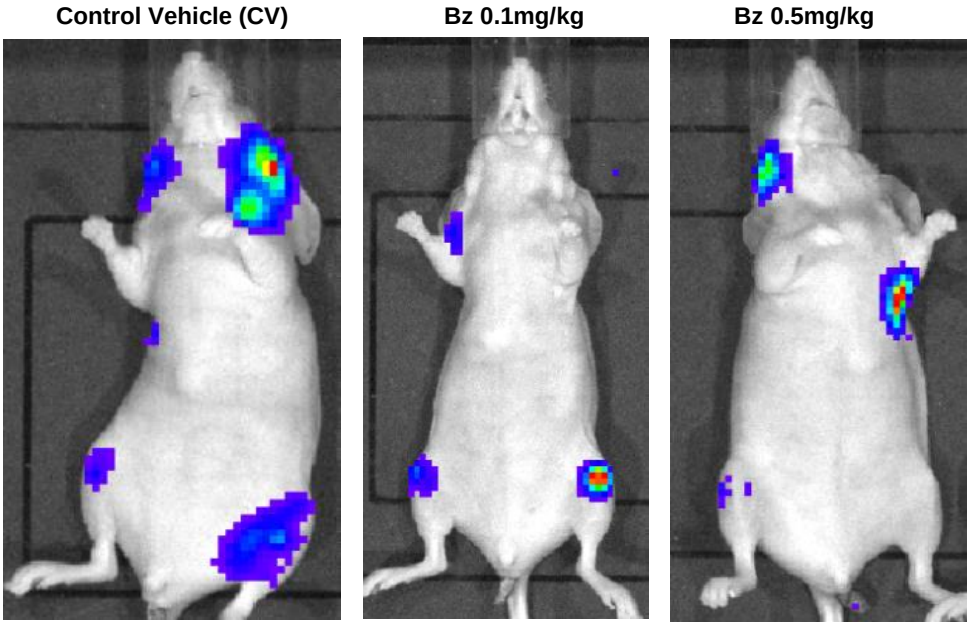

Figure 6.4 ***Effects of Bz on Overall Tumour Burden:***
Representative images of ventral IVIS Lumina II images of the luciferase signal after injection of D-luciferin taken on 56 days post injection of Luciferase labelled MDA-MB-231 breast cancer cells (i.c.) The number and size of the metastatic burden present was lower in the Bz treated animals compared with the control vehicle (CV) group.

A

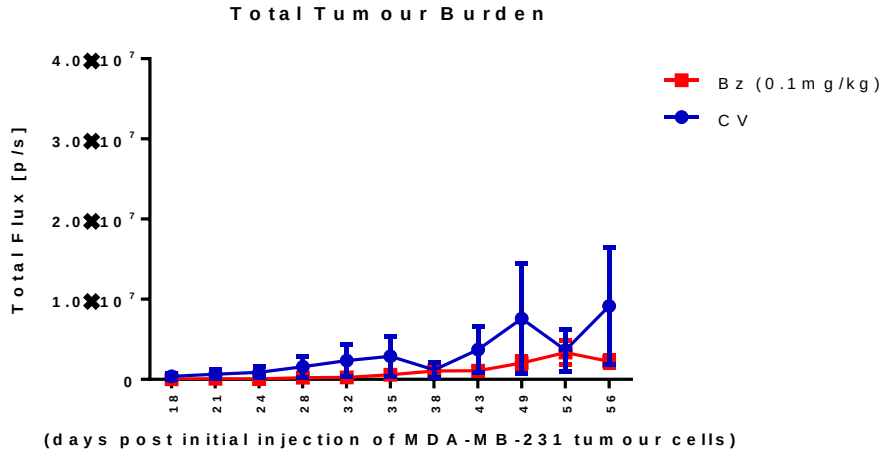

B

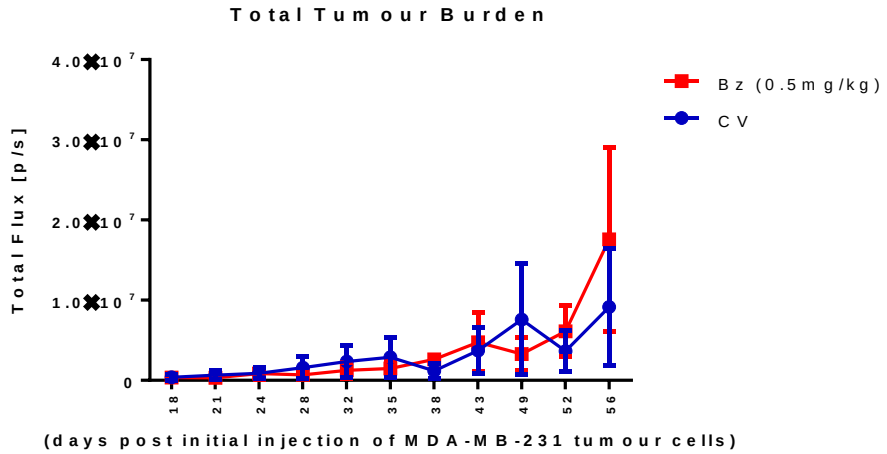

Figure 6.5 ***Effects of Bz on Overall Tumour Burden*** (**A**) Bz at 0.1mg/kg reduced the total tumour burden compared to the control vehicle (CV), this was not significant at any time point (**B**) In contrast, Bz at 0.5mg/kg increased the total tumour burden compared to the control vehicle (CV), this was not significant at any time point.

Data is presented as mean±SEM total flux; CV n=8 and Bz (0.1mg/kg & 0.5mg/kg) n=4, NS. Statistical analysis was performed using the One Way ANOVA (Sigmaplot 11 software).

A

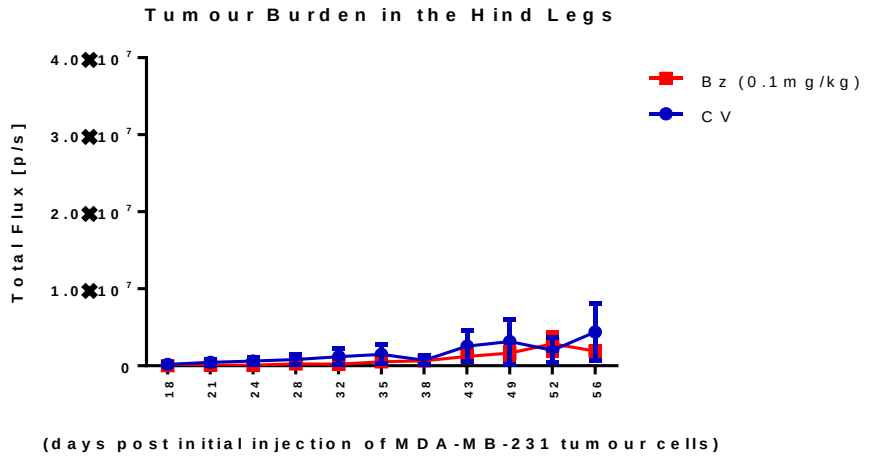

B

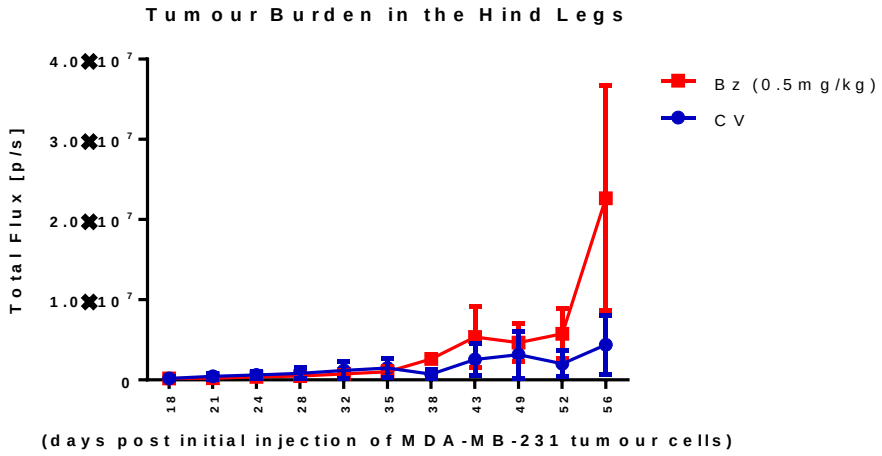

Figure 6.6 ***Effects of Bz on Metastasis in the Hind Limbs:***
(**A**) Bz at 0.1mg/kg reduced hind leg tumour burden compared with the control vehicle (CV), this was not significant at any time point (**B**) In contrast, Bz at 0.5mg/kg increased the hind leg tumour burden compared with the control vehicle (CV), this was not significant at any time point.

Data is presented as mean±SEM total flux; CV n=8 and Bz (0.1mg/kg & 0.5mg/kg) n=4, NS Statistical analysis was performed using The One Way ANOVA (Sigmaplot 11 software)

A

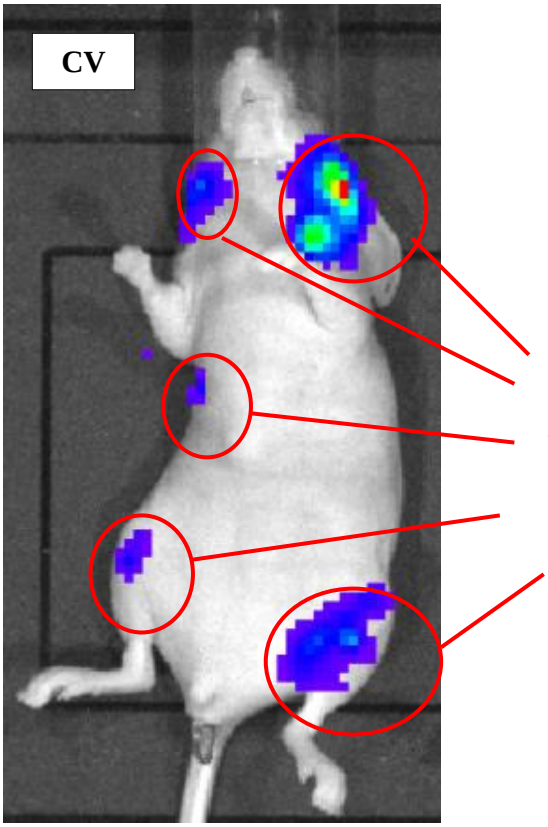

Five Individual metastatic regions within one control vehicle treated animal

B

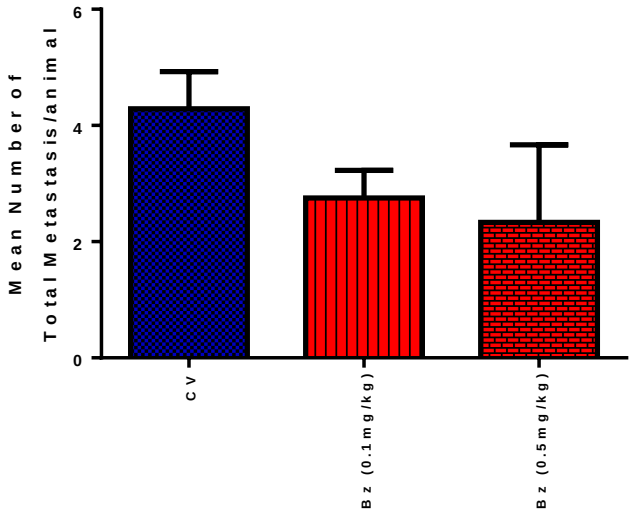

Figure 6.7 ***Effects of Bz on the Number of Bone Metastasis Present:***
(A) A representative image illustrating how the mean number of bone metastasis in each individual animal at the end of the experiment (Day 56) was measured. (**B**) Both Bz (0.1mg/kg) and Bz (0.5mg/kg) reduced the number of metastasis present in each individual animal compared with the control vehicle (CV)

Data is presented as mean±SEM number of metastasis; CV n=8 and Bz (0.1mg/kg & 0.5mg/kg) n=4, NS. Statistical analysis was performed using a t-test (Sigmaplot software)

Bone metastasis was evident in the jaw, shoulders, hind legs and rib cage of animals injected with MDA-MB-231 breast cancer cells by the end of the study (day 56). There was also differences in the of location of the breast cancer induced bone metastasis between the different treatment groups, with the control vehicle treated animals observing a higher incidence of metastasis (**Figure 6.8**) to the jaw and the rib cage compared with the Bz treated animals (**Figure 6.8**). In animals treated with Bz there was a higher incidence of bone metastasis to the hind legs (**Figure 6.8**).

A

	Jaw	Shoulder	Hind Legs	Rib Cage
CV (n=8)	71.4%	42.9%	71.4%	85.7%
Bz 0.1mg/kg (n=4)	50%	50%	100%	0
Bz 0.5mg/kg (n=4)	0	33.3%	100%	33.3%

B

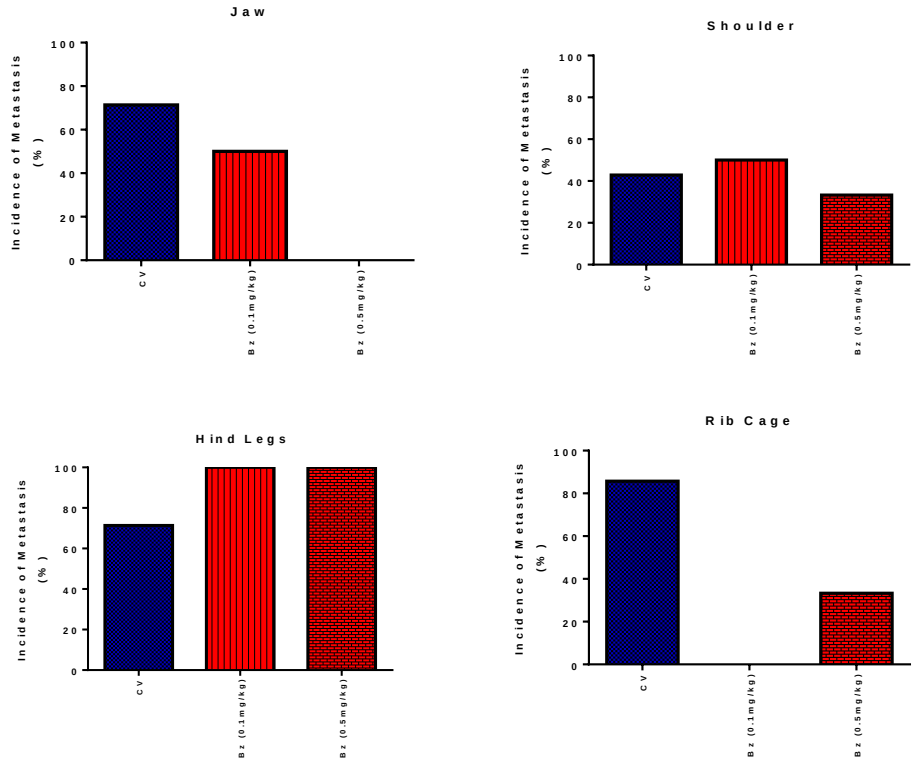

Figure 6.8 ***Incidence of Bone Metastasis:***
(**A**) Summarises the incidence of metastasis in different locations with the two doses of Bz (0.1mg/kg and 0.5mg/kg) (**B**) Treatment with Bz with both doses reduces the further dissemination of breast cancer cells to distant sites compared with the control vehicle (CV).

Data is presented as % of incidence; CV n=8 and Bz (0.1mg/kg & 0.5mg/kg) n=4.

6.3.2 Effects of Bz on Bone Structure

The mechanism of the reduction in MDA-MB-231Luciferase tumour burden in the tibia of mice treated with Bz was investigated. Micro-CT analysis was carried out to assess the effects of Bz on trabecular bone, including a list of parameters (**Figure 6.9**).

Bone mineral density was measured with no differences observed between Bz treated (0.1mg/kg and 0.5mg/kg) compared with the CV control group (respectively). However, further analysis was carried out on the trabecular bone to establish if any changes in the micro-architecture were observed after treatment with Bz.

Trabecular Bone Morphometry

A number of parameters can be quantified using μCT that assess the effects of Bz treatment on the micro-architecture of the trabecular bone with the following five considered the most relevant, 1) trabecular bone volume (bv/tv) 2) trabecular number (Tb) (3) trabecular thickness, (4) trabecular separation and (5) the structure model index (SMI) (***Bouxsein et al, 2010***). The SMI measures the change in trabecular bone structure from a plate-like to rod-like morphology. These measures are reflective of the strength and health of the bone structure. For the analysis on bone histomorphometry, a representative number of hind limbs with a tumour signal at the end of the experiment (n=3/group) were assessed using μ-CT.

Bone Volume: Trabecular Bone Volume (bv/tv)

The bv/tv measure is indicative of total bone volume occupied by mineralised bone, with a higher bv/tv value indicating healthier bone. In the current study, treatment with Bz (0.1mg/kg) significantly (*p=0.031*) increased the percentage bv/tv compared with the CV control group (mean±SEM % bv/tv; Bz (0.1mg/kg) vs. CV; 12±0 vs. 9±0; n=3, *p=0.031*) (**Figure 6.10**). A similar trend was observed with Bz (0.5mg/kg), (mean±SEM % bv/tv; Bz (0.5mg/kg) vs. CV; 12±1 vs. 9±0.4; n=3, *p=0.074*) however this increase did not reach statistical significance (*p=0.074*) (**Figure 6.10**).

Trabecular Number

This quantifies the average number of trabeculae per unit length. Treatment with Bz (0.1mg/kg) significantly (*p=0.022*) increased the Tb number compared with the CV control group (mean±SEM number (mm^3); Bz (0.1mg/kg) vs. CV; 3±0.3 vs. 2±0.1; n=3, *p= 0.022*) (**Figure 6.10**). The higher dose of Bz (0.5mg/kg) displayed a similar trend (mean±SEM number (mm^3); 3±0.3 vs. 2±0.1; n=3, *p=0.100*) however the increase did not reach statistical significance (*p= 0.100*) (**Figure 6.10**).

Trabecular Thickness

Treatment with Bz (0.1mg/kg) displayed no significant (*p=0.065*) effects on Tb. thickness compared with the CV control group (mean±SEM thickness (mm); Bz (0.1mg/kg) vs. CV; 0.04±0.002 vs. 0.05±0.002; n=3, *p=0.065*) (**Figure 6.10**). In contrast, Bz (0.5mg/kg) significantly reduced the Tb. thickness compared with the CV control group (mean±SEM thickness (mm); Bz (0.5mg/kg) vs. CV; 0.04±0.001 vs. 0.05±0.002; n=3, *p=0.011*) (**Figure 6.10**).

Trabecular Separation

Measurement of Tb.Sp demonstrated a significant decrease in trabecular separation after treatment with Bz (0.1mg/kg) compared with the CV control group (mean±SEM Tb.Sp; Bz (0.1mg/kg) vs. CV; 0.2±0.01 vs. 0.3±0.01; n=3, *p=0.017*) (**Figure 6.10**). Similarly Bz (0.5mg/kg) demonstrated Tb. separation compared with the CV control group (mean±SEM Tb.Sp; Bz (0.5mg/kg) vs. CV 0.2±0.01 vs. 0.3±0.01; n=3, *p=0.005*) (**Figure 6.10**).

Structure Model Index (SMI)

Treatment with Bz at both concentrations (0.1mg/kg and 0.5mg/kg) significantly (*p=0.024* and *p=0.008* respectively) decreased the SMI ratio compared with the CV control group (1.7±0.05 and 1.7±0.01 vs. 1.9±0.1 respectively) (**Figure 6.10**).

A

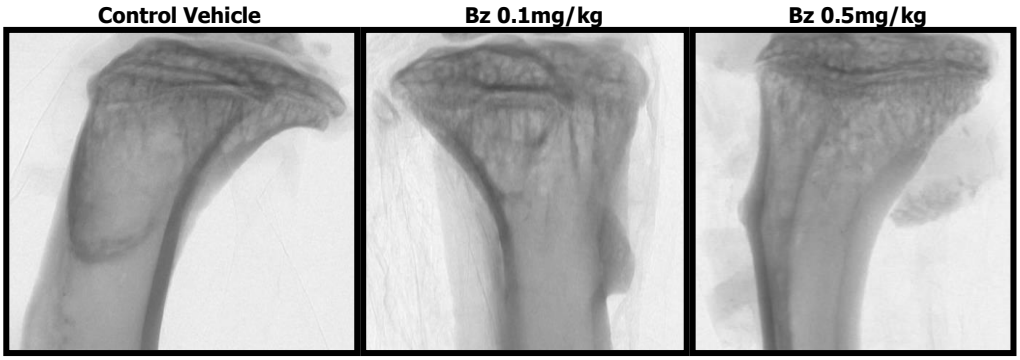

B

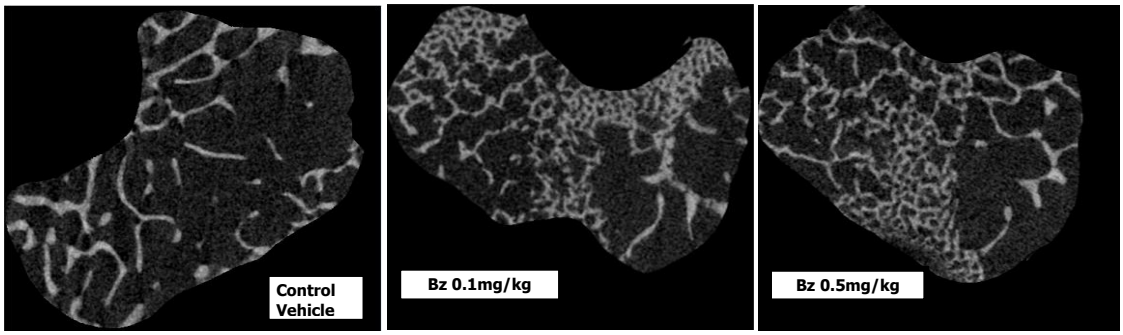

Figure 6.9 ***Effects of Bz on Bone Structure:***
Representative images from the (**A**) micro-CT scan of the tibia that were used to create the 2D and 3D required for further analysis of the bone structure. (**B**) 3D reconstructions of the trabecular. From the images, it can be observed that the spacing of the trabecular bone is more compact in the Bz treated animals, suggesting that Bz is modulating the bone micro-environment.

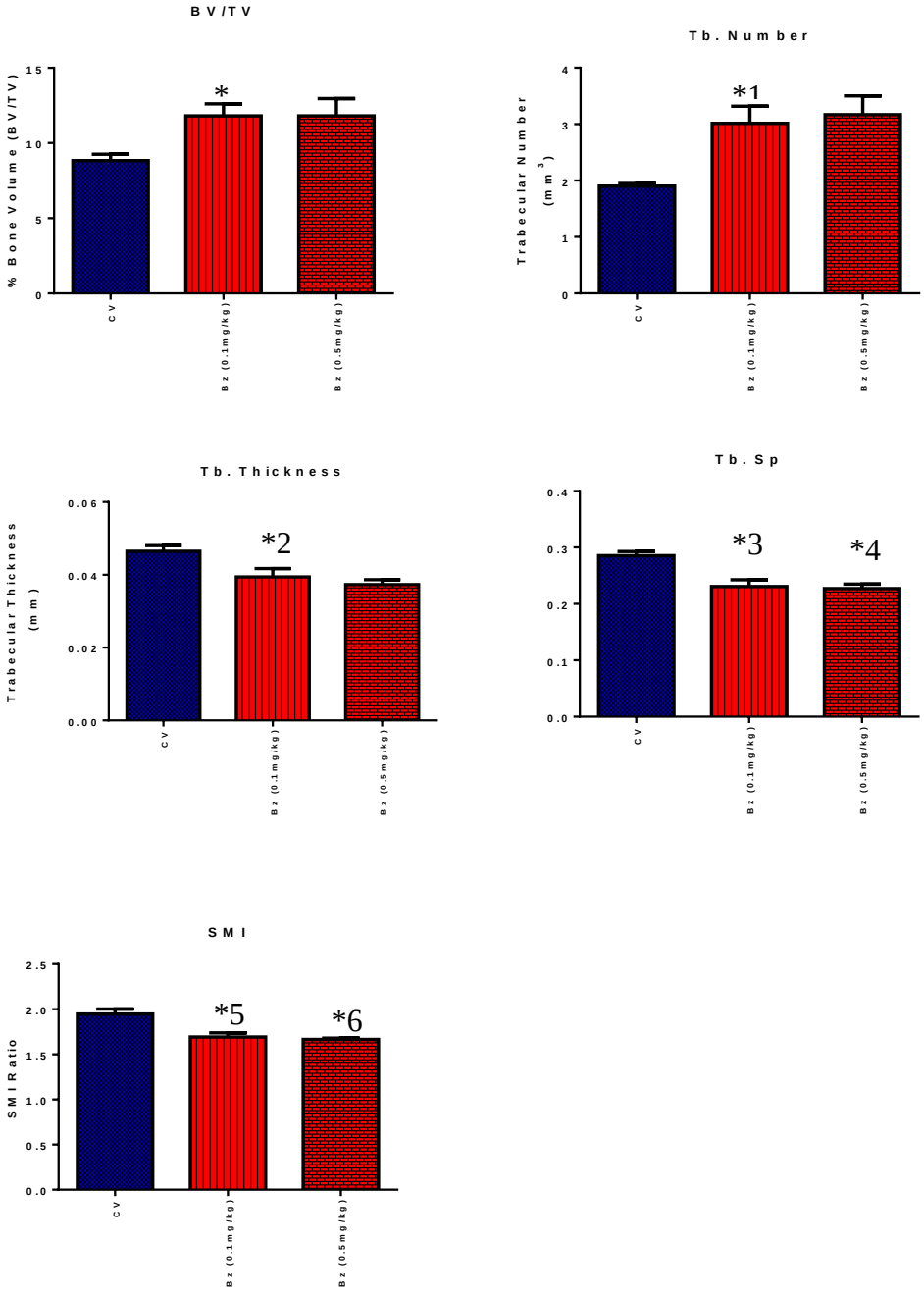

Figure 6.10 ***Effects of Bz on Bone Micro-architecture:***
From the different measures above, it appears that Bz treatment is modulating the bone environment and is aiding health of the bone. The different parameters indicate the bone strength and from data, there is evidence to suggest that Bz is interacting with the bone remodelling cells, either directly or indirectly, in order to modulate changes in the bone micro-environment, leading to increased bone strength.

Data is presented as mean±SEM; n=3, p<0.05. Statistical analysis was performed using a t-test (Sigmaplot 11 software).
**p=0.074; *1 p=0.022; *2 p= 0.011; *3 p=0.005; *4 p=0.024 and *5 p=0.008*

6.3.3 Effects of Bz on Bone Turnover

As most breast cancer induced bone metastasis is of an osteolytic nature, the bone remodelling process is usually favoured towards a higher presence of osteoclast numbers versus osteoblast, as this allows for bone destruction and tumour cell expansion in the new bone environment, thus balancing this ratio would be an important mechanism of therapy.

Treatment with Bz with either dose did not change the number of osteoclasts per mm of trabecular bone surface that was not in contact with the tumour, compared with the CV control group (mean±SEM; Bz 0.1 and 0.5mg/kg vs. CV; 11±19 and 0.4±0.4 vs. 3±5; n=3, ns) (**Figure 6.11**). Similarly, the number of osteoblast numbers not in contact with the tumour after treatment with either Bz dose remained unchanged compared with the CV control group (mean±SEM; Bz 0.1 and 0.5mg/kg vs. CV; 1±2 and 3±3 vs. 4±6; n=3, ns) (**Figure 6.11**). The number of osteoclast and osteoblasts in the sections were relatively low. Analysis on these bone sections were carried out at a depth of 3μM , thus analysis of sections cut deeper into the bone may reflect more accurately, the bone remodelling events occurring in both the control and the Bz treated groups.

Additionally due to the nature of Bz and the proposed mechanism of action associated with this anti-angiogenic drug, CD34 analysis was carried out on the bone sections. However CD34 staining on the bone sections was not as obvious as that observed in the earlier tumour sections and due to time constraints, a repeat staining experiment could not be carried out, however this is a potential stain that would be useful in establishing further the role of Bz in breast cancer induced bone metastasis.

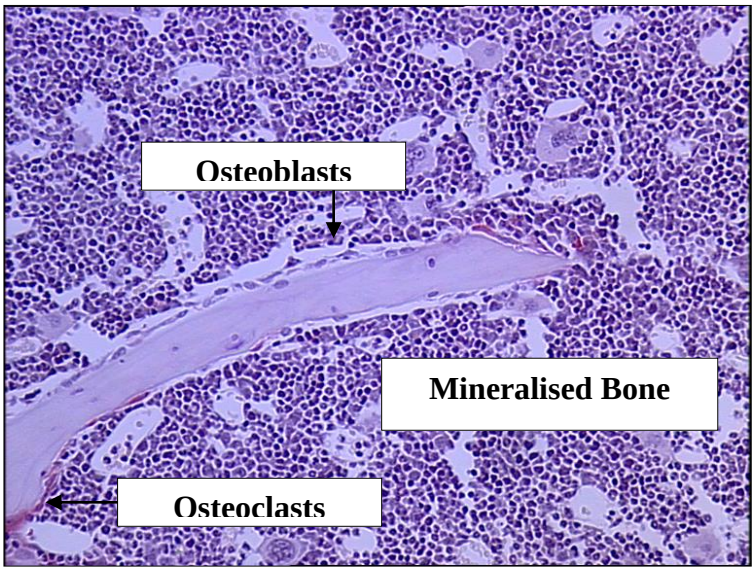

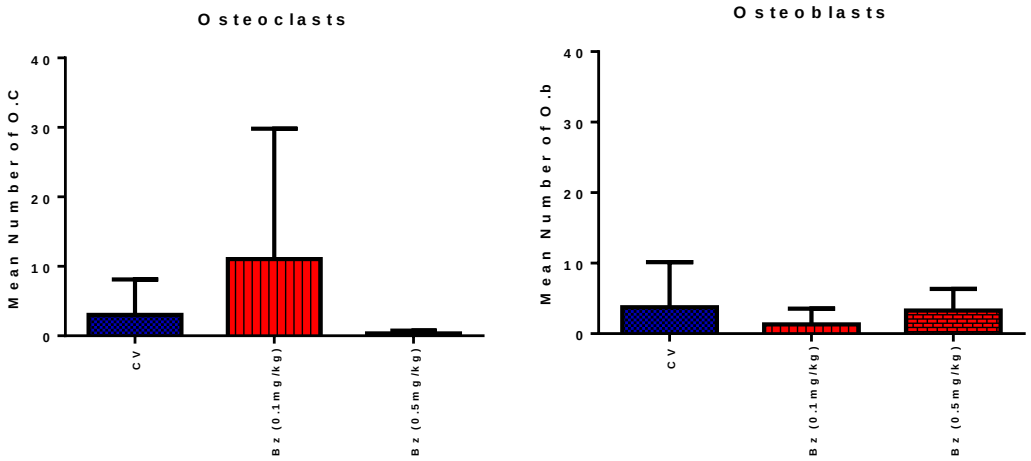

Figure 6.11 **Effects of Bz on Bone Remodelling:**
(**A**) Representative image of TRAP staining and morphological identification of osteoblasts (**B**) The levels of osteoclasts and osteoblast remained unchanged following treatment with Bz

Data is presented as mean±SEM osteoclast or osteoblast number; n=3; NS. Statistical analysis was performed using test (Sigmaplot software).

KEYPOINT

The bone metastasis model demonstrated clear distinction between the actions of Bz compared with the control vehicle

6.4 BONE METASTASIS

DISCUSSION

6.4.1 Effects of Bz on Breast Cancer Induced Bone Metastasis

Breast cancer induced metastasis is a major cause of morbidity in breast cancer patients with no current curative treatment. The current pilot study suggests that Bz (0.1mg/kg) is capable of both reducing the number of bone metastasis present and also the size of the metastasis., however a larger data set would be required to confirm this data, as the decrease in tumour burden, suggested as trend but was not significant.

The bone mineral density remains unchanged after treatment. VEGF is an important regulator of bone cell activity, and although TRAP staining allows osteoclast and osteoblast numbers to be quantified, this does not necessarily reflect the functional ability of these cells. Thus treatment with Bz may effect bone turnover via direct actions on the bone cells, which may not be reflected by the numbers present. The different parameters measured to assess trabecular bone morphometry suggested that Bz is capable of modulating the bone micro-environment to induce micro-architectural changes allowing improvement of bone strength. This is an important finding as many breast cancer patients that have bone metastasis suffer from fractures and bone pain. This suggests that VEGF inhibition, maybe offer an enhancement to the treatment currently provided by BPs, in that it could exert both palliative effects (see with the BPs), in addition to limiting metastatic tumour burden. Although there is increasing evidence that suggests that BPs display some anti-tumour activity there are still advantages for using anti-VEGF agents such as Bz in addition to BPs. The use of BPs in bone disease is ideal as these agents have a high affinity for bone (***Holen & Coleman et al, 2010***) and rapidly 'home' to the bone after administration where they are retained for long periods of time, up-to several years (***Holen & Coleman et al, 2010***). However this suggests that the distribution of BPs outside the bone maybe limited, thus the use of BPs as anti-cancer agents alone, may not be as efficacious as using drugs that display a more wide-spread distribution, such as Bz.

There is minimal literature available (PubMed) assessing the effects of Bz on breast cancer induced bone metastasis in experimental model. The majority of pre-clinical translation studies investigate the use of Bz for lung and lymph metastasis (***Matsui et al, 2008 &Volk et al, 2011***). In these studies MDA-MB-231 fragments were implanted into the mammary fat pad, allowed to grow for two weeks, after which treatment with Bz commenced. The experiment lasted for 56 days and the number of animals with metastasis in the lung and

lymph nodes were measured. Bz reduced the number of metastasis present in both lymph and the lungs, with a significant reduction being observed with lung metastasis (***Matsui et al, 2008***). To my knowledge this pilot study is novel, assessing the role of Bz therapy in breast cancer induced bone metastasis. There has been a similar study (***Bauerle et al, 2008)*** that assessed the effects of Bz on breast cancer-induced bone metastasis. However, the analysis carried out during the above study focused on imaging analysis of vessel formation and oseotolysis but effects on tumour metastasis on the bone micro-environment were not identified, therefore the mechanism by which Bz acts as both an inhibitor of primary and secondary tumour growth can not be established using the method in the ***Bauerle et al*** study. In addition, the model required injection of cancer cells into the femoral artery of the hind leg. This method is much more invasive then the intra-cardiac technique used during this PhD. This is important, as VEGF is a stress related protein and an invasive technique is more likely to cause an increase in VEGF expression around the bone micro-environment, thus creating false positive results. With that in my, the technique used during this PhD is more relevant and simulates bone metastasis to a greater extent than that observed in the ***Bauerle et al*** paper.

However, it is important to note that the data from this bone metastasis study is preliminary and further experiments are required to make a full assessment of any role for Bz in bone metastasis, however the results are promising. Further studies are required to confirm the preliminary experiments and investigate the mechanism by which Bz is modulating the bone micro-environment.

6.5 CHAPTER CONCLUSION

From the *in vivo* experiments, it can be concluded that the classical VEGF signalling pathway plays an important role in both primary breast cancer growth and subsequent progression to metastasis as Bz effectively reduced both breast tumour growth and the tumour burden associated with breast cancer induced metastasis. Further work enabling mechanistic studies would be useful.

Chapter Seven

Final Discussion

7. FINAL DISCUSSION

Breast cancer represents a major challenge for researchers due to the heterogeneous nature of the disease and the more recent sub-classification of invasive breast cancer. The key proposition initially suggested by Folkman (1973) that angiogenesis plays a crucial role in solid tumour development and the subsequent development of the anti-angiogenic agent, Bz, the first agent of its kind to gain FDA approval provided great promise for breast cancer therapy. As angiogenesis is a perquisite for all solid tumours, it was thought that anti-angiogenic therapy could be applied universally to all tumours that require establishment of a vasculature in order to progress. This would over-come the common side effects associated with chemotherapy and resistance to systemic therapy, since this anti-angiogenic therapy primarily targets the endothelial cells, a cell type thought to be genetically more stable then cancer cells. However, the results of clinical trials have modest effects with Bz even in combination with chemotherapy. Therefore this project aimed to test the hypothesis 'that inhibition of both VEGF receptor families simultaneously, enhances the efficacy of Bz'.

7.1 Breast Cancer Cell Lines as Representative Models of Breast Cancer

The relevance of using breast-tumour cell-lines to represent breast cancer has been questioned, especially after the identification of further molecular classifications of invasive breast cancer (***Holliday & Speirs, 2011***). However, it has been shown that specific breast cancer cell lines display similar molecular profiles and characteristics of the different sub-types of invasive breast cancers, such as luminal, basal, HER breast cancer types (***Holliday & Speirs, 2011***).

The two metastatic breast cancer cell lines (MDA-MB-231 and MDA-MB-436) used in this study displayed differential responses to treatment with the Np1 peptides *in vitro*. This further confirms the heterogeneous nature of breast cancer, as despite displaying similarities in hormone receptor status, morphology and other features that classify both cell lines as being reflective of basal B, triple negative breast cancer types (***Lehmann et al, 2011***) these two cell lines also have different mutations (such as BRCA1), expression of factors and preferentially metastasise to different locations (***Chavez et al, 2010 & Lehmann et al, 2011***). These variations are the potential explanation for the differential responses to targeted therapy, including the Np1 peptides. These findings emphasise the need for personalised medicine or biomarker analysis (***Lambrechts et al, 2013***) in identifying patients or cancer sub-types that would benefit from different therapies. Grouping sub-types of breast cancer is not likely to be an adequate approach for assigning therapy.

Xenograft models of primary breast cancer commonly consist of either implantation of human tumour cells via sub-cutaneous injection into the flank region or orthotopic injection into the mammary fat pad. It can be argued that implantation of tumour cells does not represent the entire process of breast cancer development described in the human disease and that the Polyoma middle T antigen (MMTV-PyMT) mouse models offers certain advantages over xenograft models of breast cancer. In the MMTV-PyMT murine model, mice develop the spectrum of breast disease (hyperplastic, in situ, invasive and metastatic stages) in the mammary fat pad and thereby more accurately reflecting the development of breast cancer (***Lin et al, 2003***). However, obviously, human cells are more relevant to human breast cancer, being syngenic, and of the same origin for which the drugs or therapy are designed. Thus drugs that are effective in a murine model of breast cancer may not translate to the human disease. The MMTV-PyMT model is difficult to monitor tumour growth over time, as the lesions are not clearly visible, making accurate caliper measurements of tumour volume difficult. Thus, unless MMTV-PyMT tumour implants are used, the use of the MMTV-PyMT may be limited to experiments that are looking at specific experimental time points or specific stages of the disease process, rather then monitoring tumour growth over time. More recently, a breast cancer metastasis model has been developed, that measures the entire process of metastasis (***Iorns et al, 2012).*** In this model breast cancer cell injected into the mammary fat pad resulted in spontaneous and frequent, metastasis to the lungs, lymph nodes and liver and interestingly, found that the cells present in these distant metastasis, differ greatly in gene expression. In addition, breast cancer-induced bone metastasis is a focus in this project as the majority of breast cancer patients with metastasis have evidence of bone metastasis. In the PyMT metastatic model, disease tends to localise to the lung, making the process of breast cancer-induced bone metastasis impossible to assess. There are several *in vivo* models of breast cancer available, however all have limitations, and therefore utilising the appropriate model to address the objectives of the study is an important consideration.

7.2 Bevacizumab

Bevacizumab (Bz) is a monoclonal antibody that binds to VEGF and subsequently blocks interactions with the classical VEGF receptors; VEGF receptor 1 and 2. Bz is considered an anti-angiogenic agent, that primarily targets the vasculature, (rather then the tumour epithelium) and therefore inhibits tumour progression indirectly. As expected Bz inhibited both microvascular endothelial cell differentiation and migration *in vitro* (Chapter 3) with no effects on the breast cancer cells. The effects of Bz on primary breast cancer growth *in vivo* confirms previous literature that Bz has the ability of effectively inhibiting breast cancer growth *in vivo*, both alone (alone) and in combination with other agents (paclitaxel/doxectaxel) (Chapter 5). Unfortunately, in the current study the control vehicle

for Bz displayed similar effects on primary breast cancer growth *in vivo*, as those observed with Bz. Closer inspection of the literature reveals that the vehicle in which Bz is reconstituted has not been used in previous experimental *in vitro* and *in vivo* studies. Based on the data from this current study the effects of the control vehicle itself require further investigation and future experiments assessing the effects of Bz should always include the control vehicle to allow discrimination between control vehicle induced effects and direct anti-angiogenic. The control vehicle consists of mostly sodium salts and tween20. More recent papers have demonstrated the effects of excipients such as tween20 on a number of cell types including breast cancer cell activity (***Yamagata et al, 2009, Yang et al, 2012 & Eskandani et al, 2013***). One paper reported inhibition of the levels of breast cancer resistance protein, BCRP/ABCG2 in response to tween20 both *in vitro* and *in vivo*. This provides confirmatory evidence suggesting that the inhibition induced by the Bz control vehicle may be a result of direct anti-tumour activity on the breast cancer cells and/or endothelial cells, due to the presence of tween20, especially since the control experiments in showed significant inhibition in endothelial cell differentiation in the presence of tween20 alone. Although the mechanism by which the control vehicle is inducing inhibitory effects is not likely to be via BCRP/ABCG2, the study by ***Yamagata et al,*** supports the data from the current project. Treating breast cancer cells and endothelial cells *in vitro* with tween20 alone and then using either Western blotting or protein arrays, to measure the downstream effectors associated with inhibiting breast cancer growth would be an informative study.

7.3 Neuropilin Peptides

Neuropilin receptors were originally identified as receptors for the semaphorin protein family involved in neuronal guidance (***Staton et al, 2007***). More recently the role of the neuropilin receptors in VEGF signalling is associated with angiogenesis and hence are being investigated (***Staton et al, 2007***). To date the majority of breast cancer research has focused on Np1, however the potential for Np2 in tumour progression is currently under investigation.

The responses to dual targeting observed *in vitro* with p7b (Np1) and p10 (Np1 and 2) in combination with Bz on both the microvascular endothelial cells and the breast cancer cells suggests that inhibition of VEGF interaction with either Np1 alone or both neuropilin receptors may be more beneficial then Bz alone. However, *in vivo* p7b alone failed to inhibit breast cancer growth whereas p10 displayed an inhibitory trend. The amino acid structure of the carboxy-terminus of the two peptides differs; p7b (**DKPRR**) and p10 (**RPPR**) and leads to differences in Np1 affinity. The RPPR sequence displays greater affinity to Np1 *in vitro* (***Cebe-Suarez et al, 2008***) and also shows the greatest ability to inhibit radio-labelled

$VEGF_{165}$ from binding to Np1 (***Cebe-Suarez et al, 2008***). In addition, p10 is thought to also bind Np2, therefore it is possible that *in vivo* p7b is readily displaced by endogenous $VEGF_{165}$, which provides an explanation for the disparity in the results between the *in vitro* and *in vivo* studies.

The design of the peptides could potentially be modified to produce a more effective inhibition of neuropilin activity both *in vitro* and *in vivo* and we are in discussion with Prof. Ballmer-Hofer regarding this. The neuropilin blocking peptides are short in length and also potentially have a short half-life and therefore may not be able to maintain long-term inhibition due to displacement of the peptides and subsequent instability. However limitations in the design of the peptide can be solved by peptide modification such as incorporation of a cyclic structure.

7.4 Combination Studies

In summary, the Np1 binding peptides displayed no additive inhibition on breast cancer growth compared to Bz alone either in the *in vitro* or *in vivo* setting. However the potential role that the neuropilin receptors play in providing a mechanism of escape following Bz treatment remains inconclusive, as a number of questions with regards to the design and the efficacious of the inhibitory activity of the neuropilin peptides have been raised. In addition, inhibitory effects with the two peptides alone were observed *in vitro*, however this did not translate to the *in vivo* setting for p7b, therefore raising the question of efficient delivery of p7b into the tumour. An important note to also consider is the dosing regime in combination therapy, as the order of administration of two adjuvant therapies could prove to be essential as to whether a combination treatment will ultimately prove efficacious (***Ottewell et al, 2009).*** As p10 alone suggested a trend that reduced tumour growth, however, when combined with Bz, a reduction in efficacy was observed, suggesting that either the combination of p10 and Bz does not work or that the order in which these two treatments are given is essential (***van der Veldt et al, 201***2). Therefore based on some of the questions raised in the discussion, the data from this current study is not enough to dismiss the potential of inhibiting neuropilins in breast cancer therapy.

Additionally targeting the VEGF pathway alone may not be sufficient in maintaining inhibitory effects observed with either Bz alone, anti-Np1 agents or a combination of the two, as breast cancer cells produce a repertoire of cytokines and growth factors/receptors that can aid progression of the tumour such as IL-6, IL-8, MCP-1 , RANTES (***Chavey et al, 2006***) , transforming growth factor beta (TGF-β) (***Barcellos-Hoff & Akhurst, 2009***) and fibroblast growth factor receptor (FGFR) (***Tenhagen et al, 2012***). Therefore combining Bz

or anti-neuropilin agents with inhibitors of other cytokines involved in breast cancer progression may prove more effective especially when aiming to over-come resistance associated with targeted therapy. Resistance to Bz activity is not only associated with up-regulation of factors involved in compensatory signalling pathways but can occur due to (1) induction of a more aggressive phenotype post Bz treatment, (2) selection of cancer stem cell (CSC) sub-populations and (3) induction of autophagy (***Giuliano & Pages et al, 2013***). Therefore combining anti-VEGF or other anti-angiogenic agents with a therapy that may limit the occurrence of the above mechanism may prove more beneficial in providing long-term inhibitory effects on breast cancer.

A major challenge in the use of Bz and other targeted agents, is the identification of a sub-population of patients that are likely to respond to and benefit from Bz therapy. Two recent papers reviewed the status of biomarker identification for Bz (***Lambrechts et al, 2013&Maru et al, 2013***). The papers highlighted the current challenges associated with finding useful predictive biomarker, the first being due to the vast number of angiogenic factors that are produced by tumour cells, such as FGF, angiopoeitin and PDGFs, any one of these factors could elicit a compensatory response to Bz, resulting in escape from therapy (***Lambrechts et al, 2013***). Secondly, pre-clinical analysis suggests that inhibiting VEGF results in a diverse response that ranges from inhibiting the formation of newly formed vasculature, causing regression of the pre-existing vessels and inhibiting the recruitment of bone–derived and endothelial progenitor cells (***Lambrechts et al, 2013***), these differing responses potentially lead to consequential events that may effect the outcome of response to Bz therapy in different patients. Lastly, the end points that measure clinical outcome may not allow identification of patients likely to respond to Bz (***Lambrechts et al, 2013***). High levels of VEGF correlated to significantly higher response rates to Bz treatment in breast cancer patients (***Lambrechts et al, 2013***).

7.5 Bone Metastasis

Although there are studies that investigate the use of Bz in lymph and lung metastasis (***Volk et al, 2012***) a less studied avenue of breast cancer research is the use of Bz in breast cancer induced bone metastasis *in vivo*. The current project observes very preliminary data that suggests that treatment with Bz alone could potentially be used as a curative therapy for bone metastasis, as not only was a trend that suggested a reduction in metastatic tumour burden evident but also significant improvements in the bone micro-architecture of Bz treated animals was observed. Currently, there is very little treatment beyond the use of bisphosphonates as palliative therapy for bone metastasis therefore the potential effects observed with Bz is encouraging. In addition combining Bz with a peptide that inhibits the

neuropilin receptors would be useful as in the clinical setting Bz treatment is thought to induce a more aggressive phenotype post-treatment, thus combining Bz with anti-neuropilins peptides may have more potential in reducing metastasis then Bz alone, especially with the identification of stem cell like cells that express Np1 (***Glinka et al, 2012***) making the neuropilin receptors an even more attractive target for bone metastasis. However, combination treatment with Bz should be investigated with some caution as there is some evidence in the literature that suggests that osteonecrosis is a side-effect associated with both BP and Bz treatment. Since bone remodelling requires angiogenic signalling pathways combining agents that target this process may lead to serious side effects, therefore investigating the mechanism by which Bz is reducing bone metastasis is required initially prior to any combination studies.

However, despite the encouraging data obtained with Bz treatment the translation of pre-clinical success of such agents to the clinic have yet to be observed in breast cancer treatment. Bz in the clinic has proven successful for other solid tumours such as metastatic colorectal cancer, therefore, identifying potential differences between these different tumour types could prove useful in establishing why the same success in the clinic has not been observed with Bz in breast cancer patients. Bz was the first anti-angiogenic inhibitor to be approved for use in the clinic thus more basic research needs to be carried out on the mechanisms and subsequent effects that Bz has both locally and systemically. This 'back to basics' approach might aid in the appropriate use of Bz in the right setting for breast cancer therapy which might then allow better understanding of how Bz is working . With all the data and literature in mind, the studies with anti-VEGF agents such as Bz highlight that tumour development and progression is an extremely dynamic process that involves a whole host of different cell types and the plethora of cytokines that are released by these different cells types that may provide mechanisms of resistance to anti-VEGF therapy thus as mentioned previously, combining anti-VEGF therapy with inhibitors of alternative pathways or functions (such as immune modulators) may prove more efficacious.

Ultimately the use of peptides is an important step in cancer research as peptides offer certain advantages over monoclonal antibody therapy that may help to over-come some of the problems that arise in the clinic as a result of antibody therapy. Monoclonal antibodies are large in size, which can result in poor delivery to the tumour, and are often associated with higher levels of toxicity (***Thundimadathil et al, 2012***). Additionally, monoclonal antibodies are expensive to produce, whereas in contrast peptides are easier to manufacture and are cheaper to produce, therefore decrease the financial burden required to pay for these treatments. Peptides are also smaller in size and therefore penetrate into the tumour more

easily and issues such as rapid degradation can be over-come by modification to the peptide design (***Thundimadathil et al, 2012***). Currently, peptide therapies have been approved for either use in breast cancer patients in the clinic such as Zoladex or are undergoing clinical trails (Triptorelin) in ER+ patients (***Thundimadathil et al, 2012***) suggesting the application of peptide targeted therapy is relevant to the biological treatment of breast cancer.

With all the data in mind, **Figure 7.1** summarises the potential *in vivo* actions of peptide 7b., which may help explain why this peptide failed to enhance inhibit breast cancer growth when the *in vitro* data suggested that this human Np1 binding peptide exerted inhibitory activity on both breast cancer and micro-vascular endothelial cells.

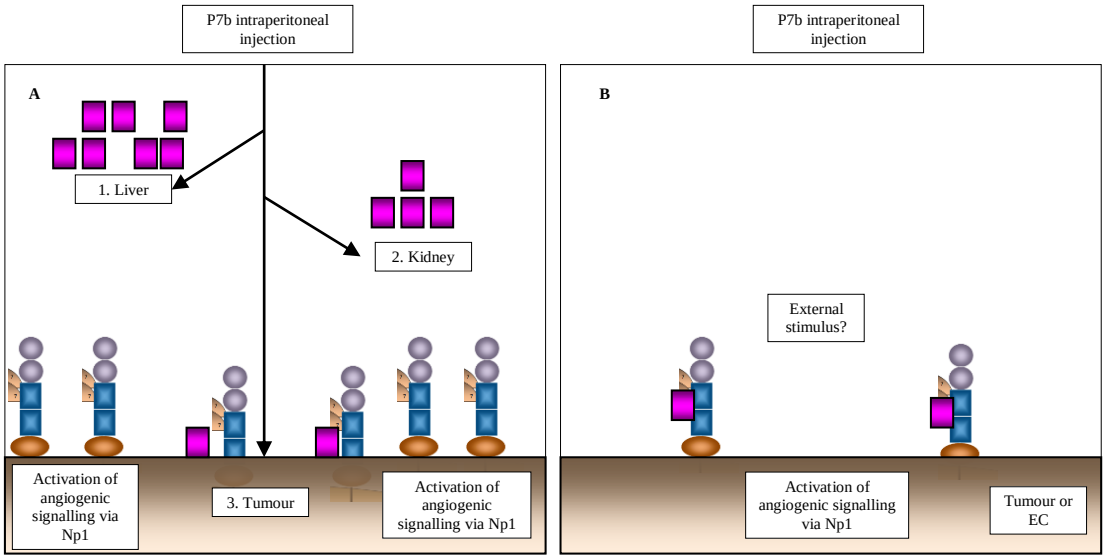

Figure 7.1 ***Peptide 7b- Potential Mechanisms of Action***:
(**A**) Post i.p. injection of p7b, the peptide is distributed throughout the circulatory system. The liver and kidneys highly express Np1 and since the circulation delivers p7b to these organs prior to reaching the tumour, it is possible that delivery of p7b at the dose administered results in inefficient delivery to the tumour, resulting in the lack of breast cancer growth *in vivo*, as observed in this current study after p7b treatment alone . (**B**) Alternatively, as p7b is derived from the $VEGF_{165}$ sequence, it is possible that the peptide is being delivered to the tumour, but is activating the Np1 receptor, rather then inhibiting it. The stimulus that dictates whether p7b inhibits or stimulates breast cancer activity either *in vitro* or *in vivo* is yet unknown.

7.6 FUTURE WORK

The future work based on the studies from this project are either work that can be carried out on the samples collected from this current study or ideas that have stemmed from the work from this project but would require additional studies to be set up.

Firstly, from the samples already available, Ki67, Caspase 3 and CD34 staining analysis needs to be carried out on the normal tissue harvested from the different treatment groups is an important future experiment to carry out to establish if there are any 'off-target' effects exerted by either Bz , p7b/p10 or the combination treatment. This is especially important since the recent revoking of Bz from use in breast cancer therapy is partly due to a high and serious toxicity profile. Of interest the difference, if any, in 'off-target' effects between the higher dose of Bz (5mg/kg) versus the lower ranges (1-0.1mg/kg) could potentially prove interesting and useful if a lower dose of Bz with less severe side effects can translate to the clinical setting. In addition, a toxicity test should be carried out to determine if the inhibitory effects observed with the Np1 peptides is a result of a toxic effect, rather then a functional consequence. It was discussed that the MTS assay may have reflected this to some level as the assay requires ATP for the colour reaction to occur, which can also be produced by dying cells. Therefore, a cell viability test would be more appropriate.

As mentioned in the earlier *in vitro* discussions (see section 3.3.1), *in vitro* flow cytometry studies that allow for the assessment of differential receptor expression under normoxic and hypoxic conditions would be useful in determining the levels of VEGF cell surface receptor expression, especially since hypoxia is known to regulate receptor expression (***Bae et al, 2008***) and is one of the hallmarks of cancer (***Hannahan &Weinberg, 2011).*** In addition, as ELISA assay could then be used to measure the levels of secreted VEGF related factors such as soluble receptors or other angiogenic agents into the conditioned media from the hypoxia experiments. This would be would be useful in determining the ratio of soluble versus membrane bound receptor present, which might also explain why peptide required to reach active membrane bound receptors in order to produce a therapeutic effect that results in biological relevance.

Protein arrays on protein extracted from the frozen tumour tissue would be useful in measuring the downstream activity occurring in response to the different treatment groups especially in the combination groups, as these arrays could provide information on the pathways that are potentially inducing resistance. There are a number of diverse pathways that can be either down-regulated or up-regulated in response to Bz or blockade of the

neuropilin/VEGF signalling pathway. One of the possible mechanisms of resistance to Bz treatment is the induction of a more aggressive phenotype after Bz treatment. Comparing the downstream signalling events associated with Bz and the combination therapy may prove useful as although the combination of Bz and p7b/p10 had no additive effects on primary growth, the array studies may identify a potential difference in downstream activity that may show that the combination treatment leads to a less aggressive response to therapy by the tumour and thus may provide more long term benefits, which potentially may relate to significant increases in overall survival in patients treated with a combination of Bz and anti-Np1 therapy, a clinical end-point which has not yet been met in breast cancer clinical trials using Bz in combination with chemotherapy. Protein arrays (R&D Systems) that assess downstream signalling events associated with angiogenic activity are available to buy commercially therefore this analysis can easily be carried out on the frozen samples already collected from this study.

The data from this project suggests that there are a numbers of different studies that can be designed or continued. The most interesting avenues of research that would be worth pursuing, as a result of this PhD is the potential role of Bz in inhibiting breast cancer-induced bone metastasis. The preliminary metastasis experiments are promising; yet future experiments to increase the numbers in the experimental groups are required to confirm these initial results. In addition the mechanism by which Bz alone is both reducing metastatic tumour burden and modulating the bone microenvironment to improve bone health in animals with breast cancer induced bone metastasis needs to be addressed. As Bz is an anti-angiogenic agent, CD31 or CD34 vessel staining would be useful to carry out on the bone sections, in order to establish a potential mechanism of action for Bz on reducing tumour metastatic burden.

From the literature surrounding the role of the neuropilin receptors and some of the *in vitro* analysis, it would be worth pursing the neuropilin receptors as potential therapeutic targets. However, a slightly different approach to therapy may be required in order to assess if there is a potential role for the neuropilin receptors in combination therapy. Investing time into the downstream signalling pathway associated with Np1 signalling would be extremely beneficial. This could better inform the best downstream target that would provide a more wide-spread inhibitory action on Np1 function. As the neuropilin receptors act as co-receptors for a number of different ligands, inhibiting these receptors may has the potential for a more wide-spread use in cancer therapy compared with agents that target VEGF alone. Designing a peptide that inhibits both Np1 and Np2 would prove beneficial. In addition, combining these re-designed peptides with an agent that targets another angiogenic activator,

such as FGF may prove beneficial although prior to carrying out any combination experiments, the use of anti-VEGF peptides alone needs to be tested.

In light of potential binding of the Np1 peptides to other receptors an NCBI protein-protein BLAST (basic local alignment search tool) search was carried out on the four Np1 peptides using a position specific alignment search (PSI-BLAST). The PSI-BLAST search looks for conservation pattern alignments between the target sequence and proteins in a given database. Below is a table (**Table 7.1**) that summaries some of the more interesting protein matches to the four Np1 peptides that help to explain why the Np1 peptides failed display inhibitory effects of tumour growth. The list of all the protein matches for the peptides can be found in the **appendix**. The blast search confirmed that the peptides used during this PhD are not specific to Np1 and therefore may help to explain some of the results observed both *in vitro* (all four peptides) and *in vivo* (p7b and p10). For example multiple epidermal growth factor-like domains protein 8 is involved in cellular communication and Hsp70 is involved in increased breast cancer cell migration which may explain why p10 in combination with Bz resulted in reduced efficacy compared with Bz. Emphasis on blocking intracellular signalling pathways is backed by the blastp search cancer progression involved a plethora of cytokines and factors that will alternatively bind and activate downstream signalling pathways which promote tumour progression.

p10 PSI-BLAST search	**Human**	**Mus musculus**
Multiple epidermal growth factor-like domains protein 8 precursor	**Y**	**Y**
PML-RARA-regulated adapter molecule 1	**N**	**Y**
Hsp70-binding protein 1 isoform 1	**Y**	**Y**
p7b PSI-BLAST search	**Human**	**Mus musculus**
Protein Smaug homolog 2	**Y**	**N**
Heat shock protein beta-3	**N**	**Y**
Immunoglobulin super family member 1 isoform 1	**Y**	**N**
p1 PSI-BLAST search	**Human**	**Mus musculus**
Arrestin domain containing protein 2 isoform 1	**Y**	Not tested
Hsp70-binding protein 1 isoform 1	**Y**	Not tested
WD repeat containing protein 7 isoform 1	**Y**	Not tested
p2 PSI-BLAST search	**Human**	**Mus musculus**
Coiled-coil domain containing protein 107 isoform A precursor	**Y**	Not tested

Coiled-coil domain containing protein 107 isoform B precursor	**Y**	Not tested

Table 7.1. Protein Blast Search:
The table summarises a few known proteins that share sequence alignment to the four Np1 peptides. This suggests that the peptides are not necessarily specific to Np1. A full list of refseq proteins that matched the sequence of the peptides can be found in the appendix.

In addition, tagging peptides with a detectable probe will allow quantitative analysis on delivery of the peptides to the tumour versus the normal organs. The IVIS imaging system not only measures bioluminescence but also detects a range of fluorophores therefore tagging peptides with a fluorescent tag would allow distribution analysis to be carried out. As the IVIS system is non-invasive it would also allow for continual monitoring of the movement of the peptide over the treatment period especially in terms of clearance of peptides from the body. Also delivery of the peptides to the tumour in a more targeted manner would improve delivery to the tumour thus enhance inhibitory actions and would also reduce any 'off-target' effects that may occur from targeting a receptor that is widely distributed under physiological conditions in other tissues other then the tumour. Examples of targeted therapy could include packaging the peptides in liposome that may be taken up by other cells types such as macrophages, and delivered to the tumour microenvironment.

The VEGF splice variants are becoming increasingly important in cancer research. Initially, it was thought that the role of the different variants was to form a VEGF gradient and thus regulating VEGF bio-availability. However, the interaction of these splice variants with the VEGF receptors are potentially important in cancer progression. For example the MDA-MB-436 tumours are thought to express higher levels of $VEGF_{145}$ in comparison with the other VEGF variants (***Stimpfl et al, 2002)***. In addition, $VEGF_{145}$ binds to Np2 but not Np1 (***Gluzman-Poltorak et al, 2000***) thus MDA-MB-436 tumours may be more responsive to Np2 inhibition due to the ratio of relevant VEGF isoforms being present, which may explain why treatment with p10 (potentially binds both Np1 and Np2) alone reduced tumour growth in comparison to p7b alone. The role of the different VEGF splice variants is therefore important to investigate when blocking receptor interactions. Lastly, similar to Bz not all breast cancer sub-types will respond to anti-neuropilin treatment therefore a tissue array that includes a large panel of breast cancer cell lines would be useful to identify more quickly breast cancer sub-types that are likely to respond to individual and combination anti-VEGF therapies prior to *in vivo* experimentation.

7.7 CONCLUSION

To conclude, the data from this PhD project suggests that VEGF is a key player in breast cancer progression as inhibiting the VEGF pathway resulted in inhibition of primary breast cancer growth and a trend that suggested a reduction in the metastatic tumour burden after treatment with Bz. However, the use of short neuropilin peptides as inhibitors of subsequent cellular activity has not proved efficacious and the role of the neuropilin receptors in the resistance to current anti-angiogenic therapy in breast cancer still remains un-answered.

References

References

Abdullah, L. N. and E. K.-H. Chow (2013). "Mechanisms of chemoresistance in cancer stem cells." Clinical and Translational Medicine **2**(1): 3.

Aesoy, R., B. C. Sanchez, et al. (2008). "An autocrine VEGF/VEGFR2 and p38 signaling loop confers resistance to 4-hydroxytamoxifen in MCF-7 breast cancer cells." Mol Cancer Res **6**(10): 1630-8.

Akerman, S., M. Fisher, et al. (2013). "Influence of soluble or matrix-bound isoforms of vascular endothelial growth factor-A on tumor response to vascular-targeted strategies." Int J Cancer.

Amini, A., S. Masoumi Moghaddam, et al. (2012). "The critical role of vascular endothelial growth factor in tumor angiogenesis." Curr Cancer Drug Targets **12**(1): 23-43.

Anan, K., T. Morisaki, et al. (1996). "Vascular endothelial growth factor and platelet-derived growth factor are potential angiogenic and metastatic factors in human breast cancer." Surgery **119**(3): 333-9.

Avastin®. Summary of product characteristics. 2014.

Azam, F., S. Mehta, et al. (2010). "Mechanisms of resistance to antiangiogenesis therapy." Eur J Cancer **46**(8): 1323-32.

Bachelder, R. E., A. Crago, et al. (2001). "Vascular endothelial growth factor is an autocrine survival factor for neuropilin-expressing breast carcinoma cells." Cancer Res **61**(15): 5736-40.

Bachelder, R. E., E. A. Lipscomb, et al. (2003). "Competing Autocrine Pathways Involving Alternative Neuropilin-1 Ligands Regulate Chemotaxis of Carcinoma Cells." Cancer Research **63**(17): 5230-5233.

Bachelder, R. E., M. A. Wendt, et al. (2002). "Vascular endothelial growth factor promotes breast carcinoma invasion in an autocrine manner by regulating the chemokine receptor CXCR4." Cancer Res **62**(24): 7203-6.

Bae, D., S. Lu, et al. (2008). "Metabolic stress induces the lysosomal degradation of neuropilin-1 but not neuropilin-2." J Biol Chem **283**(42): 28074-80.

Banerjee, A., J. Y. Lang, et al. (2011). "Unfolded protein response is required in nu/nu mice microvasculature for treating breast tumor with tunicamycin." J Biol Chem **286**(33): 29127-38.

Barcellos-Hoff, M. and R. Akhurst (2009). "Transforming growth factor-beta in breast cancer: too much, too late." Breast Cancer Research **11**(1): 202.

Barleon, B., G. Siemeister, et al. (1997). "Vascular endothelial growth factor up-regulates its receptor fms-like tyrosine kinase 1 (FLT-1) and a soluble variant of FLT-1 in human vascular endothelial cells." Cancer Res **57**(23): 5421-5.

Barr, M. P., D. J. Bouchier-Hayes, et al. (2008). "Vascular endothelial growth factor is an autocrine survival factor for breast tumour cells under hypoxia." Int J Oncol **32**(1): 41-8.

Barr, M. P., A. M. Byrne, et al. (2005). "A peptide corresponding to the neuropilin-1-binding site on VEGF(165) induces apoptosis of neuropilin-1-expressing breast tumour cells." Br J Cancer **92**(2): 328-33.

Bates, D. O., T. G. Cui, et al. (2002). "VEGF165b, an inhibitory splice variant of vascular endothelial growth factor, is down-regulated in renal cell carcinoma." Cancer Res **62**(14): 4123-31.

Bauerle T., Hilbig H, et al. (2008). “Bevacizumab inhibits breast cancer-induced osteolysis, surrounding soft tissue metastasis, and angiogenesis in rats as visualized by VCT and MRI.” Neoplasia **10** (5): 511-520.

Bear, H. D., G. Tang, et al. (2012). "Bevacizumab added to neoadjuvant chemotherapy for breast cancer." N Engl J Med **366**(4): 310-20.

Beck, B., G. Driessens, et al. (2011). "A vascular niche and a VEGF-Nrp1 loop regulate the initiation and stemness of skin tumours." Nature **478**(7369): 399-403.

Bernatchez, P. N., S. Soker, et al. (1999). "Vascular Endothelial Growth Factor Effect on Endothelial Cell Proliferation, Migration, and Platelet-activating Factor Synthesis Is Flk-1-dependent." Journal of Biological Chemistry **274**(43): 31047-31054.

Biswas, S. K. and A. Mantovani (2010). "Macrophage plasticity and interaction with lymphocyte subsets: cancer as a paradigm." Nat Immunol **11**(10): 889-96.

Borgan, E., E. M. Lindholm, et al. (2012). "Subtype-specific response to bevacizumab is reflected in the metabolome and transcriptome of breast cancer xenografts." Mol Oncol **7**(1): 130-42.

Borm, B., R. P. Requardt, et al. (2005). "Membrane ruffles in cell migration: indicators of inefficient lamellipodia adhesion and compartments of actin filament reorganization." Exp Cell Res **302**(1): 83-95.

Boudreau, N. and C. Myers (2003). "Breast cancer-induced angiogenesis: multiple mechanisms and the role of the microenvironment." Breast Cancer Res **5**(3): 140-6.

Bouxsein, M. L., S. K. Boyd, et al. (2010). "Guidelines for assessment of bone microstructure in rodents using micro-computed tomography." J Bone Miner Res **25**(7): 1468-86.

Brasch, R., C. Pham, et al. (1997). "Assessing tumor angiogenesis using macromolecular MR imaging contrast media." J Magn Reson Imaging **7**(1): 68-74.

Brogi, E., G. Schatteman, et al. (1996). "Hypoxia-induced paracrine regulation of vascular endothelial growth factor receptor expression." The Journal of Clinical Investigation **97**(2): 469-476.

Brooks, P. C., A. M. Montgomery, et al. (1994). "Integrin alpha v beta 3 antagonists promote tumor regression by inducing apoptosis of angiogenic blood vessels." Cell **79**(7): 1157-64.

Brown, H. K., P. D. Ottewell, et al. (2012). "Location matters: osteoblast and osteoclast distribution is modified by the presence and proximity to breast cancer cells in vivo." Clin Exp Metastasis **29**(8): 927-38.

Brufsky, A. M., S. Hurvitz, et al. (2011). "RIBBON-2: A Randomized, Double-Blind, Placebo-Controlled, Phase III Trial Evaluating the Efficacy and Safety of Bevacizumab in Combination With Chemotherapy for Second-Line Treatment of Human Epidermal Growth Factor Receptor 2â€“Negative Metastatic Breast Cancer." Journal of Clinical Oncology **29**(32): 4286-4293.

Bumbaca, D., H. Xiang, et al. (2012). "Maximizing tumour exposure to anti-neuropilin-1 antibody requires saturation of non-tumour tissue antigenic sinks in mice." Br J Pharmacol **166**(1): 368-77.

Bussolati, B., C. Dunk, et al. (2001). "Vascular endothelial growth factor receptor-1 modulates vascular endothelial growth factor-mediated angiogenesis via nitric oxide." Am J Pathol **159**(3): 993-1008.

Byrne, A. M., D. J. Bouchier-Hayes, et al. (2005). "Angiogenic and cell survival functions of vascular endothelial growth factor (VEGF)." J Cell Mol Med **9**(4): 777-94.

Cackowski, F. C., L. Xu, et al. (2004). "Identification of two novel alternatively spliced Neuropilin-1 isoforms." Genomics **84**(1): 82-94.

Cai, J., W. G. Jiang, et al. (2006). "Vascular endothelial growth factor-induced endothelial cell proliferation is regulated by interaction between VEGFR-2, SH-PTP1 and eNOS." Microvasc Res **71**(1): 20-31.

Campbell, J. P., A. R. Merkel, et al. (2012). "Models of bone metastasis." J Vis Exp(67): e4260.

Cao, Y. (2004). "Antiangiogenic cancer therapy." Semin Cancer Biol **14**(2): 139-45.

Carmeliet, P. (2005). "Angiogenesis in life, disease and medicine." Nature **438**(7070): 932-936.

Carmeliet, P. and R. K. Jain (2000). "Angiogenesis in cancer and other diseases." Nature **407**(6801): 249-57.

Carneiro, A., M. Falcao, et al. (2009). "Multiple effects of bevacizumab in angiogenesis: implications for its use in age-related macular degeneration." Acta Ophthalmol **87**(5): 517-23.

Carneiro, A., M. Falcao, et al. (2009). "Comparative effects of bevacizumab, ranibizumab and pegaptanib at intravitreal dose range on endothelial cells." Exp Eye Res **88**(3): 522-7.

Catena, R., L. Larzabal, et al. (2010). "VEGF121b and VEGF165b are weakly angiogenic isoforms of VEGF-A." Molecular Cancer **9**(1): 320.

Cebe-Suarez, S., F. S. Grunewald, et al. (2008). "Orf virus VEGF-E NZ2 promotes paracellular NRP-1/VEGFR-2 coreceptor assembly via the peptide RPPR." FASEB J **22**(8): 3078-86.

Cebe-Suarez, S., A. Zehnder-Fjallman, et al. (2006). "The role of VEGF receptors in angiogenesis; complex partnerships." Cell Mol Life Sci **63**(5): 601-15.

Chavey, C., F. Bibeau, et al. (2007). "Oestrogen receptor negative breast cancers exhibit high cytokine content." Breast Cancer Res **9**(1): R15.

Chavez, K. J., S. V. Garimella, et al. (2010). "Triple negative breast cancer cell lines: One tool in the search for better treatment of triple negative breast cancer." Breast Disease **32**(1): 35-48.

Cho, S.-H., J. Jeon, et al. (2012). "Personalized Medicine in Breast Cancer: A Systematic Review." J Breast Cancer **15**(3): 265-272.

Chougule, M. B., A. R. Patel, et al. (2011). "Antitumor activity of Noscapine in combination with Doxorubicin in triple negative breast cancer." PLoS One **6**(3): e17733.

Claffey, K. P. and G. S. Robinson (1996). "Regulation of VEGF/VPF expression in tumor cells: consequences for tumor growth and metastasis." Cancer Metastasis Rev **15**(2): 165-76.

Cobleigh, M. A., V. K. Langmuir, et al. (2003). "A phase I/II dose-escalation trial of bevacizumab in previously treated metastatic breast cancer." Semin Oncol **30**(5 Suppl 16): 117-24.

Conley, S. J., E. Gheordunescu, et al. (2012). "Antiangiogenic agents increase breast cancer stem cells via the generation of tumor hypoxia." Proc Natl Acad Sci U S A **109**(8): 2784-9.

Costa, R., A. Carneiro, et al. (2009). "Bevacizumab and ranibizumab on microvascular endothelial cells: A comparative study." J Cell Biochem **108**(6): 1410-7.

Costa, R., A. Carneiro, et al. (2009c). "Bevacizumab and ranibizumab on microvascular endothelial cells: A comparative study." J Cell Biochem **108**(6): 1410-7.

Cross, M. J., J. Dixelius, et al. (2003). "VEGF-receptor signal transduction." Trends Biochem Sci **28**(9): 488-94.

Cudmore, M. J., P. W. Hewett, et al. (2012). "The role of heterodimerization between VEGFR-1 and VEGFR-2 in the regulation of endothelial cell homeostasis." Nat Commun **3**: 972.

Deckers, M. M., M. Karperien, et al. (2000). "Expression of vascular endothelial growth factors and their receptors during osteoblast differentiation." Endocrinology **141**(5): 1667-74.

Del Bufalo, D., L. Ciuffreda, et al. (2006). "Antiangiogenic Potential of the Mammalian Target of Rapamycin Inhibitor Temsirolimus." Cancer Research **66**(11): 5549-5554.

Des Guetz, G., B. Uzzan, et al. (2006). "Microvessel density and VEGF expression are prognostic factors in colorectal cancer. Meta-analysis of the literature." Br J Cancer **94**(12): 1823-32.

Eichhorn, M. E., A. Kleespies, et al. (2007). "Angiogenesis in cancer: molecular mechanisms, clinical impact." Langenbecks Arch Surg **392**(3): 371-9.

Elkin, M., A. Orgel, et al. (2004). "An angiogenic switch in breast cancer involves estrogen and soluble vascular endothelial growth factor receptor 1." J Natl Cancer Inst **96**(11): 875-8.

Emlet, D. R., A. Pollice, et al. (2006). "Growth inhibitory effects of trastuzumab, erlotinib, and bevacizumab are proportional to average cellular levels of HER2 expression in breast cancer cell lines, and the effects of combinations of the three are additive in cell lines with high HER2 expression." AACR Meeting Abstracts **2006**(1): 290-c-291.

Eroles, P., A. Bosch, et al. (2011). "Molecular biology in breast cancer: intrinsic subtypes and signaling pathways." Cancer Treat Rev **38**(6): 698-707.

Eskandani, M., H. Hamishehkar, et al. (2013). "Cyto/Genotoxicity study of polyoxyethylene (20) sorbitan monolaurate (tween 20)." DNA Cell Biol **32**(9): 498-503.

Eskens, F. A. and S. Sleijfer (2008). "The use of bevacizumab in colorectal, lung, breast, renal and ovarian cancer: where does it fit?" Eur J Cancer **44**(16): 2350-6.

Favier, B., A. Alam, et al. (2006). "Neuropilin-2 interacts with VEGFR-2 and VEGFR-3 and promotes human endothelial cell survival and migration." Blood **108**(4): 1243-50.

Ferrara, N. (2004). "Vascular endothelial growth factor: basic science and clinical progress." Endocr Rev **25**(4): 581-611.

Ferrara, N., K. Carver-Moore, et al. (1996). "Heterozygous embryonic lethality induced by targeted inactivation of the VEGF gene." Nature **380**(6573): 439-42.

Ferrara, N., K. J. Hillan, et al. (2004). "Discovery and development of bevacizumab, an anti-VEGF antibody for treating cancer." Nat Rev Drug Discov **3**(5): 391-400.

Ferrara, N., K. J. Hillan, et al. (2005). "Bevacizumab (Avastin), a humanized anti-VEGF monoclonal antibody for cancer therapy." Biochem Biophys Res Commun **333**(2): 328-35.

Folkman, J. (1990). "What is the evidence that tumors are angiogenesis dependent?" J Natl Cancer Inst **82**(1): 4-6.

Fong, G.-H., J. Rossant, et al. (1995). "Role of the Flt-1 receptor tyrosine kinase in regulating the assembly of vascular endothelium." Nature **376**(6535): 66-70.

Fournier, P. G., V. Stresing, et al. (2010). "How do bisphosphonates inhibit bone metastasis in vivo?" Neoplasia **12**(7): 571-8.

Franco, M., S. Man, et al. (2006). "Targeted anti-vascular endothelial growth factor receptor-2 therapy leads to short-term and long-term impairment of vascular function and increase in tumor hypoxia." Cancer Res **66**(7): 3639-48.

Frank, Ed. (2007). Dynamics of Cancer: Incidence, Inheritance and Evolution, Chapter 3.

Fuckar, D., A. Dekanic, et al. (2006). "VEGF expression is associated with negative estrogen receptor status in patients with breast cancer." Int J Surg Pathol **14**(1): 49-55.

Funahashi, Y., C. J. Shawber, et al. "Notch modulates VEGF action in endothelial cells by inducing Matrix Metalloprotease activity." Vasc Cell **3**(1): 2.

Gabhann, F. M. and A. S. Popel (2006). "Targeting Neuropilin-1 to Inhibit VEGF Signaling in Cancer: Comparison of Therapeutic Approaches." PLoS Comput Biol **2**(12): e180.

Gasparini, G., E. Bonoldi, et al. (1997). "Prognostic Significance of Vascular Endothelial Growth Factor Protein in Node-Negative Breast Carcinoma." Journal of the National Cancer Institute **89**(2): 139-147.

Gasparini, G., R. Longo, et al. (2005). "Combination of antiangiogenic therapy with other anticancer therapies: results, challenges, and open questions." J Clin Oncol **23**(6): 1295-311.

Gerber, H. P., F. Condorelli, et al. (1997). "Differential transcriptional regulation of the two vascular endothelial growth factor receptor genes. Flt-1, but not Flk-1/KDR, is up-regulated by hypoxia." J Biol Chem **272**(38): 23659-67.

Gerber, H. P., V. Dixit, et al. (1998). "Vascular endothelial growth factor induces expression of the antiapoptotic proteins Bcl-2 and A1 in vascular endothelial cells." J Biol Chem **273**(21): 13313-6.

Gerber, H. P. and N. Ferrara (2005). "Pharmacology and pharmacodynamics of bevacizumab as monotherapy or in combination with cytotoxic therapy in preclinical studies." Cancer Res **65**(3): 671-80.

Gerber, H. P., J. Kowalski, et al. (2000). "Complete inhibition of rhabdomyosarcoma xenograft growth and neovascularization requires blockade of both tumor and host vascular endothelial growth factor." Cancer Res **60**(22): 6253-8.

Gerber, H. P., X. Wu, et al. (2007). "Mice expressing a humanized form of VEGF-A may provide insights into the safety and efficacy of anti-VEGF antibodies." Proc Natl Acad Sci U S A **104**(9): 3478-83.

Gerhardt, H., M. Golding, et al. (2003). "VEGF guides angiogenic sprouting utilizing endothelial tip cell filopodia." The Journal of Cell Biology **161**(6): 1163-1177.

Ghosh, S., C. A. Sullivan, et al. (2008). "High levels of vascular endothelial growth factor and its receptors (VEGFR-1, VEGFR-2, neuropilin-1) are associated with worse outcome in breast cancer." Hum Pathol **39**(12): 1835-43.

Gille, H., J. Kowalski, et al. (2000). "A repressor sequence in the juxtamembrane domain of Flt-1 (VEGFR-1) constitutively inhibits vascular endothelial growth factor-dependent

phosphatidylinositol 3[prime]-kinase activation and endothelial cell migration." EMBO J **19**(15): 4064-4073.

Giuliano, S. and G. Pages (2013). "Mechanisms of resistance to anti-angiogenesis therapies." Biochimie **95**(6): 1110-9.

Glinka, Y., N. Mohammed, et al. "Neuropilin-1 is expressed by breast cancer stem-like cells and is linked to NF-kappaB activation and tumor sphere formation." Biochem Biophys Res Commun **425**(4): 775-80.

Gluzman-Poltorak, Z., T. Cohen, et al. (2000). "Neuropilin-2 is a receptor for the vascular endothelial growth factor (VEGF) forms VEGF-145 and VEGF-165 [corrected]." J Biol Chem **275**(24): 18040-5.

Goel, H. L., B. Pursell, et al. (2013). "GLI1 regulates a novel neuropilin-2/alpha6beta1 integrin based autocrine pathway that contributes to breast cancer initiation." EMBO Mol Med **5**(4): 488-508.

Goel, H. L., B. Pursell, et al. (2012). "Neuropilin-2 regulates alpha6beta1 integrin in the formation of focal adhesions and signaling." J Cell Sci **125**(Pt 2): 497-506.

Goel, S., D. G. Duda, et al. (2011). "Normalization of the Vasculature for Treatment of Cancer and Other Diseases." Physiological Reviews **91**(3): 1071-1121.

Goh, L. K. and A. Sorkin (2013). "Endocytosis of receptor tyrosine kinases." Cold Spring Harb Perspect Biol **5**(5): a017459.

Goldman, C. K., R. L. Kendall, et al. (1998). "Paracrine expression of a native soluble vascular endothelial growth factor receptor inhibits tumor growth, metastasis, and mortality rate." Proc Natl Acad Sci U S A **95**(15): 8795-800.

Gordon, M. S., K. Margolin, et al. (2001). "Phase I Safety and Pharmacokinetic Study of Recombinant Human Anti-Vascular Endothelial Growth Factor in Patients With Advanced Cancer." Journal of Clinical Oncology **19**(3): 843-850.

Grepin, R. and G. Pages (2010). "Molecular mechanisms of resistance to tumour anti-angiogenic strategies." J Oncol **2010**: 835680.

Grunewald, F. S., A. E. Prota, et al. (2010). "Structure-function analysis of VEGF receptor activation and the role of coreceptors in angiogenic signaling." Biochim Biophys Acta **1804**(3): 567-80.

Guarneri, V., D. Miles, et al. (2010). "Bevacizumab and osteonecrosis of the jaw: incidence and association with bisphosphonate therapy in three large prospective trials in advanced breast cancer." Breast Cancer Res Treat **122**(1): 181-8.

Guidi, A. J., D. A. Berry, et al. (2000). "Association of Angiogenesis in Lymph Node Metastases With Outcome of Breast Cancer." Journal of the National Cancer Institute **92**(6): 486-492.

Guise, T. A., J. J. Yin, et al. (2002). "Parathyroid hormone-related protein (PTHrP)-(1-139) isoform is efficiently secreted in vitro and enhances breast cancer metastasis to bone in vivo." Bone **30**(5): 670-6.

Guo, S., L. S. Colbert, et al. "Vascular endothelial growth factor receptor-2 in breast cancer." Biochim Biophys Acta **1806**(1): 108-21.

Hanahan, D. and R. A. Weinberg (2011). "Hallmarks of cancer: the next generation." Cell **144**(5): 646-74.

Harris, S., M. Craze, et al. (2012). "Do Anti-Angiogenic VEGF (VEGFxxxb) Isoforms Exist? A Cautionary Tale." PLoS One **7**(5): e35231.

Heinzman, J. M., S. L. Brower, et al. (2008). "Comparison of angiogenesis-related factor expression in primary tumor cultures under normal and hypoxic growth conditions." Cancer Cell Int **8**: 11.

Henriksen, K., M. Karsdal, et al. (2003). "RANKL and vascular endothelial growth factor (VEGF) induce osteoclast chemotaxis through an ERK1/2-dependent mechanism." J Biol Chem **278**(49): 48745-53.

Herve, M. A., H. Buteau-Lozano, et al. (2008). "Overexpression of vascular endothelial growth factor 189 in breast cancer cells leads to delayed tumor uptake with dilated intratumoral vessels." Am J Pathol **172**(1): 167-78.

Herzog, B., C. Pellet-Many, et al. (2011). "VEGF binding to NRP1 is essential for VEGF stimulation of endothelial cell migration, complex formation between NRP1 and VEGFR2, and signaling via FAK Tyr407 phosphorylation." Mol Biol Cell **22**(15): 2766-76.

Higgins, B., K. Kolinsky, et al. (2007). "Antitumor activity of capecitabine and bevacizumab combination in a human estrogen receptor-negative breast adenocarcinoma xenograft model." Anticancer Res **27**(4B): 2279-87.

Hoang, T., S. Huang, et al. (2012). "Enhancement of radiation response with bevacizumab." Journal of Experimental & Clinical Cancer Research **31**(1): 37.

Holen, I. and R. E. Coleman (2010). "Anti-tumour activity of bisphosphonates in preclinical models of breast cancer." Breast Cancer Res **12**(6): 214.

Holliday, D. L. and V. Speirs (2011). "Choosing the right cell line for breast cancer research." Breast Cancer Res **13**(4): 215.

Holmes, D. I. and I. Zachary (2005). "The vascular endothelial growth factor (VEGF) family: angiogenic factors in health and disease." Genome Biol **6**(2): 209.

Hsu, Y. P., C. A. Staton, et al. "Anti-angiogenic properties of ADAMTS-4 in vitro." Int J Exp Pathol **93**(1): 70-7.

Huang, K., C. Andersson, et al. (2001). "Signaling properties of VEGF receptor-1 and -2 homo- and heterodimers." Int J Biochem Cell Biol **33**(4): 315-24.

Huang, Y., J. Yuan, et al. (2012). "Vascular normalizing doses of antiangiogenic treatment reprogram the immunosuppressive tumor microenvironment and enhance immunotherapy." Proc Natl Acad Sci U S A **109**(43): 17561-6.

Hunter, F., J. Xie, et al. (2006). "Rhodamine-RCA in vivo labeling guided laser capture microdissection of cancer functional angiogenic vessels in a murine squamous cell carcinoma mouse model." Mol Cancer **5**: 5.

Hurwitz, H., L. Fehrenbacher, et al. (2004). "Bevacizumab plus irinotecan, fluorouracil, and leucovorin for metastatic colorectal cancer." N Engl J Med **350**(23): 2335-42.

Iorns, E., K. Drews-Elger, et al. (2012). "A New Mouse Model for the Study of Human Breast Cancer Metastasis." PLoS One **7**(10): e47995.

Ishihara, A., H. Tsuda, et al. (2009). "Morphological characteristics of basal-like subtype of breast carcinoma with special reference to cytopathological features." Breast Cancer **16**(3): 179-85.

Jain, R. K. (2001). "Normalizing tumor vasculature with anti-angiogenic therapy: a new paradigm for combination therapy." Nat Med **7**(9): 987-9.

Jenkins, D., Y. Hornig, et al. (2005). "Bioluminescent human breast cancer cell lines that permit rapid and sensitive in vivo detection of mammary tumors and multiple metastases in immune deficient mice." Breast Cancer Research **7**(4): R444 - R454.

Jones, A., C. Fujiyama, et al. (2001). "Relation of vascular endothelial growth factor production to expression and regulation of hypoxia-inducible factor-1 alpha and hypoxia-inducible factor-2 alpha in human bladder tumors and cell lines." Clin Cancer Res **7**(5): 1263-72.

Jubb, A. M., K. D. Miller, et al. (2011). "Impact of exploratory biomarkers on the treatment effect of bevacizumab in metastatic breast cancer." Clin Cancer Res **17**(2): 372-81.

Kao, J., K. Salari, et al. (2009). "Molecular Profiling of Breast Cancer Cell Lines Defines Relevant Tumor Models and Provides a Resource for Cancer Gene Discovery." PLoS One **4**(7): e6146.

Kaplan, R. N., B. Psaila, et al. (2006). "Bone marrow cells in the 'pre-metastatic niche': within bone and beyond." Cancer Metastasis Rev **25**(4): 521-9.

Kaplan, R. N., R. D. Riba, et al. (2005). "VEGFR1-positive haematopoietic bone marrow progenitors initiate the pre-metastatic niche." Nature **438**(7069): 820-7.

Kawasaki, T., T. Kitsukawa, et al. (1999). "A requirement for neuropilin-1 in embryonic vessel formation." Development **126**(21): 4895-902.

Kerbel, R. and J. Folkman (2002). "Clinical translation of angiogenesis inhibitors." Nat Rev Cancer **2**(10): 727-39.

Kim, Y. M., S. Hwang, et al. (2002). "Endostatin blocks vascular endothelial growth factor-mediated signaling via direct interaction with KDR/Flk-1." J Biol Chem **277**(31): 27872-9.

Kodera, Y., Y. Katanasaka, et al. (2011). "Sunitinib inhibits lymphatic endothelial cell functions and lymph node metastasis in a breast cancer model through inhibition of vascular endothelial growth factor receptor 3." Breast Cancer Res **13**(3): R66.

Konecny, G. E., Y. G. Meng, et al. (2004). "Association between HER-2/neu and vascular endothelial growth factor expression predicts clinical outcome in primary breast cancer patients." Clin Cancer Res **10**(5): 1706-16.

Konopatskaya, O., A. J. Churchill, et al. (2006). "VEGF165b, an endogenous C-terminal splice variant of VEGF, inhibits retinal neovascularization in mice." Mol Vis **12**: 626-32.

Kowalski, P. J., M. A. Rubin, et al. (2003). "E-cadherin expression in primary carcinomas of the breast and its distant metastases." Breast Cancer Res **5**(6): R217-22.

Kozlow, W. and T. A. Guise (2005). "Breast cancer metastasis to bone: mechanisms of osteolysis and implications for therapy." J Mammary Gland Biol Neoplasia **10**(2): 169-80.

Kubota, Y., H. K. Kleinman, et al. (1988). "Role of laminin and basement membrane in the morphological differentiation of human endothelial cells into capillary-like structures." J Cell Biol **107**(4): 1589-98.

Lamalice, L., F. Le Boeuf, et al. (2007). "Endothelial Cell Migration During Angiogenesis." Circulation Research **100**(6): 782-794.

Lambrechts, D., H. J. Lenz, et al. (2013). "Markers of response for the antiangiogenic agent bevacizumab." J Clin Oncol **31**(9): 1219-30.

Langley, R. R. and I. J. Fidler (2011). "The seed and soil hypothesis revisited--the role of tumor-stroma interactions in metastasis to different organs." Int J Cancer **128**(11): 2527-35.

Lee, E., J. E. Koskimaki, et al. (2013). "Inhibition of lymphangiogenesis and angiogenesis in breast tumor xenografts and lymph nodes by a peptide derived from transmembrane protein 45A." Neoplasia **15**(2): 112-24.

Lee, T. H., S. Seng, et al. (2007). "Vascular endothelial growth factor mediates intracrine survival in human breast carcinoma cells through internally expressed VEGFR1/FLT1." PLoS Med **4**(6): e186.

Lehmann, B. D., J. A. Bauer, et al. (2011). "Identification of human triple-negative breast cancer subtypes and preclinical models for selection of targeted therapies." The Journal of Clinical Investigation **121**(7): 2750-2767.

Li, Q., S. Yano, et al. (2007). "The Therapeutic Efficacy of Antiâ€"Vascular Endothelial Growth Factor Antibody, Bevacizumab, and Pemetrexed against Orthotopically Implanted Human Pleural Mesothelioma Cells in Severe Combined Immunodeficient Mice." Clinical Cancer Research **13**(19): 5918-5925.

Liang, Y., R. A. Brekken, et al. (2006). "Vascular endothelial growth factor induces proliferation of breast cancer cells and inhibits the anti-proliferative activity of anti-hormones." Endocr Relat Cancer **13**(3): 905-19.

Lin E., Jones JG, (2003). “Progression to malignancy in the polyoma middle T oncoprotein mouse breast cancer model provides a reliable model for human disease.” American Journal of Pathology **163 (**5): 2113-2126.

Lin, M. I. and W. C. Sessa (2004). "Antiangiogenic therapy: creating a unique "window" of opportunity." Cancer Cell **6**(6): 529-31.

Linardou, H., K. T. Kalogeras, et al. (2012). "The prognostic and predictive value of mRNA expression of vascular endothelial growth factor family members in breast cancer: a study in primary tumors of high-risk early breast cancer patients participating in a randomized Hellenic Cooperative Oncology Group trial." Breast Cancer Res **14**(6): R145.

Linderholm, B., K. Grankvist, et al. (2000). "Correlation of vascular endothelial growth factor content with recurrences, survival, and first relapse site in primary node-positive breast carcinoma after adjuvant treatment." J Clin Oncol **18**(7): 1423-31.

Loges, S., T. Schmidt, et al. "Mechanisms of resistance to anti-angiogenic therapy and development of third-generation anti-angiogenic drug candidates." Genes Cancer **1**(1): 12-25.

Lorquet, S., S. Berndt, et al. (2010). "Soluble forms of VEGF receptor-1 and -2 promote vascular maturation via mural cell recruitment." FASEB J **24**(10): 3782-95.

Lu, Y., H. Xiang, et al. (2009). "Identification of circulating neuropilin-1 and dose-dependent elevation following anti-neuropilin-1 antibody administration." MAbs **1**(4): 364-9.

Margolin, K., M. S. Gordon, et al. (2001). "Phase Ib trial of intravenous recombinant humanized monoclonal antibody to vascular endothelial growth factor in combination with chemotherapy in patients with advanced cancer: pharmacologic and long-term safety data." J Clin Oncol **19**(3): 851-6.

Marxsen, J. H., O. Schmitt, et al. (2001). "Vascular endothelial growth factor gene expression in the human breast cancer cell line MX-1 is controlled by O2 availability in vitro and in vivo." Ann Anat **183**(3): 243-9.

Mathot, L. and J. Stenninger (2012). "Behavior of seeds and soil in the mechanism of metastasis: a deeper understanding." Cancer Sci **103**(4): 626-31.

Matsui, J., Y. Funahashi, et al. (2008). "Multi-kinase inhibitor E7080 suppresses lymph node and lung metastases of human mammary breast tumor MDA-MB-231 via inhibition of vascular endothelial growth factor-receptor (VEGF-R) 2 and VEGF-R3 kinase." Clin Cancer Res **14**(17): 5459-65.

Matsui, J., Y. Funahashi, et al. (2008). "Multi-kinase inhibitor E7080 suppresses lymph node and lung metastases of human mammary breast tumor MDA-MB-231 via inhibition of

vascular endothelial growth factor-receptor (VEGF-R) 2 and VEGF-R3 kinase." Clin Cancer Res **14**(17): 5459-65.

McMahon, G. (2000). "VEGF receptor signaling in tumor angiogenesis." Oncologist **5 Suppl 1**: 3-10.

Melnyk, O., M. Zimmerman, et al. (1999). "Neutralizing anti-vascular endothelial growth factor antibody inhibits further growth of established prostate cancer and metastases in a pre-clinical model." J Urol **161**(3): 960-3.

Mezquita, B., J. Mezquita, et al. (2010). "A novel intracellular isoform of VEGFR-1 activates Src and promotes cell invasion in MDA-MB-231 breast cancer cells." J Cell Biochem **110**(3): 732-42.

Miles, D. W., A. Chan, et al. (2010). "Phase III Study of Bevacizumab Plus Docetaxel Compared With Placebo Plus Docetaxel for the First-Line Treatment of Human Epidermal Growth Factor Receptor 2â€“Negative Metastatic Breast Cancer." Journal of Clinical Oncology **28**(20): 3239-3247.

Miles, D. W., S. L. de Haas, et al. (2013). "Biomarker results from the AVADO phase 3 trial of first-line bevacizumab plus docetaxel for HER2-negative metastatic breast cancer." Br J Cancer **108**(5): 1052-60.

Miller, K., M. Wang, et al. (2007). "Paclitaxel plus bevacizumab versus paclitaxel alone for metastatic breast cancer." N Engl J Med **357**(26): 2666-76.

Miller, K. D., L. I. Chap, et al. (2005). "Randomized phase III trial of capecitabine compared with bevacizumab plus capecitabine in patients with previously treated metastatic breast cancer." J Clin Oncol **23**(4): 792-9.

Mimeault, M. and S. K. Batra (2010). "New advances on critical implications of tumor- and metastasis-initiating cells in cancer progression, treatment resistance and disease recurrence." Histol Histopathol **25**(8): 1057-73.

Mo, M. L., J. Okamoto, et al. (2013). "Down-Regulation of SIX3 is Associated with Clinical Outcome in Lung Adenocarcinoma." PLoS One **8**(8): e71816.

Morikawa, S., P. Baluk, et al. (2002). "Abnormalities in pericytes on blood vessels and endothelial sprouts in tumors." Am J Pathol **160**(3): 985-1000.

Muller, Y. A., B. Li, et al. (1997). "Vascular endothelial growth factor: Crystal structure and functional mapping of the kinase domain receptor bindingâ€‰site." Proceedings of the National Academy of Sciences **94**(14): 7192-7197.

Muramatsu, M., S. Yamamoto, et al. (2010). "Vascular endothelial growth factor receptor-1 signaling promotes mobilization of macrophage lineage cells from bone marrow and stimulates solid tumor growth." Cancer Res **70**(20): 8211-21.

Murga, M., O. Fernandez-Capetillo, et al. (2005). "Neuropilin-1 regulates attachment in human endothelial cells independently of vascular endothelial growth factor receptor-2." Blood **105**(5): 1992-9.

Nakagawa, M., T. Kaneda, et al. (2000). "Vascular endothelial growth factor (VEGF) directly enhances osteoclastic bone resorption and survival of mature osteoclasts." FEBS Lett **473**(2): 161-4.

Nasarre, P., B. Constantin, et al. (2003). "Semaphorin SEMA3F and VEGF have opposing effects on cell attachment and spreading." Neoplasia **5**(1): 83-92.

Nor, J. E., J. Christensen, et al. (1999). "Vascular endothelial growth factor (VEGF)-mediated angiogenesis is associated with enhanced endothelial cell survival and induction of Bcl-2 expression." Am J Pathol **154**(2): 375-84.

Olsson, A. K., A. Dimberg, et al. (2006). "VEGF receptor signalling - in control of vascular function." Nat Rev Mol Cell Biol **7**(5): 359-71.

Ortholan, C., J. Durivault, et al. (2010). "Bevacizumab/docetaxel association is more efficient than docetaxel alone in reducing breast and prostate cancer cell growth: a new paradigm for understanding the therapeutic effect of combined treatment." Eur J Cancer **46**(16): 3022-36.

O'Shaughnessy, J. A. and A. M. Brufsky (2008). "RiBBON 1 and RiBBON 2: phase III trials of bevacizumab with standard chemotherapy for metastatic breast cancer." Clin Breast Cancer **8**(4): 370-3.

Ottewell, P. D., D. V. Lefley, et al. (2010). "Sustained inhibition of tumor growth and prolonged survival following sequential administration of doxorubicin and zoledronic acid in a breast cancer model." Int J Cancer **126**(2): 522-32.

Ottewell, P. D., J. K. Woodward, et al. (2009). "Anticancer mechanisms of doxorubicin and zoledronic acid in breast cancer tumor growth in bone." Mol Cancer Ther **8**(10): 2821-32.

Pan, Q., Y. Chathery, et al. (2007). "Neuropilin-1 Binds to VEGF121 and Regulates Endothelial Cell Migration and Sprouting." Journal of Biological Chemistry **282**(33): 24049-24056.

Papetti, M. and I. M. Herman (2002). "Mechanisms of normal and tumor-derived angiogenesis." Am J Physiol Cell Physiol **282**(5): C947-70.

Park, J. E., G. A. Keller, et al. (1993). "The vascular endothelial growth factor (VEGF) isoforms: differential deposition into the subepithelial extracellular matrix and bioactivity of extracellular matrix-bound VEGF." Mol Biol Cell **4**(12): 1317-26.

Patan, S. (2004). "Vasculogenesis and angiogenesis." Cancer Treat Res **117**: 3-32.

Pham, C. D., T. P. Roberts, et al. (1998). "Magnetic resonance imaging detects suppression of tumor vascular permeability after administration of antibody to vascular endothelial growth factor." Cancer Invest **16**(4): 225-30.

Plank, M. J. and B. D. Sleeman (2003). "A reinforced random walk model of tumour angiogenesis and anti-angiogenic strategies." Math Med Biol **20**(2): 135-81.

Prabhakaran, P., F. Hassiotou, et al. (2013). "Cisplatin induces differentiation of breast cancer cells." Front Oncol **3**: 134.

Prager, G. W., J. M. Breuss, et al. (2004). "Vascular Endothelial Growth Factor Receptor-2â€"Induced Initial Endothelial Cell Migration Depends on the Presence of the Urokinase Receptor." Circulation Research **94**(12): 1562-1570.

Prager, G. W., E.-M. Lackner, et al. (2010). "Targeting of VEGF-dependent transendothelial migration of cancer cells by bevacizumab." Molecular oncology **4**(2): 150-160.

Prager, G. W., M. Poettler, et al. (2012). "Angiogenesis in cancer: anti-VEGF escape mechanisms." Translational Lung Cancer Research **1**(1): 14-25.

Price, D. J., T. Miralem, et al. (2001). "Role of vascular endothelial growth factor in the stimulation of cellular invasion and signaling of breast cancer cells." Cell Growth Differ **12**(3): 129-35.

Przybyla, B. D., G. Shafirstein, et al. (2012). "Conductive thermal ablation of 4T1 murine breast carcinoma reduces severe hypoxia in surviving tumour." Int J Hyperthermia **28**(2): 156-62.

Przybyla, B. D., G. Shafirstein, et al. (2012). "Conductive thermal ablation of 4T1 murine breast carcinoma reduces severe hypoxia in surviving tumour." Int J Hyperthermia **28**(2): 156-62.

Qiu, Y., H. Bevan, et al. (2008). "Mammary alveolar development during lactation is inhibited by the endogenous antiangiogenic growth factor isoform, VEGF165b." FASEB J **22**(4): 1104-12.

Qu Z., Van Ginkel S, et al (2008). “Vascular endothelial growth factor reduces tamoxifen efficacy and promotes metastatic colonization and desmoplasia in breast tumours”. Cancer Research **68**: 6232-6240.

Rennel, E., E. Waine, et al. (2008). "The endogenous anti-angiogenic VEGF isoform, VEGF165b inhibits human tumour growth in mice." Br J Cancer **98**(7): 1250-7.

Robert, N. J., V. Dieras, et al. (2011). "RIBBON-1: randomized, double-blind, placebo-controlled, phase III trial of chemotherapy with or without bevacizumab for first-line treatment of human epidermal growth factor receptor 2-negative, locally recurrent or metastatic breast cancer." J Clin Oncol **29**(10): 1252-60.

Robinson, C. J. and S. E. Stringer (2001). "The splice variants of vascular endothelial growth factor (VEGF) and their receptors." J Cell Sci **114**(Pt 5): 853-65.

Roland, C. L., S. P. Dineen, et al. (2009a). "Inhibition of vascular endothelial growth factor reduces angiogenesis and modulates immune cell infiltration of orthotopic breast cancer xenografts." Mol Cancer Ther **8**(7): 1761-71.

Roland, C. L., K. D. Lynn, et al. (2009b). "Cytokine levels correlate with immune cell infiltration after anti-VEGF therapy in preclinical mouse models of breast cancer." PLoS One **4**(11): e7669.

Rose, A. A. and P. M. Siegel (2006). "Breast cancer-derived factors facilitate osteolytic bone metastasis." Bull Cancer **93**(9): 931-43.

Rugo, H. S., A. J. Chien, et al. "A phase II study of lapatinib and bevacizumab as treatment for HER2-overexpressing metastatic breast cancer." Breast Cancer Res Treat **134**(1): 13-20.

Ryan, A. M., D. B. Eppler, et al. (1999). "Preclinical safety evaluation of rhuMAbVEGF, an antiangiogenic humanized monoclonal antibody." Toxicol Pathol **27**(1): 78-86.

Ryden, L., B. Linderholm, et al. (2003). "Tumor specific VEGF-A and VEGFR2/KDR protein are co-expressed in breast cancer." Breast Cancer Res Treat **82**(3): 147-54.

Sakurai, Y., K. Ohgimoto, et al. (2005). "Essential role of Flk-1 (VEGF receptor 2) tyrosine residue 1173 in vasculogenesis in mice." Proc Natl Acad Sci U S A **102**(4): 1076-81.

Schmidt, U., J. Ahmed, et al. (2008). "Comparative VEGF receptor tyrosine kinase modeling for the development of highly specific inhibitors of tumor angiogenesis." Genome Inform **20**: 243-51.

Schneider, B. P. and K. D. Miller (2005). "Angiogenesis of breast cancer." J Clin Oncol **23**(8): 1782-90.

Schneider, B. P., M. Wang, et al. (2008). "Association of vascular endothelial growth factor and vascular endothelial growth factor receptor-2 genetic polymorphisms with outcome in a trial of paclitaxel compared with paclitaxel plus bevacizumab in advanced breast cancer: ECOG 2100." J Clin Oncol **26**(28): 4672-8.

Scott, P. A., J. M. Gleadle, et al. (1998). "Role of the hypoxia sensing system, acidity and reproductive hormones in the variability of vascular endothelial growth factor induction in human breast carcinoma cell lines." Int J Cancer **75**(5): 706-12.

Semenza, G. L. (2001). "Regulation of hypoxia-induced angiogenesis: a chaperone escorts VEGF to the dance." J Clin Invest **108**(1): 39-40.

Senger, D. R., S. J. Galli, et al. (1983). "Tumor cells secrete a vascular permeability factor that promotes accumulation of ascites fluid." Science **219**(4587): 983-5.

Shalaby, F., J. Rossant, et al. (1995). "Failure of blood-island formation and vasculogenesis in Flk-1-deficient mice." Nature **376**(6535): 62-6.

Shibuya, M. (2010). "Tyrosine Kinase Receptor Flt/VEGFR Family: Its Characterization Related to Angiogenesis and Cancer." Genes Cancer **1**(11): 1119-23.

Shibuya, M. and L. Claesson-Welsh (2006). "Signal transduction by VEGF receptors in regulation of angiogenesis and lymphangiogenesis." Exp Cell Res **312**(5): 549-60.

Shih, T. and C. Lindley (2006). "Bevacizumab: an angiogenesis inhibitor for the treatment of solid malignancies." Clin Ther **28**(11): 1779-802.

Shojaei, F. (2012). "Anti-angiogenesis therapy in cancer: current challenges and future perspectives." Cancer Lett **320**(2): 130-7.

Shojaei, F. and N. Ferrara (2008). "Role of the microenvironment in tumor growth and in refractoriness/resistance to anti-angiogenic therapies." Drug Resist Updat **11**(6): 219-30.

Soker, S., S. Gollamudi-Payne, et al. (1997). "Inhibition of vascular endothelial growth factor (VEGF)-induced endothelial cell proliferation by a peptide corresponding to the exon 7-encoded domain of VEGF165." J Biol Chem **272**(50): 31582-8.

Soker, S., S. Takashima, et al. (1998). "Neuropilin-1 is expressed by endothelial and tumor cells as an isoform-specific receptor for vascular endothelial growth factor." Cell **92**(6): 735-45.

Soldi, R., S. Mitola, et al. (1999). "Role of alphavbeta3 integrin in the activation of vascular endothelial growth factor receptor-2." EMBO J **18**(4): 882-92.

Starzec, A., P. Ladam, et al. (2007). "Structure-function analysis of the antiangiogenic ATWLPPR peptide inhibiting VEGF(165) binding to neuropilin-1 and molecular dynamics simulations of the ATWLPPR/neuropilin-1 complex." Peptides **28**(12): 2397-402.

Starzec, A., R. Vassy, et al. (2006). "Antiangiogenic and antitumor activities of peptide inhibiting the vascular endothelial growth factor binding to neuropilin-1." Life Sci **79**(25): 2370-81.

Staton, C. A., I. Kumar, et al. (2007). "Neuropilins in physiological and pathological angiogenesis." J Pathol **212**(3): 237-48.

Stimpfl, M., D. Tong, et al. (2002). "Vascular endothelial growth factor splice variants and their prognostic value in breast and ovarian cancer." Clin Cancer Res **8**(7): 2253-9.

Street, J. and B. Lenehan (2009). "Vascular endothelial growth factor regulates osteoblast survival â€“ evidence for an autocrine feedback mechanism." Journal of Orthopaedic Surgery and Research C7 - 19 **4**(1): 1-13.

Suva, L. J., R. J. Griffin, et al. (2009). "Mechanisms of bone metastases of breast cancer." Endocr Relat Cancer **16**(3): 703-13.

Svensson, S., K. Jirstrom, et al. (2005). "ERK phosphorylation is linked to VEGFR2 expression and Ets-2 phosphorylation in breast cancer and is associated with tamoxifen treatment resistance and small tumours with good prognosis." Oncogene **24**(27): 4370-9.

Takahashi, T. and M. Shibuya (1997). "The 230 kDa mature form of KDR/Flk-1 (VEGF receptor-2) activates the PLC-gamma pathway and partially induces mitotic signals in NIH3T3 fibroblasts." Oncogene **14**(17): 2079-89.

Takashima, S., M. Kitakaze, et al. (2002). "Targeting of both mouse neuropilin-1 and neuropilin-2 genes severely impairs developmental yolk sac and embryonic angiogenesis." Proc Natl Acad Sci U S A **99**(6): 3657-62.

Talmadge, J. E. and I. J. Fidler (2010). "AACR Centennial Series: The Biology of Cancer Metastasis: Historical Perspective." Cancer Research **70**(14): 5649-5669.

Tenhagen, M., P. J. van Diest, et al. (2012). "Fibroblast growth factor receptors in breast cancer: expression, downstream effects, and possible drug targets." Endocr Relat Cancer **19**(4): R115-29.

Thompson, A., K. Brennan, et al. (2008). "Evaluation of the current knowledge limitations in breast cancer research: a gap analysis." Breast Cancer Research **10**(2): R26.

Thundimadathil, J. "Cancer treatment using peptides: current therapies and future prospects." J Amino Acids **2012**: 967347.

Timoshenko, A. V., S. Rastogi, et al. (2007). "Migration-promoting role of VEGF-C and VEGF-C binding receptors in human breast cancer cells." British Journal of Cancer **97**(8): 1090-1098.

Tozer, G. M., S. Akerman, et al. (2008). "Blood vessel maturation and response to vascular-disrupting therapy in single vascular endothelial growth factor-A isoform-producing tumors." Cancer Res **68**(7): 2301-11.

Tu, Y. F., B. A. Kaipparettu, et al. (2011). "Mitochondria of highly metastatic breast cancer cell line MDA-MB-231 exhibits increased autophagic properties." Biochim Biophys Acta **1807**(9): 1125-32.

Underwood, J. G. S. P., Churchill Livingstone., Ed. (1996). General and Systemic Pathology.

Uniewicz, K. A., M. J. Cross, et al. (2011). "Exogenous recombinant dimeric neuropilin-1 is sufficient to drive angiogenesis." J Biol Chem **286**(1): 12-23.

van der Pluijm, G., B. Sijmons, et al. (2001). "Monitoring metastatic behavior of human tumor cells in mice with species-specific polymerase chain reaction: elevated expression of angiogenesis and bone resorption stimulators by breast cancer in bone metastases." J Bone Miner Res **16**(6): 1077-91.

Van der Veldt, Astrid A. M., M. Lubberink, et al. (2012). "Rapid Decrease in Delivery of Chemotherapy to Tumors after Anti-VEGF Therapy: Implications for Scheduling of Anti-Angiogenic Drugs." Cancer Cell **21**(1): 82-91.

Varey, A. H., E. S. Rennel, et al. (2008). "VEGF 165 b, an antiangiogenic VEGF-A isoform, binds and inhibits bevacizumab treatment in experimental colorectal carcinoma: balance of pro- and antiangiogenic VEGF-A isoforms has implications for therapy." Br J Cancer **98**(8): 1366-79.

Vintonenko, N., I. Pelaez-Garavito, et al. (2011). "Overexpression of VEGF189 in breast cancer cells induces apoptosis via NRP1 under stress conditions." Cell Adh Migr **5**(4): 332-43.

Volk, L. D., M. J. Flister, et al. (2008). "Nab-paclitaxel efficacy in the orthotopic model of human breast cancer is significantly enhanced by concurrent anti-vascular endothelial growth factor A therapy." Neoplasia **10**(6): 613-23.

Volk, L. D., M. J. Flister, et al. (2011). "Synergy of nab-paclitaxel and bevacizumab in eradicating large orthotopic breast tumors and preexisting metastases." Neoplasia **13**(4): 327-38.

Volk-Draper, L. D., S. Rajput, et al. "Novel model for basaloid triple-negative breast cancer: behavior in vivo and response to therapy." Neoplasia **14**(10): 926-42.

von Tell, D., A. Armulik, et al. (2006). "Pericytes and vascular stability." Exp Cell Res **312**(5): 623-9.

Voorzanger-Rousselot, N., F. Juillet, et al. (2006). "Association of 12 serum biochemical markers of angiogenesis, tumour invasion and bone turnover with bone metastases from breast cancer: a crossectional and longitudinal evaluation." Br J Cancer **95**(4): 506-14.

Waltenberger, J., L. Claesson-Welsh, et al. (1994). "Different signal transduction properties of KDR and Flt1, two receptors for vascular endothelial growth factor." J Biol Chem **269**(43): 26988-95.

Wanami, L. S., H. Y. Chen, et al. (2008). "Vascular endothelial growth factor-A stimulates Snail expression in breast tumor cells: implications for tumor progression." Exp Cell Res **314**(13): 2448-53.

Wang, D., D. B. Donner, et al. (2000). "Homeostatic Modulation of Cell Surface KDR and Flt1 Expression and Expression of the Vascular Endothelial Cell Growth Factor (VEGF) Receptor mRNAs by VEGF." Journal of Biological Chemistry **275**(21): 15905-15911.

Wang, L., H. Zeng, et al. (2003). "Neuropilin-1-mediated vascular permeability factor/vascular endothelial growth factor-dependent endothelial cell migration." J Biol Chem **278**(49): 48848-60.

Wang, Y., D. Fei, et al. (2004). "Biological activity of bevacizumab, a humanized anti-VEGF antibody in vitro." Angiogenesis **7**(4): 335-45.

Weidner, N., J. P. Semple, et al. (1991). "Tumor Angiogenesis and Metastasis â€" Correlation in Invasive Breast Carcinoma." New England Journal of Medicine **324**(1): 1-8.

Weigand, M., P. Hantel, et al. (2005). "Autocrine vascular endothelial growth factor signalling in breast cancer. Evidence from cell lines and primary breast cancer cultures in vitro." Angiogenesis **8**(3): 197-204.

Weigelt, B., F. C. Geyer, et al. (2010). "Histological types of breast cancer: how special are they?" Mol Oncol **4**(3): 192-208.

Weilbaecher, K. N., T. A. Guise, et al. (2011). "Cancer to bone: a fatal attraction." Nat Rev Cancer **11**(6): 411-425.

Weinberg, R. A. (2007). "The Biology of Cancer."

Wey, J. S., M. J. Gray, et al. (2005). "Overexpression of neuropilin-1 promotes constitutive MAPK signalling and chemoresistance in pancreatic cancer cells." Br J Cancer **93**(2): 233-41.

Wey, J. S., M. J. Gray, et al. (2005). "Overexpression of neuropilin-1 promotes constitutive MAPK signalling and chemoresistance in pancreatic cancer cells." Br J Cancer **93**(2): 233-41.

Woolard, J., W. Y. Wang, et al. (2004). "VEGF165b, an inhibitory vascular endothelial growth factor splice variant: mechanism of action, in vivo effect on angiogenesis and endogenous protein expression." Cancer Res **64**(21): 7822-35.

Workman, P., E. O. Aboagye, et al. (2010). "Guidelines for the welfare and use of animals in cancer research." Br J Cancer **102**(11): 1555-77.

Wu, Y., Z. Zhong, et al. (2006). "Anti-vascular endothelial growth factor receptor-1 antagonist antibody as a therapeutic agent for cancer." Clin Cancer Res **12**(21): 6573-84.

Xue, Y., P. Religa, et al. (2008). "Anti-VEGF agents confer survival advantages to tumor-bearing mice by improving cancer-associated systemic syndrome." Proc Natl Acad Sci U S A **105**(47): 18513-8.

Yamagata, T., M. Morishita, et al. (2009). "Characterization of the inhibition of breast cancer resistance protein-mediated efflux of mitoxantrone by pharmaceutical excipients." Int J Pharm **370**(1-2): 216-9.

Yang, S., J. Liu, et al. (2012). "Reversal effect of Tween-20 on multidrug resistance in tumor cells in vitro." Biomed Pharmacother **66**(3): 187-94.

Yang, S., X. Xin, et al. (2001). "Vascular endothelial cell growth factor-driven endothelial tube formation is mediated by vascular endothelial cell growth factor receptor-2, a kinase insert domain-containing receptor." Arterioscler Thromb Vasc Biol **21**(12): 1934-40.

Yang, Y.-Q., Y.-Y. Tan, et al. (2012). "The role of vascular endothelial growth factor in ossification." In J Oral Sci **4**(2): 64-68.

Yasuoka, H., R. Kodama, et al. (2009). "Neuropilin-2 expression in breast cancer: correlation with lymph node metastasis, poor prognosis, and regulation of CXCR4 expression." BMC Cancer **9**(1): 220.

Yokota, J. (2000). "Tumor progression and metastasis." Carcinogenesis **21**(3): 497-503.

Yoneda, T. (1997). "Arterial microvascularization and breast cancer colonization in bone." Histol Histopathol **12**(4): 1145-9.

Yoneda, T., A. Sasaki, et al. (1994). "Osteolytic bone metastasis in breast cancer." Breast Cancer Res Treat **32**(1): 73-84.

Zamarron, B. F. and W. Chen (2011). "Dual roles of immune cells and their factors in cancer development and progression." Int J Biol Sci **7**(5): 651-8.

Zeng, H., H. F. Dvorak, et al. (2001). "Vascular Permeability Factor (VPF)/Vascular Endothelial Growth Factor (VEGF) Receptor-1 Down-modulates VPF/VEGF Receptor-2-mediated Endothelial Cell Proliferation, but Not Migration, through

Phosphatidylinositol 3-Kinase-dependent Pathways." Journal of Biological Chemistry **276**(29): 26969-26979.

Zhang, W., S. Ran, et al. (2002). "A monoclonal antibody that blocks VEGF binding to VEGFR2 (KDR/Flk-1) inhibits vascular expression of Flk-1 and tumor growth in an orthotopic human breast cancer model." Angiogenesis **5**(1-2): 35-44.

Zhang, X. H., Q. Wang, et al. (2009). "Latent bone metastasis in breast cancer tied to Src-dependent survival signals." Cancer Cell **16**(1): 67-78.

VI APPENDIX

Acetate Buffer	
Sodium acetate	5.44g
water	50ml
Sodium tartrate	4.6ml

Napthol/dimethyformide Buffer	
Napththol AS-BI Phosphate	0.02g
Dimethlformamide	1ml
Acetate Buffer	50ml

PBS Buffer (5L)	
PBS Tablets	50
dH_2O	5000ml

PBST Buffer (5L)	
PBS Tablets	50
Tween20	5ml
dH_2O	5000ml

4X Reducing Buffer	VOLUME (ml)
Stacking Buffer	2.5
10% SDS	0.8g
Glycerol	4
2-mecaptoethanol	2
dH_2O	1.1
Bromophenol Blue (1% stock)	0.1

Resolving Gel (for 1 gel)	VOLUME (ml)
Resolving Buffer	2.5
30% Arcrlaymide	2.5
APS	50µl
TEMED	5µl
dH_2O	4.85

Running Buffer (10x) pH 8.3	VOLUME (ml)
Tris Base (25mM)	30g
Glycine (0.192M)	144g
SDS (0.1%)	10g
dH20	1000

Sodium Citrate Buffer (pH 6)	
Sodium citrate	
Tween20	0.5ml
dH_2O	1000ml
Adjust to pH 6, add tween20 and make up to 1L with dH_2O. Store at r.t.p	

Sodium Nitrile Buffer	
Sodium Nitrile	0.08g
water	2ml
Pararosanliline	2ml
Add 2.5ml of this solution to 50ml acetate buffer	

Stacking Gel (for 2 gels)	VOLUME (ml)
Stacking Buffer	2.5
30% Arcrlaymide	1.3
APS	100µ
TEMED	10µl
dH_2O	6.1ml

Transfer Buffer (10x) (25mM Tris, 192mM Glycine) pH 8.2-8,4	VOLUME (ml)
Tris Base	3.03g
Glycine	14.10g
dH2O	1000

Protein- p10 Blastp search	Human	Mus musculus
Arginine/serine-rich protein PNISR	N	Y
Atrial natriuretic peptide receptor 3 isoform a precursor	N	Y
Atrial natriuretic peptide receptor 3 isoform b precursor	N	Y
Austism susceptibility gene 2 protein	N	Y
Austism susceptibility gene 2 protein isoform 3	Y	N
Autism susceptibility gene 2 protein isoform 1	Y	N
Autism susceptibility gene 2 protein isoform 2	Y	N
Class A basic helix-loop-helix protein 15	Y	Y
Coiled-coil domain-containing protein 74A isoform 1	Y	N
Coiled-coil domain-containing protein 74A isoform 2	Y	N
Coiled-coil domain-containing protein 74A isoform 3	Y	N
Coiled-coil domain-containing protein 74A isoform 4	Y	N
Cystin-1	Y	Y
Dual specificity protein phosphatise 8	N	Y
Ecotropic viral integration site 5 protein homolog	Y	N
Endothelin-2 precursor	N	Y
Endothelin-2 preproprotein	Y	N
Fibrosin-1-like protein	Y	N
Fibrosin-1-like protein isoform 1	Y	Y
Growth/differentiation factor 9 precursor	N	Y
G patch domain-containing protein 8	Y	Y
Helicase SRCAP	Y	N
Hepatitis A virus cellular receptor 1 homolog isoform b precursor	N	Y
Hepatitis A virus cellular receptor 1 homolog isoform a precursor	N	Y
HHIP-like protein 1 precursor	N	Y
Hsp70-binding protein 1 isoform 1	Y	Y
Hsp70-binding protein 1 isoform 2	Y	N
Laminin subunit alpha-2 isoform a precursor	Y	Y
Laminin subunit alpha-2 isoform b precursor	Y	N

Meiotic recombination protein REC8 homolog	**Y**	**N**
MICAL-like protein 2	**Y**	**N**
Multiple epidermal growth factor-like domains protein 8 isoform 1 precursor	**Y**	**N**
Multiple epidermal growth factor-like domains protein 8 isoform 2 precursor	**Y**	**N**
Multiple epidermal growth factor-like domains protein 8 precursor	**N**	**Y**
NK 1 transcription factor-related protein 2	**Y**	**Y**
PML-RARA-regulated adapter molecule 1	**N**	**Y**
Pre-mRNA-processing factor 40 homolog B	**N**	**Y**
Pre-mRNA-processing factor 40 homolog B isoform 1	**Y**	**N**
Pre-mRNA-processing factor 40 homolog B isoform 2	**Y**	**N**
Protein FAM189A2	**N**	**Y**
Protein LSM14 homolog B	**N**	**Y**
PWWP domain-containing protein MUM1	**Y**	**N**
Retinal dehydrogenase 8	**N**	**Y**
Rho-related GTP binding protein RhoV	**N**	**Y**
Reproductive homeobox 13	**N**	**Y**
Serine/arginine repetitive matrix protein 1	**N**	**Y**
Serine/arginine repetitive matrix protein 1 isoform 1	**N**	**Y**
Serine/arginine repetitive matrix protein 2	**N**	**Y**
Serine/arginine rich splicing factor 2	**N**	**Y**
Synaptonemal complex protein 2		
Thrombospondin-4 precursor		
Transcription factor SPT20 homolog-like 1	**Y**	
Ubiquitin carboxyl-terminal hydrolase 1		**Y**
Zinc finger CCCH domain-containing protein 18 isoform b		**Y**
Zinc finger CCCH domain-containing protein 18 isoform a		**Y**
Zinc finger protein 341		**Y**
Zinc finger protein 414 isoform 1	**Y**	
Zinc finger protein 414 isoform 2	**Y**	

Protein- p7b Blastp search	Human	Mus musculus
Arrestin domain containing 4 isoform 1	N	Y
Arrestin domain containing 4 isoform 2	N	Y
B cell CLL/lymphoma 7 protein family member C isoform 1	Y	N
B cell CLL/lymphoma 7 protein family member C isoform 2	Y	N
Coiled-coil domain containing protein 13	Y	N
Colorectal mutant cancer protein isoform 1	Y	N
Colorectal mutant cancer protein isoform 2	Y	N
Cyclin T1 domain	Y	Y
DNA polymerase theta isoform 1	N	Y
DNA polymerase theta isoform 2	N	Y
E3 ubiquitin protein ligase HERC2	N	Y
G1/S-specific cyclin-E2	Y	Y
G1/S-specific cyclin-E2 isoform 1	N	Y
Glutamyl-Trna amidotransferase subunit A, mitochondrial	Y	Y
Heat shock protein beta-3	N	Y
Immunoglobulin super family member 1 isoform 1	Y	N
Immunoglobulin super family member 1 isoform 3	Y	N
Immunoglobulin super family member 1 isoform 4	Y	Y
Interleukin-1 receptor accessory protein-like 1 precursor	N	Y
NAD-dependent protein deacetylase sirtuin 1 isoform a	Y	Y
NAD-dependent protein deacetylase sirtuin 1 isoform b	Y	Y
Pro-interleukin-16 isoform 2	Y	N
Pro-interleukin-16 isoform 3	Y	N
Protein PRR2C	Y	Y
Protein PRRC2A	Y	Y
Protein PRRC2B	Y	N
Protein SCAI	N	Y
Protein shroom2 isoform 4	N	Y
Protein Smaug homolog-2	Y	Y

Protocadherin fat 2 precursor	**N**	**Y**
RNA-binding E3 ubiqutin-protein ligase MEX3C	**Y**	**Y**
Ryanodine receptor 3 isoform 1	**Y**	**N**
Ryanodine receptor 3 isoform 2	**Y**	**N**
Serine/threonine-protein kinase MARK2 isoform 1	**N**	**Y**
Serine/threonine-protein kinase MARK2 isoform 2	**N**	**Y**
Serine/threonine-protein kinase MARK2 isoform 3	**N**	**Y**
Serine/threonine-protein kinase MARK2 isoform 4	**N**	**Y**
SH3 and cysteine-rich domain-containing protein	**N**	**Y**
SIDI transmembrane family member 2 isoform 1 precursor	**N**	**Y**
SIDI transmembrane family member 2 isoform 2 precursor	**N**	**Y**
SPARC-related modular calcium binding protein 1 isoform 1 precursor	**Y**	**N**
SPARC-related modular calcium binding protein 1 isoform 2 precursor	**Y**	**N**
Spermatogenesis associated protein 6	**N**	**Y**
Spermatogenesis associated protein 6 isoform 1 precursor	**Y**	**N**
Spermatogenesis associated protein 6 isoform 2	**Y**	**N**
Spermatogenesis associated protein 6 isoform 3	**Y**	**N**
Transcription factor Sp7	**N**	**Y**
Transcription factor TFIIIB component B" homolog	**N**	**Y**
Transcriptional adapter 2-alpha isoform a	**Y**	**N**
Transcriptional adapter 2-alpha isoform b	**Y**	**N**
Tyrosine-protein kinase SgK223	**N**	**Y**
WD repeat domain phosphoinositide-interacting protein 3	**Y**	**Y**
X-linked interleukin-1 receptor accessory protein-like 2 precursor	**Y**	**N**
X-linked interleukin-1 receptor accessory protein-like 2 precursor	**N**	**Y**
Zinc finger CCCH domain containing protein 4	**Y**	**N**
Zinc finger CCCH-type with G patch domain containing protein isoform d	**Y**	**N**
Zinc finger CCCH-type with G patch domain containing protein isoform c	**Y**	**N**
Zinc finger CCCH-type with G patch domain containing protein isoform a	**Y**	**N**

Zinc finger FYVE domain-containing protein 26	**Y**	**N**
Zinc finger protein 446	**Y**	**N**
Zinc finger protein 451 isoform 1	**N**	**Y**
Zinc finger protein 451 isoform 2	**N**	**Y**
Zinc finger protein 469	**Y**	**N**
Zinc finger protein 622	**N**	**Y**

Protein- p1 Blastp search	Human
55 kDa erythrocyte membrane protein isoform 1	**Y**
55 kDa erythrocyte membrane protein isoform 2	**Y**
55 kDa erythrocyte membrane protein isoform 3	**Y**
Arrestin domain containing protein 2 isoform 1	**Y**
Arrestin domain containing protein 2 isoform 2	**Y**
Arrestin domain containing protein 2 isoform 3	**Y**
Aspartate beta-hydroxylase domain-containing protein 1	**Y**
Ataxin-7-like protein	**Y**
Cat eye syndrome critical region protein 2 isoform 1	**Y**
Cat eye syndrome critical region protein 2 isoform 2	**Y**
Cholecystokinin receptor type A	**Y**
CUB-domain containing protein 2 precursor	**Y**
Ectonucleoside triphosphate diphosphohydrolase 6 isoform 1	**Y**
Ectonucleoside triphosphate diphosphohydrolase 6 isoform 2	**Y**
FERM, RhoGEF and pleckstrin domain-containing protein 2 isoform a	**Y**
FH2 domain-containing protein 1	**Y**
Hsp70-binding protein 1 isoform 1	**Y**
Hsp70-binding protein 1 isoform 2	**Y**
Hypermethylated in cancer 2 protein	**Y**
Iporin	**Y**
Melatonin receptor type 1B	**Y**
Methyl-CpG-binding protein 2 isoform 1	**Y**
Methyl-CpG-binding protein 2 isoform 2	**Y**

Mucin-19 receptor	**Y**
Multiple epidermal growth factor-like domains protein 6 isoform 1 precursor	**Y**
Multiple epidermal growth factor-like domains protein 8 isoform 2 precursor	**Y**
Nesprin-2-isoform 4	**Y**
Nesprin-2-isoform 5	**Y**
OUT domain-containing protein7B	**Y**
Ras-interacting protein 1	**Y**
RNA-binding protein raly isoform 1	**Y**
RNA-binding protein raly isoform 2	**Y**
Suppression of tumourgenicity 5 protein isoform 1	**Y**
Thrombospondin-4 precursor	**Y**
Transcription factor Sp7 isoform a	**Y**
Transcription factor Sp7 isoform b	**Y**
Usherin isoform 8	**Y**
WD repeat containing protein 7 isoform 1	**Y**
WD repeat containing protein 7 isoform 2	**Y**
WD repeat-containing protein 86 isoform 1	**Y**

Protein- p2 Blastp search	Human
Activating transcription factor 7-interacting protein 1 isoform 1	**Y**
Activating transcription factor 7-interacting protein 1 isoform 2	**Y**
AF4/MR2 family member 1 isoform 1	**Y**
AF4/MR2 family member 1 isoform 2	**Y**
Arginine-fifty homeobox	**Y**
Aryl-hydrocarbon-interacting protein-like 1 isoform 2	**Y**
Aryl-hydrocarbon-interacting protein-like 1 isoform 3	**Y**
Aryl-hydrocarbon-interacting protein-like 1 isoform 4	**Y**
Aryl-hydrocarbon-interacting protein-like 1 isoform 5	**Y**
Aryl-hydrocarbon-interacting protein-like 1 isoform 6	**Y**
Aryl-hydrocarbon-interacting protein-like 1 isoform 7	**Y**
Cat eye syndrome critical region protein 2 isoform 1	**Y**

Cat eye syndrome critical region protein 2 isoform 2	**Y**
Cleavage and polyadenylation specificity factor subunit 7 isoform 3	**Y**
Cleavage and polyadenylation specificity factor subunit 7 isoform 2	**Y**
Cleavage and polyadenylation specificity factor subunit 7 isoform 1	**Y**
Coiled-coil domain containing protein 107 isoform A precursor	**Y**
Coiled-coil domain containing protein 107 isoform B precursor	**Y**
Coiled-coil domain containing protein 107 isoform C precursor	**Y**
Coiled-coil domain containing protein 107 isoform D precursor	**Y**
CUB domain containing protein 2 precursor	**Y**
D-dopachrome decarboxylase	**Y**
D-dopachrome decarboxylase like protein	**Y**
D-dopachrome decarboxylase related protein	**Y**
Downs syndrome cell adhesion molecule-like protein 1	**Y**
G patch domain-containing protein 8	**Y**
GRB2-asscoiated binding protein 4	**Y**
GTP-binding protein 10 isoform 1	**Y**
Hepatoma-derived growth factor-related protein 2 isoform 1	**Y**
Hepatoma-derived growth factor-related protein 2 isoform 2	**Y**
Integrin alpha-E precursor	**Y**
Interleuckin-17 receptor C isoform 2 precursor	**Y**
Melanoma-associated antigen 1	**Y**
Pro-neuregulin-3, membrane bound isoform 1	**Y**
Pro-neuregulin-3, membrane bound isoform 2	**Y**
Protein phosphatise slingshot homolog 1 isoform 1	**Y**
Protein spire homolog 2	**Y**
Rho/guanine nucleoside exchange factor 17	**Y**
Sarcalumenin precursor	**Y**
Sodium/hydrogen exchanger 1	**Y**
Vacuolar fusion protein MON1 homolog A	**Y**
Zinc finger protein 839 isoform 1	**Y**

Appendix